Summer 9-1-2014

Contribution of the Microenvironment in Bone Resident Cancer: the Role of Thrombospondin-1 in Bone and Risk Loci Contributing to Multiple Myeloma

Sarah R. Amend
Washington University in St. Louis

WASHINGTON UNIVERSITY IN SAINT LOUIS

Division of Biology and Biomedical Sciences
Molecular Genetics and Genomics

Dissertation Examination Committee:

Katherine N. Weilbaecher, Chair
Michael Tomasson, Co-Chair
Kendall Blumer
John DiPersio
William Frazier
Deborah Veis Novack

Contribution of the Microenvironment in Bone Resident Cancer:
the Role of Thrombospondin-1 in Bone and Risk Loci Contributing to Multiple Myeloma

by

Sarah R. Amend

A dissertation presented to the
Graduate School of Arts & Sciences
of Washington University in
partial fulfillment of the
requirements for the degree
of Doctor of Philosophy

August 2014
St. Louis, Missouri

Table of Contents

Chapter 1: Introduction

Chapter 2: Thrombospondin-1 regulates bone homeostasis through effects on bone matrix integrity and nitric oxide signaling in osteoclasts

Chapter 3: Samsn1 underlies genetic susceptibility to monoclonal gammopathy of undetermined significance in KaLwRij mice

Chapter 4: Summary of work, future directions, and clinical relevancy

Appendix

Curriculum Vitae

List of Figures

Chapter 3: *Samsn1* **deletion contributes to monoclonal gammopathy of undetermined significance and multiple myeloma susceptibility through effects on multiple cell types**

Chapter 4: Summary of work, future directions, and clinical relevancy

List of Abbreviations

BIP – benign idiopathic paraproteinemia
BMM – bone marrow macrophage
BMSC – bone marrow stromal cell
ECM – extracellular matrix
MGUS – monoclonal gammopathy of undetermined significance
MM – multiple myeloma
NCP – non-collagenous protein
NO – nitric oxide
NOS – nitric oxide synthase
OB – osteoblast
OC – osteoclast
SNP – single nucleotide polymorphism
SPEP – serum protein electrophoresis
TAM – tumor associated macrophage
TSP1 – Thrombospondin-1
WGAA – whole genome association study

Acknowledgements

I owe a debt of gratitude to my thesis advisor, Katherine Weilbeacher. Kathy, you pushed me to be independent, encouraged creative thinking, and showed unwavering confidence in my abilities and thought processes. Thank you for your patience, your sense of humor, and your dedication to your trainees.

One of my major graduate projects was possible because of Michael Tomasson's confidence in my skills and ideas. Thank you for teaching me to be a better communicator and collaborator.

Thank you to all of the Weilbaecher lab members during my tenure in the lab, but most especially Xinming Su, Jingyu "Jerry" Xiang, Alison Esser, Yalin Xu, and Michael Ross. I couldn't ask for better lab mates. Special thanks to Michelle: voice of reason, math-checker extraordinaire, and, most especially, friend.

My thesis committee has been wonderful: Deb Novack, Bill Frazier, Ken Blumer, and John DiPersio. Thank you for your guidance and thoughtful feedback.

To the members of the Experimental Skeletal Biology group, most especially Steve Teitelbaum, Deb Novack, Roberta Faccio, Roberto Civitelli, and Matt Silva: your suggestions and help have been invaluable. To the myeloma and MGUS translational research group, most especially Jacob Paasch, Ravi Vij, and Graham Colditz, thank you for your feedback and practical support.

My graduate school experience certainly wouldn't have been as successful (or as fun) without my friends. Special recognition goes to the Too Cute Tuesday group. Thanks to Danka, for always being there, when I knew I needed it and when I didn't; to Anne, for everything, most especially pizza and beer night; and to Emily, for your love and encouragement. Ben, Katie, and Renee: thanks for making sure I was more than "just" a scientist. Brian, thank you for your patient support. Ida, thanks for entrusting me with your horses and allowing me the opportunity to pursue my other passion.

Finally, I couldn't have done this without my parents, Elisabeth and Fred Amend. Mum, thanks for helping me with the many top-crisis-secrets and for sharing my love of science with everyone you know. Dad, your reminders that "even bad-news data tells you something new!" have gotten me through more experiments than you realize. Thank you both for your unconditional confidence and constant support.

This work is dedicated to the teachers who encouraged me to pursue a career in science, to ask challenging questions, and to always be excited about discovery.

Middle school teachers of Camp Einstein
Marilu Morse; MathCounts coach, St. Paul Education Center
Chip Duncan; Biology, New Bern High School
Bill Smith; Resource Seeds, Inc.
Bruce Novack; Dept. of Chemistry, NC State University
Barbara Shew; Dept. of Plant Pathology, NC State University
Ron Korstanje; The Jackson Laboratory

ABSTRACT OF THE DISSERTATION

Contribution of the Microenvironment in Bone Resident Cancer:
the Role of Thrombospondin-1 in Bone and Risk Loci Contributing to Multiple Myeloma

by

Sarah R. Amend

Doctor of Philosophy in Biology and Biomedical Sciences
Molecular Genetics and Genomics
Washington University in Saint Louis, 2014

Katherine Weilbaecher, Chair
Michael Tomasson, Co-Chair

Cancer growth in bone, a defining characteristic of multiple myeloma and common in many solid tumors including breast and prostate cancer, is characterized by the active participation of host microenvironment cells. Tumor cells stimulate the vicious cycle through stimulation of bone remodeling by osteoclasts and osteoblasts, resulting in increased release of growth factors and cytokines to further promote local tumor growth. Notably, cancer cells are unable to remodel bone independently, and require the metabolically active bone cells for this support.

A specific role for the bone microenvironment in mediating tumor growth was first discussed in 1889 with the introduction of Paget's seed-and-soil hypothesis that tumor cells will only grow in a favorable microenvironment. This dissertation is focused on investigating the properties of a "congenial soil." In Chapter 2 we discuss the role of bone-resident Thrombospondin-1 (TSP1), a glycoprotein with well-documented roles in promoting cancer growth. Chapter 3 is focused on the identification of genes conferring inherited susceptibility to

multiple myeloma that participate both in malignant cells and in host supportive cells.

TSP1 is a large matricellular protein that interacts β3 integrin, CD47, and other receptors to regulate cell migration, adhesion, and proliferation with effects on tumor angiogenesis, inflammation, and wound healing. We examined the role of TSP1 in the bone microenvironment. TSP1-/- mice had increased trabecular bone volume and increased cortical bone area and thickness compared to wild type controls. Surprisingly, TSP1-/- mouse bones did not resist bending as much as anticipated, and we confirmed a bone materials defect, indicating that TSP1 was important for maintaining bone quality. In addition to the mechanical defects, TSP1-/- mice had decreased serum CTX compared to controls, indicating an osteoclast defect. Primary osteoclast cultures require TSP1 at early stages of osteoclastogenesis, though exogenous TSP1 is dispensable at later stages of maturation. Interestingly, we found that TSP1-deplete osteoclast cultures had a significant and dramatic increase in inducible nitric oxide synthase (iNOS) expression. Moreover, upon administration of a NOS inhibitor to mice, the TSP1-/- bone resorption defect was rescued to wild type levels. To test whether osteoblast-deposited bone-resident TSP1 inhibits early osteoclast NO signaling, we plated osteoclasts on either wild type or TSP1-/- bone and found that only wild type bone was sufficient to block iNOS expression. Thus, we conclude that TSP1 is a paracrine signaling molecule that couples OB activity to OC formation and targeting of the TSP1 signaling pathway, currently under investigation for treating cancer and modulating blood pressure, may have additional effects on bone.

The second part of this dissertation focuses on host susceptibility to multiple myeloma (MM) and its requisite precursor, monoclonal gammopathy of undetermined significance (MGUS). The C57Bl/KaLwRij (KaLwRij) mouse strain has increased susceptibility to benign idiopathic paraproteinemia (BIP), analogous to human MGUS, and is a common mouse model

for the disease. Following immunization, KaLwRij mice developed a sustained M-spike at a higher frequency than 12 other genetically diverse mouse strains, most notably, the highly related C57Bl/6J (B6) strain. To query the genetic basis for BIP susceptibility in KaLwRij mice, we completed SNP analysis to identify variation between KaLwRij and B6. We found that KaLwRij is a unique inbred strain, completely distinct from the closely related B6. We identified several thousand variants between KaLwRij and B6 and compiled a candidate gene list of 419 genes. To ensure that we would pursue genes applicable to human disease, we completed whole genome association analysis between MM patients and healthy controls and identified SNPs located in 180 gene loci. Combining these two gene sets resulted in a candidate gene list of 5 genes, one of which, *Samsn1*, is annotated as a negative regulator of B-cell activation. Upon closer examination of the *Samsn1* locus, we found that KaLwRij harbored a germline deletion of all coding exons of the gene, resulting in absent RNA and protein expression. Consistent with the published role of SAMSN1 in genetically deficient mice, KaLwRij mice had enhanced B-cell function as evaluated by B-cell proliferation in primary culture and in vivo IgG2b response. To investigate the role of *Samsn1* in host cells, we profiled *Samsn1* expression in bone microenvironment cells and found that macrophages were high expressers. KaLwRij macrophages had enhanced expression of polarization markers, suggesting that they are pre-activated under homeostatic conditions. Further, we found that KaLwRij macrophages stimulated to a pro-tumorigenic M2 polarization promoted 5TG myeloma tumor growth more than B6 control macrophages in mice. In conclusion, we identified candidate gene lists underlying murine and human susceptibility to MGUS and myeloma. Specifically, we found that *Samsn1* contributes to KaLwRij susceptibility to BIP, and likely to human MGUS, through effects in pre-malignant B-cells and in macrophages.

Chapter 1

Introduction

The seed and soil hypothesis of metastasis

Metastasis is the dissemination of primary tumor cells to a distant site. In 1889, Stephen Paget, a physician in the West London hospital, analyzed the autopsies of 735 fatal breast cancer patients. He noted that secondary growth was more often seen in some organs than others, even in those with the same potential for metastasis (e.g. liver vs. spleen). Furthermore, he noted that "the bones [of breast cancer patients] suffer in a special way," more than would be predicted based on the circulation of tumor cells alone, based on evidence from other cancer types (Paget, 1889).

These observations led to his proposal of the "seed and soil" hypothesis: "when a plant goes to seed, its seeds are carried in all directions, but they can only live and grow if they fall on congenial soil." Cancer biologists, then, must be "scientific botanists," concerned not just with the malignant seed, but also with the "properties of the soil" that make up a favorable tumor microenvironment (Paget, 1889).

The goal of this thesis is to contribute to the understanding of the "congenial soil." First, we will address the role of the antiangiogenic Thrombospondin-1 in the "fertile soil" of bone, a common site of metastasis. Second, we will identify genetic risk loci that confer whole-host "congeniality" to multiple myeloma (MM) and its precursor syndrome monoclonal gammopathy of undetermined significance (MGUS).

Part I: The role of the bone microenvironment in metastasis.

Homeostatic bone remodeling requires coupled bone formation and destruction

Bone is a dynamic connective organ that, together with the cartilage, comprises the skeleton and provides mechanical, protective, and metabolic support for the rest of the body. Cancellous bone is made of a lattice of trabeculae localized to the metaphysis of long bones with high surface area for mineral metabolism. Cortical bone forms the outer shell of the metaphysis and the diaphysis (shaft) of long bones to provide mechanical support. The bone marrow found in the marrow space formed by the cortical bone is made up of hematopoietic and stromal cells that give rise to blood cells, platelets, endothelial cells, fibroblasts, adipocytes, osteoblasts (OBs), and osteoclasts (OCs) (Baron, 1996).

The bone matrix is composed of two compartments: osteoid (primarily collagen type I fibers–90%, and non-collagenous proteins–10%) and mineral (calcium-phosphate hydroxyapatite crystals). The numerous noncollagenous proteins include growth factors, proteoglycans, and adhesion molecules. These molecules contribute to maintenance of homeostatic bone remodeling, promoting cell attachment, differentiation, and growth of bone remodeling cells. In addition, some molecules aid in osteoid and mineral matrix organization, directly influencing bone strength.

Bone-forming OB arise from mesenchymal stem cells and express specific markers during differentiation including Runx2, alkaline phosphatase, osteonectin, and osteocalcin, useful for tracking OB formation in an experimental setting. To form bone, OBs deposit collagen fibers to form the extracellular matrix that is subsequently calcified with hydroxyapatite crystals. Osteoid also contains non-collagenous proteins secreted by the OBs including

thrombospondin-1 (TSP1), BMPs, IGFs, and TGFβ that play diverse roles in maintaining matrix structure and as signaling molecules to promote adhesion, survival, and differentiation of cells within the bone marrow (Puzas, 1996). OBs also directly promote OC formation through pre-OB secretion of MCSF and expression of RANKL, key cytokines necessary for osteoclastogenesis.

OCs arise from the MCSF- and RANKL-dependent fusion of macrophages. Following fusion, pre-OCs polarize and form the characteristic ruffled membrane necessary for bone resorption. OCs form a contractile actin ring to create a highly acidic sealing zone, the site of bone resorption (Baron, 1996; Novack and Teitelbaum, 2008). Cells committed to the OC lineage are TRAP+, useful for in vitro staining. Furthermore, each stage of OC formation is characterized by a unique gene expression signature: early OC precursors express N-FATc1, fusing OC express DC-STAMP and CD47, polarized cells express αvβ3 integrin, and mature resorbing cells express Cathepsin K. Dissolving of the mineral and underlying matrix releases growth factors and cytokines essential for OB activity, thus recruiting bone formation to a site of recent bone destruction.

Bone remodeling is a tightly regulated process that requires the coupled activity of bone forming OBs and bone resorbing OCs. Bone remodeling is necessary to preserve the integrity of the skeleton and to maintain calcium and phosphate levels (Baron, 1996; Hadjidakis and Androulakis, 2006). Misregulation of the basal bone remodeling, as in osteoporosis or bone metastasis, leads to decreased bone integrity, resulting in hypercalcemia, nerve-compression, and pathologic fracture.

Bone is a favorable microenvironment for metastatic invasion and growth

Bone metastasis is common to many cancers, including breast (70%), prostate (70%) and lung (35%), and bone disease is characteristic of multiple myeloma (Coleman, 2001; Lipton, 2004; Mundy, 2002). The consequences of bone metastases are devastating and cause pain, pathologic fracture, spinal cord and other nerve-compression syndromes, and life-threatening hypercalcemia (Roodman, 2004). Both osteolytic lesions and osteoblastic bone metastases are associated with increased OC activity and disrupted bone micro-architecture (Coleman et al., 2005; Lipton et al., 2001). Notably, while cancer cells are unable to resorb bone independently, they secrete soluble factors that promote bone remodeling resulting in the release of additional bone matrix-bound growth factors which further activates OCs and OBs and promotes tumor growth (Bendre et al., 2003; Clines and Guise, 2008; Guise et al., 2006; Hirbe et al., 2006; Hirbe et al., 2007; Kakonen et al., 2002; Kingsley et al., 2007; Kozlow and Guise, 2005; Mundy, 2002; Pfeilschifter et al., 1987; Roodman, 2004; Yin et al., 1999). This process of pathologic induction of bone remodeling by the cancer cells results in a "vicious cycle" of tumor growth and bone destruction (**Figure 1.1**). Anti-resorptive therapy, e.g. with bisphosphonates or denosumab, significantly decreases skeletal complications of cancer and is a standard of care for patients with bone metastases (Body et al., 2009; Fizazi et al., 2009; Hamdy, 2008; Hirbe et al., 2006; Roodman, 2004).

Integrins play a critical role in bone metastasis in both tumor cells and host stromal cells

The site of metastasis is tumor cell specific depending on adhesion molecule and chemokine receptor expression profiles of both the cancer cell and the host organ cells (Kang et al., 2003; Marcellini et al., 2006; Wei et al., 2005; Yoneda, 2000). At the metastatic site, normal

physiology is changed towards increased secretion of cytokines and activation of adhesion molecules to support recruitment, survival, and growth of tumor cells. Integrins expressed by tumor cells, in concert with bone microenvironment chemokine secretion and further adhesion molecule activation, determines the osteotropic characteristics of metastasizing cancer cells and represent an ideal target for skeletal metastatic cancer therapy.

Integrins are heterodimeric transmembrane glycoproteins that facilitate cell-cell and cell-extracellular matrix adhesion and cell migration (Schwartz et al., 1995). Integrins recruit many intracellular signaling molecules and can activate survival, proliferation, and motility signaling pathways (Hynes, 1992). Tumor cells localize to specific tissues through integrin-mediated contacts with extracellular matrix and stromal cells. Integrin expression and signaling are perturbed in cancer cells, allowing them to "escape" from cell-cell and cell-matrix tethers, invade, migrate, and colonize within new tissues and matrices. Integrin signaling through αvβ3 and VLA-4 on tumor cells promotes tumor metastasis to and proliferation in the bone microenvironment. As described above, misregulated OC-mediated bone resorption is a hallmark of bone metastasis and promotes tumor expansion in the marrow space. αvβ3 integrins are critical for OC function and development (Faccio et al., 1998; Faccio et al., 2003; Feng et al., 2001), and β3-/- mice have reduced tumor burden in bone and are protected from tumor-associated osteolysis due to defective OC (Bakewell et al., 2003; Morgan et al., 2009)

Integrin-mediated cell signaling plays a critical role in many of these processes during bone metastasis, including platelet aggregation (αIIbβ3), hematopoietic/immune cell mobilization (VLA-4, osteopontin, TSP1), neoangiogenesis (αvβ3,αvβ5, α6β4, β1 integrins, TSP1, CD47) and stromal function (osteopontin, VLA-4) (**Figure 1.2**). The mechanisms by which integrin signaling mediates the pathogenesis of bone metastasis, both from the tumor cell

and the host microenvironment, is an area of active research. Integrin pathway signaling is critical in the pathogenesis of bone metastasis at many stages and further study to define integrin dysregulation by cancer cells will yield new therapeutic targets for the prevention and treatment of bone metastasis.

Integrin signaling is critical for cell adhesion and survival

There are 8 beta and 18 alpha integrin subunits that assemble into 24 different known combinations in different cell types, each characterized by distinct ligand binding specificities, signaling abilities, and regulatory mechanisms(Hynes, 2002). Integrins are activated by conformational changes in the integrin extracellular domains ("inside-out" signaling). When the integrin α and β subunit cytoplasmic and transmembrane domains remain closely juxtaposed, the extracellular domains are held in a closed conformation. Activation by intracellular signals to the cytoplasmic tails results in separation of the α and β cytoplasmic and transmembrane domains and exposure of the extracellular ligand binding domain (Shattil et al., 2010) ("inside-out" signaling). In addition to activation by inside-out signaling, ligand binding and integrin clustering can be significantly modulated by growth factor receptor interactions and other integrin interacting proteins, as reviewed in (Desgrosellier and Cheresh; Hynes, 2002; Shattil et al., 2010). The open conformation facilitates high affinity ligand binding and triggers integrin-mediated cell signaling cascades ("outside-in" signaling) (Offermanns, 2006; Qin et al., 2004), critical for growth, migration, adhesion, and survival.

Maintaining adhesion to the extracellular matrix, in part through integrin signaling, is critical to cell survival (Frisch and Screaton, 2001). Altered cell-cell or cell-matrix interactions can result in disruption of downstream survival signaling and anchorage-dependent non-

transformed cells undergo anoikis (Frisch and Screaton, 2001). Under normal conditions, because each cell type expresses a unique set of integrins that recognize underlying extracellular matrix ligands, this form of apoptosis ensures that detached cells do not colonize inappropriate locations (Frisch and Screaton, 2001). Cells that resist anoikis, such as metastatic cells, take advantage of aberrant integrin expression that enables the cell to adhere to a novel extracellular matrix (Bissell and Radisky, 2001) and colonize a distant site.

Integrin signaling in tumor cells that metastasize to bone

Tumor progression, invasion, and metastasis require the activity of many adhesion proteins, including the integrin superfamily. At each stage of cancer progression, subsets of integrin heterodimers are activated, providing the necessary signaling pathways for adhesion, migration, and cell survival. Metastatic tumor cells show differential integrin heterodimerization and activation compared to non-metastatic tumor cells that enable the cell to home to and colonize in a metastatic site, such as the bone marrow cavity (Edlund et al., 2001; Yoneda, 2000). In order for primary epithelial cancers to metastasize, the tumor cells must become resistant to anoikis and detach from the primary tumor site extracellular matrix, enter the vasculature, and eventually colonize a distant site. Upon reaching a successful metastatic site, however, tumor cells use both anoikis and anoikis-resistance to their advantage, in some cases forming micro-metastases that are resistant to cancer treatment via integrin binding to the underlying bone matrix as reviewed in (Clezardin, 2009). In addition to evading apoptosis, tumor cells must also form interactions between the tumor cell and bone stroma to establish and maintain skeletal metastasis.

8

The β3 integrin signaling pathway has been implicated in tumor cell-host bone stroma interactions during bone metastasis and tumor growth in bone (**Figure 1.2**). Breast cancer cells that overexpress αvβ3 have increased levels of bone metastasis and associated tumor burden and osteolysis (Nakamura et al., 2007; Pecheur et al., 2002; Sloan et al., 2006; Van der Velde-Zimmermann et al., 1997; Zhao et al., 2007). This overexpression of αvβ3 in the tumor cells leads to increased tumor cell adhesion, migration, and invasion to bone as well as enhanced OC recruitment within the bone microenvironment (Pecheur et al., 2002; Sloan et al., 2006), implicating a role of tumor-specific αvβ3 expression in breast cancer metastasis to bone as well as tumor-associated osteolysis. Likewise, in prostate cancer cells, active αvβ3 is necessary for the adherence and migration to bone matrix proteins at early stages of skeletal metastasis. This tumor cell αvβ3 integrin expression allows cancer cells to adhere to the bone matrix and interact directly with the native bone cells, OBs and OCs, as well as with the bone matrix itself (Nakamura et al., 2007).

CD47 and TSP1 augment αvβ3 integrin signaling

β3 integrins are activated upon binding to an Arg-Gly-Asp (RGD) protein motif, contained in many extracellular matrix proteins including vitronectin, fibronectin, osteopontin, bone sialoprotein, and TSP1, among others. Importantly, integrin associated protein CD47 augments integrin activation and affects the ability of αvβ3 integrin to cluster upon ligand binding (Brown and Frazier, 2001). CD47 augments β3 integrin-dependent adhesion, with CD47-deficient β3-expressing cells showing decreased adhesion to vitronectin (Lindberg et al., 1996). Notably, TSP1 ligation of CD47 further enhances adhesion (Gao et al., 1996), suggesting that TSP1-binding of CD47 mediates the enhancement of β3 function. Pertussis toxin inhibits

these effects, providing evidence that the mechanism likely involves Gαi GTPase activity

(Frazier et al., 1999; Green et al., 1999). Investigation of the role of TSP1 in the bone

microenvironment will be discussed in **Chapter 2**.

αvβ3 integrin and thrombospondin-1 regulate tumor angiogenesis

Tumor neovascularization is essential for tumor growth and metastasis, providing the

cancer cells with host nutrients and access to the circulation for the dissemination for metastatic

cells. The ability of tumor cells to activate the normally quiescent vasculature is proposed to be

controlled by an "angiogenic switch" mechanism, whereby tumor or stromal cells induce

changes in the relative balance of inducers (VEGF, TGFβ) and inhibitors (TSP-1) of

angiogenesis (reviewed in (Desgrosellier and Cheresh; Hanahan and Weinberg, 2000; Hodivala-

Dilke, 2008; Hood and Cheresh, 2002; Silva et al., 2008; Stupack and Cheresh, 2004)).

Many integrins have been implicated in angiogenesis, but one of the best characterized is

αvβ3. Integrin αvβ3 is highly expressed on tumor-associated vasculature, and angiogenesis is

inhibited with β3 neutralizing antibodies. Interestingly, however, β3-/- mice have enhanced (not

reduced) tumor-associated angiogenesis in subcutaneous tumors (Reynolds et al., 2002). In β3

floxed mice crossed with endothelial-specific Cre mice, depletion of β3 integrin in endothelial

cells inhibits angiogenesis and tumor growth in a preventative setting, but not in established

tumors. Moreover, these tumor effects are transient, and long-term endothelial cell β3 deletion is

ineffective to reduce angiogenesis (Steri et al., 2014). Reports that low dose integrin antagonists

can increase tumor growth and angiogenesis while higher doses suppress tumor growth and

angiogenesis (Reynolds et al., 2009) (Carmeliet, 2002; Martin et al., 2002; Wang et al., 2001;

Zhao et al., 2005) further underscore the complexity of targeting β3 integrins for angiogenesis and cancer therapy.

In some scenarios, β3 integrin influences angiogenesis through interactions with ligand TSP1. TSP1 was the first identified endogenous anti-angiogenic factor (Isenberg et al., 2007a) and plays a role in neoangiogenesis in endothelial cells and platelets through its interactions with CD47 and β3 integrin. In numerous studies, TSP1 has tumor suppressing effects in the tumor microenvironment and many tumors have low expression of TSP1 (reviewed in (Kazerounian et al., 2008)). TSP1-/- mice have increased tumor burden and tumor-associated vasculature in a primary tumor model, while mice that over-express TSP1 have delayed tumor growth and reduced tumor-associated vasculature (Rodriguez-Manzaneque et al., 2001). In contrast, other studies demonstrate a role for TSP1 in promoting tumor progression (Dias et al., 2012; John et al., 2010; Tuszynski et al., 1987) in part through TSP1 stimulation of endothelial cell migration through interactions with the α6 integrin pathway (Dias et al., 2012; John et al., 2010). Thus, TSP-1 can play both pro- and anti-angiogenic roles, depending on its specific integrin interaction.

The role of αvβ3 integrin in tumor-associated angiogenesis is complex, not only involving integrin-ligand interactions and associated signaling pathways, but also specific temporal regulation and indirect effects through proteins such as TSP1, and are important for the progression of angiogenesis and eventual metastasis.

Integrin αvβ3 is necessary for osteoclast function and plays a key role in bone metastasis

Bone invading metastatic tumor cells co-opt integrin signaling pathways that enhance OC function and recruitment. As part of bone remodeling, OC bind to the bone matrix, form an actin

ring mediated sealing zone, secrete enzymes and acid to degrade bone, and then migrate to a new site. Each of these functions is regulated in part by integrins located on the membrane surface of the OC, interacting with neighboring cells and with the extracellular matrix (Teitelbaum and Ross, 2003).

αvβ3 is the predominant integrin found on OCs and plays roles in multiple components of osteoclastogenesis and resorption (Novack and Teitelbaum 2008; Ross and Teitelbaum 2005. αvβ3 is responsible for mediating OC∶∶bone matrix recognition (Crippes et al., 1996; Liapis et al., 1996; Ross et al., 1993; Zambonin Zallone et al., 1989), adhesion (Chellaiah, 2006; Ross et al., 1993), formation of the ruffled border, and overall organization of the cytoskeleton (Faccio et al., 2003; McHugh, 2000; Rucci et al., 2005; Zhang et al., 2000). Antibody inhibition of αvβ3 inhibits OC attachment to the bone matrix and OC-mediated bone resorption(Ross et al., 1993). In addition, β3-/- have defective OC function (McHugh, 2000) and are protected from tumor associated osteolysis (Bakewell et al., 2003).

Integrin αvβ3 ligand CD47 also plays important roles in OC formation and tumor-associated osteolysis, both through augmenting β3 activity, and in an integrin-independent manner. CD47-/- mice have increased bone volume due in part to reduced OC number and function (Koskinen et al., 2013; Uluckan et al., 2009), and CD47-/- mice are partially protected from tumor-associated osteolysis (Uluckan et al., 2009). CD47 in OC include binding to SIRPα in hematopoietic cells is an important "self-signal" to prevent phagocytosis. CD47:SIRPα binding is also important for macrophage fusion, an early event in OC formation (Han et al., 2000; Lundberg et al., 2007; Vignery, 2005). Interestingly, CD47-/- OCs have increased levels of inducible nitric oxide synthase and the CD47-/- OC formation defect is rescued in vitro through blockade of nitric oxide signaling (Uluckan et al., 2009). Notably, in other cell types

TSP1-CD47 binding inhibits nitric oxide signaling; we will investigate the role of TSP1 in nitric oxide mediated regulation of OC in **Chapter 2**.

OC targeted therapy is a standard of care for the treatment of bone metastasis and myeloma bone disease. Tumor cells recruit OCs resulting in bone destruction and pain (Clohisy and Ramnaraine, 1998; Honore et al., 2000; Mundy, 2002). Because of its known role in OC function and its high expression in skeletal metastatic tumors as discussed above, much research has focused on αvβ3 integrin and its ligands in bone. Elucidating the role of β3 integrin pathway member TSP1 is the subject of **Chapter 2**.

β3-/-, CD47-/-, and TSP1-/- mice have phenotypic overlap suggesting a common pathway

Mice with genetic deficiency in individual components of the αvβ3 pathway, including β3, CD47, and TSP1, show phenotypic overlap in characteristics essential for bone metastasis (**Table 1.1**). Importantly, both β3-/- and TSP1-/- mice have increased primary tumor growth and neoangiogenesis (Reynolds et al., 2002; Rodriguez-Manzaneque et al., 2001), while CD47-/- mice have decreased tumor burden with no apparent effect on angiogenesis, suggesting that the β3-CD47 signaling pathway may not participate in primary tumorigenesis. In the bone microenvironment, however, β3-/- and CD47-/- mice both have increased bone volume and decreased tumor-associated osteolysis (Bakewell et al., 2003; Uluckan et al., 2009), largely due to decreased OC activity. While the TSP1-/- mouse bone phenotype has not been fully evaluated, there is some evidence implicating TSP1 in OC activity (Carron et al., 2000; Carron et al., 1995).

Together, these data led us to hypothesize that the β3 – CD47 – TSP1 signaling axis is important in the bone microenvironment, both under homeostatic and pathologic states. Investigation of the role of TSP1 in the bone is the topic of **Chapter 2**.

Thrombospondin-1 is expressed in the bone matrix, but its role remains unknown

TSP1 is a large matricellular glycoprotein (350 kDa) that is ligand for at least 11 unique receptors, including αvβ3 integrin, CD47, and CD36, as well as many extracellular matrix proteins, including collagen, calcium, and osteopontin, among others. It is expressed and secreted by all vascular, endothelial, and hematopoietic cells, but is most highly secreted by activated platelets as part of wound healing. As a matricellular protein, TSP1 has dual function, both as a member of the ECM and as a signaling molecule.

TSP1 deficient mice are reported to have mild spine deformation(Crawford et al., 1998) and mild growth plate cartilage disorganization (Posey et al., 2008) but detailed analysis of bone has not been reported. TSP1 is expressed by OBs and is present in osteoid and mineralized bone matrix (Grzesik and Robey, 1994; Kannus et al., 1998; Robey et al., 1989) where it is directly deposited by bone-forming OBs (Clezardin et al., 1989; Robey et al., 1989). TSP1 participates in OB differentiation in part through activation of latent TGF-β (Bailey Dubose et al., 2012; Ueno et al., 2006), and TSP1 receptors CD47 and CD36 also regulate OB (Kevorkova et al., 2013; Koskinen et al., 2013). TSP1 has been implicated in OC activity, but its mechanism of action remains unknown(Carron et al., 1995). TSP1-CD47 interactions play a role in the formation of multiple myeloma-dendritic cell fusions with bone-resorbing capacity (Kukreja et al., 2009), and TSP1-CD36 ligation can promote osteoclastic resorption on dentine slices (Carron et al., 2000). Together these data led us to hypothesize that OB-secreted TSP1 sequestered in bone matrix will

modulate OC function thereby coupling OB activity to OC formation which we will investigate in **Chapter 2**.

Nitric oxide signaling modulates endothelial cell and osteoclast activity

Nitric oxide (NO) is synthesized by NO synthases (NOSs): eNOS and nNOS synthesize low levels of NO(Tsutsui, 2004) while higher levels are produced by iNOS, induced upon inflammatory cell activation (**Figure 1.2**) (Ridnour et al., 2005; Ridnour et al., 2006). NO binds sGC to catalyze the reaction of cGMP (Roy and Garthwaite, 2006), responsible for regulating signaling that controls proliferation, migration, cell cycle and apoptosis (Thomas et al., 2008). NO exerts a biphasic effect with low (<10 nM) levels of NO necessary for maintaining normal cell function (Isenberg et al., 2007b), while high (>100 nM) levels of NO are toxic (Lau, 2003) (**Figure 1.3**). Thus, tight regulation of NO is critical for normal cell function and unregulated increases in NO is typical of many pathologic conditions, including cancer, and can lead to cell toxicity or disrupted cell function.

NO signaling is a critical signaling pathway during homeostatic bone resorption. Upon stimulation with RANKL, OC precursors upregulate iNOS expression through an NFκB-dependent mechanism and the subsequent high NO concentration inhibits further OC formation (Zheng et al., 2006). iNOS deficient bone marrow macrophages show increased OC formation and resorption (Zheng et al., 2006). Misregulation of NO signaling, therefore, may lead to aberrant bone remodeling, compromising skeletal integrity.

TSP1 is a regulator of NO in endothelial cells, platelets, and vascular smooth muscle cells(Bergseth et al., 2000; Chen et al., 2000). Notably, only TSP1 receptors CD36 and CD47 have been implicated in NO regulation. TSP1-/- mice show elevated levels of endothelial cell

15

cGMP compared to wild type, and primary cultures show increased proliferation, migration, and adhesion (Isenberg et al., 2005). NO-stimulated endothelial cells and vascular smooth muscle cells have increased proliferation and migration and elevated cGMP (Isenberg et al., 2005). These responses are blocked upon addition of TSP1, CD47-binding peptide, or CD36-binding peptide (Isenberg et al., 2005). Vascular outgrowth is increased in TSP1-/- mice, an effect that is augmented with NO stimulation (Isenberg et al., 2006). Interestingly, while addition of TSP1 inhibits the NO-stimulated vascular outgrowth in CD36-/- mice, it has no effect in CD47-/- mice (Isenberg et al., 2006), indicating that CD47 is necessary for NO-mediated endothelial cell function. Despite identification of CD36 as a regulator of eNOS (Isenberg et al., 2007b), the direct mechanism of action for CD47 inhibition of NO has not been identified. Our lab reported that CD47 suppression of NO signaling in OCs plays an important role in pathologic osteolysis (Uluckan et al., 2009), but the CD47-activating ligand in OCs has not been defined. We will explore the role of TSP1-regulation of NO signaling in OC in **Chapter 2**. We hypothesize that TSP1 is a negative regulator of NO signaling in OC, promoting early stages of OC formation.

Goals of the present study

The seed-and-soil hypothesis of cancer metastasis has been accepted for decades, and the field of cancer biology acknowledges the necessity of host support for tumor growth. While many molecules have been implicated in host-cell support of tumor growth, the components of "congenial soil" remain incomplete. Therapeutic targeting of the host cells, specifically the uncoupling of the "vicious cycle" within the bone microenvironment, represents a promising site of intervention for the treatment of bone metastasis.

In **Chapter 2**, we elucidate the role of potent anti-angiogenic TSP1 in bone in order to better understand the impacts of TSP1-pathway directed therapeutics. While many receptors of TSP1 are known to be important for bone integrity, both in the bone matrix and in metabolically active bone cells, the role of the matricellular ligand is unclear. We demonstrated that TSP1 played both structural and signaling roles to maintain bone homeostasis. Using TSP1-null mice, we showed that TSP1 contributed to bone quality and that it was essential for OC formation. We found that pharmacologic inhibition of NO signaling in TSP1-/- mice restored OC activity, placing TSP1 upstream of NO regulation of OC formation. Importantly, we present strong evidence for TSP1 as a paracrine signaling molecule, coupling OB activity to OC formation, thus building upon the literature of critical bone remodeling factors.

Part II: Genetic susceptibility to monoclonal gammopathy of undetermined significance, the requisite precursor to multiple myeloma

Monoclonal gammopathy of undetermined significance is a common disorder of aging

Monoclonal gammopathy of undetermined significance (MGUS) is a common syndrome of aging, with a prevalence of 3.2 – 5.2 percent in 50 – 70 year olds, respectively (Kyle et al., 2006; Landgren et al., 2009). MGUS is characterized by the presence of a constant serum level of monoclonal paraprotein (less than 3 g/dl) termed "M-spike" as detected by a persistent band in the gamma region of a serum protein electrophoresis (SPEP, **Figure 1.4a**) in the absence of end-organ damage. While largely benign, MGUS is associated with increased fracture risk and osteoporosis (Melton et al., 2005), and MGUS patients have elevated serum levels of OC-activating (MIP1α) and OB-inhibiting (DKK1) factors (Ng et al., 2011). Importantly, MGUS is the requisite precursor to multiple myeloma (MM), and progresses to overt malignancy at a rate of 1% per year. Due to the largely asymptomatic state and low rate of transformation to myeloma (lifetime risk of 10-30% (Kyle et al., 2010; Sirohi and Powles, 2006; Zingone and Kuehl, 2011)), MGUS is not clinically treated, though patients are monitored with annual blood chemistry tests.

Step-wise transformation from MGUS multiple myeloma

MM is the second most common hematological malignancy and is invariably fatal with a ~6 year median survival (Kumar et al., 2013). MM is a malignancy of plasma B-cells that is clinically diagnosed by an M-spike of >3 g/dL and the presence of CRAB syndromes: hypercalcemia, renal insufficiency, anemia, and lytic bone lesions, highlighting its dependence on the bone microenvironment (**Figure 1.4b**).

Normal plasma B-cell development results in a long-lived non-proliferative antibody-producing cell. One of the hallmarks of B-cell differentiation is a DNA rearrangement for increased variation: VDJ recombination in immunoglobulin (Ig) heavy and light chains, somatic hypermutation, and Ig heavy change switch recombination. In the bone marrow, pro- and pre-B-cells undergo Ig heavy and light chain recombination, respectively. Immature B-cells that undergo receptor editing and express IgM receptor leave the bone marrow and travel to the spleen or lymph nodes as antigen-presenting cells. Upon encountering an antigen, the B-cell will endocytose the antigen and presents the antigenic peptides as part of the MHC II complex. These activated B-cells enter a germinal center and undergo somatic hypermutation of both the heavy and light chains. Cells that express high-binding antigen-receptors undergo Ig class switch recombination then home to the bone marrow as mature, antibody producing plasma B-cells.

The affected cell in MGUS and MM is the typically non-proliferative terminally-differentiated post-germinal center B-cell. In MGUS, there is a clonal expansion of one or more of these plasma cells, resulting in an elevated level of immunoglobulin in the serum. MM is characterized by a further expansion of one or more of these clones to fill the marrow space, again resulting in an elevated immunoglobulin level, but now accompanied with more significant end-organ damage.

The bone microenvironment contributes to MGUS and MM pathology

Differentiation and function of normal plasma cells is dependent on the bone marrow microenvironment. Bone marrow stromal cells and OBs support B-cell lymphopoiesis, proliferation, and plasma cell homing to the marrow. Likewise, MM::microenvironment

interactions parallel normal B-cell::microenvironment cross-talk, with similar mechanisms

identified for homing (CXCR4/SDF1 gradient) and proliferation (IL-6, IGF1, TGFB) (reviewed

in (Kuehl and Bergsagel, 2002)). In addition, myelomas further modulate the bone

microenvironment and produce OC-stimulatory (Basak et al., 2009; Esteve and Roodman, 2007;

Oyajobi et al., 2003) and OB-inhibitory factors (Giuliani et al., 2005; Yaccoby, 2010) that

deregulate the coupled process of healthy bone remodeling (Mundy, 2002; Weilbaecher et al.,

2011). This results in osteolytic lesions in 70-80% of MM patients (Terpos et al., 2007) (**Figure

1.4b**). Such pathologic bone resorption releases tumor growth factors stored within the bone

matrix. Bone marrow stromal cells, a heterogeneous population including mesenchymal stem

cells, support myeloma growth through adhesion-dependent mechanisms (VLA-4/VCAM) and

the production of soluble growth factors including IL-6(Terpos et al., 2007). MM causes

significant bone destruction, hypercalceimia, bone pain, and facture.

Tumor associated macrophages promote myeloma progression

In addition to the crucial role of bone remodeling cells, there is a growing literature

implicating tumor-associated macrophages (TAMs) in the pathogenesis of MM (reviewed in

(Asimakopoulos et al., 2013; Berardi et al., 2013; Ribatti et al., 2013)). TAMs are typically

categorized as classically-activated pro-inflammatory macrophages (M1) or alternatively-

activated anti-inflammatory macrophages (M2), though the distinction between the two classes

likely represents a spectrum rather than specific identity. M1 macrophages, activated by bacterial

lipopolysaccharide (LPS) and interferon-gamma (IFNg), promote a strong host immune

response. In contrast, M2 macrophages, activated by IL-4, IL-13, and TGFβ, suppresses Th1-

mediated inflammation and promotes wound healing, including angiogenesis and destruction of

the extracellular matrix. Thus, even within their normal physiologic roles, M1 macrophages are inherently anti-tumor while M2 macrophages promote tumor progression.

MM patients with active disease have higher percentage of macrophages in the bone marrow than either MGUS patients or patients with non-active disease (Scavelli et al., 2008). In addition, these macrophages are functionally distinct from non-affected patients and contribute to angiogenesis through vasculogenic mimicry (Scavelli et al., 2008). MM TAMs have increased pro-MM factor secretion such as IL-6 (Kim et al., 2012; Zheng et al., 2009) and higher levels of pro-angiogenic VEGF expression compared to non-MM macrophages (Ribatti et al., 2006; Scavelli et al., 2008; Vacca and Ribatti, 2011). The role of *Samsn1* in macrophages will be explored in **Chapter 3**.

Genetic risk factors contributing to MGUS and MM susceptibility

Human population studies suggest that genetic risk factors underlie susceptibility to MGUS and MM. Interestingly, however, the majority of plasma-cell intrinsic genetic events in MM cells are present in MGUS-affected B-cells (Davies et al., 2003), though not in normal plasma B-cells. Epidemiological studies have identified a higher incidence for MM in African Americans and that this is the result of elevated risk to MGUS, rather than an increased rate of conversion from MGUS to MM (Kyle et al., 2010; Kyle et al., 2006; Landgren et al., 2006). In addition, studies in affected families showed a higher risk of MM in patients with an MGUS-affected relative (Jain et al., 2009; Kyle et al., 2004; Vachon et al., 2009).

Genome wide significance studies of MM have identified seven SNPs that confer a significant increase in MM risk (Broderick et al., 2012; Chubb et al., 2013). Interestingly, a recent study in an MGUS patient population showed that these SNPs also conferred increased

risk to MGUS (Weinhold et al., 2014), providing further evidence that increased MM risk is due to increased MGUS risk. These studies highlight the need for a better understanding of the genetic predisposition to MGUS that will be the subject of **Chapter 3**.

C57Bl/KaLwRij is a spontaneous mouse model of MGUS and MM

One of the most common experimental models for MGUS and MM is the C57BL/KaLwRij mouse (KaLwRij). KaLwRij was first identified to have a high frequency of benign idiopathic paraproteinaemia (BIP), the murine counterpoint to human MGUS, in 1974 (Radl and Hollander, 1974). KaLwRij mice have increased serum levels of homogeneous immunoglobulin by SPEP, similar to the M-spike observed in MGUS and MM patients, by 12 months of age with a penetrance of ~45% (Radl et al., 1978). Affected mice progress to overt malignancy at a rate of approximately 1% with similar clinical features as human MM, including severe bone pathology (Radl et al., 1978).

5T myeloma cell lines were generated from spontaneous myelomas in KaLwRij mice, and can be transplanted into KaLwRij mice to propagate the myeloma (Alici et al., 2004; Asosingh et al., 2000; Vanderkerken et al., 2003). Intravenous injection into KaLwRij mice yields robust bone marrow-disseminated myeloma with significant osteolytic bone lesions and increased monoclonal paraprotein (M-spike) within 28 days (Dallas et al., 1999; Edwards et al., 2009; Garrett et al., 1997). Importantly, the 5TMM cell lines will not engraft in the closely related C57Bl/6 (B6) strain (Asosingh et al., 2000), highlighting the requirement of a supportive host microenvironment for establishment of early disease. Notably, while KaLwRij represents an ideal model for MGUS and for a MM-supportive host microenvironment, the genetic basis of

BIP susceptibility in these mice remains largely unknown. We characterized the genetic

variation between KaLwRij and B6 using SNP mapping which is presented in **Chapter 3**.

Mouse genetic mapping to identify genetic susceptibility loci for BIP

The KaLwRij mouse strain is an ideal model to dissect genetic risk loci contributing to

the complex trait of BIP susceptibility, analogous to human MGUS. Importantly, identifying

germline risk alleles will encompass genes at play in all cell types participating in the step-wise

progression from a normal plasma cell to overt MM, including host stromal cells predicted to

contribute to MGUS and MM. In our studies presented in **Chapter 3** we use a variety of genetic

techniques to identify MGUS risk alleles using KaLwRij mice and human MM samples.

The BIP-prone KaLwRij strain has been interbred since approximately 1978, and we

demonstrated that it is distinct from, but closely related to, the commonly used wild type (and

BIP-resistant) strain, B6 (**Chapter 3, Figure 3.1**). We used SNP analysis, also known as linkage

disequilibrium mapping, to identify candidate loci underlying risk to MGUS. Haplotype

analysis, while uncommon in the genomic era, is used to narrow quantitative trait loci regions

and to characterize regions of interest contributing to phenotype in recombinant inbred strain

analysis (Burgess-Herbert et al., 2008).

Linkage disequilibrium is the non-random assortment of alleles based on physical

proximity. Loci that are physically proximal to each other are more likely to be inherited

together than expected by random assortment, due to low rates of recombination in short

physical space. Contiguous loci that are inherited together represent a haplotype. Therefore, by

identifying regions which are shared in "high" phenotype mouse strains and not in "low"

phenotype mouse strains allows for the identification of candidate gene loci. Traditional

haplotype block analysis assumes that any variation between strains is a result of ancestral variation rather than recent variation, resulting in large DNA regions that are identical by descent. We modified the approach to identify smaller units of variation between the closely related KaLwRij and B6, and therefore used a lower threshold than is typical for this analysis.

In our analyses presented in **Chapter 3**, we identified candidate lists of genes underlying susceptibility to (1) murine BIP, (2) human MM/MGUS, and (3) both murine BIP and human MM/MGUS.

Goals of the present study

Epidemiological evidence points to genetic risk to MGUS and subsequent progression to MM, representing a "congenial soil" for malignant cell transformation, both inherent to the pre-malignant B-cell and to the non-cancerous host cells contributing to disease progression.

In **Chapter 3**, we focus on whole-host "congeniality" to MGUS and MM. We identify genetic risk loci contributing to susceptibility to microenvironment-dependent MGUS. Using a combinatorial approach, we compiled candidate gene lists derived from mouse SNP analysis and human MM patient association studies to ultimately identify a shared candidate list of five genes and focused our studies on *Samsn1*. We show that the most common murine model for human MGUS and myeloma, KaLwRij mouse strain, has a germline deletion for the B-cell inhibitor *Samsn1*. We present compelling evidence that *Samsn1* confers genetic risk to B-cell malignancy through effects both in pre-malignant cells inn cooperating cells of the host microenvironment, namely TAMs. Therefore, *Samsn1* represents a single tumor-suppressor gene contributing to myeloma progression through two mutually exclusive mechanisms.
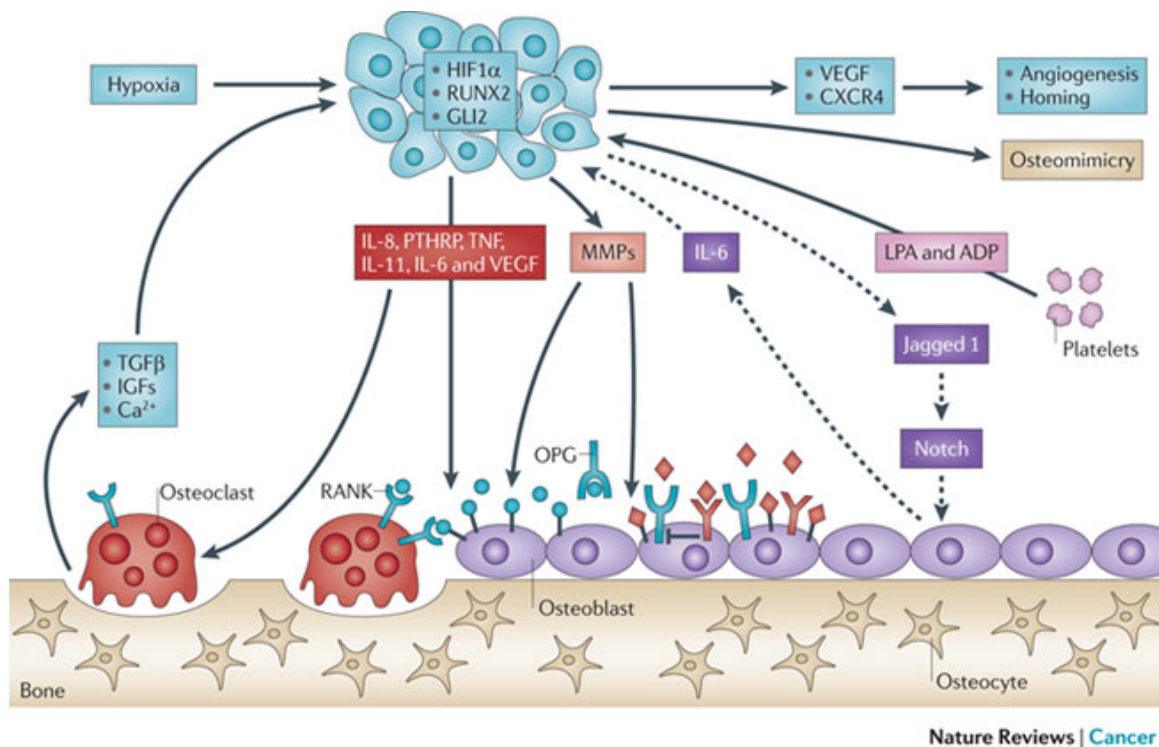
Figure 1.1. The "vicious cycle" of bone metastasis.

In the bone marrow space, metastatic cells secrete factors (including PTHrP, IL-6, VEGF, TNF, and MMPs) to stimulate bone resorption, through both direct and indirect effects on osteoclasts. In turn, osteoclasts releases bone-sequestered growth actors (including TGFβ and IGFs) that further stimulate tumor growth.

Reproduced from (Weilbaecher et al., 2011).

Integrin Expression During Bone Metastasis
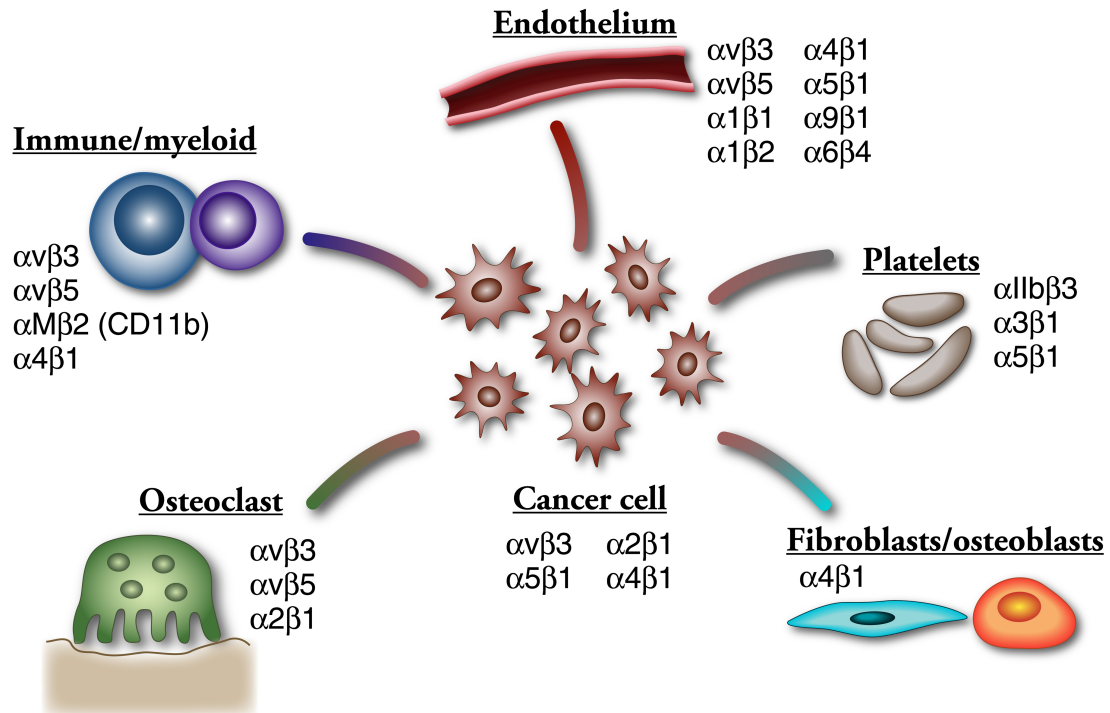
Figure 1.2.
Expression of integrins in tumor cells and host microenvironment cells during metastasis.
Reproduced from (Schneider et al., 2011).
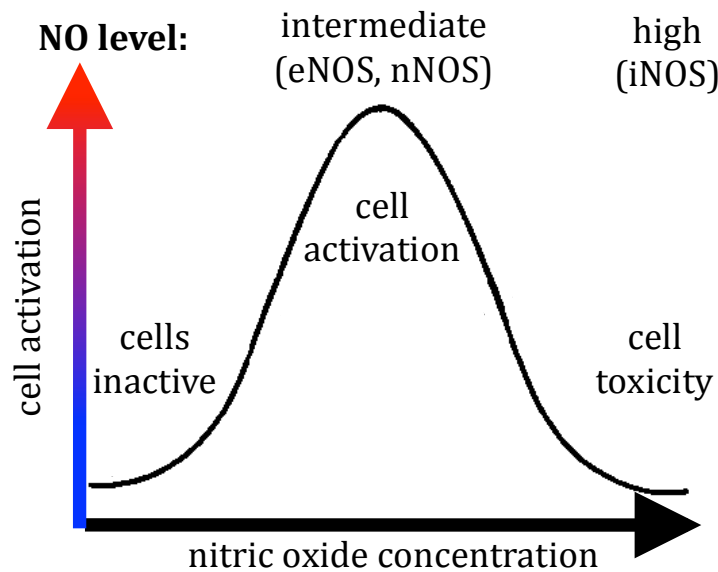
Figure 1.3. Nitric oxide (NO) exerts a biphasic (or "Goldilocks") effect on cell activation. In the absence of nitric oxide, cells remain inactive or fail to differentiate. Under tonic levels of NO, synthesized by the constitutive nitric oxide synthases (NOSs) endothelial NOS and neuronal NOS, cells are activated or differentiate. High levels of NO, produced by inducible NOS, results in cell toxicity.
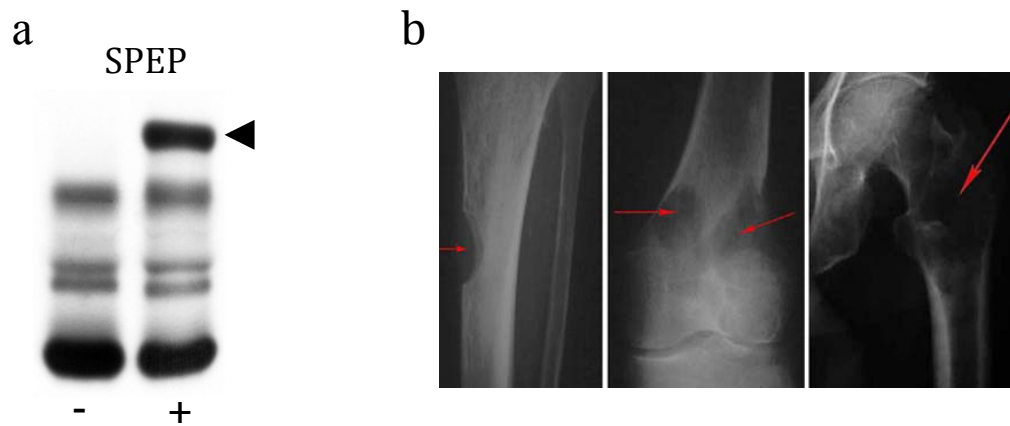
Figure 1.4. Clinical diagnosis of MGUS and multiple myeloma.
(a) Serum protein electrophoresis (SPEP). Arrowhead indicates band in the gamma region, indicative of an accumulation of monoclonal paraprotein (M-spike). Negative (left) and positive (right) M-spike.
(b) X-ray of a multiple myeloma patient with characteristic "hole-punch" bone lesions (arrows). Reproduced from the American Academy of Orthopedic Surgeons.

Table 1.1. Integrin β3-/-, CD47-/-, and TSP1-/- mouse model phenotypic overlap

Mouse model	Primary tumor		Bone metastasis		Homeostatic bone	
	Tumor	Angiogenesis	Tumor	Osteolysis	Bone volume	Osteoclasts
β3-/-	↑	↑	↓	↓	↑	↓
CD47-/-	↓	- - -	↓	↓	↑	↓
TSP1-/-	↑	↑	?	?	?	?

References

Alici, E., Konstantinidis, K.V., Aints, A., Dilber, M.S., and Abedi-Valugerdi, M. (2004). Visualization of 5T33 myeloma cells in the C57BL/KaLwRij mouse: establishment of a new syngeneic murine model of multiple myeloma. Experimental hematology *32*, 1064-1072.

Asimakopoulos, F., Kim, J., Denu, R.A., Hope, C., Jensen, J.L., Ollar, S.J., Hebron, E., Flanagan, C., Callander, N., and Hematti, P. (2013). Macrophages in multiple myeloma: emerging concepts and therapeutic implications. Leukemia & lymphoma *54*, 2112-2121.

Asosingh, K., Radl, J., Van Riet, I., Van Camp, B., and Vanderkerken, K. (2000). The 5TMM series: a useful in vivo mouse model of human multiple myeloma. The hematology journal : the official journal of the European Haematology Association / EHA *1*, 351-356.

Bailey Dubose, K., Zayzafoon, M., and Murphy-Ullrich, J.E. (2012). Thrombospondin-1 inhibits osteogenic differentiation of human mesenchymal stem cells through latent TGF-beta activation. Biochem Biophys Res Commun *422*, 488-493.

Bakewell, S.J., Nestor, P., Prasad, S., Tomasson, M.H., Dowland, N., Mehrotra, M., Scarborough, R., Kanter, J., Abe, K., Phillips, D.*, et al.* (2003). Platelet and osteoclast beta3 integrins are critical for bone metastasis. Proc Natl Acad Sci U S A *100*, 14205-14210.

Baron, R.E. (1996). Anatomy and Ultrastructure of Bone. In Primer on the Metabolic Bone Diseases and Disorders of Mineral Metabolism, M.J. Favus, ed. (New York: Lippincott - Raven Publishers).

Basak, G.W., Srivastava, A.S., Malhotra, R., and Carrier, E. (2009). Multiple myeloma bone marrow niche. Current pharmaceutical biotechnology *10*, 345-346.

Bendre, M.S., Montague, D.C., Peery, T., Akel, N.S., Gaddy, D., and Suva, L.J. (2003). Interleukin-8 stimulation of osteoclastogenesis and bone resorption is a mechanism for the increased osteolysis of metastatic bone disease. Bone *33*, 28-37.

Berardi, S., Ria, R., Reale, A., De Luisi, A., Catacchio, I., Moschetta, M., and Vacca, A. (2013). Multiple myeloma macrophages: pivotal players in the tumor microenvironment. J Oncol *2013*, 183602.

Bergseth, G., Lappegard, K.T., Videm, V., and Mollnes, T.E. (2000). A novel enzyme immunoassay for plasma thrombospondin. Comparison with beta-thromboglobulin as platelet activation marker in vitro and in vivo. Thromb Res *99*, 41-50.

Bissell, M.J., and Radisky, D. (2001). Putting tumours in context. Nat Rev Cancer *1*, 46-54.

Body, J.J., Lipton, A., Gralow, J., Steger, G.G., Gao, G., Yeh, H., and Fizazi, K. (2009). Effects of Denosumab in Patients with Bone Metastases, with and without Previous Bisphosphonate Exposure. J Bone Miner Res.

Broderick, P., Chubb, D., Johnson, D.C., Weinhold, N., Forsti, A., Lloyd, A., Olver, B., Ma, Y.P., Dobbins, S.E., Walker, B.A.*, et al.* (2012). Common variation at 3p22.1 and 7p15.3 influences multiple myeloma risk. Nature genetics *44*, 58-61.

Brown, E.J., and Frazier, W.A. (2001). Integrin-associated protein (CD47) and its ligands. Trends Cell Biol *11*, 130-135.

Burgess-Herbert, S.L., Cox, A., Tsaih, S.W., and Paigen, B. (2008). Practical applications of the bioinformatics toolbox for narrowing quantitative trait loci. Genetics *180*, 2227-2235.

Carmeliet, P. (2002). Integrin indecision. Nat Med *8*, 14-16.

Carron, J.A., Wagstaff, S.C., Gallagher, J.A., and Bowler, W.B. (2000). A CD36-binding peptide from thrombospondin-1 can stimulate resorption by osteoclasts in vitro. Biochem Biophys Res Commun *270*, 1124-1127.

Carron, J.A., Walsh, C.A., Fraser, W.D., and Gallagher, J.A. (1995). Thrombospondin promotes resorption by osteoclasts in vitro. Biochem Biophys Res Commun *213*, 1017-1025.

Chellaiah, M.A. (2006). Regulation of podosomes by integrin alphavbeta3 and Rho GTPase-facilitated phosphoinositide signaling. Eur J Cell Biol *85*, 311-317.

Chen, H., Herndon, M.E., and Lawler, J. (2000). The cell biology of thrombospondin-1. Matrix Biol *19*, 597-614.

Chubb, D., Weinhold, N., Broderick, P., Chen, B., Johnson, D.C., Forsti, A., Vijayakrishnan, J., Migliorini, G., Dobbins, S.E., Holroyd, A.*, et al.* (2013). Common variation at 3q26.2, 6p21.33, 17p11.2 and 22q13.1 influences multiple myeloma risk. Nature genetics *45*, 1221-1225.

Clezardin, P. (2009). Integrins in bone metastasis formation and potential therapeutic implications. Curr Cancer Drug Targets *9*, 801-806.

Clezardin, P., Jouishomme, H., Chavassieux, P., and Marie, P.J. (1989). Thrombospondin is synthesized and secreted by human osteoblasts and osteosarcoma cells. A model to study the different effects of thrombospondin in cell adhesion. European journal of biochemistry / FEBS *181*, 721-726.

Clines, G.A., and Guise, T.A. (2008). Molecular mechanisms and treatment of bone metastasis. Expert Rev Mol Med *10*, e7.

Clohisy, D.R., and Ramnaraine, M.L. (1998). Osteoclasts are required for bone tumors to grow and destroy bone. J Orthop Res *16*, 660-666.

Coleman, R.E. (2001). Metastatic bone disease: clinical features, pathophysiology and treatment strategies. Cancer Treat Rev *27*, 165-176.

Coleman, R.E., Major, P., Lipton, A., Brown, J.E., Lee, K.A., Smith, M., Saad, F., Zheng, M., Hei, Y.J., Seaman, J.*, et al.* (2005). Predictive value of bone resorption and formation markers in

cancer patients with bone metastases receiving the bisphosphonate zoledronic acid. J Clin Oncol *23*, 4925-4935.

Crawford, S.E., Stellmach, V., Murphy-Ullrich, J.E., Ribeiro, S.M., Lawler, J., Hynes, R.O., Boivin, G.P., and Bouck, N. (1998). Thrombospondin-1 is a major activator of TGF-beta1 in vivo. Cell *93*, 1159-1170.

Crippes, B.A., Engleman, V.W., Settle, S.L., Delarco, J., Ornberg, R.L., Helfrich, M.H., Horton, M.A., and Nickols, G.A. (1996). Antibody to beta3 integrin inhibits osteoclast-mediated bone resorption in the thyroparathyroidectomized rat. Endocrinology *137*, 918-924.

Dallas, S.L., Garrett, I.R., Oyajobi, B.O., Dallas, M.R., Boyce, B.F., Bauss, F., Radl, J., and Mundy, G.R. (1999). Ibandronate reduces osteolytic lesions but not tumor burden in a murine model of myeloma bone disease. Blood *93*, 1697-1706.

Davies, F.E., Dring, A.M., Li, C., Rawstron, A.C., Shammas, M.A., O'Connor, S.M., Fenton, J.A., Hideshima, T., Chauhan, D., Tai, I.T*., et al.* (2003). Insights into the multistep transformation of MGUS to myeloma using microarray expression analysis. Blood *102*, 4504-4511.

Desgrosellier, J.S., and Cheresh, D.A. Integrins in cancer: biological implications and therapeutic opportunities. Nat Rev Cancer *10*, 9-22.

Dias, J.V., Benslimane-Ahmim, Z., Egot, M., Lokajczyk, A., Grelac, F., Galy-Fauroux, I., Juliano, L., Le-Bonniec, B., Takiya, C.M., Fischer, A.M*., et al.* (2012). A motif within the N-terminal domain of TSP-1 specifically promotes the proangiogenic activity of endothelial colony-forming cells. Biochem Pharmacol *84*, 1014-1023.

Edlund, M., Miyamoto, T., Sikes, R.A., Ogle, R., Laurie, G.W., Farach-Carson, M.C., Otey, C.A., Zhau, H.E., and Chung, L.W. (2001). Integrin expression and usage by prostate cancer cell lines on laminin substrata. Cell Growth Differ *12*, 99-107.

Edwards, C.M., Lwin, S.T., Fowler, J.A., Oyajobi, B.O., Zhuang, J., Bates, A.L., and Mundy, G.R. (2009). Myeloma cells exhibit an increase in proteasome activity and an enhanced response to proteasome inhibition in the bone marrow microenvironment in vivo. American journal of hematology *84*, 268-272.

Esteve, F.R., and Roodman, G.D. (2007). Pathophysiology of myeloma bone disease. Best practice & research Clinical haematology *20*, 613-624.

Faccio, R., Grano, M., Colucci, S., Zallone, A.Z., Quaranta, V., and Pelletier, A.J. (1998). Activation of alphav beta3 integrin on human osteoclast-like cells stimulates adhesion and migration in response to osteopontin. Biochem Biophys Res Commun *249*, 522-525.

Faccio, R., Takeshita, S., Zallone, A., Ross, F.P., and Teitelbaum, S.L. (2003). c-Fms and the alphavbeta3 integrin collaborate during osteoclast differentiation. J Clin Invest *111*, 749-758.

Feng, X., Novack, D.V., Faccio, R., Ory, D.S., Aya, K., Boyer, M.I., McHugh, K.P., Ross, F.P., and Teitelbaum, S.L. (2001). A Glanzmann's mutation in beta 3 integrin specifically impairs osteoclast function. J Clin Invest *107*, 1137-1144.

Fizazi, K., Lipton, A., Mariette, X., Body, J.J., Rahim, Y., Gralow, J.R., Gao, G., Wu, L., Sohn, W., and Jun, S. (2009). Randomized phase II trial of denosumab in patients with bone metastases from prostate cancer, breast cancer, or other neoplasms after intravenous bisphosphonates. J Clin Oncol *27*, 1564-1571.

Frazier, W.A., Gao, A.G., Dimitry, J., Chung, J., Brown, E.J., Lindberg, F.P., and Linder, M.E. (1999). The thrombospondin receptor integrin-associated protein (CD47) functionally couples to heterotrimeric Gi. J Biol Chem *274*, 8554-8560.

Frisch, S.M., and Screaton, R.A. (2001). Anoikis mechanisms. Curr Opin Cell Biol *13*, 555-562.

Gao, A.G., Lindberg, F.P., Dimitry, J.M., Brown, E.J., and Frazier, W.A. (1996). Thrombospondin modulates alpha v beta 3 function through integrin-associated protein. J Cell Biol *135*, 533-544.

Garrett, I.R., Dallas, S., Radl, J., and Mundy, G.R. (1997). A murine model of human myeloma bone disease. Bone *20*, 515-520.

Giuliani, N., Colla, S., Morandi, F., Lazzaretti, M., Sala, R., Bonomini, S., Grano, M., Colucci, S., Svaldi, M., and Rizzoli, V. (2005). Myeloma cells block RUNX2/CBFA1 activity in human bone marrow osteoblast progenitors and inhibit osteoblast formation and differentiation. Blood *106*, 2472-2483.

Green, J.M., Zhelesnyak, A., Chung, J., Lindberg, F.P., Sarfati, M., Frazier, W.A., and Brown, E.J. (1999). Role of cholesterol in formation and function of a signaling complex involving alphavbeta3, integrin-associated protein (CD47), and heterotrimeric G proteins. J Cell Biol *146*, 673-682.

Grzesik, W.J., and Robey, P.G. (1994). Bone matrix RGD glycoproteins: immunolocalization and interaction with human primary osteoblastic bone cells in vitro. J Bone Miner Res *9*, 487-496.

Guise, T.A., Mohammad, K.S., Clines, G., Stebbins, E.G., Wong, D.H., Higgins, L.S., Vessella, R., Corey, E., Padalecki, S., Suva, L.*, et al.* (2006). Basic mechanisms responsible for osteolytic and osteoblastic bone metastases. Clin Cancer Res *12*, 6213s-6216s.

Hadjidakis, D.J., and Androulakis, II (2006). Bone remodeling. Ann N Y Acad Sci *1092*, 385-396.

Hamdy, N.A. (2008). Denosumab: RANKL inhibition in the management of bone loss. Drugs Today (Barc) *44*, 7-21.

Han, X., Sterling, H., Chen, Y., Saginario, C., Brown, E.J., Frazier, W.A., Lindberg, F.P., and Vignery, A. (2000). CD47, a ligand for the macrophage fusion receptor, participates in macrophage multinucleation. J Biol Chem *275*, 37984-37992.

Hanahan, D., and Weinberg, R.A. (2000). The hallmarks of cancer. Cell *100*, 57-70.

Hirbe, A., Morgan, E.A., Uluckan, O., and Weilbaecher, K. (2006). Skeletal complications of breast cancer therapies. Clin Cancer Res *12*, 6309s-6314s.

Hirbe, A.C., Rubin, J., Uluckan, O., Morgan, E.A., Eagleton, M.C., Prior, J.L., Piwnica-Worms, D., and Weilbaecher, K.N. (2007). Disruption of CXCR4 enhances osteoclastogenesis and tumor growth in bone. Proc Natl Acad Sci U S A *104*, 14062-14067.

Hodivala-Dilke, K. (2008). alphavbeta3 integrin and angiogenesis: a moody integrin in a changing environment. Curr Opin Cell Biol *20*, 514-519.

Honore, P., Luger, N.M., Sabino, M.A., Schwei, M.J., Rogers, S.D., Mach, D.B., O'Keefe P, F., Ramnaraine, M.L., Clohisy, D.R., and Mantyh, P.W. (2000). Osteoprotegerin blocks bone cancer-induced skeletal destruction, skeletal pain and pain-related neurochemical reorganization of the spinal cord. Nat Med *6*, 521-528.

Hood, J.D., and Cheresh, D.A. (2002). Role of integrins in cell invasion and migration. Nat Rev Cancer *2*, 91-100.

Hynes, R.O. (1992). Integrins: versatility, modulation, and signaling in cell adhesion. Cell *69*, 11-25.

Hynes, R.O. (2002). Integrins: bidirectional, allosteric signaling machines. Cell *110*, 673-687.

Isenberg, J.S., Hyodo, F., Matsumoto, K., Romeo, M.J., Abu-Asab, M., Tsokos, M., Kuppusamy, P., Wink, D.A., Krishna, M.C., and Roberts, D.D. (2007a). Thrombospondin-1 limits ischemic tissue survival by inhibiting nitric oxide-mediated vascular smooth muscle relaxation. Blood *109*, 1945-1952.

Isenberg, J.S., Jia, Y., Fukuyama, J., Switzer, C.H., Wink, D.A., and Roberts, D.D. (2007b). Thrombospondin-1 inhibits nitric oxide signaling via CD36 by inhibiting myristic acid uptake. J Biol Chem *282*, 15404-15415.

Isenberg, J.S., Ridnour, L.A., Dimitry, J., Frazier, W.A., Wink, D.A., and Roberts, D.D. (2006). CD47 is necessary for inhibition of nitric oxide-stimulated vascular cell responses by thrombospondin-1. J Biol Chem *281*, 26069-26080.

Isenberg, J.S., Ridnour, L.A., Perruccio, E.M., Espey, M.G., Wink, D.A., and Roberts, D.D. (2005). Thrombospondin-1 inhibits endothelial cell responses to nitric oxide in a cGMP-dependent manner. Proc Natl Acad Sci U S A *102*, 13141-13146.

Jain, M., Ascensao, J., and Schechter, G.P. (2009). Familial myeloma and monoclonal gammopathy: a report of eight African American families. American journal of hematology *84*, 34-38.

John, A.S., Rothman, V.L., and Tuszynski, G.P. (2010). Thrombospondin-1 (TSP-1) Stimulates Expression of Integrin alpha6 in Human Breast Carcinoma Cells: A Downstream Modulator of TSP-1-Induced Cellular Adhesion. J Oncol *2010*, 645376.

Kakonen, S.M., Selander, K.S., Chirgwin, J.M., Yin, J.J., Burns, S., Rankin, W.A., Grubbs, B.G., Dallas, M., Cui, Y., and Guise, T.A. (2002). Transforming growth factor-beta stimulates parathyroid hormone-related protein and osteolytic metastases via Smad and mitogen-activated protein kinase signaling pathways. J Biol Chem *277*, 24571-24578.

Kang, Y., Siegel, P.M., Shu, W., Drobnjak, M., Kakonen, S.M., Cordon-Cardo, C., Guise, T.A., and Massague, J. (2003). A multigenic program mediating breast cancer metastasis to bone. Cancer Cell *3*, 537-549.

Kannus, P., Jozsa, L., Jarvinen, T.A., Jarvinen, T.L., Kvist, M., Natri, A., and Jarvinen, M. (1998). Location and distribution of non-collagenous matrix proteins in musculoskeletal tissues of rat. The Histochemical journal *30*, 799-810.

Kazerounian, S., Yee, K.O., and Lawler, J. (2008). Thrombospondins in cancer. Cell Mol Life Sci *65*, 700-712.

Kevorkova, O., Martineau, C., Martin-Falstrault, L., Sanchez-Dardon, J., Brissette, L., and Moreau, R. (2013). Low-Bone-Mass Phenotype of Deficient Mice for the Cluster of Differentiation 36 (CD36). PloS one *8*, e77701.

Kim, J., Denu, R.A., Dollar, B.A., Escalante, L.E., Kuether, J.P., Callander, N.S., Asimakopoulos, F., and Hematti, P. (2012). Macrophages and mesenchymal stromal cells support survival and proliferation of multiple myeloma cells. British journal of haematology *158*, 336-346.

Kingsley, L.A., Fournier, P.G., Chirgwin, J.M., and Guise, T.A. (2007). Molecular biology of bone metastasis. Mol Cancer Ther *6*, 2609-2617.

Koskinen, C., Persson, E., Baldock, P., Stenberg, A., Bostrom, I., Matozaki, T., Oldenborg, P.A., and Lundberg, P. (2013). Lack of CD47 impairs bone cell differentiation and results in an osteopenic phenotype in vivo due to impaired signal regulatory protein alpha (SIRPalpha) signaling. J Biol Chem *288*, 29333-29344.

Kozlow, W., and Guise, T.A. (2005). Breast cancer metastasis to bone: mechanisms of osteolysis and implications for therapy. J Mammary Gland Biol Neoplasia *10*, 169-180.

Kuehl, W.M., and Bergsagel, P.L. (2002). Multiple myeloma: evolving genetic events and host interactions. Nat Rev Cancer *2*, 175-187.

Kukreja, A., Radfar, S., Sun, B.H., Insogna, K., and Dhodapkar, M.V. (2009). Dominant role of CD47-thrombospondin-1 interactions in myeloma-induced fusion of human dendritic cells: implications for bone disease. Blood *114*, 3413-3421.

Kumar, S.K., Dispenzieri, A., Lacy, M.Q., Gertz, M.A., Buadi, F.K., Pandey, S., Kapoor, P., Dingli, D., Hayman, S.R., Leung, N.*, et al.* (2013). Continued improvement in survival in multiple myeloma: changes in early mortality and outcomes in older patients. Leukemia.

Kyle, R.A., Durie, B.G., Rajkumar, S.V., Landgren, O., Blade, J., Merlini, G., Kroger, N., Einsele, H., Vesole, D.H., Dimopoulos, M.*, et al.* (2010). Monoclonal gammopathy of undetermined significance (MGUS) and smoldering (asymptomatic) multiple myeloma: IMWG consensus perspectives risk factors for progression and guidelines for monitoring and management. Leukemia *24*, 1121-1127.

Kyle, R.A., Therneau, T.M., Rajkumar, S.V., Larson, D.R., Plevak, M.F., and Melton, L.J., 3rd (2004). Long-term follow-up of 241 patients with monoclonal gammopathy of undetermined significance: the original Mayo Clinic series 25 years later. Mayo Clinic proceedings *79*, 859-866.

Kyle, R.A., Therneau, T.M., Rajkumar, S.V., Larson, D.R., Plevak, M.F., Offord, J.R., Dispenzieri, A., Katzmann, J.A., and Melton, L.J., 3rd (2006). Prevalence of monoclonal gammopathy of undetermined significance. N Engl J Med *354*, 1362-1369.

Landgren, O., Gridley, G., Turesson, I., Caporaso, N.E., Goldin, L.R., Baris, D., Fears, T.R., Hoover, R.N., and Linet, M.S. (2006). Risk of monoclonal gammopathy of undetermined significance (MGUS) and subsequent multiple myeloma among African American and white veterans in the United States. Blood *107*, 904-906.

Landgren, O., Kyle, R.A., Pfeiffer, R.M., Katzmann, J.A., Caporaso, N.E., Hayes, R.B., Dispenzieri, A., Kumar, S., Clark, R.J., Baris, D.*, et al.* (2009). Monoclonal gammopathy of undetermined significance (MGUS) consistently precedes multiple myeloma: a prospective study. Blood *113*, 5412-5417.

Lau, H.K. (2003). Cytotoxicity of nitric oxide donors in smooth muscle cells is dependent on phenotype, and mainly due to apoptosis. Atherosclerosis *166*, 223-232.

Liapis, H., Flath, A., and Kitazawa, S. (1996). Integrin alpha V beta 3 expression by bone-residing breast cancer metastases. Diagn Mol Pathol *5*, 127-135.

Lindberg, F.P., Gresham, H.D., Reinhold, M.I., and Brown, E.J. (1996). Integrin-associated protein immunoglobulin domain is necessary for efficient vitronectin bead binding. J Cell Biol *134*, 1313-1322.

Lipton, A. (2004). Pathophysiology of bone metastases: how this knowledge may lead to therapeutic intervention. J Support Oncol *2*, 205-213; discussion 213-204, 216-207, 219-220.

Lipton, A., Costa, L., Ali, S., and Demers, L. (2001). Use of markers of bone turnover for monitoring bone metastases and the response to therapy. Semin Oncol *28*, 54-59.

Lundberg, P., Koskinen, C., Baldock, P.A., Lothgren, H., Stenberg, A., Lerner, U.H., and Oldenborg, P.A. (2007). Osteoclast formation is strongly reduced both in vivo and in vitro in the absence of CD47/SIRPalpha-interaction. Biochem Biophys Res Commun *352*, 444-448.

Marcellini, M., De Luca, N., Riccioni, T., Ciucci, A., Orecchia, A., Lacal, P.M., Ruffini, F., Pesce, M., Cianfarani, F., Zambruno, G.*, et al.* (2006). Increased melanoma growth and metastasis spreading in mice overexpressing placenta growth factor. Am J Pathol *169*, 643-654.

Martin, K.H., Slack, J.K., Boerner, S.A., Martin, C.C., and Parsons, J.T. (2002). Integrin connections map: to infinity and beyond. Science *296*, 1652-1653.

McHugh, K.P. (2000). Mice lacking b3 integrins are osteosclerotic because of dysfunctional osteoclasts. Journal of Clinical Investigation *105*, 433-440.

Melton, L.J., 3rd, Kyle, R.A., Achenbach, S.J., Oberg, A.L., and Rajkumar, S.V. (2005). Fracture risk with multiple myeloma: a population-based study. J Bone Miner Res *20*, 487-493.

Morgan, E.A., Schneider, J., T., B., Uluckan, O., Heller, E.A., Hurchla, M.A., Deng, H., Floyd, D.H., Berdy, A., Prior, J.L.*, et al.* (2009). Dissection of platelet and myeloid cell defects by conditional targeting of the β3 integrin subunit. FASEB *in press*.

Mundy, G.R. (2002). Metastasis to bone: causes, consequences and therapeutic opportunities. Nat Rev Cancer *2*, 584-593.

Nakamura, I., Duong le, T., Rodan, S.B., and Rodan, G.A. (2007). Involvement of alpha(v)beta3 integrins in osteoclast function. J Bone Miner Metab *25*, 337-344.

Ng, A.C., Khosla, S., Charatcharoenwitthaya, N., Kumar, S.K., Achenbach, S.J., Holets, M.F., McCready, L.K., Melton, L.J., 3rd, Kyle, R.A., Rajkumar, S.V.*, et al.* (2011). Bone microstructural changes revealed by high-resolution peripheral quantitative computed tomography imaging and elevated DKK1 and MIP-1alpha levels in patients with MGUS. Blood *118*, 6529-6534.

Novack, D.V., and Teitelbaum, S.L. (2008). The osteoclast: friend or foe? Annu Rev Pathol *3*, 457-484.

Offermanns, S. (2006). Activation of platelet function through G protein-coupled receptors. Circ Res *99*, 1293-1304.

Oyajobi, B.O., Franchin, G., Williams, P.J., Pulkrabek, D., Gupta, A., Munoz, S., Grubbs, B., Zhao, M., Chen, D., Sherry, B.*, et al.* (2003). Dual effects of macrophage inflammatory protein-1alpha on osteolysis and tumor burden in the murine 5TGM1 model of myeloma bone disease. Blood *102*, 311-319.

Paget, S. (1889). The distribution of secondary growths in cancer of the breast. 1889. Cancer metastasis reviews *8*, 98-101.

Pecheur, I., Peyruchaud, O., Serre, C.M., Guglielmi, J., Voland, C., Bourre, F., Margue, C., Cohen-Solal, M., Buffet, A., Kieffer, N.*, et al.* (2002). Integrin alpha(v)beta3 expression confers on tumor cells a greater propensity to metastasize to bone. FASEB J *16*, 1266-1268.

Pfeilschifter, J., D'Souza, S.M., and Mundy, G.R. (1987). Effects of transforming growth factor-beta on osteoblastic osteosarcoma cells. Endocrinology *121*, 212-218.

Posey, K.L., Hankenson, K., Veerisetty, A.C., Bornstein, P., Lawler, J., and Hecht, J.T. (2008). Skeletal abnormalities in mice lacking extracellular matrix proteins, thrombospondin-1, thrombospondin-3, thrombospondin-5, and type IX collagen. Am J Pathol *172*, 1664-1674.

Puzas, J.E. (1996). Osteoblast Cell Biology -- Lineage and Function. In Primer on the Metabolic Bone Diseases and Disorders of Mineral Metabolism, M.J. Favus, ed. (New York: Lippincott-Raven Publishers).

Qin, J., Vinogradova, O., and Plow, E.F. (2004). Integrin bidirectional signaling: a molecular view. PLoS Biol *2*, e169.

Radl, J., and Hollander, C.F. (1974). Homogeneous immunoglobulins in sera of mice during aging. J Immunol *112*, 2271-2273.

Radl, J., Hollander, C.F., van den Berg, P., and de Glopper, E. (1978). Idiopathic paraproteinaemia. I. Studies in an animal model--the ageing C57BL/KaLwRij mouse. Clinical and experimental immunology *33*, 395-402.

Reynolds, A.R., Hart, I.R., Watson, A.R., Welti, J.C., Silva, R.G., Robinson, S.D., Da Violante, G., Gourlaouen, M., Salih, M., Jones, M.C.*, et al.* (2009). Stimulation of tumor growth and angiogenesis by low concentrations of RGD-mimetic integrin inhibitors. Nat Med *15*, 392-400.

Reynolds, L.E., Wyder, L., Lively, J.C., Taverna, D., Robinson, S.D., Huang, X., Sheppard, D., Hynes, R.O., and Hodivala-Dilke, K.M. (2002). Enhanced pathological angiogenesis in mice lacking beta3 integrin or beta3 and beta5 integrins. Nat Med *8*, 27-34.

Ribatti, D., Moschetta, M., and Vacca, A. (2013). Macrophages in multiple myeloma. Immunology letters.

Ribatti, D., Nico, B., and Vacca, A. (2006). Importance of the bone marrow microenvironment in inducing the angiogenic response in multiple myeloma. Oncogene *25*, 4257-4266.

Ridnour, L.A., Isenberg, J.S., Espey, M.G., Thomas, D.D., Roberts, D.D., and Wink, D.A. (2005). Nitric oxide regulates angiogenesis through a functional switch involving thrombospondin-1. Proc Natl Acad Sci U S A *102*, 13147-13152.

Ridnour, L.A., Thomas, D.D., Donzelli, S., Espey, M.G., Roberts, D.D., Wink, D.A., and Isenberg, J.S. (2006). The biphasic nature of nitric oxide responses in tumor biology. Antioxid Redox Signal *8*, 1329-1337.

Robey, P.G., Young, M.F., Fisher, L.W., and McClain, T.D. (1989). Thrombospondin is an osteoblast-derived component of mineralized extracellular matrix. J Cell Biol *108*, 719-727.

Rodriguez-Manzaneque, J.C., Lane, T.F., Ortega, M.A., Hynes, R.O., Lawler, J., and Iruela-Arispe, M.L. (2001). Thrombospondin-1 suppresses spontaneous tumor growth and inhibits activation of matrix metalloproteinase-9 and mobilization of vascular endothelial growth factor. Proc Natl Acad Sci U S A *98*, 12485-12490.

Roodman, G.D. (2004). Mechanisms of bone metastasis. N Engl J Med *350*, 1655-1664.

Ross, F.P., Chappel, J., Alvarez, J.I., Sander, D., Butler, W.T., Farach-Carson, M.C., Mintz, K.A., Robey, P.G., Teitelbaum, S.L., and Cheresh, D.A. (1993). Interactions between the bone matrix proteins osteopontin and bone sialoprotein and the osteoclast integrin alpha v beta 3 potentiate bone resorption. J Biol Chem *268*, 9901-9907.

Roy, B., and Garthwaite, J. (2006). Nitric oxide activation of guanylyl cyclase in cells revisited. Proc Natl Acad Sci U S A *103*, 12185-12190.

Rucci, N., DiGiacinto, C., Orru, L., Millimaggi, D., Baron, R., and Teti, A. (2005). A novel protein kinase C alpha-dependent signal to ERK1/2 activated by alphaVbeta3 integrin in osteoclasts and in Chinese hamster ovary (CHO) cells. J Cell Sci *118*, 3263-3275.

Scavelli, C., Nico, B., Cirulli, T., Ria, R., Di Pietro, G., Mangieri, D., Bacigalupo, A., Mangialardi, G., Coluccia, A.M., Caravita, T.*, et al.* (2008). Vasculogenic mimicry by bone marrow macrophages in patients with multiple myeloma. Oncogene *27*, 663-674.

Schneider, J.G., Amend, S.R., and Weilbaecher, K.N. (2011). Integrins and bone metastasis: integrating tumor cell and stromal cell interactions. Bone *48*, 54-65.

Schwartz, M.A., Schaller, M.D., and Ginsberg, M.H. (1995). Integrins: emerging paradigms of signal transduction. Annu Rev Cell Dev Biol *11*, 549-599.

Shattil, S.J., Kim, C., and Ginsberg, M.H. (2010). The final steps of integrin activation: the end game. Nat Rev Mol Cell Biol *11*, 288-300.

Silva, R., D'Amico, G., Hodivala-Dilke, K.M., and Reynolds, L.E. (2008). Integrins: the keys to unlocking angiogenesis. Arterioscler Thromb Vasc Biol *28*, 1703-1713.

Sirohi, B., and Powles, R. (2006). Epidemiology and outcomes research for MGUS, myeloma and amyloidosis. Eur J Cancer *42*, 1671-1683.

Sloan, E.K., Pouliot, N., Stanley, K.L., Chia, J., Moseley, J.M., Hards, D.K., and Anderson, R.L. (2006). Tumor-specific expression of alphavbeta3 integrin promotes spontaneous metastasis of breast cancer to bone. Breast Cancer Res *8*, R20.

Steri, V., Ellison, T.S., Gontarczyk, A.M., Weilbaecher, K., Schneider, J.G., Edwards, D., Fruttiger, M., Hodivala-Dilke, K.M., and Robinson, S.D. (2014). Acute depletion of endothelial beta3-integrin transiently inhibits tumor growth and angiogenesis in mice. Circ Res *114*, 79-91.

Stupack, D.G., and Cheresh, D.A. (2004). Integrins and angiogenesis. Curr Top Dev Biol *64*, 207-238.

Teitelbaum, S.L., and Ross, F.P. (2003). Genetic regulation of osteoclast development and function. Nat Rev Genet *4*, 638-649.

Terpos, E., Sezer, O., Croucher, P., and Dimopoulos, M.A. (2007). Myeloma bone disease and proteasome inhibition therapies. Blood *110*, 1098-1104.

Thomas, D.D., Ridnour, L.A., Isenberg, J.S., Flores-Santana, W., Switzer, C.H., Donzelli, S., Hussain, P., Vecoli, C., Paolocci, N., Ambs, S.*, et al.* (2008). The chemical biology of nitric oxide: implications in cellular signaling. Free Radic Biol Med *45*, 18-31.

Tsutsui, M. (2004). Neuronal nitric oxide synthase as a novel anti-atherogenic factor. J Atheroscler Thromb *11*, 41-48.

Tuszynski, G.P., Gasic, T.B., Rothman, V.L., Knudsen, K.A., and Gasic, G.J. (1987). Thrombospondin, a potentiator of tumor cell metastasis. Cancer Res *47*, 4130-4133.

Ueno, A., Miwa, Y., Miyoshi, K., Horiguchi, T., Inoue, H., Ruspita, I., Abe, K., Yamashita, K., Hayashi, E., and Noma, T. (2006). Constitutive expression of thrombospondin 1 in MC3T3-E1 osteoblastic cells inhibits mineralization. J Cell Physiol *209*, 322-332.

Uluckan, O., Becker, S.N., Deng, H., Zou, W., Prior, J.L., Piwnica-Worms, D., Frazier, W.A., and Weilbaecher, K.N. (2009). CD47 regulates bone mass and tumor metastasis to bone. Cancer Res *69*, 3196-3204.

Vacca, A., and Ribatti, D. (2011). Angiogenesis and vasculogenesis in multiple myeloma: role of inflammatory cells. Recent results in cancer research Fortschritte der Krebsforschung Progres dans les recherches sur le cancer *183*, 87-95.

Vachon, C.M., Kyle, R.A., Therneau, T.M., Foreman, B.J., Larson, D.R., Colby, C.L., Phelps, T.K., Dispenzieri, A., Kumar, S.K., Katzmann, J.A.*, et al.* (2009). Increased risk of monoclonal gammopathy in first-degree relatives of patients with multiple myeloma or monoclonal gammopathy of undetermined significance. Blood *114*, 785-790.

Van der Velde-Zimmermann, D., Verdaasdonk, M.A., Rademakers, L.H., De Weger, R.A., Van den Tweel, J.G., and Joling, P. (1997). Fibronectin distribution in human bone marrow stroma: matrix assembly and tumor cell adhesion via alpha5 beta1 integrin. Exp Cell Res *230*, 111-120.

Vanderkerken, K., Asosingh, K., Croucher, P., and Van Camp, B. (2003). Multiple myeloma biology: lessons from the 5TMM models. Immunol Rev *194*, 196-206.

Vignery, A. (2005). Macrophage fusion: are somatic and cancer cells possible partners? Trends Cell Biol *15*, 188-193.

Wang, X.Q., Sun, P., and Paller, A.S. (2001). Inhibition of integrin-linked kinase/protein kinase B/Akt signaling: mechanism for ganglioside-induced apoptosis. J Biol Chem *276*, 44504-44511.

Wei, S.C., Tsao, P.N., Yu, S.C., Shun, C.T., Tsai-Wu, J.J., Wu, C.H., Su, Y.N., Hsieh, F.J., and Wong, J.M. (2005). Placenta growth factor expression is correlated with survival of patients with colorectal cancer. Gut *54*, 666-672.

Weilbaecher, K.N., Guise, T.A., and McCauley, L.K. (2011). Cancer to bone: a fatal attraction. Nat Rev Cancer *11*, 411-425.

Weinhold, N., Johnson, D.C., Rawstron, A.C., Forsti, A., Doughty, C., Vijayakrishnan, J., Broderick, P., Dahir, N.B., Begum, D.B., Hosking, F.J.*, et al.* (2014). Inherited genetic susceptibility to monoclonal gammopathy of unknown significance. Blood *123*, 2513-2517.

Yaccoby, S. (2010). Osteoblastogenesis and tumor growth in myeloma. Leukemia & lymphoma *51*, 213-220.

Yin, J.J., Selander, K., Chirgwin, J.M., Dallas, M., Grubbs, B.G., Wieser, R., Massague, J., Mundy, G.R., and Guise, T.A. (1999). TGF-beta signaling blockade inhibits PTHrP secretion by breast cancer cells and bone metastases development. J Clin Invest *103*, 197-206.

Yoneda, T. (2000). Cellular and molecular basis of preferential metastasis of breast cancer to bone. J Orthop Sci *5*, 75-81.

Zambonin Zallone, A., Teti, A., Gaboli, M., and Marchisio, P.C. (1989). Beta 3 subunit of vitronectin receptor is present in osteoclast adhesion structures and not in other monocyte-macrophage derived cells. Connect Tissue Res *20*, 143-149.

Zhang, Z., Baron, R., and Horne, W.C. (2000). Integrin engagement, the actin cytoskeleton, and c-Src are required for the calcitonin-induced tyrosine phosphorylation of paxillin and HEF1, but not for calcitonin-induced Erk1/2 phosphorylation. J Biol Chem *275*, 37219-37223.

Zhao, H., Ross, F.P., and Teitelbaum, S.L. (2005). Unoccupied alpha(v)beta3 integrin regulates osteoclast apoptosis by transmitting a positive death signal. Mol Endocrinol *19*, 771-780.

Zhao, Y., Bachelier, R., Treilleux, I., Pujuguet, P., Peyruchaud, O., Baron, R., Clement-Lacroix, P., and Clezardin, P. (2007). Tumor alphavbeta3 integrin is a therapeutic target for breast cancer bone metastases. Cancer Res *67*, 5821-5830.

Zheng, H., Yu, X., Collin-Osdoby, P., and Osdoby, P. (2006). RANKL stimulates inducible nitric-oxide synthase expression and nitric oxide production in developing osteoclasts. An autocrine negative feedback mechanism triggered by RANKL-induced interferon-beta via NF-kappaB that restrains osteoclastogenesis and bone resorption. J Biol Chem *281*, 15809-15820.

Zheng, Y., Cai, Z., Wang, S., Zhang, X., Qian, J., Hong, S., Li, H., Wang, M., Yang, J., and Yi, Q. (2009). Macrophages are an abundant component of myeloma microenvironment and protect myeloma cells from chemotherapy drug-induced apoptosis. Blood *114*, 3625-3628.

Zingone, A., and Kuehl, W.M. (2011). Pathogenesis of monoclonal gammopathy of undetermined significance and progression to multiple myeloma. Seminars in hematology *48*, 4-12.

Chapter 2

Thrombospondin-1 regulates bone homeostasis through effects on bone matrix integrity and nitric oxide signaling in osteoclasts

Abstract

Thrombospondin-1 (TSP1), an endogenous antiangiogenic, is a widely expressed secreted ligand with roles in migration, adhesion and proliferation and is a target for new therapeutics. While TSP1 is present in the bone matrix and several TSP1 receptors play roles in bone biology, the role of TSP1 in bone remodeling has not been fully elucidated. Bone turnover is characterized by coordinated activity of bone-forming osteoblasts (OB) and bone-resorbing osteoclasts (OC). TSP1-/- mice had increased bone mass and increased cortical bone size and thickness compared to wild type (WT). However, despite increased size, TSP1-/- femurs showed less resistance to bending than expected, indicative of diminished bone quality and a bone material defect. Additionally, we found that TSP1 deficiency resulted in decreased OC activity in vivo and reduced OC differentiation. TSP1 was critical during early osteoclastogenesis, and TSP1 deficiency resulted in a substantial overexpression of inducible nitric oxide synthase (iNOS). Importantly, administration of a NOS inhibitor rescued the OC functional defects of TSP1-/- mice in vivo. To investigate the role of bone-derived TSP1 in osteoclastogenesis, we found that wild type (WT) pre-OCs had defective iNOS expression when cultured on TSP1-/- bone compared to WT bone, suggesting that TSP1 in bone plays a critical role in iNOS signaling during OC development. These data implicate a new role for TSP1 in bone homeostasis with roles in maintaining bone matrix integrity and regulating OC formation. It will be critical to monitor bone health of patients administered TSP1-pathway directed therapeutics in clinical use and under development.

Introduction

      Bone is a dynamic tissue, characterized by balanced bone resorption and formation. This bone remodeling is necessary to preserve the structural integrity of the skeleton and to maintain calcium and phosphate homeostasis (Baron, 1996; Hadjidakis and Androulakis, 2006). Bone is a matrix composed of two compartments: osteoid (primarily collagen type I fibers) and mineral (calcium-phosphate hydroxyapatite crystals). The bone matrix also contains numerous noncollagenous proteins including growth factors, proteoglycans, and adhesion molecules. These molecules contribute to maintenance of homeostatic bone remodeling, promoting cell attachment, differentiation, and growth of bone remodeling cells. In addition, some molecules aid in osteoid and mineral matrix organization, directly influencing bone strength.

      Mesenchymal osteoblasts (OBs) form bone by depositing collagen and other molecules to form osteoid and subsequently calcify this matrix to form rigid bone. Osteoclasts (OCs), polarized multi-nucleated hematopoietic cells formed from the fusion of macrophages, resorb bone through protease- and acid-dependent processes. The formation and activity of OCs and OBs is a tightly coupled process. OCs are activated by OB-derived cytokines such as M-CSF and RANK-L. In turn, OCs promote osteoblastic bone formation by releasing stored growth factors including bone morphogenic proteins, TGFβ, and insulin growth factor from the bone matrix. Misregulation of healthy bone remodeling, as in cancer metastasis, arthritis, or osteoporosis, leads to decreased bone integrity, pathologic fracture, nerve-compression syndromes, and hypercalcemia (Weilbaecher et al., 2011). While many factors that individually regulate OC and OB formation and activity have been identified, our understanding of the role of OB-deposited bone matrix-sequestered proteins in homeostatic OC activity remains incomplete.

Thrombospondin-1 (TSP1) is a large secreted protein that binds at least 11 distinct receptors, including β3 integrin, CD47, and CD36, thereby influencing downstream pathways. By regulating migration, adhesion and proliferation, TSP1 participates in diverse processes including angiogenesis, inflammation, and wound healing. TSP1 was the first identified endogenous antiangiogenic molecule, and TSP1 mimetics have entered clinical trials as cancer therapeutics (Taraboletti et al., 2010). Antibodies against the TSP1 receptor CD47, used to induce macrophage phagocytosis of cancer cells, have completed pre-clinical studies(Tseng et al., 2013; Weiskopf et al., 2013), and a humanized antibody is under clinical development. In addition, nitric oxide (NO) signaling, a pathway regulated by TSP1, is being therapeutically targeted for vasodilation (NO donors) or hypotension (NO synthase inhibitors)(Deshpande et al., 2012). As these TSP1 pathway-targeted therapies enter broad clinical use, it is important to consider the action of TSP1 in other systems, including the skeleton, where TSP1 receptors CD47, β3 integrin, and CD36 (Faccio et al., 2003b; Kevorkova et al., 2013; Koskinen et al., 2013; McHugh et al., 2000; Schneider et al., 2011; Uluckan et al., 2009) are involved in OC and OB signaling. Bone-related off-target effects will be especially crucial to consider in advanced cancer patients at risk for skeletal metastasis and post-menopausal women who are at risk for osteoporosis.

TSP1 deficient mice are reported to have mild spine deformation (Crawford et al., 1998) and mild growth plate cartilage disorganization (Posey et al., 2008) in addition to enhanced angiogenesis (Smadja et al., 2011) but detailed analysis of bone has not been reported. TSP1 is expressed by OBs and is present in osteoid and mineralized bone matrix (Grzesik and Robey, 1994; Kannus et al., 1998; Robey et al., 1989) where it is directly deposited by bone-forming OBs (Clezardin et al., 1989; Robey et al., 1989). TSP1 is involved in OB differentiation in part

through activation of latent TGF-β (Bailey Dubose et al., 2012; Ueno et al., 2006), and TSP1 receptors CD47 and CD36 also regulate OB (Kevorkova et al., 2013; Koskinen et al., 2013). TSP1 is a regulator of nitric oxide (NO) in endothelial cells, platelets, and vascular smooth muscle cells (Chen et al., 2000; Isenberg et al., 2009), but only receptors CD36 and CD47 have been implicated in NO regulation (Isenberg et al., 2009; Isenberg et al., 2006; Isenberg et al., 2005). TSP1 has been implicated in OC activity, but its mechanism of action remains unknown (Carron et al., 1995). TSP1-CD47 interactions play a role in the formation of multiple myeloma-dendritic cell fusions with bone-resorbing capacity (Kukreja et al., 2009), and TSP1-CD36 ligation can promote osteoclastic resorption on dentine slices (Carron et al., 2000). CD47-/- mice have a bone resorption defect (Koskinen et al., 2013; Lundberg et al., 2007; Uluckan et al., 2009), which we have shown is due to increased iNOS in OCs (Uluckan et al., 2009). Together these data led us to hypothesize that OB-secreted TSP1 sequestered in bone matrix will modulate OC function thereby coupling OB activity to OC formation.

In this study, we describe the role of bone-sequestered TSP1 in the maintenance of bone homeostasis, both as a structural protein contributing to bone strength and as a signaling ligand promoting OC formation. Here we have used mice genetically deficient in TSP1 and neutralizing anti-TSP1 antibody to investigate the role of TSP1 in bone homeostasis. Together, these data implicate a novel role for TSP1 in bone homeostasis, both in mediating bone matrix integrity and by regulating OC formation as a matrix-derived paracrine signaling molecule. Our findings provide an important rationale to monitor the effects on bone health of TSP1 pathway-directed therapeutics, currently in clinical use and under development, especially in patients affected by bone pathology such as osteoporosis and skeletal metastasis.

Materials and Methods

Animals

TSP1-/- mice were originally obtained from Jack Lawler (Lawler et al., 1998) and backcrossed over 20 times to C57BL/6J. TSP1-/- and TSP1+/+ mice were housed in shared pathogen-free conditions according to the guidelines of the Division of Comparative Medicine, Washington University School of Medicine. The animal ethics committee approved all experiments.

Reagents

Anti-TSP1 function blocking antibody, clone A4.1 (IgM, mouse anti-human)(Annis et al., 2006) was purchased from Thermo Scientific (Waltham, MA). TSP1 is highly conserved among species and clone A4.1 has cross-species reactivity with mouse and bovine TSP1. IgM istoype control was purchased from eBioscience (San Diego, CA).

Micro-computed tomography

Tibiae and femurs from TSP1-/- and WT sex-matched mice were suspended in agarose and tibial metaphyses and femoral mid-diaphysis were scanned by micro-computed tomography (uCT-40; Scanco Medical) as described previously (Heller et al., 2012; Uluckan et al., 2009). For image acquisition, the long bones were placed in a 13-mm holder and scanned. The cancellous region was selected using contours inside the cortical shell on each 2d image. The growth plate was used as a marker to determine a consistent location to start analysis and 40 slices were analyzed. A 3-dimentional cubical voxel model of bone was built and calculations made: relative trabecular bone volume over total volume, trabecular number, and trabecular spacing. The cortical region was selected using contours outside the cortical shell at the mid-diaphysis and 50 slices were analyzed. The average cross-sectional geometry measurements were calculated for

cortical thickness and total cross-sectional area. The bending moment of inertia was determined using standard engineering parallel-axis theory as previously described (Brodt et al., 1999; Silva et al., 2006).

Bone biomechanics

Immediately following dissection, femurs were frozen at -20°C for a minimum of 12 hours. Femurs were thawed in phosphate-buffered saline for 1 h prior to use, and testing was carried out at room temperature using a servohydraulic testing machine (8841 Dynamite, Instron, Norwood, MA). Femurs were positioned on two supports 7 mm apart, and the central loading point was the mid-diaphysis. Displacement was applied transverse to the long axis of the bone at a rate of 0.03 mm/s until failure. Force-displacement data were recorded at 60 Hz and analyzed to determine stiffness (a measure of elastic resistance to bending), yield force (a measure of the force required to permanently deform the bone), ultimate force (the highest force attained prior to failure), post-yield displacement (a measure of ductility) and energy-to-fracture (a measure of overall resistance to fracture) (Brodt et al., 1999; Silva et al., 2006). Estimated material properties (elastic modulus, yield stress, ultimate stress) were calculated using standard engineering beam theory that normalizes for bone size.

Reference point indentation

Femurs were subjected to reference point indentation as previously described (Randall et al., 2009). A 25 μm testing probe was placed on the cortical bone surface and a preload force of 0.1N and a waveform of 10 cycles of 2N force was applied as a frequency of 2 Hz (Biodent, Active Life Sciences, Santa Barbara, CA). Each bone was subjected to 3 indents 1 mm apart. Measurements were made for each indent: initial indentation distance and indentation distance increase (cycle 1 – cycle 10).

Serum CTX assay

Carboxy-terminal telopeptide collagen crosslinks (CTX) was measured in the serum of overnight fasted mice by ELISA (RatLaps; Immunodiagnostic Systems, Scottsdale, AZ) according to the manufacturer's instructions.

Serum P1NP assay

N-terminal propeptide of type I procollagen (P1NP) was measured in serum of overnight fasted mice using ELISA (Immunadiagnostic Systems, Scottsdale, AZ) according to the manufacturer's instructions.

L-NAME administration

L-NAME (Sigma Aldrich, St. Louis, MO) was administered in the drinking water of 8 week old mice for 6 weeks, changed every 2 days (40 mg/kg/day).

In vitro osteoclast differentiation

To generate macrophages, whole bone marrow cells were cultured in αMEM, 10% FBS, 1% penicillin-streptomycin, 100 ng/ml MCSF for 3 days as previously described (Morgan et al., 2010). To generate OCs, $9x10^4$/ml were plated on plastic or bone powder as indicated and cultured in αMEM, 10% FBS (on plastic), 1% penicillin-streptomycin, 50 ng/ml MCSF, 50 ng/ml RANKL, refed every 48 hours. Where indicated, macrophages were cultured with 5 μg/ml antibody. TRAP staining was performed according to the manufacturer's instructions (Sigma-Aldrich, St. Louis, MO).

In vitro osteoblast differentiation

To generate bone marrow stromal cells (BMSCs), whole bone marrow cells were cultured in ascorbic-acid free αMEM, 10% FBS, 1% penicillin-streptomycin for 7 days. For OB differentiation, $2x10^5$ BMSC/ml were cultured in αMEM, 10% FBS, 1% penicillin-streptomycin,

10 mM β-glycerophosphate, 50 ug/ml ascorbic acid for 14 days, refed every 7 days. Cultures were fixed in 10% neutral buffered formalin and stained with Alkaline Phosphatase (Fast Blue RR salt, Sigma Aldrich) and 0.4% Alizarin Red. Chromogenic alkaline phosphatase was quantitated according to manufacturer's instructions (Sigma-Aldrich, St. Louis, MO). Alizarin red stain was measured using the Osteogenesis Quantitation Kit according to manufacturer's instructions (Millipore, Billerica, MA).

Bone powder coated plates

Plates were coated with bone powder as previously described(Cremasco et al., 2012) with modifications. Bone marrow was flushed from the long bones of WT and TSP1-/- mice, and the bones were frozen at $-20^{O}C$. Frozen bones were crushed to powder using a Bullet Blender Bead Lysis Kit (Midsci, St. Louis, MO), and the powder was washed 3 times in 70% ethanol. Plates were coated with 1:20 bone powder:PBS + 4 ug/ml poly-l-lysine for 4 hours at $68^{O}C$. Plates were sterilized under UV light and experiments completed as described.

Quantitative reverse-transcription PCR

RNA was extracted using RNeasy Mini kit (Qiagen, Venlo, Netherlands) and cDNA generated using iScript (Bio-Rad, Hercules, CA). Quantitative PCR was completed using SsoFast EVA Green Supermix (Bio-Rad, Hercules, CA).

qRT-PCR primer sequences (forward/reverse)

NFATc1:

GGTAACTCTGTCTTTCTAACCTTAAGC / GTGATGACCCCAGCATGCACCAGTCA

DC-STAMP: ACAAACAGTTCCAAAGCTTGC / TCCTTGGGTTCCTTGCTTC

TRAP: CAGCTGTCCTGGCTCAAAA / ACATAGCCCACACCGTTCTC

β3 integrin: TGGTGCTCAGATGAGACTTTGTC / GACTCTGGAGCACAATTGTCCTT

Cathepsin K: GAGGGCCAACTCAAGAAGAA / GCCGTGGCGTTATACATACA

iNOS: GGCAGCCTGTGAGACCTTTG / GCATTGGAAGTGAAGCGTTTC

cyclophilin: AGCATACAGGTCCTGGCATC / TTCACCTTCCCAAAGACCAC

In vivo calcein labeling

Calcein labeling was completed as previously described (Su et al., 2012). Briefly, mice were injected 8 and 2 days prior to sacrifice with 20 mg/kg calcein (Sigma-Aldrich, St. Louis, MO) in a 2% sodium bicarbonate solution i.p. Calveria were fixed in 70% ethanol and embedded in methylmethacrylate and sectioned.

Bone histomorphometry

Bones were prepared and analyzed as previously described. Mouse tibiae were fixed in 10% formalin for 24 hours and decalcified in 14% EDTA solution for 2 weeks. Paraffin embedded sections were stained with TRAP. Sections were analyzed by a blinded operator according to standard protocol using Bioquant Osteo V7 10.10 (Bioquant Image Analysis Corp.).

Statistical analysis

All experiments were analyzed using Student's t-test. In calculating two-tailed significance levels for equality of means, equal variances were assumed for both populations. Results were considered to reach significance at $p<0.05$. *$p<0.05$; **$p<0.01$; ***$p<0.001$.

<center>**Results**</center>

TSP1-/- mice had increased cancellous and cortical bone mass

We have previously shown that mice deficient in the TSP1-receptor CD47 have modestly increased bone mass (Koskinen et al., 2013; Lundberg et al., 2007; Uluckan et al., 2009). To determine if TSP1-/- mice would similarly display increased bone volume, we performed microCT analysis on WT and TSP1-/- mice to evaluate cancellous and cortical bone. We observed a significant increase in trabecular bone volume in 8 week-old (+32.6%), 16 week-old (+112.1%), and 32 week old (+158.8%) TSP1-/- mice (**Figure 2.1 A-B**). Coordinately, trabecular number was increased and trabecular spacing was decreased in TSP1-/- mice (**Figure 2.2**). This dramatic increase in trabecular bone volume is in contrast to the modest bone volume phenotypes of TSP1-receptor deficient mice (CD47, CD36, β3 integrin-/- (Faccio et al., 2003a; Kevorkova et al., 2013; Koskinen et al., 2013; McHugh et al., 2000; Uluckan et al., 2009)), and is consistent with TSP1 binding to multiple receptors. TSP1-/- mice also had significantly increased cortical bone thickness and total cortical area at 12 weeks (**Figure 2.1 C-E**), indicating a geometrically larger bone in TSP1-/- compared to WT mice. Therefore, TSP1-/- mice had both increased size and increased relative bone mass compared to WT mice.

TSP1 improved bone strength through effects on the bone material properties

Because TSP1 null mice showed enhanced cortical thickness and cross-sectional area (**Figure 2.1 C-E**), and because TSP1 is a known component of the bone matrix (Clezardin et al., 1989; Robey et al., 1989), we hypothesized that TSP1 deletion may influence bone mechanical

<center>52</center>

properties. Bone mechanical properties are influenced by many factors including overall structural morphology and the material properties ("quality") of the bone matrix.

MicroCT analysis of the femoral mid-diaphysis showed a striking increase in moment of inertia in TSP1-/- mice (+67.1%), predicting increased strength based on morphology (**Figure 2.3 A**). Interestingly, however, direct measurement of mechanical strength by 3-point bending did not recapitulate these results. Bone is permanently deformed upon reaching its yield force and eventually fractures after reaching its highest (ultimate) force. TSP1-/- femurs showed only a modest increase ultimate force (+16.7%) and no difference compared to WT in yield force (**Figure 2.3 B-C**). Notably, a normalized measure of yield force that accounts for differences in morphology (yield stress) is significantly decreased in TSP1-/- femurs (**Figure 2.3 D**). This suggests a bone material defect in TSP1-/- mice that offsets the morphological size advantage.

To directly evaluate the local material properties of the bone matrix, we performed reference point indentation by applying a repetitive force on the cortical bone surface through a small probe. TSP1-/- femurs had increased initial indentation distance and a larger increase in indentation at the end of 10 cycles (**Figure 2.3 E-F**). These data indicate that TSP1-/- bone material had less resistance to microfracture compared to WT control. Dynamic histomorphometric analysis to quantitate bone formation rate and mineral apposition rates were difficult to perform because of fuzzy and poor bone mineral labeling in the TSP1-/- mice (**Figure 2.4 B**), consistent with a bone mineral defect. Taken together, these mechanical and material properties demonstrate that TSP1 plays a role in maintaining the matrix quality necessary for normal bone strength.

TSP1-/- mice had decreased bone resorption and OC formation

While we identified differences in long bone size and bone material properties that contribute to reduced bone quality, the underlying mechanism leading to the increased bone mass in TSP1-/- mice remained unclear. The progressive increase in trabecular bone volume with age in TSP1 null animals (**Figure 2.1 A-B**) is consistent with a failure in bone resorption. To test this, we measured serum markers of bone turnover, which include CTX (carboxy-terminal telopeptide collagen crosslinks), a measure of osteoclastic bone resorption and P1NP (pro-collagen type I N-terminal telopeptide), a measure of OB function. There were no statistically significant differences in serum P1NP at 8, 16, or 32 weeks of age (**Figure 2.4 A**) and no differences in ex vivo OB formation assays (**Figure 2.4 C-E**). We did observe significant decreases in serum CTX levels in TSP1-/- mice compared to WT controls at 8 weeks and 16 weeks of age (**Figure 2.5 A**) consistent with a defect in OC resorption. Histomorphometric analysis of mouse tibiae showed that TSP1-/- mice did not have significantly different OC number/bone surface at 8 or 32 weeks of age (**Figure 2.6**). To investigate the role of TSP1 in osteoclastogenesis and function, we differentiated WT primary OCs from bone marrow macrophages in vitro. TSP1 is secreted by activated platelets, leading to high levels of the protein in blood serum. Fetal bovine serum (FBS), necessary in OC culture media, contains approximately 100 ng/ml TSP1 (data not shown). To neutralize FBS-derived TSP1, we treated cultures with TSP1 neutralizing antibody (clone A4.1). Notably, in control cultures, TSP1-/- OCs were indistinguishable from WT OCs, indicating that exogenous, FBS-derived TSP1 was sufficient to maintain normal OC formation (**Figure 2.7**). In contrast, OC differentiation in the presence of anti-TSP1 antibody was dramatically reduced**,** while cells treated with the IgM control antibody developed large multinucleated TRAP+ OCs (**Figure 2.5 B, left panels; Figure**

2.7). Interestingly, while there was no change in NFATc1, a marker of OC lineage commitment, RT-qPCR analysis showed decreased expression of OC differentiation markers (DC-STAMP, TRAP, β3 integrin, Cathepsin K) in anti-TSP1 antibody treated cultures, consistent with reduced osteoclastogenesis (**Figure 2.5 C**).

To define the temporal requirement of TSP1 in OC formation, we treated early (d0-2), mid (d3-4), or late (d4-5) stage OC cultures with A4.1 to neutralize TSP1 at different times during OC formation. We found that neutralizing TSP1 in early OC precursors (d0-2) was sufficient to decrease OC differentiation, while mid- or late-stage TSP1 neutralization had no effect (**Figure 2.5 B**). These data indicate that TSP1 promotes early-stage OC formation while it is dispensable for later maturation.

Inhibition of NOS rescued TSP1-/- bone resorption phenotype

TSP1 is an established mediator of NO signaling in endothelium and inflammatory macrophages (Chen et al., 2000; Isenberg et al., 2009), and we have previously shown that TSP1-receptor CD47 null mice show reduced OC formation due to increased levels of iNOS transcription (Uluckan et al., 2009). In primary OC cultures treated with TSP1 neutralizing antibody, we saw a dramatic elevation of iNOS expression compared to isotype control (**Figure 2.8 A**). Neither nNOS nor eNOS were elevated in anti-TSP1 antibody treated cultures (data not shown). To test whether the bone resorption defect in TSP1-/- mice was attributable to elevated NO signaling, we inhibited NO production in vivo by administration of the pan-NOS inhibitor L-NAME in the drinking water of TSP1-/- and WT mice (40 mg/kg/day) for six weeks. L-NAME-treatment increased the serum CTX level of TSP1-/- mice to that of their WT counterparts, demonstrating that osteoclastic bone resorption was restored (**Figure 2.8 B**). Together, these data

indicate that aberrant NO signaling in TSP1-/- mice was in part responsible for decreased OC function in vitro and in vivo.

TSP1 in bone was sufficient to inhibit OC iNOS

It is well established that TSP1 is secreted by OBs and is present in the bone matrix (Clezardin et al., 1989; Robey et al., 1989). We found that TSP1 contributes to maintaining bone strength (**Figure 2.3**), but its role as matricellular signaling molecule in the bone remained unknown.

We hypothesized that bone-sequestered TSP1 signals to immature OCs to inhibit RANK-L-induced iNOS. We therefore differentiated WT bone marrow macrophages into OC on plates coated with bone powder derived from WT or TSP1-/- mice. The osteoclastogenic culture medium was serum free to ensure that the bone was the only source of TSP1. OCs plated on TSP1-/- bone powder had increased iNOS expression compared to the same cells plated on WT bone after 24 hours of differentiation (**Figure 2.9 A**). Notably, the lineage marker NFATc1 was unchanged between cells plated on WT and TSP1-/- bone, indicating that osteoclastogenic signaling was initiated equally (**Figure 2.9 A**). Together, these data indicate that bone-sequestered TSP1 plays a critical role in iNOS signaling during early osteoclastogenesis.

Discussion

We demonstrate here that TSP1 is critical for the maintenance of bone homeostasis, contributing both to matrix material integrity and regulation of OC formation (**Figure 2.9 B**). TSP1-/- mice were protected from age-associated bone loss and had increased cross-sectional area, but failed to show proportional resistance to bending. Instead, we found that TSP1 null mice had a bone material properties defect, resulting in decreased bone material quality and reduced strength. The increased trabecular bone mass in TSP1-/- mice was due to decreased osteoclastic resorption that was rescued upon in vivo pharmacologic inhibition of NO signaling. We demonstrated that TSP1 inhibition of iNOS was necessary for early OC formation, but was dispensable for later OC maturation. Finally, we showed that bone-sequestered TSP1 modulated OC iNOS levels, indicating TSP1 as a novel paracrine signaling molecule, coupling OB function to OC formation.

The bone matrix is composed of two compartments: mineral of calcium-phosphate hydroxyapatite crystals and osteoid of collagen (90%) and other non-collagenous proteins (10%, NCP). Many diseases including osteogenesis imperfecta and rickets impact bone quality through modification of the osteoid tissue or mineralized matrix leading to increased risk of fragility fracture. Notably, TSP1 binds many components of the bone matrix, including collagen and hydroxyapatite, as well as numerous NCPs including osteonectin, fibronectin, osteopontin, and proteoglycans, among others (reviewed in (Tan and Lawler, 2009)). These NCPs are critical for bone matrix organization, both for collagen organization and hydroxyapatite deposition (Termine and Robey, 1996). In osteogenesis imperfecta patient OBs, secretion of TSP1 and its NCP binding partners are misregulated, suggesting that TSP1 participates with collagen and other

NCPs for osteoid organization (Fedarko et al., 1995). Our data indicate that TSP1 is critical for maintaining the material properties of bone necessary for high bone quality. We postulate that TSP1 mediates the proper physical organization and protein stoichiometry of the bone matrix through its interactions with other bone matrix components. Further work is necessary to understand the role of the matrix proteins that interact with TSP1 to mediate bone quality.

The TSP1-/- bones had both cancellous and cortical bone phenotypes. The increased area and cortical thickness of the TSP1-/- bones suggest an effect of TSP1 loss on OB bone formation. Assessment of bone formation rate and mineral apposition rates by dynamic histomorphometry in the TSP1-/- mice were hampered by the lack of double labels and diffuse single labels (**Figure 2.4 B**). These labeling abnormalities are consistent with a bone matrix defect. Ex vivo OB formation assays were not abnormal in the TSP1-/- cells or in WT cells in the presence of TSP1 neutralizing antibody (data not shown). It is possible that there was a compensatory increase in bone mineral formation due to defects in bone quality or that there are effects of TSP1 on osteocyte and OB formation and function that may be present early in development. Experiments are underway to explore the role of TSP1 in OBs.

In addition to its role in maintaining bone matrix material integrity, we also found that TSP1 binding to early OC precursors promotes differentiation. While our data supports the hypothesis that bone-resident TSP1 regulates iNOS in early OC, it is also possible that TSP1 modulation of the matrix, including stoichiometry of NCPs and protein presentation, may indirectly influence NO signaling. As ongoing research better characterizes the protein interactions in the bone matrix, the impact of matricellular TSP1 on cell signaling will be elucidated. Our data shows that exogenous TSP1 promotes osteoclastogenesis through modulation of NO signaling in OC precursors, similar to its function in endothelial cells,

platelets, and vascular smooth muscle cells through CD36 and CD47 (Chen et al., 2000; Isenberg et al., 2009; Isenberg et al., 2006; Isenberg et al., 2005). The dramatic OC phenotype of TSP1 deficiency, in contrast with the modest effects reported for receptors CD47 and CD36 (Carron et al., 2000; Kevorkova et al., 2013; Koskinen et al., 2013; Lundberg et al., 2007; Uluckan et al., 2009), suggests that TSP1 binds multiple receptors to influence OC formation. We have previously reported that CD47 promotes OC formation through inhibition of iNOS (Uluckan et al., 2009). In the setting of bone homeostasis, OCs sense increased NO produced by iNOS early in differentiation as negative feedback to regulate the extent of osteoclastic bone resorption (Zheng et al., 2006). We demonstrated in vitro that TSP1 inhibits iNOS expression in OC precursors, thereby permitting OC formation. Notably, inhibition of NO synthesis in vivo rescued the TSP1-/- bone resorption defect, consistent with TSP1's influence on OC through modulation of NO signaling.

We present data to support novel roles of TSP1 that place it as a critical member of the bone microenvironment. We propose the following model: TSP1 is directionally secreted by OB into the matrix during bone formation (Clezardin et al., 1989; Robey et al., 1989). In the bone, TSP1 promotes matrix material integrity through interactions with other essential bone matrix proteins. Moreover, the matrix-derived TSP1 acts as a paracrine signaling molecule to promote OC formation via inhibition of iNOS, thus linking OB function to OC formation via the bone matrix (**Figure 2.9 B**).

Due to its pleiotropic nature, with roles in inflammation, angiogenesis, and bone health, the TSP1-signaling axis represents a promising therapeutic target for many disease states. NOS inhibitors, including the compound L-NAME used in our study, are under clinical investigation to modulate blood pressure. Their converse, nitric oxide donors, have been in clinical use for

decades to relieve angina and hypertension. Given our data of elevated OC activity upon administration of L-NAME to TSP1-/- mice, it will be important to monitor the bone health of patients administered these NO-targeted drugs long-term, especially in an elderly patient population with common bone pathological comorbidities such as osteoporosis and osteoarthritis.

Bone pathologies such as osteoporosis and bone metastasis are characterized by a disruption of healthy bone turnover leading to pathologic fracture, hypercalcemia, and nerve compression. Modulation of OCs and OBs represent an attractive point for therapeutic intervention with agents such as bisphosphonates and anti-RANKL antibody (denosumab) in clinical use (Weilbaecher et al., 2011). Our findings provide further rationale to target the TSP1-pathway, especially in comorbidities such as osteoporosis and bone metastasis. Importantly, we showed that TSP1-/- mice are protected from age-associated bone loss, but the increased bone mass was accompanied by a loss in bone quality. This provides important rationale to monitor bone health, both bone density and bone quality, as part of studies investigating TSP1-pathway directed therapeutics for bone-related and other indications. As targeted drugs, including anti-CD47 antibodies, TSP1 mimetics, and NOS inhibitors, enter development and clinical use, it will be important to further investigate the role of TSP1, its receptors, and its downstream signaling molecules in bone health, to identify and monitor both harmful and positive bone effects.
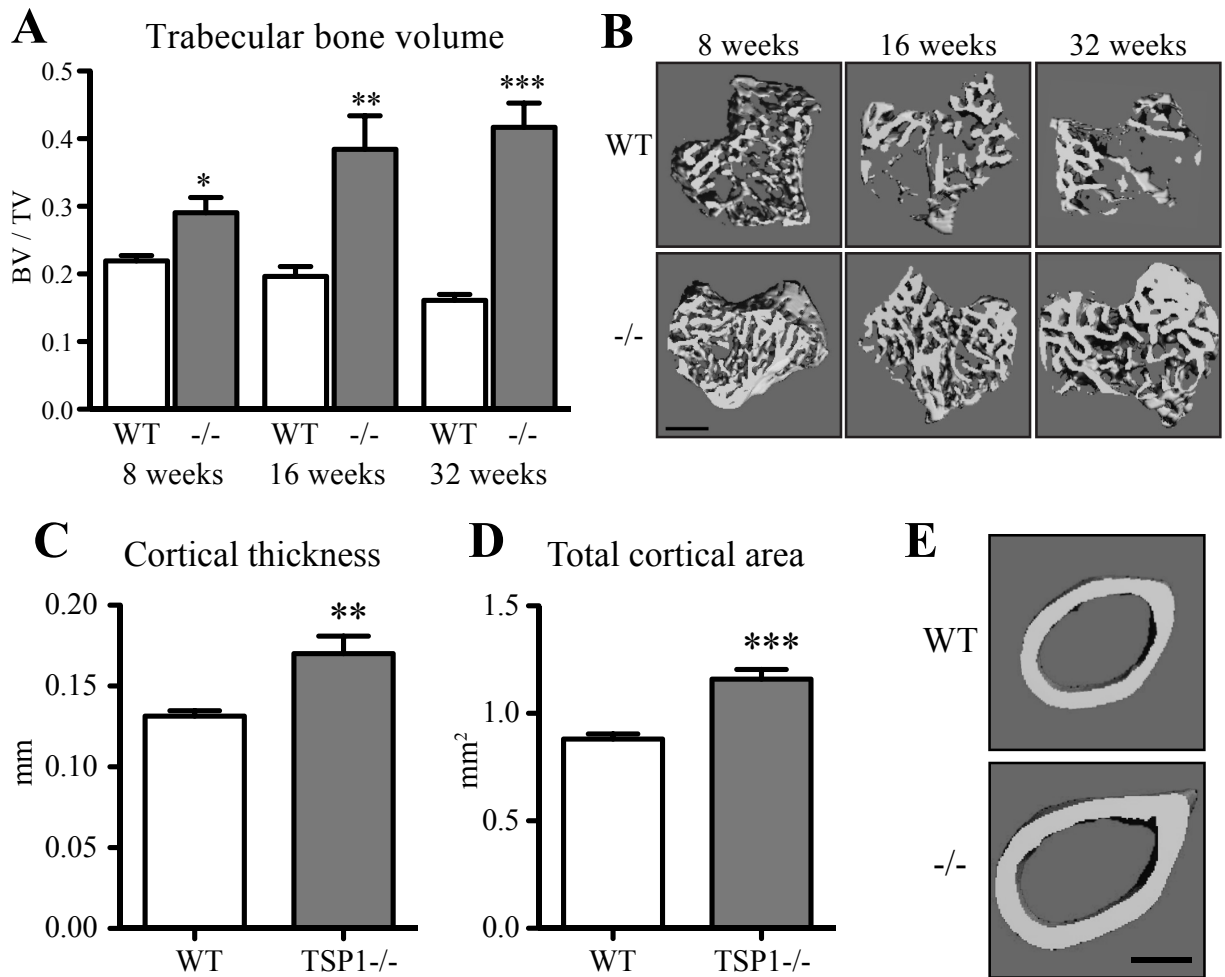
Figure 2.1.
TSP1-/- mice had increased bone mass.
MicroCT analysis for calculation of bone morphological parameters: (A) Trabecular bone volume of 8-, 16-, and 32-week-old WT and TSP1-/- mice tibiae (8- and 32-week n=6/group; 16-week n=5/group). (B) Representative images of three- dimensional microCT reconstruction. (C) Cortical bone thickness and (D) total area of 12-week-old WT and TSP-/- mice femurs (WT n=5; TSP1-/- n=4). (E) Representative images of three-dimensional microCT reconstruction. (scale bars = 500 um)

A Trabecular number

B Trabecular spacing
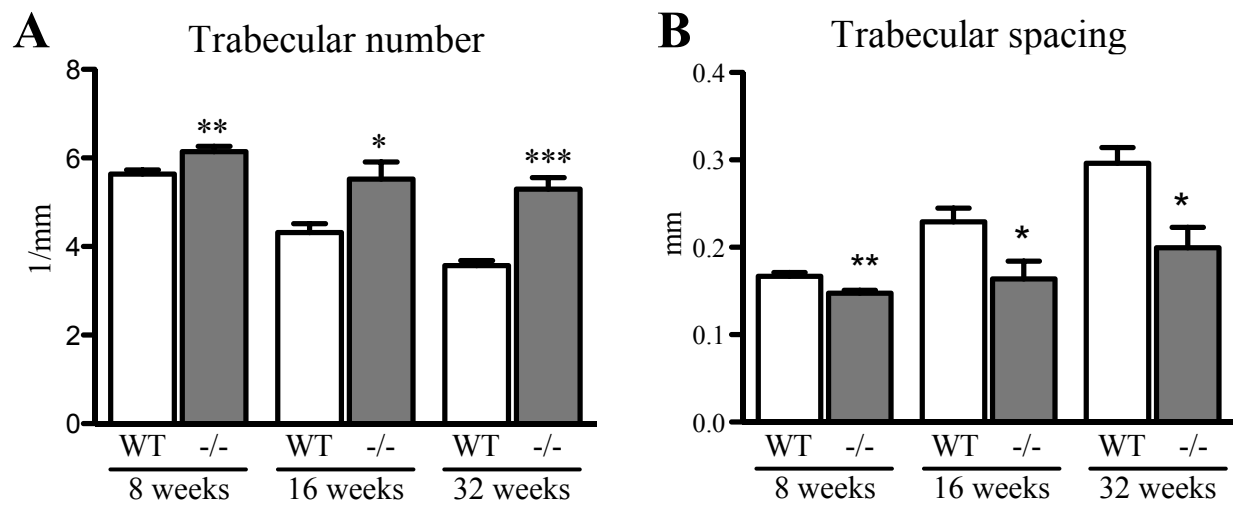
Figure 2.2.
TSP1-/- mice had altered trabecular morphology.
MicroCT analysis for calculation of bone morphological parameters: (A) Trabeculae number and (B) trabecular spacing of 8-, 16-, and 32-week-old WT and TSP1-/- mice tibiae (8- and 32-week n=6/group; 16-week n=5/group).
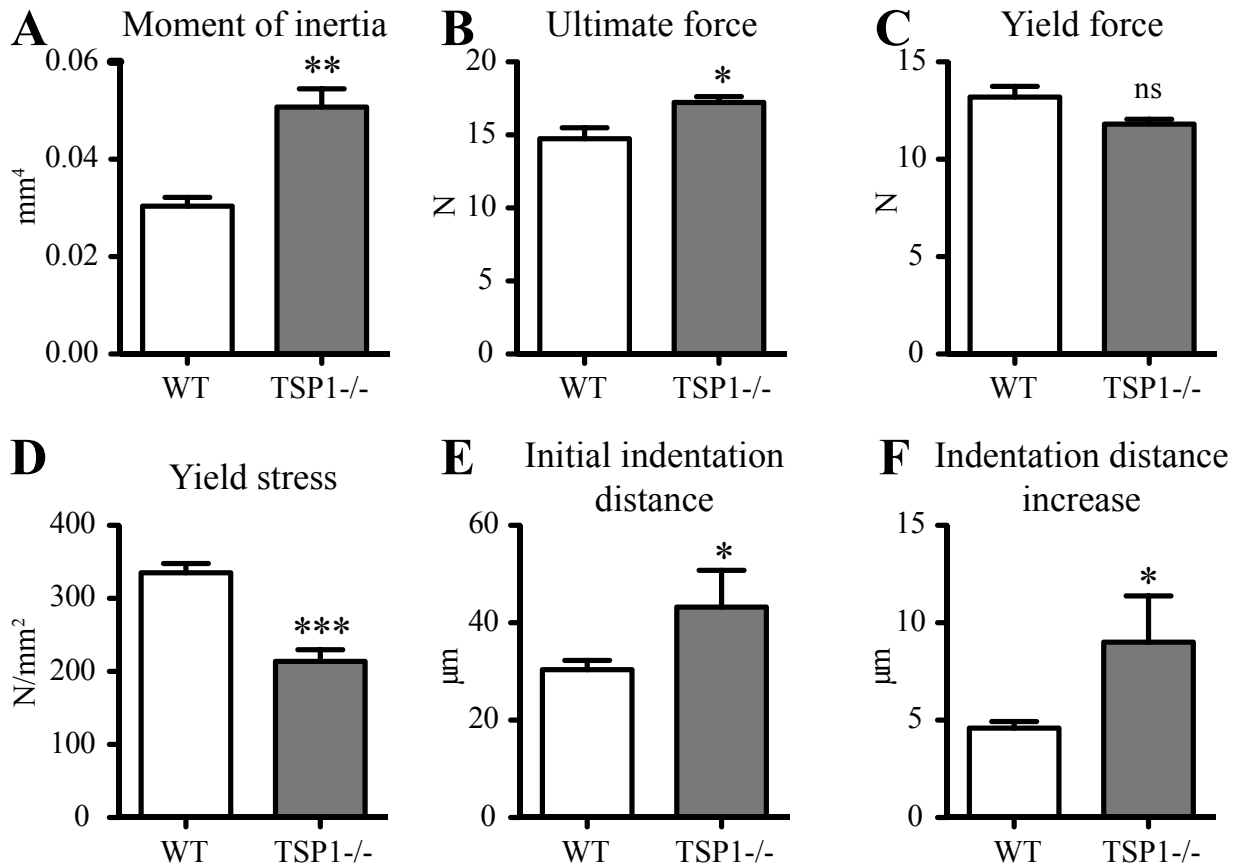
Figure 2.3.
TSP1 improved bone strength through effects on bone material properties.
12-week old WT and TSP1-/- femurs were evaluated for structural and material
strength. (A) MicroCT analysis of WT and TSP1-/- mice femurs for minimum moment
of inertia. Femurs were subjected to three-point bending to evaluate structural
mechanical parameters (B) ultimate force and (C) yield force (ns, p=0.0727). (D) Yield
stress was calculated to normalize for differences in cortical bone morphology (WT
n=5; TSP1-/- n=4). Reference point indentation was completed to evaluate local
material properties: (E) initial indentation distance, (F) indentation distance increase.
(n=3 tests/femur; WT n=5 femurs; TSP1-/- n = 3 femurs)
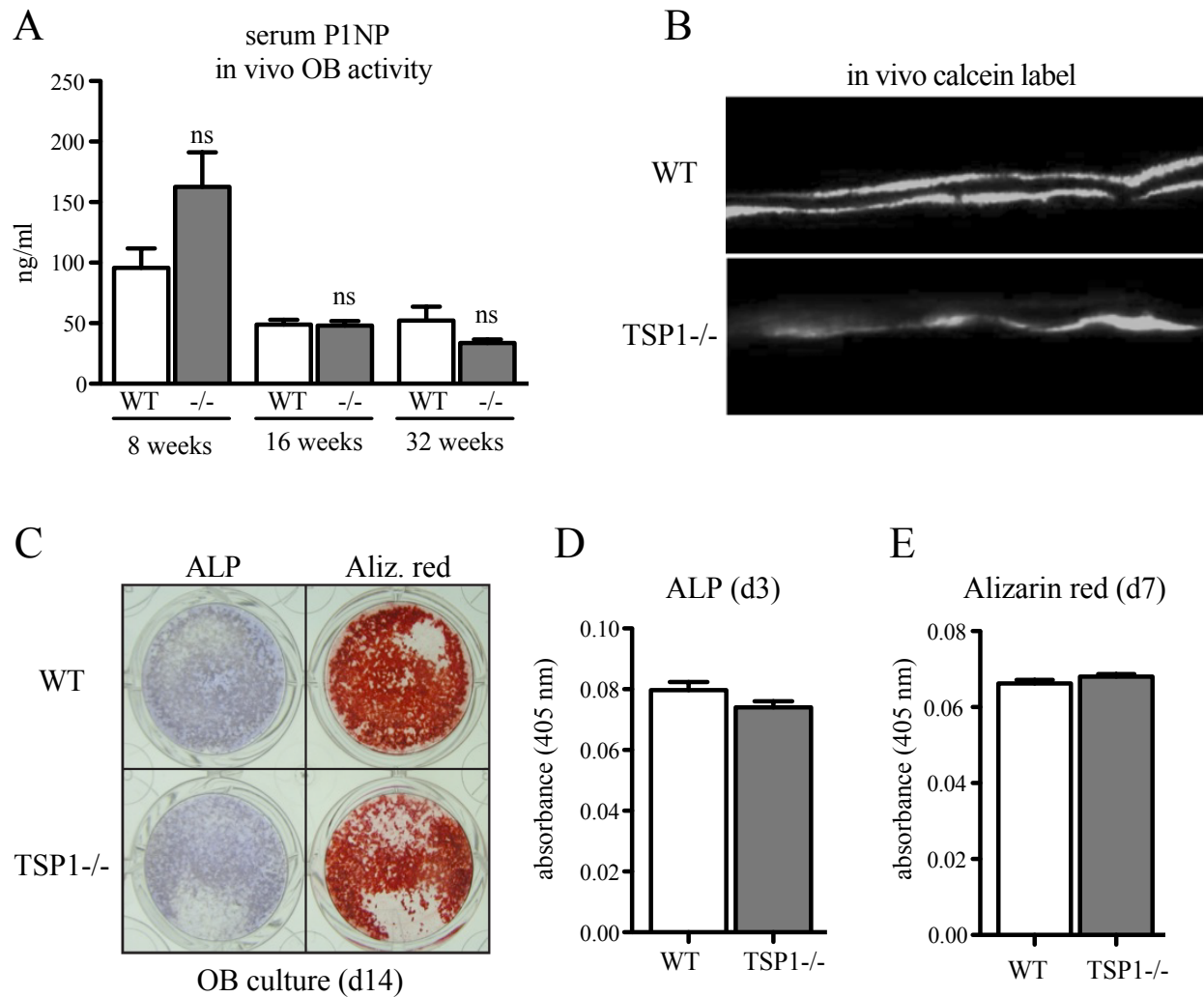
Figure 2.4.

TSP1-/- mice had normal bone formation parameters.

(A) Pro-collagen type I (P1NP) was measured in the serum of fasted WT and TSP1-/-mice (8-week WT n=6, TSP1-/- n=5; 16- and 32-week n=5/group). (B) Double calcein labeling of 16-week old WT and TSP1-/- mice. (C) WT and TSP1-/- bone marrow stromal cells were differenitated into OB in osteogenic media and stained for alkaline phosphatase (ALP) and alizarin red on day 14. (D) ALP and (E) alizarin red were quantitated on day 3 and day 7.
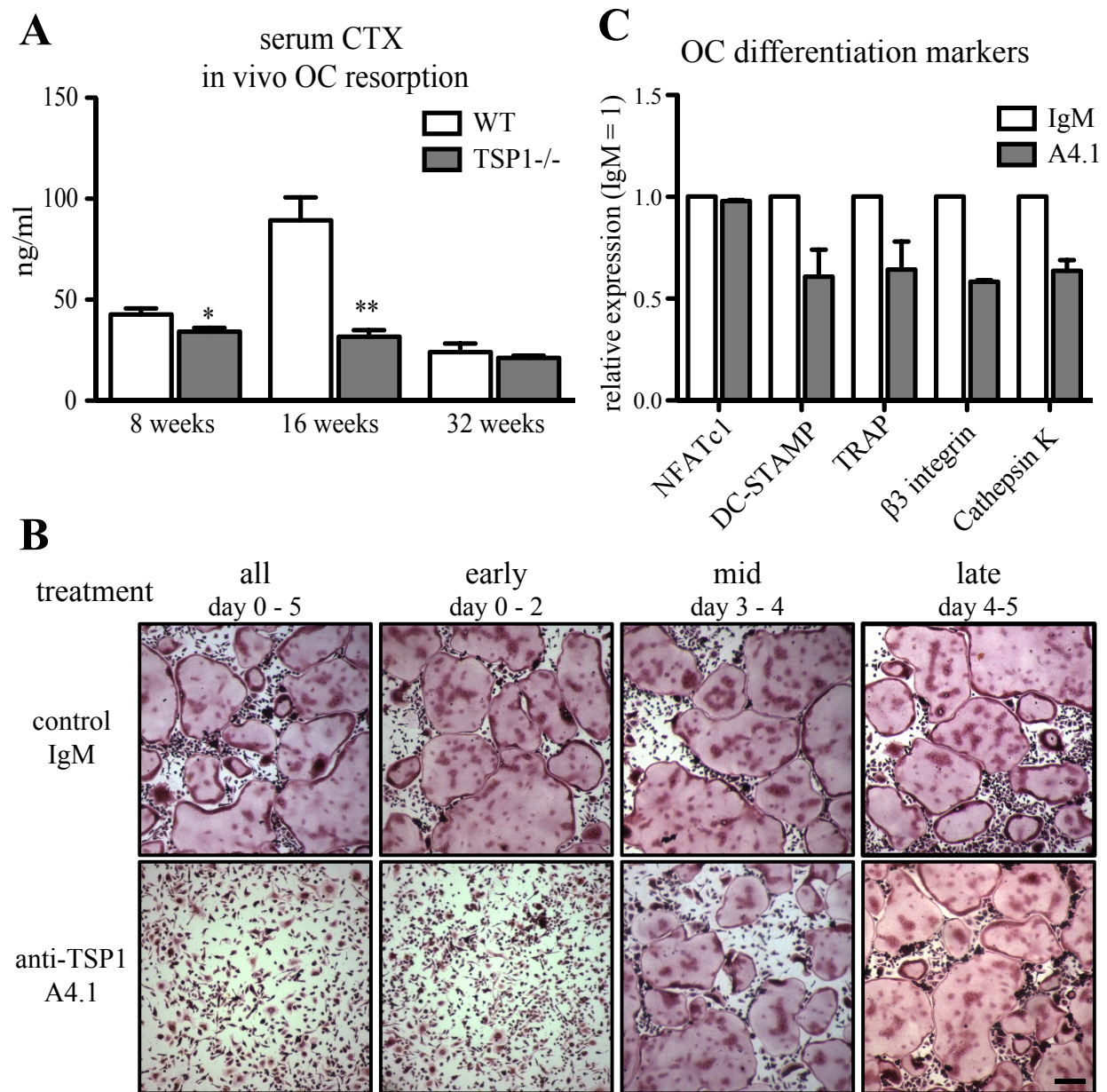
Figure 2.5.
TSP1 deficiency resulted in decreased osteoclast function in vivo and reduced osteoclast formation in vitro.

(A) Collagen breakdown products (CTX) was measured in the serum of fasted WT and TSP1-/- mice (8-week n=5/group; 16-week n=4/group; 32-week n=7/group). (B) WT bone marrow macrophages differentiated into OC in the presence of anti-TSP1 A4.1 antibody or IgM isotype control antibody at indicated days. TRAP staining for multinucleated OC at day 5 shown (representative images of n>3 biological replicates, scale bar = 0.25 mm). (C) qRT-PCR analysis for day 3 OC cultured with anti-TSP1 A4.1 or IgM control (n=3 biological replicates).
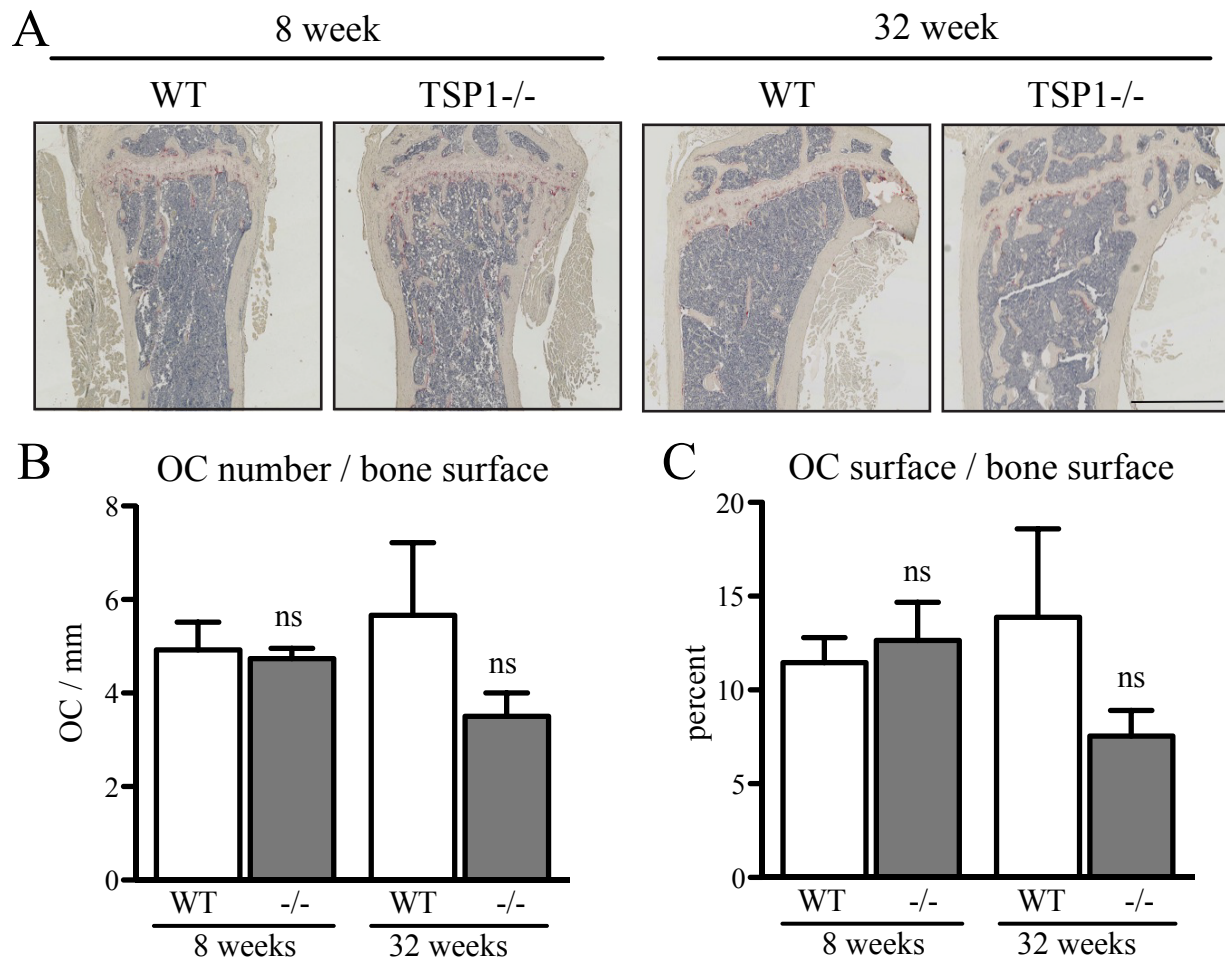
Figure 2.6.
TSP1-/- mice did not have significantly reduced osteoclast numbers in vivo.
(A) 8-week old (left panels) and 32-week old (right panels) WT and TSP1-/- tibiae were sectioned and stained for TRAP (scale bar = 2 mm; representative images of n > 3). (B) OC per bone surface and (C) OC surface per bone surface of 8- and 32-week WT and TSP1-/- mice.
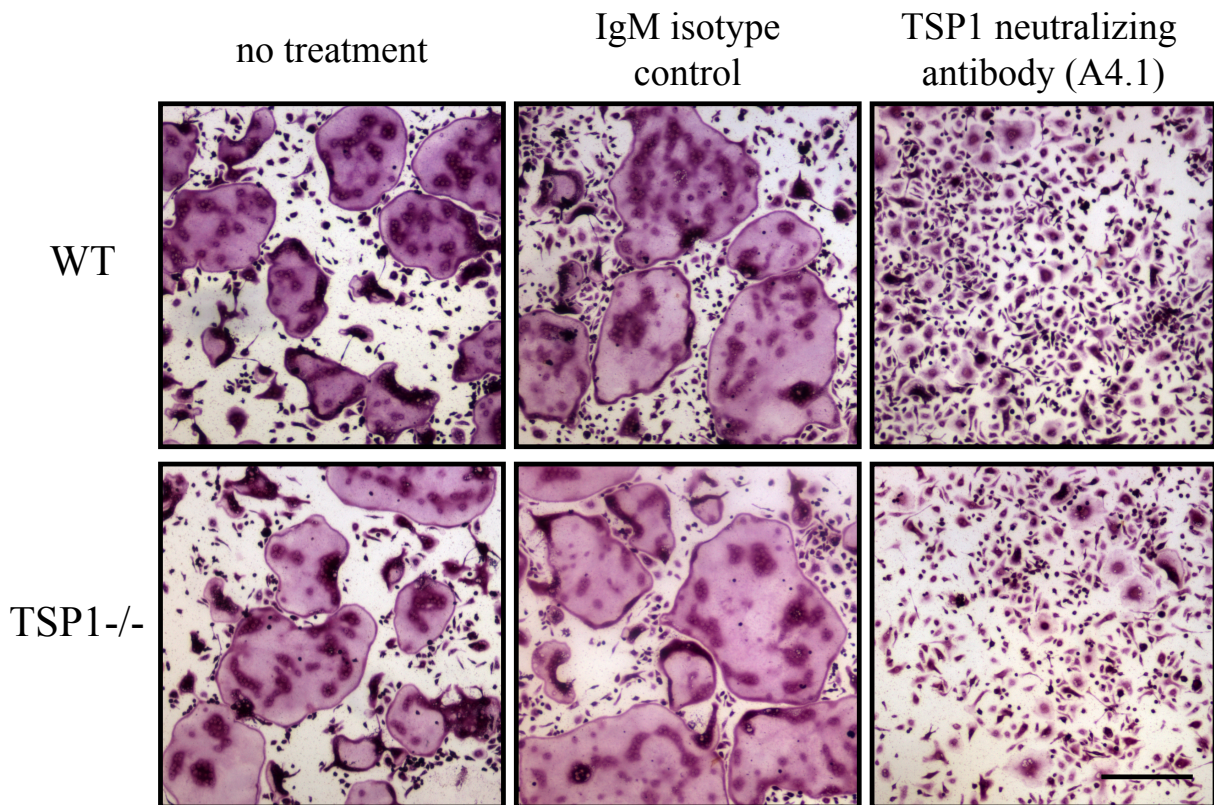
Figure 2.7.
Neutralization of exogenous TSP1 prevents OC formation in wild type and TSP1-/- cells. TRAP stain of WT or TSP1-/- bone marrow macrophages differentiated into OC in IgM isotype control of TSP1 neutralizing antibody (clone A4.1). TRAP staining for multinucleated OC at day 5 shown. (scale bar = 0.25 mm; representative images of n>3 biological replicates)
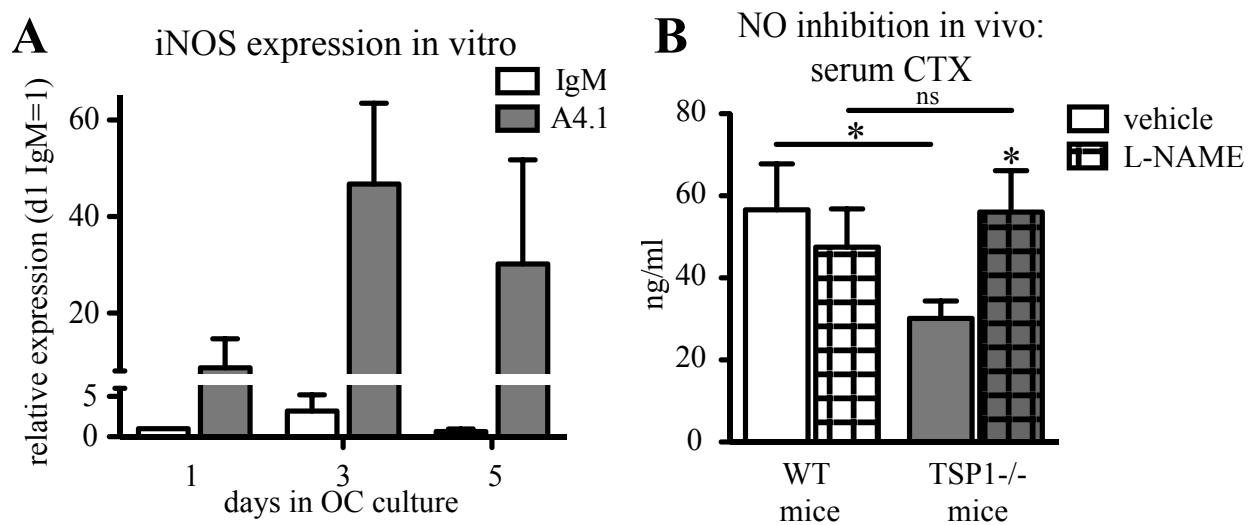
Figure 2.8.
TSP1 regulates osteoclasts through inhibition of iNOS.
(A) qRT-PCR of iNOS from WT OC cultures in the presence of TSP1 neutralizing antibody (A4.1) or istoype control (IgM). (n=3 biological replicates). (B) WT and TSP1-/- mice were administered pan-NOS inhibitor L-NAME, 40 mg/kg/day for 6 weeks, and fasted serum CTX was measured (WT n=7/group; TSP1-/- n=8/vehicle, n=10/L-NAME).

A Wild type OC on bone gene expression

☐ WT bone
▨ TSP1-/- bone

relative expression (WT bone = 1)

NFATc1   iNOS

B OBs secrete TSP1 into the bone matrix

pre-OC bind matrix TSP1 to promote OC formation

Matrix- TSP1 promotes bone quality
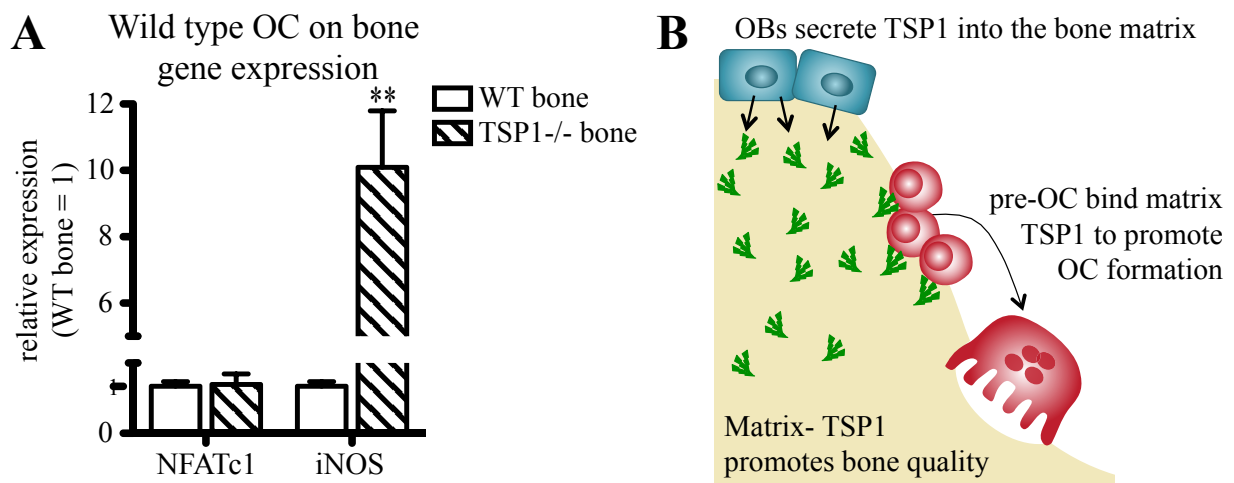
Figure 2.9.
Bone-derived TSP1 is sufficient to inhibit iNOS in osteoclasts.
(A) qRT-PCR of early OC marker NFATc1 and iNOS from WT OC cultured on WT or TSP1-/- bone powder (n=2 biological replicates) for 24 hours. (B) Model of the role of TSP1 in bone biology.

Table 2.1. Mechanical properties of WT and TSP1-/- femurs

Property	WT (n=5)	TSP1-/- (n=4)	p-value
Stiffness (N/mm)	58.71 ± 14.34	70.41 ± 7.961	0.5294
Yield displacement (mm)	0.1180 ± 0.02089	0.1190 ± 0.01096	0.9699
Post-yield displacement (mm)	0.2248 ± 0.01568	0.3100 ± 0.02640	0.0225
Energy to fracture (N*mm)	2.806 ± 0.2241	3.940 ± 0.4317	0.0419

Data are expressed as mean ± SEM

References

Annis, D.S., Murphy-Ullrich, J.E., and Mosher, D.F. (2006). Function-blocking antithrombospondin-1 monoclonal antibodies. Journal of thrombosis and haemostasis : JTH *4*, 459-468.

Bailey Dubose, K., Zayzafoon, M., and Murphy-Ullrich, J.E. (2012). Thrombospondin-1 inhibits osteogenic differentiation of human mesenchymal stem cells through latent TGF-beta activation. Biochem Biophys Res Commun *422*, 488-493.

Baron, R.E. (1996). Anatomy and Ultrastructure of Bone. In Primer on the Metabolic Bone Diseases and Disorders of Mineral Metabolism, M.J. Favus, ed. (New York: Lippincott - Raven Publishers).

Brodt, M.D., Ellis, C.B., and Silva, M.J. (1999). Growing C57Bl/6 mice increase whole bone mechanical properties by increasing geometric and material properties. Journal of bone and mineral research : the official journal of the American Society for Bone and Mineral Research *14*, 2159-2166.

Carron, J.A., Wagstaff, S.C., Gallagher, J.A., and Bowler, W.B. (2000). A CD36-binding peptide from thrombospondin-1 can stimulate resorption by osteoclasts in vitro. Biochem Biophys Res Commun *270*, 1124-1127.

Carron, J.A., Walsh, C.A., Fraser, W.D., and Gallagher, J.A. (1995). Thrombospondin promotes resorption by osteoclasts in vitro. Biochem Biophys Res Commun *213*, 1017-1025.

Chen, H., Herndon, M.E., and Lawler, J. (2000). The cell biology of thrombospondin-1. Matrix Biol *19*, 597-614.

Clezardin, P., Jouishomme, H., Chavassieux, P., and Marie, P.J. (1989). Thrombospondin is synthesized and secreted by human osteoblasts and osteosarcoma cells. A model to study the different effects of thrombospondin in cell adhesion. European journal of biochemistry / FEBS *181*, 721-726.

Crawford, S.E., Stellmach, V., Murphy-Ullrich, J.E., Ribeiro, S.M., Lawler, J., Hynes, R.O., Boivin, G.P., and Bouck, N. (1998). Thrombospondin-1 is a major activator of TGF-beta1 in vivo. Cell *93*, 1159-1170.

Cremasco, V., Decker, C.E., Stumpo, D., Blackshear, P.J., Nakayama, K.I., Nakayama, K., Lupu, T.S., Graham, D.B., Novack, D.V., and Faccio, R. (2012). Protein kinase C-delta deficiency perturbs bone homeostasis by selective uncoupling of cathepsin K secretion and ruffled border formation in osteoclasts. Journal of bone and mineral research : the official journal of the American Society for Bone and Mineral Research *27*, 2452-2463.

Deshpande, S.R., Satyanarayana, K., Rao, M.N., and Pai, K.V. (2012). Nitric oxide modulators: an emerging class of medicinal agents. Indian journal of pharmaceutical sciences *74*, 487-497.

Faccio, R., Novack, D.V., Zallone, A., Ross, F.P., and Teitelbaum, S.L. (2003a). Dynamic changes in the osteoclast cytoskeleton in response to growth factors and cell attachment are controlled by beta3 integrin. The Journal of cell biology *162*, 499-509.

Faccio, R., Takeshita, S., Zallone, A., Ross, F.P., and Teitelbaum, S.L. (2003b). c-Fms and the alphavbeta3 integrin collaborate during osteoclast differentiation. J Clin Invest *111*, 749-758.

Fedarko, N.S., Robey, P.G., and Vetter, U.K. (1995). Extracellular matrix stoichiometry in osteoblasts from patients with osteogenesis imperfecta. Journal of bone and mineral research : the official journal of the American Society for Bone and Mineral Research *10*, 1122-1129.

Grzesik, W.J., and Robey, P.G. (1994). Bone matrix RGD glycoproteins: immunolocalization and interaction with human primary osteoblastic bone cells in vitro. J Bone Miner Res *9*, 487-496.

Hadjidakis, D.J., and Androulakis, II (2006). Bone remodeling. Ann N Y Acad Sci *1092*, 385-396.

Heller, E., Hurchla, M.A., Xiang, J., Su, X., Chen, S., Schneider, J., Joeng, K.S., Vidal, M., Goldberg, L., Deng, H.*, et al.* (2012). Hedgehog signaling inhibition blocks growth of resistant tumors through effects on tumor microenvironment. Cancer Res *72*, 897-907.

Isenberg, J.S., Martin-Manso, G., Maxhimer, J.B., and Roberts, D.D. (2009). Regulation of nitric oxide signalling by thrombospondin 1: implications for anti-angiogenic therapies. Nature reviews Cancer *9*, 182-194.

Isenberg, J.S., Ridnour, L.A., Dimitry, J., Frazier, W.A., Wink, D.A., and Roberts, D.D. (2006). CD47 is necessary for inhibition of nitric oxide-stimulated vascular cell responses by thrombospondin-1. J Biol Chem *281*, 26069-26080.

Isenberg, J.S., Ridnour, L.A., Perruccio, E.M., Espey, M.G., Wink, D.A., and Roberts, D.D. (2005). Thrombospondin-1 inhibits endothelial cell responses to nitric oxide in a cGMP-dependent manner. Proc Natl Acad Sci U S A *102*, 13141-13146.

Kannus, P., Jozsa, L., Jarvinen, T.A., Jarvinen, T.L., Kvist, M., Natri, A., and Jarvinen, M. (1998). Location and distribution of non-collagenous matrix proteins in musculoskeletal tissues of rat. The Histochemical journal *30*, 799-810.

Kevorkova, O., Martineau, C., Martin-Falstrault, L., Sanchez-Dardon, J., Brissette, L., and Moreau, R. (2013). Low-Bone-Mass Phenotype of Deficient Mice for the Cluster of Differentiation 36 (CD36). PloS one *8*, e77701.

Koskinen, C., Persson, E., Baldock, P., Stenberg, A., Bostrom, I., Matozaki, T., Oldenborg, P.A., and Lundberg, P. (2013). Lack of CD47 impairs bone cell differentiation and results in an osteopenic phenotype in vivo due to impaired signal regulatory protein alpha (SIRPalpha) signaling. J Biol Chem *288*, 29333-29344.

Kukreja, A., Radfar, S., Sun, B.H., Insogna, K., and Dhodapkar, M.V. (2009). Dominant role of CD47-thrombospondin-1 interactions in myeloma-induced fusion of human dendritic cells: implications for bone disease. Blood *114*, 3413-3421.

Lawler, J., Sunday, M., Thibert, V., Duquette, M., George, E.L., Rayburn, H., and Hynes, R.O. (1998). Thrombospondin-1 is required for normal murine pulmonary homeostasis and its absence causes pneumonia. The Journal of clinical investigation *101*, 982-992.

Lundberg, P., Koskinen, C., Baldock, P.A., Lothgren, H., Stenberg, A., Lerner, U.H., and Oldenborg, P.A. (2007). Osteoclast formation is strongly reduced both in vivo and in vitro in the absence of CD47/SIRPalpha-interaction. Biochem Biophys Res Commun *352*, 444-448.

McHugh, K.P., Hodivala-Dilke, K., Zheng, M.H., Namba, N., Lam, J., Novack, D., Feng, X., Ross, F.P., Hynes, R.O., and Teitelbaum, S.L. (2000). Mice lacking beta3 integrins are osteosclerotic because of dysfunctional osteoclasts. The Journal of clinical investigation *105*, 433-440.

Morgan, E.A., Schneider, J.G., Baroni, T.E., Uluckan, O., Heller, E., Hurchla, M.A., Deng, H., Floyd, D., Berdy, A., Prior, J.L.*, et al.* (2010). Dissection of platelet and myeloid cell defects by conditional targeting of the beta3-integrin subunit. FASEB journal : official publication of the Federation of American Societies for Experimental Biology *24*, 1117-1127.

Posey, K.L., Hankenson, K., Veerisetty, A.C., Bornstein, P., Lawler, J., and Hecht, J.T. (2008). Skeletal abnormalities in mice lacking extracellular matrix proteins, thrombospondin-1, thrombospondin-3, thrombospondin-5, and type IX collagen. Am J Pathol *172*, 1664-1674.

Randall, C., Mathews, P., Yurtsev, E., Sahar, N., Kohn, D., and Hansma, P. (2009). The bone diagnostic instrument III: testing mouse femora. The Review of scientific instruments *80*, 065108.

Robey, P.G., Young, M.F., Fisher, L.W., and McClain, T.D. (1989). Thrombospondin is an osteoblast-derived component of mineralized extracellular matrix. J Cell Biol *108*, 719-727.

Schneider, J.G., Amend, S.R., and Weilbaecher, K.N. (2011). Integrins and bone metastasis: integrating tumor cell and stromal cell interactions. Bone *48*, 54-65.

Silva, M.J., Brodt, M.D., Wopenka, B., Thomopoulos, S., Williams, D., Wassen, M.H., Ko, M., Kusano, N., and Bank, R.A. (2006). Decreased collagen organization and content are associated with reduced strength of demineralized and intact bone in the SAMP6 mouse. Journal of bone and mineral research : the official journal of the American Society for Bone and Mineral Research *21*, 78-88.

Smadja, D.M., d'Audigier, C., Bieche, I., Evrard, S., Mauge, L., Dias, J.V., Labreuche, J., Laurendeau, I., Marsac, B., Dizier, B.*, et al.* (2011). Thrombospondin-1 is a plasmatic marker of peripheral arterial disease that modulates endothelial progenitor cell angiogenic properties. Arterioscler Thromb Vasc Biol *31*, 551-559.

Su, X., Floyd, D.H., Hughes, A., Xiang, J., Schneider, J.G., Uluckan, O., Heller, E., Deng, H., Zou, W., Craft, C.S.*, et al.* (2012). The ADP receptor P2RY12 regulates osteoclast function and pathologic bone remodeling. J Clin Invest *122*, 3579-3592.

Tan, K., and Lawler, J. (2009). The interaction of Thrombospondins with extracellular matrix proteins. Journal of cell communication and signaling *3*, 177-187.

Taraboletti, G., Rusnati, M., Ragona, L., and Colombo, G. (2010). Targeting tumor angiogenesis with TSP-1-based compounds: rational design of antiangiogenic mimetics of endogenous inhibitors. Oncotarget *1*, 662-673.

Termine, J.D., and Robey, P.G. (1996). Bone Matrix Proteins and the Mineralization Process. In Primer on the Metabolic Bone Diseases and Disorders of Mineral Metabolism, M.J. Favus, ed. (New York: Lippincott-Raven).

Tseng, D., Volkmer, J.P., Willingham, S.B., Contreras-Trujillo, H., Fathman, J.W., Fernhoff, N.B., Seita, J., Inlay, M.A., Weiskopf, K., Miyanishi, M.*, et al.* (2013). Anti-CD47 antibody-mediated phagocytosis of cancer by macrophages primes an effective antitumor T-cell response. Proceedings of the National Academy of Sciences of the United States of America *110*, 11103-11108.

Ueno, A., Miwa, Y., Miyoshi, K., Horiguchi, T., Inoue, H., Ruspita, I., Abe, K., Yamashita, K., Hayashi, E., and Noma, T. (2006). Constitutive expression of thrombospondin 1 in MC3T3-E1 osteoblastic cells inhibits mineralization. J Cell Physiol *209*, 322-332.

Uluckan, O., Becker, S.N., Deng, H., Zou, W., Prior, J.L., Piwnica-Worms, D., Frazier, W.A., and Weilbaecher, K.N. (2009). CD47 regulates bone mass and tumor metastasis to bone. Cancer Res *69*, 3196-3204.

Weilbaecher, K.N., Guise, T.A., and McCauley, L.K. (2011). Cancer to bone: a fatal attraction. Nat Rev Cancer *11*, 411-425.

Weiskopf, K., Ring, A.M., Schnorr, P.J., Volkmer, J.P., Volkmer, A.K., Weissman, I.L., and Garcia, K.C. (2013). Improving macrophage responses to therapeutic antibodies by molecular engineering of SIRPalpha variants. Oncoimmunology *2*, e25773.

Zheng, H., Yu, X., Collin-Osdoby, P., and Osdoby, P. (2006). RANKL stimulates inducible nitric-oxide synthase expression and nitric oxide production in developing osteoclasts. An autocrine negative feedback mechanism triggered by RANKL-induced interferon-beta via NF-kappaB that restrains osteoclastogenesis and bone resorption. J Biol Chem *281*, 15809-15820.

Chapter 3

Samsn1 deletion contributes to monoclonal gammopathy of undetermined significance and multiple myeloma susceptibility through effects on multiple cell types

Abstract

Multiple myeloma (MM) is a malignancy of plasma B-cells that is invariably preceded by monoclonal gammopathy of undetermined significance (MGUS), a pre-neoplastic plasma cell proliferative disorder.   Epidemiologic and population association studies demonstrated that inherited susceptibility to MM is due to an increased risk of MGUS, rather than an increased rate of transformation to overt malignancy. Therefore, prevalence of MM is likely mediated by germline MGUS risk alleles. C57Bl/KaLwRij (KaLwRij) is a spontaneous mutant mouse strain predisposed to benign idiopathic paraproteinemia (BIP), analogous to human MGUS. Using a integrative approach, we combined KaLwRij x B6 SNP analysis (418 genes) and a MM patient association study (180 genes) to identify five candidate genes likely to contribute to both murine BIP-susceptibility and human MM risk. Surprisingly, we found KaLwRij mice had complete germline deletion of one of the five candidate genes, *Samsn1*, a negative regulator of B-cell activation. *Samsn1* is expressed in hematopoietic cells, including B-cells and macrophages. Consistent with the reported inhibitory function of SAMSN1 in B-cells, KaLwRij mice had enhanced B-cell responses in vitro and in vivo. We also found that SAMSN1 re-expression decreases proliferation in myeloma cells, demonstrating its inhibitory function in malignant B-cells. Moreover, we found KaLwRij macrophages to have increased proliferation and markedly elevated expression of pro-tumorigenic M2 macrophage markers in vitro, and increased tumor-promoting activity in vivo, suggesting that *Samsn1* regulates macrophage activation. Thus, we identified *Samsn1* as a gene contributing to BIP-susceptibility in KaLwRij mice through mutually exclusive function in multiple cell types. It is likely that SAMSN1 and its pathway members contribute to human MM progression, and may represent a point for preventative therapeutic intervention.

Introduction

Monoclonal gammopathy of undetermined significance (MGUS) is a hematological disorder characterized by an expansion of one or more antibody-producing plasma cells in the bone marrow, diagnosed by the presence of constant serum level of monoclonal paraprotein (<3 g/dL, "M-spike"). MGUS is a common syndrome of aging, with a prevalence of >3-5% in 50-70 year olds (Kyle et al., 2006; Landgren et al., 2009). While MGUS does not present with severe clinical features, the disorder is not wholly benign, and is associated with increased fracture risk and osteoporosis (Melton et al., 2005). Most significant, MGUS is the requisite precursor to multiple myeloma (MM), and MGUS patients progress to overt malignancy at an annual rate of 1%. MM is the second most common hematological malignancy and is invariably fatal with a ~6 year median survival (Kumar et al., 2013). MM is characterized by an M-spike of >3 g/dL and is clinically diagnosed by the presence of CRAB symptoms: hyper<u>c</u>alcemia, <u>r</u>enal insufficiency, <u>a</u>nemia, and lytic <u>b</u>one lesions. Because of the low rate of transformation to myeloma (lifetime risk of 10-30% (Kyle et al., 2010; Sirohi and Powles, 2006; Zingone and Kuehl, 2011)), however, MGUS is not clinically treated, and, due to lack of symptoms, most cases remain undiagnosed until the patient presents with MM.

Epidemiologic and association studies indicate germline risk alleles contribute to MM and MGUS susceptibility. Interestingly, the majority of plasma-cell intrinsic genetic events in MM cells are present in MGUS-affected B-cells (Davies 2003). There is a higher incidence for MM in African Americans that is the result of elevated risk to MGUS, rather than an increased rate of conversion from MGUS to MM (Kyle et al., 2010; Kyle et al., 2006; Landgren et al., 2006). In addition, there is a higher risk of MM in individuals with an MGUS-affected first degree relative (Jain et al., 2009; Kyle et al., 2004; Vachon et al., 2009). Seven common variants

were identified to confer a significant increase in MM risk in patients (Broderick et al., 2012; Chubb et al., 2013). Interestingly, these SNPs also confer increased risk to MGUS, (Weinhold et al., 2014), providing further evidence that MM risk is a consequence of increased risk to MGUS. These studies highlight the necessity for a better understanding of the genetic predisposition to MGUS.

A common spontaneous model for MGUS and MM is the C57Bl/KaLwRij mouse (KaLwRij). KaLwRij has been inbred separate from the other C57Bl strains, including the common wild-type C57Bl/6 (B6) strain, since approximately 1978. KaLwRij mice develop benign idiopathic paraproteineima (BIP), analogous to human MGUS, with a penetrance of ~45% by 12 months of age (Radl and Hollander, 1974; Radl et al., 1978). Affected mice may also progress to overt malignancy (~1%) with similar clinical features as MM, including severe bone pathology (Alici et al., 2004; Asosingh et al., 2000; Vanderkerken et al., 2003). The 5T myeloma cell lines were subcloned from these spontaneous myelomas, and may be transplanted into KaLwRij mice to propagate the myeloma (Radl et al., 1979). Importantly, the 5TMM cell lines will not engraft in closely related C57Bl/6 (B6) mice (Asosingh et al., 2000). Notably, while KaLwRij is a model that recapitulates many features of human disease, the genetic basis of BIP susceptibility in these mice remains unknown.

In this study, we identify *Samsn1* as a candidate gene contributing to inherited risk of KaLwRij mice to BIP, analogous to human MGUS. We used KaLwRij x B6 mouse SNP analysis and a human MM population association study to identify a candidate gene list. We found that KaLwRij mice were null for *Samsn1*, a negative regulator of B-cell activation, and show that *Samsn1* plays a role in B-cells, myeloma cells, and macrophages. We sequenced *Samsn1* in unaffected tissue from MM patients and found genetic variability that suggests that

the SAMSN1 pathway may be relevant to human disease. Together, these data suggest that

Samsn1 underlies predisposition to BIP in KaLwRij mice and that the SAMSN1 pathway may be

involved in human MGUS and MM.

Materials and Methods

Mice

129S1/SvImJ, A/J, AKR/J, BALB/cByJ, CBA/J, C3H/HeJ, C57BL/6J, DBA/2J, FVB/NJ, NOD/ShiLtJ, SJL/J, and NOD-scid –IL2Rγ mice were purchased from Jackson Laboratory (Bar Harbor, ME). C57Bl/KaLwRij mice were originally obtained from Dr. Gregory Mundy at Vanderbilt University. Mice were housed in shared pathogen-free conditions according the guidelines of the Division of Comparative Medicine, Washington University School of Medicine. The animal ethics committee approved all experiments.

Immunization

Mice were immunized with 50 μg chicken gamma globulin (Biosearch Technologies, Novato, CA) in complete or incomplete Freund's adjuvant (Sigma-Aldrich, St. Louis, MO) by intraperitoneal injection at 6 (primary immunization) and 7.5 (boosting immunization) months of age. Blood samples were collected serially as indicated and stored frozen.

Immunoglobulin ELISA

Serum levels of immunoglobulins were monitored by ELISA for IgG and IgG2b according to manufacture's instructions (Bethyl Laboratories, Montgomery, TX).

Serum protein electrophoresis (SPEP)

SPEP test was performed with the SPIFE 3000 analyzer according to the manufacturer's instructions, using SPIFE SPE gel (Helena Laboratories, Beaumont, TX). The protein fractions were quantified by densitometer (QuickScan 2000, Helena Laboratories, Beaumont, TX).

Mouse phylogenetic analysis

KaLwRij genomic DNA was isolated from kidney using DNeasy blood & tissue kit as described by the manufacturer (QIAGEN, Valencia, CA). SNP array analysis was performed using the Affymetrix mouse diversity genotyping array. Sample preparation, hybridization and scanning were performed by Jackson Laboratory according to the standard Affymetrix genotyping protocol. The PHYLIP package (University of Washington, Seattle, WA) was used for the phylogenetic analysis. A distance matrix was created by the Neighbor program based on the KaLwRij and the published SNP data of other 11 strains (Didion et al., 2012; Yang et al., 2009). The neighbor-joining algorithm was used to calculate a phylogenetic tree followed by the Drawtree program for drawing the tree.

B6xKaLwRij mouse strain SNP analysis

SNP analysis was completed as previously described (Burgess-Herbert et al., 2008). KaLwRij SNPs identified from the Affymetrix mouse diversity genotyping array were compared the published SNP data of B6 mice (Yang et al., 2009). All genes annotated in Ensembl mouse genome build 37 with $\geq$ 5 variants were included as candidate genes for further analysis.

Human subjects

DNA for WGAA and sequencing analysis was extracted from skin cells. The study cohort consisting of 183 MM patients and 105 unaffected controls was approved by the Human Research Protection Office at Washington University School of Medicine and at the Mayo Clinic. Informed consent from the patients was obtained in accordance with the Declaration of Helsinki.

81

Whole-genome association analysis (WGAA)

305 MM patients and 353 unaffected volunteers were genotyped using Affymetrix 6.0 platform.

Data was analyzed by logistic regression analysis, adjusted for sex and group using PLINK

software (http://pngu.mgh.harvard.edu/purcell/plink/) (Purcell et al., 2007). SNPs in the 99th

significance percentile were included in further analysis. Genes containing these SNPs were

included as human candidate genes.

Sequencing of *SAMSN1* in MM patients

Coding exons and adjacent intronic regions of *SAMSN1* were sequenced in non-affected tissue

from 183 MM patients and 105 unaffected volunteers by the Genome Technology Access Center

at Washington University School of Medicine. PCR amplicons were constructed using the

Fluidigm Access Array (Fluidigm, San Francisco, CA). Samples were harvested and indexed

using the BioMark HD system (Fluidigm, San Francisco, CA). Samples were pooled into

sample libraries and sequenced on a MiSeq sequencer (Illumina, San Diego, CA). Following

annotation, variants in the case and control population were analyzed using logistic regression of

reference allele dosage in cases and controls.

Immunoblotting

Western blot was performed as previously described(Chu et al., 2012). Antibodies: SAMSN1

(Sigma-Aldrich, St. Louis, MO), actin (Sigma), and GFP (Santa Cruz Biotechnology, Dallas,

TX). Blots were incubated with horseradish conjugated secondary antibodies (GE Healthcare,

Fairfield, CT) and visualized by chemiluminescence (Pierce Biotechnology, Rockford, IL).

Primary cell culture

Splenic B-cells were negatively selected via MACS with anti-CD43 beads (Miltenyi Biotec,

Cologne, Germany). Cells were cultured in RPMI1650 media, 10% FBS, BME, 1% penicillin-

streptomycin and stimulated with 10 ng/ml LPS and 20 ng/ml IL-4 for 72 hours. To generate

macrophages, whole bone marrow or peritoneal fluid was cultured in αMEM, 10% FBS, 1%

penicillin-streptomycin, 50 ng/ml MCSF for 3 days (bone marrow macrophages) or 12 hours

(peritoneal macrophages). Proliferation was measured by standard MTT assay (Sigma-Aldrich,

St Louis, MO). M2 polarized macrophages were generated by stimulating day 3 bone marrow

macrophages with 5 ng/ml IL-4 for 24 hours. Osteoclasts were generated by culturing bone

marrow macrophages in 50 ng/ml MCSF and 50 ng/ml RANKL for 3 days. Bone marrow

macrophages were generated by plating whole bone marrow cells in ascorbic acid-free αMEM,

10% FBS, 1% penicillin-streptomycin for 7 days in 5% oxygen followed by negative selection

via MACS with anti-CD45 beads (Miltenyi Biotec, Cologne, Germany).

5TGM1 cell culture

The 5TGM1 murine myeloma line was originally obtained from Dr. Gregory Mundy at

Vanderbilt University. 5TGM1 stably overexpressing *Samsn1* were generated using lentivirus

transduction. Briefly, full-length mouse *Samsn1* cDNA was subconed into an MSCV-PGK-Puro

plasmid (MPP). To generate lentivirus, SAMSN1-MPP or MPP control and lentiviral vectors

pCMVΔ8.9 and pM2G were transfected into HEK293T cells. Cell supernatant containing

lentivirus was then plated on 5TGM1 cells and selected with puromycin for 72 hours. *Samsn1*

expression was assayed by Western Blot. Cells were maintained in DMEM, 10% FBS, 1%

penicillin-streptomycin. Proliferation was measured by BrdU ELISA according to the

manufacture's instructions (Roche Diagnostics, Indianapolis, IN).

M2-macrophage injection into 5TGM1 subcutaneous tumors

1×10^6 5TGM1 cells were injected subcutaneously in the right flank of NOD-scid –IL2Rγ female

mice. 14 days following tumor inoculation, 3×10^6 in vitro M2 polarized macrophages from B6

or KaLwRij mice were injected directly into the tumor. Tumor burden was monitored by serum murine IgG2b ELISA (Bethyl Laboratories, Montgomery, TX).

Macrophage comparison by microarray

Bone marrow macrophages were isolated from B6 and KaLwRij mice (n = 3 biologic replicates) and RNA extracted using RNeasy Mini kit (Qiagen, Venlo, Netherlands). RNA samples were submitted to the Genome Technology Access Center at Washington University School of Medicine for hybridization using the GeneChip Mouse Gene 1.0 ST array (Affymetrix, Santa Clara, CA). Data was analyzed using Partek Genomics Suite (Partek Inc., St. Louis, MO). Differentially expressed genes were based on changes of 1.5 fold or more between B6 and KaLwRij.

Quantitative reverse-transcription PCR

RNA was extracted using RNeasy Mini kit (Qiagen, Venlo, Netherlands) and cDNA generated using iScript (Bio-Rad, Hercules, CA). Quantitative PCR was completed using SsoFast EVA Green Supermix (Bio-Rad, Hercules, CA). All samples run with biological replicates of ≥ 2. Primer sequences (forward/reverse):

Cyclophilin: AGCATACAGGTCCTGGCATC / TTCACCTTCCCAAAGACCAC

Samsn1: TTCACGCCAAGTCCCTATGAC / TTCCCATTGGTGTTTTGCACATA

FIZZ1: GCTGATGGTCCCAGTGAATA / CGTTACAGTGGAGGGATAGTTAG

YM1: GGGCATACCTTTATCCTGAG / CCACTGAAGTCATCCATGTC

VEGF: GGAGAGCAGAAGTCCCATGA / AGATCTCCACCAGGGTCTCA

DNA amplification

Genomic DNA was extracted from tail tissue or 5TGM1 culture using DNeasy blood & tissue kit as described by the manufacturer (QIAGEN, Valencia, CA). DNA was amplified using standard

PCR and amplified products were visualized on an agarose gel stained with ethidium bromide under UV light.

Primer sequences (forward/reverse):

Gapdh: ACTTTGTCAAGCTCATTTCC / TGCAGCGAACTTTATTGATG

Samsn1 exons:

exon 1: TCACCAAGTGCTTTCCTTCC / AAGGCAGCAACGTGACATAA

exon 2: AGTCTTCATCATGCCCTTGG / GTTGCTTGGCAGATGGAGTT

exon 3: AACACACACACCGCCAAAGT / CCAAACCTCTTTCCAAACACA

exon 4: TCCCTTTTCAGGTTTCATGG / CTGGGACTAAACCCCCAATC

exon 5: CATCCGAGGACCACTGTTTT / TTTGCCTTTTCCTTCACCTG

exon 6: GGGTTCATCCCATTTTGTTG / TCTCACCTGCTTCCTGGACT

exon 7: TTCCTGGCTTATCCTGTGCT / GGAGCATCTCTGATCTTTGGA

exon 8: TAATGGGGGAAGGGATTAGG / AATGTCCTTACCTAACTCAGAAAAAT

exon 9: AGGCAGCCTGTTGAACAAT / TGTCCCAACTTAAACAATGCAC

exon 10: AATTGCAGTTGAATTCCACAAT / CATTGCACCAGATCCCTGTA

exon 11: ATGCCCTTTAAGGCAGATCA / TGCTAACAGCCACAGTCGAT

exon 12: CCCAGCACATATGAGTGAGTACTAT / GAACTGTTCTAGGAAATCAGGTTTA

Statistics

Data are shown as mean +/- SEM. Unless otherwise indicated, experiments were analyzed using Student's t-test or 1-way ANOVA as appropriate.   Sequencing results were considered to reach significance at $p < 0.05$. $*p < 0.05$; $**p < 0.01$; $***p < 0.001$.

Results

KaLwRij mice are an inbred strain susceptible to BIP

The KaLwRij mouse strain is reported to have a high frequency of BIP (Radl et al., 1978). KaLwRij has been inbred separately from the other C57Bl strains, including B6, for over 30 years.   To evaluate the relatedness of KaLwRij to B6 and other common lab strains, we performed high-density mouse SNP array analysis using KaLwRij genomic DNA. The genetic distance values were estimated based on the comparison between the KaLwRij SNP data and the published single nucleotide polymorphism (SNP) data of 11 mouse strains (Yang et al., 2009), selected for relative genetic diversity. These data demonstrated that, while closely related to B6, KaLwRij is a unique inbred strain (**Figure 3.1a**).

We hypothesized that the predisposition of KaLwRij mice to BIP and myeloma would be reflected in a unique antibody response to immune challenge. We evaluated immune response in KaLwRij and the other 11 strains of mice. We treated mice with a primary and boosting immunization, collected serial serum samples, and performed immunoglobulin ELISA and serum protein electrophoresis (SPEP) (**Figure 3.1b**). We quantitated immunoglobulin isotypes IgG (**Figure 3.1c**), IgM, and IgA. Differences in antibody isotype response among strains were highly significant, indicating that immunoglobulin response was influenced by genetic background.

In patients, SPEP is used to screen for the presence of clonal serum immunoglobulin (**Figure 1.4a**). In mice, an abnormal peak in the gamma fraction suggests an accumulation of monoclonal protein (M-spike) and indicates BIP, analogous to human MGUS. Most strains presented with an M-spike post-primary or post-boosting immunization, indicating a normal

immune response. By 18 months, however, the highest frequency of sustained M-spike was found in KaLwRij (**Table 1**.**1**). Notably, the M-spike incidence in its closest related mouse strain, B6, had resolved.

Our initial intention to map quantitative trait loci underlying murine BIP was confounded by the fact that the ELISA profiles we obtained appeared to reflect heterogeneity of normal immune responses rather than BIP development, and the SPEP signal took 18 months to manifest, making repeated crosses impractical.

SNP analysis identified 418 genes divergent between B6 and KaLwRij haplotypes

To identify candidate loci underlying susceptibility to BIP, we compared B6 and KaLwRij genotypes using high-density genome-wide SNP data. Of the 562,061 SNPs queried across the 19 mouse autosomes, 21,133 SNPs varied between KaLwRij and B6. 11,323 were single nucleotide variation (53.6% of variation observed), while the remaining 9,810 SNPs grouped into 3,468 blocks of two or more consecutive non-identical SNPs. Included in the observed SNP variation between B6 and KaLwRij, SNP no-calls in KaLwRij were also identified. While most of these were solitary, there were 48 groups of two or greater consecutive SNP no-calls, suggesting possible deletions affecting the locus. The largest blocks of no-calls (two instances of 6 SNPs) fall in the *Samsn1* locus that contains a total of 22 no-calls, the highest number of observed in a single gene locus.

SNP blocks of two or greater fell within a total of 1,519 gene loci, with the highest number of variants in *Ptprt*, containing 128 polymorphic SNPs between B6 and KaLwRij. For subsequent analysis, we used an arbitrary cut-off off blocks of five or greater consecutive SNPs, representing 56.1% of all SNPs that group in blocks of two or greater (**Figure 3.2a**). This

defined a ranked candidate gene list of 418 genes that many contribute to BIP susceptibility in KaLwRij mice (**Table 3.2**).

Association analysis of MM patients identified common variants in 180 genes

Inherited genetic susceptibility to MM is likely due to increased risk of MGUS, rather than increased risk of MGUS-to-MM transformation. We next sought to identify genetic loci contributing to increased risk of human MGUS and MM. We performed whole-genome association analysis (WGAA) in a Caucasian population of MM patients (n=305) and healthy controls (n=353) to identify common genetic variation associated with MM and its requisite precursor MGUS (**Figure 3.2b**). Relatively low sample size resulted in overall decreased significance of SNPs, and only one SNP (rs1029654 in an intergenic region) reached genome-wide significance ($p < 5 \times 10^{-8}$). Therefore, to encompass all possible genetic variation contributing to MGUS and MM risk, we queried SNPs in the 99th significance percentile as differentially represented in MM patients versus controls (343 SNPs). This identified a candidate gene list of 180 genes that may contribute to MM risk in humans (**Table 3.3**).

Integrating murine BIP and human MM genetic analyses identified 5 shared genes

To further narrow our gene list and ensure that we pursued loci of clinical relevancy, we employed an integrative cross-species approach. Combining the murine KaLwRij x B6 SNP analysis (418 genes) and human MM patient WGAA analysis (180 genes) yielded five shared genes (**Figure 3.3a**). These genes are likely to contribute to inherited susceptibility to both human MGUS/MM and murine BIP/myeloma: *Fstl14, Samsn1, Ccm2, Tenm2,* and *Csmd1* (**Figure 3.3b**).

88

KaLwRij mice have a germline homozygous deletion of *Samsn1*

MGUS is a syndrome characterized by a clonal expansion of plasma B-cells and increased monoclonal immunoglobulin production; therefore, *Samsn1*, a negative regulator of B-cell function, drew particular interest. In activated B-cells, SAMSN1 is an adaptor protein in a B-cell signaling inhibitory complex, binding SHP-1/2 and the ITIM domain of PIR-B (Wang et al., 2010; Zhu et al., 2004). We hypothesized that inactivating SNPs in the *Samsn1* locus of KaLwRij would lead dysregulation of B-cells, increased B-cell activation, and subsequent BIP development.

Close inspection of the KaLwRij SNP array data at the gene locus (Chromosome 16: 75,858,793-76,022,270; SNPs encompassing Chromosome 16: 75,815,371-75,999,906) revealed that 29 no-calls in KaLwRij, suggesting a gene deletion (**Figure 3.4a**). We amplified the coding regions of *Samsn1* from DNA of KaLwRij and B6 by PCR. Surprisingly, all protein-coding exons 1-12 of *Samsn1* failed to amplify from KaLwRij germline DNA, further implying deletion of the locus (**Figure 3.4b**). To confirm loss of protein expression anticipated by gene deletion, we probed for SAMSN1 in splenic B-cells treated with IL-4 and LPS. Following treatment, SAMSN1 was strongly expressed in B6 B-cells, but not in KaLwRij B-cells (**Figure 3.4c**). Together, these data indicate a homozygous germline deletion of the *Samsn1* gene in KaLwRij mice.

KaLwRij mice have enhanced B-cell function

SAMSN1 has been shown to regulate B-cell activity, likely through its interactions with the B-cell inhibitory protein PIR-B (Zhu et al., 2004). Samsn1-/- mice have enhanced B-cell function compared to wild type, with increased proliferation in purified splenic B-cell culture

and increased immunoglobulin response following immunization in vivo (Wang et al., 2010). To

evaluate whether KaLwRij mice showed similar increased B-cell activity, we cultured purified

CD43- splenic B-cells from KaLwRij and B6 mice. Importantly, we demonstrated loss of

SAMSN1 in KaLwRij cells, while purified splenic B-cells from B6 mice showed increased

levels of SAMSN1 protein following stimulation with IL-4 and LPS (**Figure 3.4c**). Next, we

measured proliferation of cultured primary B-cells in response to IL-4 and LPS stimulation by

MTT assay. KaLwRij B-cells displaced enhanced proliferative response to B-cell activation

compared to B6 (**Figure 3.5a**).

To test whether KaLwRij mice also had increased B-cell activity in vivo, we immunized

6 month old KaLwRij and B6 mice (**Figure 3.1b**) and monitored immunoglobulin response until

the mice reached 24 months of age. KaLwRij mice had a significant and progressive elevation in

IgG2b levels, first evident after primary immunization and continuing throughout the entirety of

the experiment, more than a year following immunization (**Figure 3.5b**). Therefore, we

demonstrated that KaLwRij mice showed considerable B-cell phenotypic overlap with Samsn1-/-

mice, both in vitro and in vivo.

***Samsn1* decreases KaLwRij MM cell line 5TGM1 proliferation**

The murine 5T myeloma cell lines were originally isolated from a myeloma-bearing

KaLwRij mouse (Asosingh et al., 2000; Radl et al., 1979), and subsequent subclones were

isolated, including 5TGM1. We confirmed *Samsn1* deletion in 5TGM1 by PCR and RT-qPCR

(**Figure 4.6a-b**). Because *SAMSN1* is down regulated in many human MM cell lines (Claudio et

al., 2001), and because of *Samsn1*'s role in regulating murine B-cell activation, we hypothesized

that *Samsn1* was a myeloma-cell intrinsic tumor suppressor. 5TGM1 cells with stable

overexpression of *Samsn1* had decreased proliferation compared to control under both basal and IL-6 stimulated conditions (**Figure 3.6b-c**). These data suggest that *Samsn1* contributes in part to myeloma tumor growth through a cell-intrinsic mechanism, consistent with its published anti-proliferative role (Wang et al., 2010; Zhu et al., 2004).

KaLwRij mice have an altered MGUS- and MM-supportive bone microenvironment

Germline risk alleles to MGUS and MM may also influence cell types beyond pre-malignant plasma B-cells. MGUS and MM are both characterized by bone microenvironment contributions from host cells including macrophages, bone marrow stromal cells, and osteoclasts (reviewed in (Kuehl and Bergsagel, 2002)). Differential gene expression in whole bone marrow of KaLwRij and B6 mice has been previously demonstrated (Fowler et al., 2011), but individual cell-type gene expression variation has not been evaluated.

To query specific components of the BIP- and myeloma-supportive bone microenvironment we cultured primary macrophages and CD45- bone marrow stromal cells from whole bone marrow of B6 and KaLwRij mice. Microarray analysis identified 31 differentially expressed genes, including *Samsn1,* in bone marrow macrophages (**Figure 3.7a**, **Table 3.4**) and eight differentially expressed genes in bone marrow stromal cells (**Figure 3.7b**, **Table 3.5**). Notably, six genes from the macrophage analysis (*Tnfrsf26, Samsn1, Lyrm7, Sparc, Lrrc27,* and *Qpct*) and three genes from the stromal cell analysis (*Tnfrsf26, Tnfrsf23,* and *Lyrm7*) are included in the list of candidate genes underlying genetic susceptibility to BIP in KaLwRij mice (**Table 3.2**).

We verified the *Samsn1* expression observed in the bone marrow macrophage and bone marrow stromal cell microarrays, and confirmed that bone marrow macrophages express *Samsn1*

while bone marrow stromal cells are non-expressors (**Figure 3.7c**). To further evaluate the role of *Samsn1* in other BIP- and myeloma-supportive host microenvironment cells, we cultured primary peritoneal macrophages and differentiated osteoclasts from bone marrow macrophages. Osteoclasts expressed low but detectable levels of *Samsn1*. Peritoneal macrophages were high *Samsn1* expressors, with 70-fold higher levels than bone marrow macrophages (**Figure 3.7c**). As a population, peritoneal macrophages are more mature and have increased activation compared to bone marrow macrophages, likely due to recruitment to the peritoneal cavity in response to infection (Wang et al., 2013). These data suggest that *Samsn1* may play a role in macrophage activation.

Enhanced macrophage function in KaLwRij mice

Gene expression data from bone marrow macrophages and peritoneal macrophages suggest that *Samsn1* may contribute to macrophage function, similar to its role in B-cells. Notably, SAMSN1 binding partners (PIR-B and SHP-1/2) and pathway members (Syk, PI3K, among others) in B-cells, also participate in macrophage biology (Brenner et al., 2004; Munitz et al., 2010; Xie et al., 2014). To assess macrophage activity in *Samsn1*-null KaLwRij mice, we cultured bone marrow macrophages from whole bone marrow and measured proliferation by MTT assay. We found that KaLwRij macrophages had increased proliferation compared to B6 (**Figure 3.8a**).

Tumor associated macrophages (TAMs) are established host microenvironment contributors to myeloma pathogenesis (reviewed in (Asimakopoulos et al., 2013; Berardi et al., 2013; Ribatti et al., 2013)). TAMs are broadly classified as anti-tumor M1 macrophages and pro-tumor M2 macrophages. In vitro, macrophage polarization to M1 requires stimulation with

interferon-gamma, while polarization to M2 is induced upon addition of IL-4. Under basal

conditions, that is, without the addition of any stimulatory cytokines, we found that KaLwRij had

significant and dramatic elevation of M2-macropahge markers FIZZ1 and YM1 in both bone

marrow macrophages (**Figure 3.8b**) and peritoneal macrophages (**Figure 3.8c**). TAMs from

MM patients promote tumor growth through vasculomimicry, including increased expression of

pro-angiogenic VEGF. We found that KaLwRij had increased levels of VEGF transcription

compared to B6 in both bone marrow (**Figure 3.8b**) and peritoneal (**Figure 3.8c**) macrophage

cultures. These data suggest that under homeostatic conditions, KaLwRij macrophages are

skewed towards a pro-tumor M2 polarization phenotype.

To evaluate the ability of KaLwRij M2 macrophages to promote tumor growth in vivo,

we inoculated 5TGM1 myeloma cells subcutaneously in NOD-scid –IL2Rγ mice. Once tumors

were established (day 14), we injected B6 or KaLwRij ex vivo M2-polarized macrophages

directly into the tumor and monitored tumor growth by IgG2b, the 5TGM1 Ig clonotype (**Figure

3.8d**). Tumors injected with KaLwRij M2 macrophages had significantly increased tumor

growth as measured by serum IgG2b compared to tumors injected with B6 M2 macrophages

(**Figure 3.8e;** representative tumors **Figure 3.8f**). Together, these findings indicate that

KaLwRij macrophages have enhanced activation and contribute to myeloma pathogenesis.

***SAMSN1* genetic variation in unaffected tissue of MM**

To directly investigate the impact of *SAMSN1* to confer risk in patients, *SAMSN1* exome

sequencing was performed on non-affected tissue from MM patients (n=183) and healthy

controls (n=105). In total, we identified 38 SNPs contained in the protein coding regions, 5' and

3' untranslated regions (UTR), and exon/intron boundaries (**Table 3.6**). Of these, 15 SNPs only

occurred in one individual. While the majority of variants were previously known and annotated in the dbSNP database, we identified six novel SNPs, all private variants. Of the annotated SNPs, six fell in the 3'UTR, three in the 5'UTR, and two SNPs were located in exon/intron splice regions. In addition, we observed seven annotated missense variants. The remainder 20 SNPs were silent mutations or fell in intronic regions or were unannotated. Two variants reached statistical significance, rs2822790 (OR = 0.5098, p = 0.0472) and rs2822792 (OR = 0.5098, p = 0.0472). Both variants were present at lower frequency in MM cases (4.12%) than controls (8.09%), suggesting that the alternate allele may be protective. While few SNPs reached statistical significance, the variability observed in MM patients suggests that the *SAMSN1* pathway may play a role in human MGUS and MM pathogenesis.

Discussion

Using a combinatorial genetics approach, we identified genes underlying inherited susceptibility to MGUS and MM in humans and in mice. Specifically, this study identifies *Samsn1* as a novel MGUS/MM susceptibility gene, likely conferring risk via effects in both pre-neoplastic B-cells as well as host supportive macrophages. We found that KaLwRij mice are null for *Samsn1,* reported to have decreased expression in human MM cell lines (Claudio et al., 2001), thus providing compelling evidence that *Samsn1* is a permissive allele in both mouse and human pathogenesis. KaLwRij mice phenocopied the published enhanced B-cell response in Samsn1-/- mice (Zhu et al., 2004). We further found a cell-intrinsic role for *Samsn1* as a tumor suppressor in malignant myeloma cells. We identified a novel putative role for *Samsn1* in macrophages, with KaLwRij macrophages exhibiting enhanced macrophage activation under basal conditions and increased ability to enhance myeloma growth in mice. Finally, we found two SNPs at reduced frequency in a MM patient population, providing further evidence that germline variants *SAMSN1* may confer increased risk to MGUS and MM in humans. Together, these data indicate that *Samsn1* confers risk to murine BIP and human MGUS with roles both in the pre-neoplastic B-cell and in the host macrophages.

While KaLwRij mice are a widely used spontaneous model of MGUS and MM, the genetic basis for its susceptibility to BIP remains largely unknown. SNP analysis of KaLwRij x B6 revealed more than 1000 genes containing multiple variants, including several deletions, in the KaLwRij strain. We generated a candidate gene list underlying inherited susceptibility to BIP in KaLwRij of 418 genes. Importantly, it is likely that multiple genes contribute to the

complex trait of BIP, and investigation of additional candidate genes in KaLwRij mice is underway.

To query genetic loci conferring risk to human MGUS and MM and ensure that we were pursuing genes with clinical relevancy in the KaLwRij mouse model, we completed a WGAA of human MM patients and healthy controls. Typically, sample sizes of greater than 2000 cases and controls are necessary to identify causal variants in WGAA; published MM WGAA analyzed 1675-4692 cases and 5903-10990 controls to identify risk loci with genome-wide significance (Jain et al., 2009; Kyle et al., 2004; Vachon et al., 2009). In the study described here, low sample size (205 cases, 353 controls) resulted in overall decreased significance of SNPs. To ensure inclusion of all biologically significant genetic variation, therefore, we queried SNPs in the 99th significance percentile that fell in 180 gene loci. Importantly, we identified SNPs in three of the seven previously published genetic loci associated with MGUS and MM risk (2p23.3, 3p22.1, and 7p15.3), validating our approach.

Finally, in order to identify candidate genes for biologic validation in the KaLwRij mouse model, we combined the mouse and human gene sets. This approach ensures clinical relevancy of further work in gene variant validation and investigation of biologic function. Moreover, combining the mouse and human datasets also guarantees that the human variants of interest have a murine counterpart, providing a practical, relevant, and immediate mouse model. Using this integrative approach, we identified five genes that may underlie susceptibly murine BIP and also contribute to MGUS and MM risk in patients.

Because it has been implicated in human MM cell lines and has an established role in regulating B-cell activation, we investigated the *Samsn1* locus in the KaLwRij mouse strain. Surprisingly, we found that KaLwRij had homozygous germline deletion for the coding regions

of *Samsn1*. Moreover, KaLwRij mice have a similar phenotype as the the published enhanced B-cell response of *Samsn1*-/- mice with increased B-cell proliferation in vitro and enhanced and sustained antibody response in vivo (Wang et al., 2010). These data strongly indicate that loss of *Samsn1* in pre-malignant plasma B-cells confers increased risk of developing BIP in mice.

Next, we evaluated the role of *Samsn1* in myeloma cells. In human MM cell lines, *Samsn1* expression is dramatically reduced (Claudio et al., 2001), suggesting a role as a tumor suppressor in myeloma. Like the KaLwRij mouse, the KaLwRij-derived myeloma cell line 5TGM1 is null for *Samsn1*. Overexpression of *Samsn1* in 5TGM1 reduces in vitro proliferation under both basal and pro-tumorigenic conditions. These data provide compelling evidence that *Samsn1* is a myeloma-autonomous intrinsic negative regulator of tumor growth.

While it is well established that genetic risk factors contribute to susceptibility to MM, the majority of genetic alterations in MM cells are already present in MGUS plasma cells (Davies et al., 2003). These data suggest that plasma-cell extrinsic factors contribute to the conversion of MGUS to MM. Rather than being confined to the affected plasma cell, it is likely that genetic susceptibility alleles are expressed in both the pre-malignant B-cell and in supportive host microenvironment cells.

To investigate specific cell types of the bone microenvironment in BIP-susceptible KaLwRij mice, we completed gene expression analysis of B6 and KaLwRij bone marrow macrophages and bone marrow stromal cells. 31 genes were differentially expressed in B6 and KaLwRij bone marrow macrophages, and eight genes were differentially expressed in bone marrow stromal cells. Interestingly, six of the 31 differentially expressed macrophage genes (including *Samsn1*) and three of the eight differentially expressed stromal cell genes contain germline variants in KaLwRij mice as identified in the B6xKaLwRij SNP analysis. This

97

suggests that genetic variation likely influences these genes' macrophage expression and provides further evidence of B-cell extrinsic activity of BIP susceptibility alleles.

Samsn1 is expressed in many cells of the hematopoietic lineage, and we found that *Samsn1* is expressed by bone marrow macrophages and, to a greater extent, peritoneal macrophages from B6 mice. Increased expression in the more mature peritoneal macrophages compared to bone marrow macrophages led us to hypothesize that *Samsn1* may participate in macrophage activation via similar mechanisms as its role in B-cells.

Host tumor-associated macrophages (TAMs) have been implicated in promoting MM progression. Macrophages from MM patient bone marrow are functionally distinct from bone marrow macrophages from MGUS patients (Scavelli et al., 2008). MM tumor-associated macrophages (TAMs) support MM progression directly through elevated secretion of pro-tumorigenic factors such as IL-6 (Kim et al., 2012; Zheng et al., 2009) and by promoting angiogenesis through elevated expression of VEGF (Ribatti et al., 2006; Scavelli et al., 2008; Vacca and Ribatti, 2011).

We investigated KaLwRij macrophages to determine whether they had increased capacity to support BIP- and myeloma cells. Non-stimulated KaLwRij bone marrow macrophages and peritoneal macrophages had significantly increased macrophage activation, with elevated pro-tumorigenic M2 macrophage markers. These data suggest that, similar to its role in B-cells, *Samsn1* negatively regulates macrophage activation. Importantly, we further demonstrated that KaLwRij M2-polarized macrophages potently increased myeloma tumor growth in vivo. Together, these data indicate that KaLwRij *Samsn1*-null macrophages have enhanced macrophage response and a greater capacity to support tumor growth in vivo.

Finally, we sought to identify whether *SAMSN1* germline variants confer risk to MM in a patients. We sequenced *SAMSN1* in 183 MM patients and 105 controls. We observed 38 SNPs and identified six rare variants that are not annotated in the dbSNP database. Two SNPs had greater frequency in the control population, suggesting that they may confer MM or MGUS resistance. Further GWAS studies and sequencing of normal tissue from MM patients in necessary to validate and expand upon these findings. *SAMSN1* does not represent the only possible locus for genetic lesions; variation in other members of the SAMSN1 signaling pathway likely also contribute to MM susceptibility. Further work is necessary to elucidate binding partners and downstream effects of SAMSN1 in human cells, and in different cell types including macrophages.

Described here is a novel integrative approach to identify candidate genes contributing to risk of murine BIP and human MGUS and MM. Combining mouse and human datasets was successful in identifying genes relevant to human disease, including *Samsn1*. BIP-prone KaLwRij mice harbor a homozygous deletion of *Samsn1*, the first germline mutation identified in the KaLwRij strain. We demonstrate that *Samsn1* plays functionally important and cell-autonomous roles in multiple cell types involved in MM pathogenesis, including B-cells (as previously published), in myeloma cells, and in host supportive macrophages. Importantly, while our work focused on the role of *Samsn1*, other identified genes listed are also promising candidates to influence MM risk in multiple cell types, and work is ongoing to investigate these candidates. In particular, candidate gene *Fstl4* is especially intriguing with possible downstream effects on B-cell immunoglobulin production and M2 macrophage activation (Ogawa et al., 2008; Sierra-Filardi et al., 2011). In conclusion, this work informs and prioritizes ongoing and future human genetics studies and mechanistic studies in mice. It is highly likely that SAMSN1

and other members of its pathway play important roles in MGUS and MM pathogenesis in humans, and future work will further define the effects of *Samsn1* in myeloma progression as well as explore other risk loci contributing to MGUS and MM susceptibility.
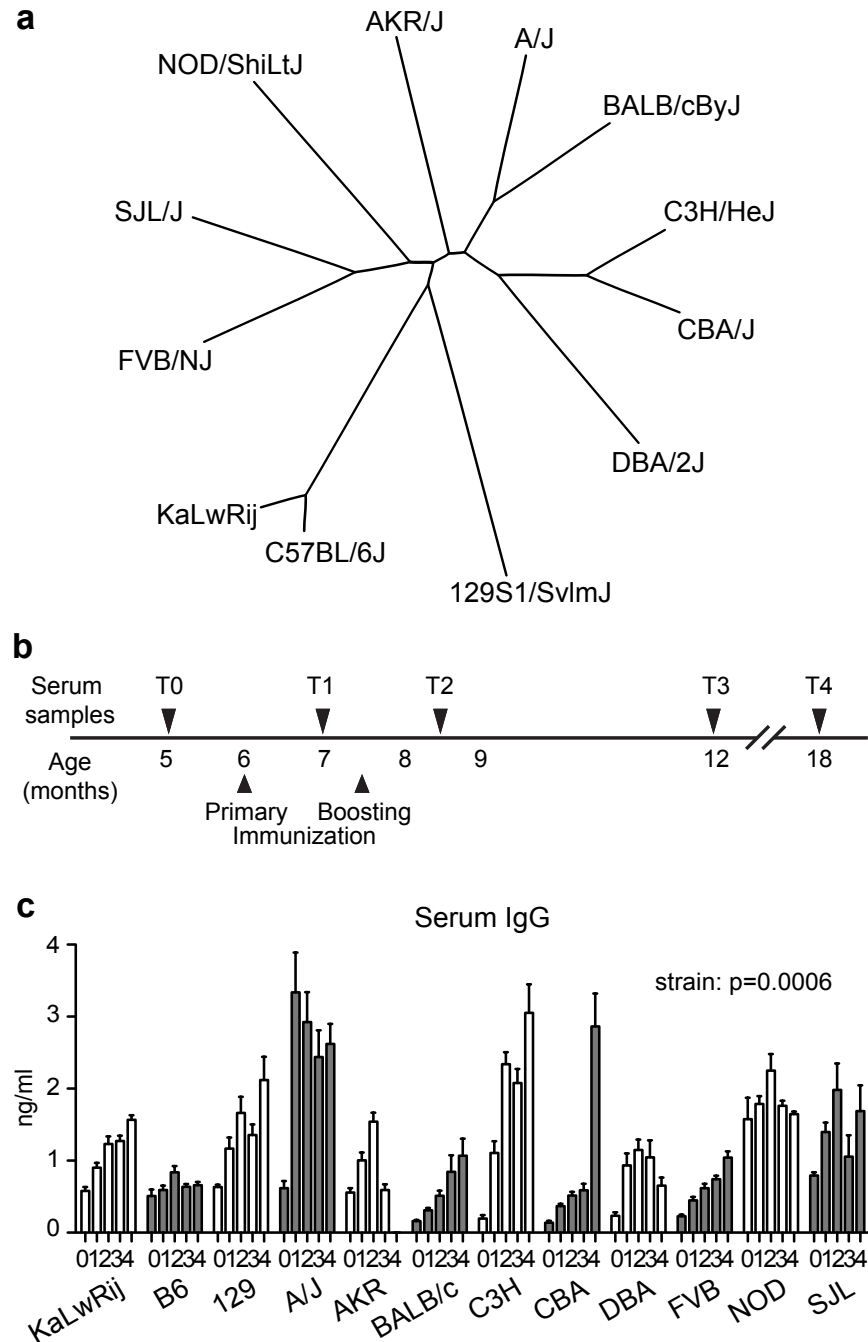
Figure 3.1.
Immunoglobulin responses are significantly different between mouse strains.
(a) Phylogenetic tree demonstrating genetic distances of 12 strains of mice by whole genome SNP array. (b) Schema for immunization and serial serum sample protocol. Serum was collected at baseline (T0), post-primary immunization (T1), post-boosting immunization (T2), 12 months (T3), and 18 months (T4). (c) Serum IgG analysis of serial serum samples by ELISA.
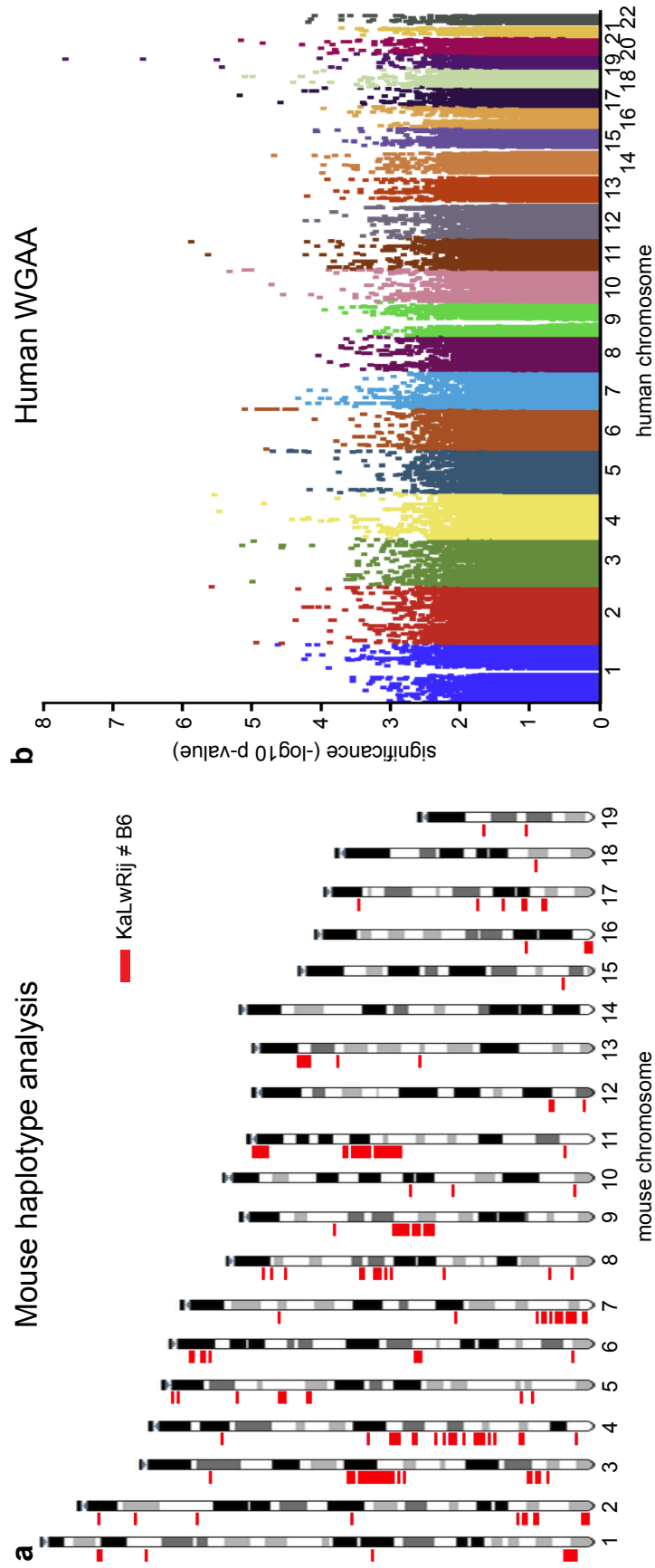
Figure 3.2.

Mouse and human genetic analyses identify candidate genes that may influence risk to BIP in mice and MM in humans

(a) Haplotype analysis identified contiguous regions of non-shared polymorphic alleles between KaLwRij and B6 mice (red bars) in 419 genes. (b) GWAS between MM patients and healthy volunteers. SNPs in the 99th percentile fell in 180 genes.

a
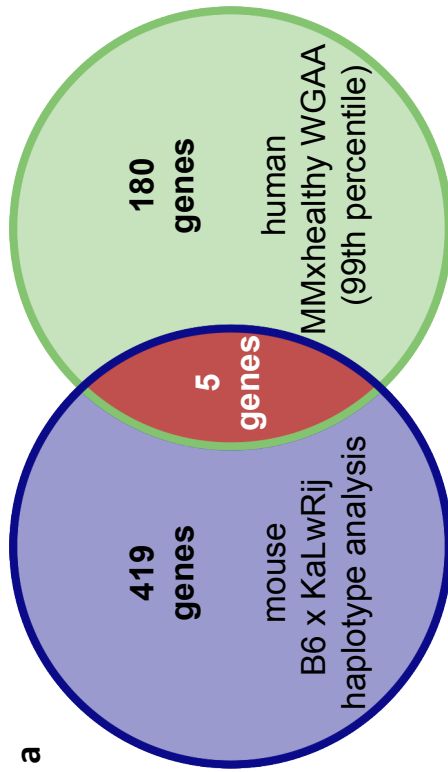
b

Gene	Mouse		Human		
	Chr	Score	Chr	SNP	P-value
Fstl4	11	54	5	rs11242158	0.00043280
Samsn1	14	33	21	rs12626593	0.00040510
Ccm2	11	11	7	rs10951785	0.00023090
Tenm3	8	6	4	rs12504374	0.00000300
Csmd1	8	5	8	rs17414486	0.00040130

Figure 3.3.

Combinatorial genetic approach identified a candidate gene list underlying human MGUS and murine BIP.

(a) Venn diagram representing combined analysis of **Figure 3.3 a** and **b** (b), resulting in a candidate gene list of 5 genes (b).

103
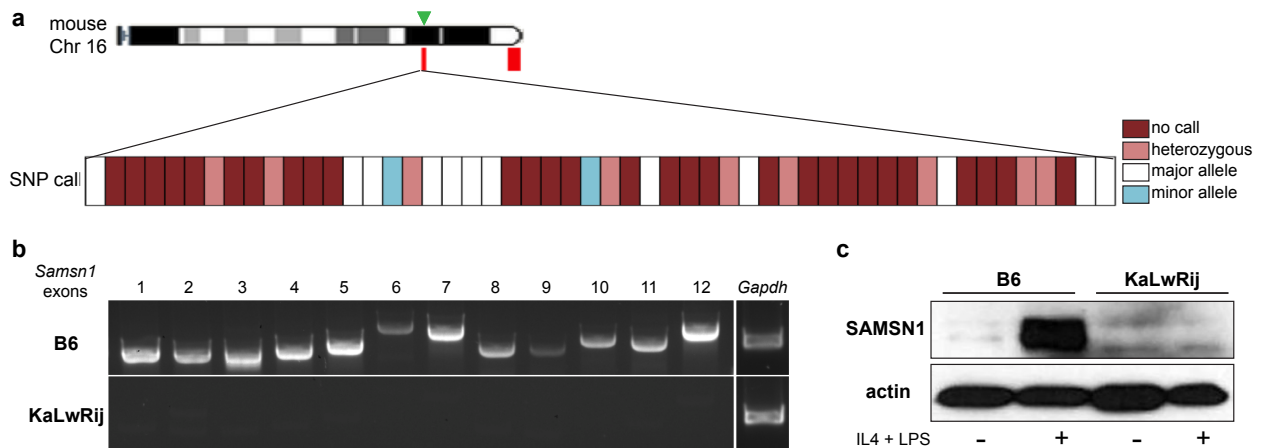
Figure 3.4.
The *Samsn1* locus is deleted in KaLwRij mice.
(a) Mouse chromosome 16 map.   Red regions are non-shared polymorphic alleles between KaLwRij and B6 mice; green arrowhead indicates MM WGAA SNP rs12626593.   Closer analysis of the region of *Samsn1* covered by the high-density genotyping SNP array (Chr16: 75,815,371–75,999,906).   Boxes represent SNP calls (red = no-call; pink = heterozygous; white = reference allele (B6); blue = alternate allele).   (b) PCR amplification of exons 1-12 of *Samsn1* and *Gapdh* control from B6 and KaLwRij tail DNA.   (c) Western blot analysis of SAMSN1 in CD43- splenic B-cells from B6 or KaLwRij mice stimulated with IL-4 and LPS for 72 hours.
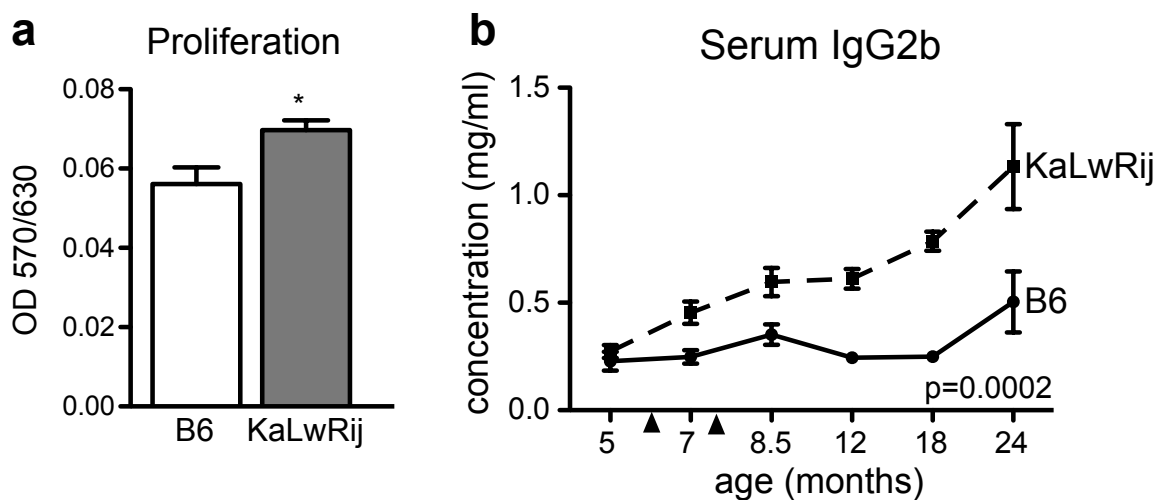
Figure 3.5.
Enhanced B-cell response in KaLwRij mice.
(a) CD43- splenic B-cells were stimulated with IL-4 and LPS for 72 hours.   Cell proliferation was measured by MTT. (b) Mice were immunized (arrowheads indicate primary and secondary immunization) and serial serum samples collected. Levels of IgG2b were determined by ELISA.
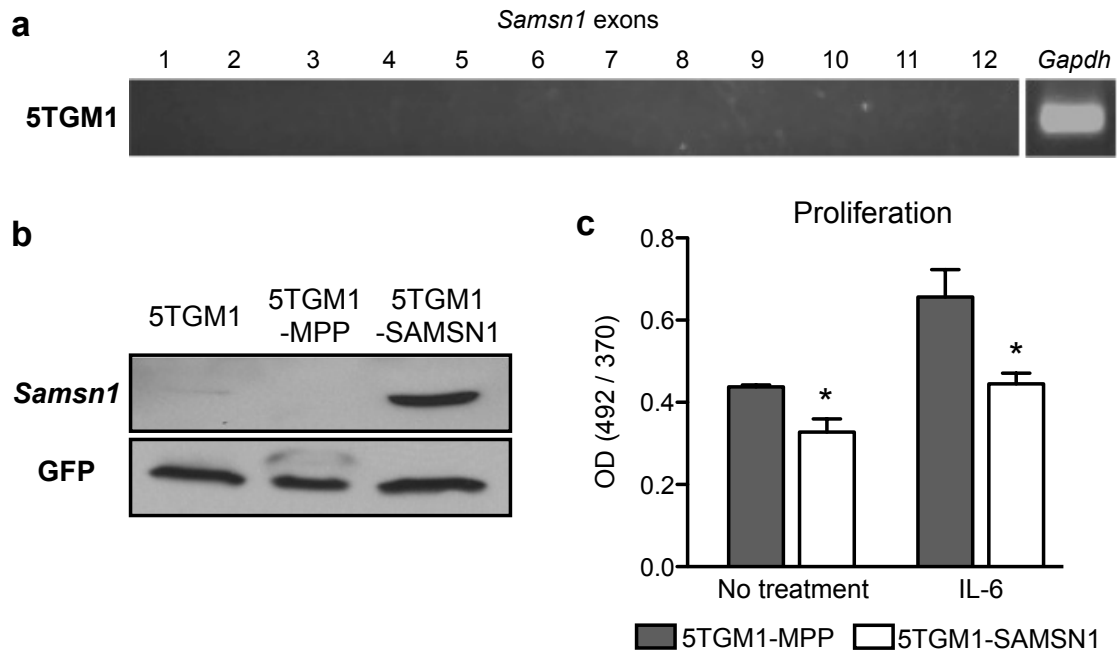
Figure 3.6.
***Samsn1* inhibits proliferation in KaLwRij myeloma cell line 5TGM1.**
(a)   PCR amplification of exons 1-12 of *Samsn1* and *Gapdh* control from the KaLwRij-derived 5TGM1 cell line DNA.   (b) RT-qPCR for *Samsn1* in parental 5TGM1 cells, control vector cells (5TGM1-MPP), and cells overexpressing *Samsn1* (5TGM1-SAMSN1).   (c) 5TGM1-MPP and 5TGM1-SAMSN1 cells were stimulated with IL-6 for 24 hours. Cell proliferation was measured by BrdU incorporation.
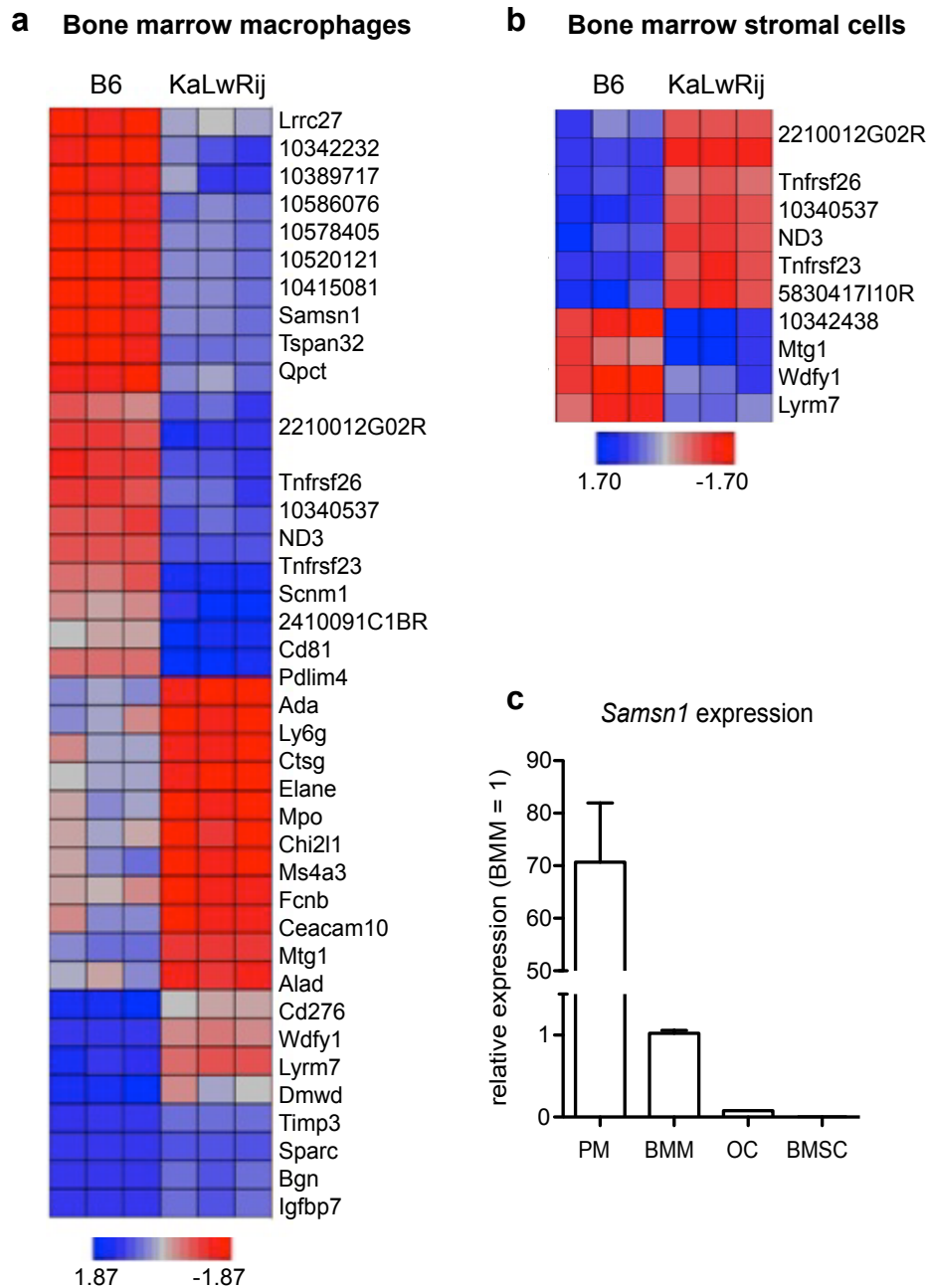
Figure 3.7.

Differential gene expression in B6 and KaLwRij bone marrow macrophages and bone marrow stromal cells.

Microarray analysis of gene expression in B6 and KaLwRij (a) bone marrow macrophages and (b) bone marrow stromal cells.. (c) *Samsn1* expression in B6 peritoneal macrophages (PM) bone marrow macrophages (BMM), osteoclasts (OC), and bone marrow stromal cells (BMSC).
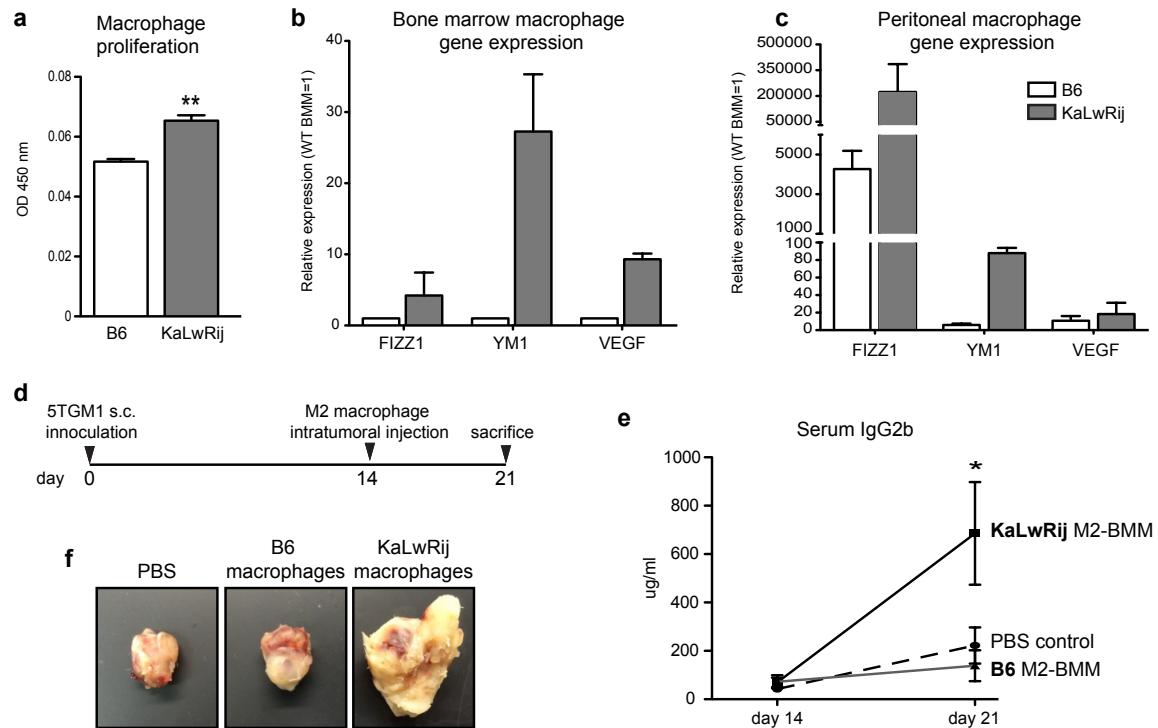
Figure 3.8.
KaLwRij mice have enhanced pro-tumorigenic macrophage activation
Proliferation of B6 and KaLwRij macrophages was measured by MTT assay. (b) M2 macrophage polarization markers (FIZZ1, YM1) and VEGF in (b) bone marrow macrophages and (c) periotoneal macrophages by qPT-PCR. (d) B6 or KaLwRij in vitro M2-polarized macrophages were injected directly into 5TGM1 tumors 14 days after tumor innoculation. Mice were sacrificed at day 21 (representative tumors (f)). (g) Tumor burden was monitored by serum levels of IgG2b (clonotype of 5TGM1 cells).

Table 3.1. Mice with positive M-spike on SPEP

Strain	Baseline	Post-PI	Post-BI	12 mo	18 mo
KaLwRij	0/12 (0)	1/12 (8)	2/11 (18)	8/11 (73)	5/9 (56)
C57BL/6J	0/10 (0)	0/10 (0)	4/10 (40)	3/9 (33)	0/7 (0)
129S1/SvlmJ	0/10 (0)	2/9 (22)	6/9 (67)	2/8 (25)	0/8 (0)
A/J	0/10 (0)	7/7 (100)	4/7 (57)	0/4 (0)	0/2 (0)
AKR/J	0/10 (0)	4/7 (57)	5/6 (83)	1/2 (50)	--
BALB/cByJ	0/10 (0)	3/10 (30)	3/9 (33)	4/9 (44)	0/7 (0)
C3H/HeJ	0/10 (0)	3/8 (38)	5/8 (63)	4/8 (50)	0/2 (0)
CBA/J	0/10 (0)	3/30 (30)	1/10 (10)	6/7 (86)	0/1 (0)
DBA/2J	0/10 (0)	1/9 (11)	1/9 (11)	0/5 (0)	0/2 (0)
FVB/NJ	0/10 (0)	1/10 (10)	6/10 (60)	4/9 (44)	0/6 (0)
NOD/ShiLtJ	2/10 (20)	7/3 (43)	4/5 (80)	0/5 (0)	0/4 (0)
SJL/J	0/10 (0)	0/9 (0)	4/5 (80)	1/5 (20)	1/3 (33)

M-spike positive mice / total mice (percentage)
No strain AKR/J mice survived to 18 months.

Table 3.2. Candidate genes underlying genetic susceptibility to BIP in KaLwRij mice

Gene	SNP score	Ensembl gene ID	Chr	Strand	Start (bp)	End (bp)	Band
Ptprt	128	ENSMUSG00000053141	2	-	161521990	162661147	H2
Thsd4	109	ENSMUSG00000032289	9	-	59966931	60522046	B
Arfip1	102	ENSMUSG00000074513	3	-	84496093	85887516	F1
Dab1	95	ENSMUSG00000028519	4	+	103619359	104744844	C6
5033411D12Rik	95	ENSMUSG00000055137	13	-	16857855	17694732	A2
Shank2	92	ENSMUSG00000037541	7	+	144001928	144424494	F5
Rora	85	ENSMUSG00000032238	9	+	68653786	69388246	C
Cdh4	75	ENSMUSG00000000305	2	+	179442431	179899373	H4
Elmo1	74	ENSMUSG00000041112	13	+	20090507	20608353	A2
Ush2a	68	ENSMUSG00000026609	1	+	188262023	188965041	H6
Esrrg	63	ENSMUSG00000026610	1	+	187608791	188214885	H5
Fgfr2	62	ENSMUSG00000030849	7	-	130162451	133123350	F3
Dock1	62	ENSMUSG00000058325	7	+	134670687	135173639	F3
Sgcd	61	ENSMUSG00000020354	11	-	46896253	47988969	B1.1
Fstl5	58	ENSMUSG00000034098	3	+	76074270	76710019	E3
Fstl4	54	ENSMUSG00000036264	11	+	52764634	53188538	B1.3
Gm12132	52	ENSMUSG00000085301	11	+	40008194	40337831	A5
Pou6f2	44	ENSMUSG00000009734	13	-	18121101	18382041	A2
Kcnq1	43	ENSMUSG00000009545	7	+	143107254	143427042	F5
Kcnq5	42	ENSMUSG00000028033	1	-	21398403	21961942	A4
Gm12239	41	ENSMUSG00000086020	11	+	55772088	56070848	B1.3
Adamtsl1	38	ENSMUSG00000066113	4	+	86053915	86428385	C4
Map2k5	37	ENSMUSG00000058444	9	-	63163769	63377902	C
A230004M16Rik	34	ENSMUSG00000087306	11	+	41710342	41973117	A5
Samsn1	33	ENSMUSG00000022876	16	-	75858793	76022270	C3.1
Stpg2	33	ENSMUSG00000047940	3	+	139205694	139710299	H1
Slc24a2	32	ENSMUSG00000037996	4	-	86983124	87230477	C4
C1qtnf7	32	ENSMUSG00000061535	5	+	43515569	43618817	B3
Ptprd	31	ENSMUSG00000028399	4	-	75941238	78211961	C3
Wdr17	30	ENSMUSG00000039375	8	-	54629055	54887184	B1.3
Col23a1	29	ENSMUSG00000063564	11	+	51289920	51583918	B1.3
Arid5b	27	ENSMUSG00000019947	10	-	68095593	68278726	B5.2
Vps41	27	ENSMUSG00000041236	13	+	18717292	18866809	A2
Ano1	26	ENSMUSG00000031075	7	-	144588549	144751974	F5
Tln2	26	ENSMUSG00000052698	9	-	67217087	67559703	C
Aoah	25	ENSMUSG00000021322	13	+	20794119	21024252	A2
Mark1	25	ENSMUSG00000026620	1	-	184896443	184999549	H5
Nxph1	25	ENSMUSG00000046178	6	+	8948431	9249032	A1
Unc5c	25	ENSMUSG00000059921	3	+	141465564	141834924	H1
Iqsec1	24	ENSMUSG00000034312	6	-	90659598	90810123	D1
Vps13c	24	ENSMUSG00000035284	9	+	67840396	67995634	C
Znrf3	24	ENSMUSG00000041961	11	-	5276324	5444847	A1
Dhx35	23	ENSMUSG00000027655	2	+	158794807	158858214	H1
D7Ertd443e	23	ENSMUSG00000030994	7	-	134266262	134385661	F3
Neo1	23	ENSMUSG00000032340	9	-	58874679	59036441	B
Focad	23	ENSMUSG00000038368	4	+	88094629	88411011	C4
Tcerg1l	22	ENSMUSG00000091002	7	-	138208974	138397730	F4
Adcy1	21	ENSMUSG00000020431	11	+	7063489	7178506	A1

Table 3.2. con't

Gene	SNP score	Ensembl gene ID	Chr	Strand	Start (bp)	End (bp)	Band
Tspan5	21	ENSMUSG00000028152	3	+	138742195	138904433	H1
Ldb2	21	ENSMUSG00000039706	5	-	44472133	44799707	B3
Ebf1	21	ENSMUSG00000057098	11	+	44617317	45008091	B1.1
Stk32c	20	ENSMUSG00000015981	7	-	139103638	139213307	F4
Tns3	20	ENSMUSG00000020422	11	-	8431652	8664535	A1
Spata17	20	ENSMUSG00000026611	1	-	187044648	187215465	H5
Prom1	20	ENSMUSG00000029086	5	-	43993625	44102032	B3
Itga11	20	ENSMUSG00000032243	9	+	62677826	62783982	B
Atg2b	20	ENSMUSG00000041341	12	-	105613539	105685241	E
Bmpr1b	20	ENSMUSG00000052430	3	-	141837136	142169425	H1
4933427D06Rik	20	ENSMUSG00000055403	6	+	88950683	89110030	D1
Kcnn3	19	ENSMUSG00000000794	3	+	89520164	89667761	F1
Rab28	19	ENSMUSG00000029128	5	-	41624976	41708155	B3
Coro2b	19	ENSMUSG00000041729	9	-	62419492	62537044	B
Tnip1	18	ENSMUSG00000020400	11	-	54910785	54962917	B1.3
Trim2	18	ENSMUSG00000027993	3	-	84160439	84305446	F1
Foxp2	18	ENSMUSG00000029563	6	+	14901349	15441977	A1
Fam196a	18	ENSMUSG00000073805	7	-	134881926	134938430	F3
Nf2	17	ENSMUSG00000009073	11	-	4765845	4849536	A1
Osbp2	17	ENSMUSG00000020435	11	-	3703731	3863903	A1
Phf14	17	ENSMUSG00000029629	6	+	11907809	12081197	A1
Etl4	17	ENSMUSG00000036617	2	+	19909780	20810713	A3
Rtel1	17	ENSMUSG00000038685	2	+	181319739	181356616	H4
Akap9	17	ENSMUSG00000040407	5	+	3928054	4080209	A1
Dscam	17	ENSMUSG00000050272	16	-	96592079	97170752	C4
Gm20388	17	ENSMUSG00000092329	8	+	119910841	124345722	E1
Lrba	16	ENSMUSG00000028080	3	+	86224690	86782693	F1
Rap1gds1	16	ENSMUSG00000028149	3	-	138925906	139075199	H1
Car12	16	ENSMUSG00000032373	9	+	66713686	66766845	C
Adamts2	16	ENSMUSG00000036545	11	+	50602084	50807573	B1.3
Ppp1r16b	16	ENSMUSG00000037754	2	+	158665398	158766334	H1
Arhgef11	16	ENSMUSG00000041977	3	+	87617559	87738034	F1
Mgmt	16	ENSMUSG00000054612	7	+	136894611	137128187	F3
Map2k1	15	ENSMUSG00000004936	9	-	64185770	64253631	C
Ankrd36	15	ENSMUSG00000020481	11	+	5569684	5689337	A1
Pdgfc	15	ENSMUSG00000028019	3	+	81036416	81214040	E3
Gpm6a	15	ENSMUSG00000031517	8	+	54954728	55060877	B1.3
Lyplal1	15	ENSMUSG00000039246	1	-	186087731	186117310	H5
Ak7	15	ENSMUSG00000041323	12	+	105705982	105782447	E
2410076I21Rik	15	ENSMUSG00000074269	9	-	58652856	58741559	B
Glra1	14	ENSMUSG00000000263	11	-	55514238	55608198	B1.3
Prdm15	14	ENSMUSG00000014039	16	-	97791467	97851850	C4
Slc22a4	14	ENSMUSG00000020334	11	-	53983123	54028090	B1.3
Vit	14	ENSMUSG00000024076	17	+	78508063	78627409	E3
Strn	14	ENSMUSG00000024077	17	-	78649913	78737196	E3
Fam83d	14	ENSMUSG00000027654	2	+	158768093	158786637	H1
Sepsecs	14	ENSMUSG00000029173	5	-	52640087	52669729	C1
Vegfc	14	ENSMUSG00000031520	8	+	54077532	54186454	B1.3

Table 3.2. con't

Gene	SNP score	Ensembl gene ID	Chr	Strand	Start (bp)	End (bp)	Band
Zfyve9	14	ENSMUSG00000034557	4	-	108637466	108780798	C7
Iqch	14	ENSMUSG00000037801	9	-	63421455	63602493	C
Gpatch2	14	ENSMUSG00000039210	1	+	187215508	187351704	H5
Myo9a	14	ENSMUSG00000039585	9	+	59750896	59928866	B
Adam12	14	ENSMUSG00000054555	7	-	133883199	134232146	F3
Atp10b	14	ENSMUSG00000055415	11	+	43149877	43262285	A5
Ppapdc1a	14	ENSMUSG00000070366	7	+	129257094	129391307	F3
Lrig3	13	ENSMUSG00000020105	10	+	125966219	126015359	D3
Ascc2	13	ENSMUSG00000020412	11	+	4637747	4685699	A1
Nup210l	13	ENSMUSG00000027939	3	+	90104132	90212017	F1
Ddah1	13	ENSMUSG00000028194	3	+	145758675	145894277	H2
Pias1	13	ENSMUSG00000032405	9	-	62880077	62980879	B
Eri3	13	ENSMUSG00000033423	4	+	117550365	117674297	D1
Mtmr3	13	ENSMUSG00000034354	11	-	4480868	4594863	A1
Rtkn2	13	ENSMUSG00000037846	10	+	67979570	68059740	B5.1
Heatr5b	13	ENSMUSG00000039414	17	-	78752906	78835381	E3
Pnldc1	13	ENSMUSG00000073460	17	-	12888902	12910000	A1
Gm12160	13	ENSMUSG00000087089	11	+	45160943	45213656	B1.1
Gm11376	13	ENSMUSG00000087140	13	+	31299628	31396579	A3.2
Igsf5	12	ENSMUSG00000000159	16	+	96361668	96525580	C4
Stard3nl	12	ENSMUSG00000003062	13	-	19357677	19395752	A2
Sh3gl2	12	ENSMUSG00000028488	4	+	85205126	85639195	C4
Fam154a	12	ENSMUSG00000028492	4	-	86444641	86558328	C4
Mllt3	12	ENSMUSG00000028496	4	-	87769925	88033364	C4
Podn	12	ENSMUSG00000028600	4	-	108014791	108096445	C7
Stra6	12	ENSMUSG00000032327	9	+	58063788	58153996	B
Nptn	12	ENSMUSG00000032336	9	+	58582240	58657955	B
Map9	12	ENSMUSG00000033900	3	+	82358072	82395268	E3
Acot11	12	ENSMUSG00000034853	4	-	106744555	106804998	C7
Nudcd3	12	ENSMUSG00000053838	11	-	6105691	6200415	A1
Fat2	12	ENSMUSG00000055333	11	-	55250609	55336564	B1.3
Tox2	12	ENSMUSG00000074607	2	+	163203125	163324170	H2
Ccm2	11	ENSMUSG00000000378	11	+	6546887	6596744	A1
Tmprss2	11	ENSMUSG00000000385	16	-	97564684	97611195	C4
Csf2	11	ENSMUSG00000018916	11	-	54247271	54249667	B1.3
Gabrg2	11	ENSMUSG00000020436	11	-	41910195	42000857	A5
Prkd3	11	ENSMUSG00000024070	17	-	78949405	79020816	E3
Eif2ak2	11	ENSMUSG00000024079	17	-	78852564	78882573	E3
Pja2	11	ENSMUSG00000024083	17	-	64281005	64331916	E1.1
4930555F03Rik	11	ENSMUSG00000031559	8	+	49370886	49521095	B1.2
Scaper	11	ENSMUSG00000034007	9	-	55549883	55919605	B
Rxfp1	11	ENSMUSG00000034009	3	-	79641611	79737880	E3
Megf11	11	ENSMUSG00000036466	9	+	64385626	64709205	C
Ppfia1	11	ENSMUSG00000037519	7	-	144476758	144553729	F5
Rapgef6	11	ENSMUSG00000037533	11	+	54522847	54699285	B1.3
Osbpl2	11	ENSMUSG00000039050	2	+	180119306	180162680	H4
Olfr56	11	ENSMUSG00000040328	11	+	48978889	49135387	B1.2
Gal3st1	11	ENSMUSG00000049721	11	+	3983636	3999326	A1

Table 3.2. con't

Gene	SNP score	Ensembl gene ID	Chr	Strand	Start (bp)	End (bp)	Band
Dlgap4	11	ENSMUSG00000061689	2	+	156613705	156764363	H1
Gm16223	11	ENSMUSG00000067285	5	+	42067960	42216798	B3
D430019H16Rik	11	ENSMUSG00000094910	12	+	105453856	105493095	E
Galntl6	11	ENSMUSG00000096914	8	-	57776225	57962564	B2
Pkn2	10	ENSMUSG00000004591	3	-	142790902	142882004	H1
Ebf3	10	ENSMUSG00000010476	7	-	137193673	137314445	F3
Mcoln2	10	ENSMUSG00000011008	3	+	146149833	146195513	H2
Kcnq2	10	ENSMUSG00000016346	2	-	181075579	181135291	H4
Sparc	10	ENSMUSG00000018593	11	-	55394500	55420080	B1.3
Lyrm7	10	ENSMUSG00000020268	11	-	54826866	54860916	B1.3
Hormad2	10	ENSMUSG00000020419	11	-	4345814	4441105	A1
Papola	10	ENSMUSG00000021111	12	+	105784694	105838944	E
Sfrp4	10	ENSMUSG00000021319	13	+	19623175	19632821	A2
Arih1	10	ENSMUSG00000025234	9	-	59388258	59486618	B
Anxa2	10	ENSMUSG00000032231	9	+	69453620	69491795	C
Ptpn9	10	ENSMUSG00000032290	9	+	56994968	57062805	B
Thsd7a	10	ENSMUSG00000032625	6	-	12311610	12749410	A1
Szt2	10	ENSMUSG00000033253	4	-	118362743	118409273	D2.1
Mnd1	10	ENSMUSG00000033752	3	-	84087934	84155786	F1
Osbpl5	10	ENSMUSG00000037606	7	-	143688762	143756985	F5
D630003M21Rik	10	ENSMUSG00000037813	2	-	158182533	158229222	H1
Lgi2	10	ENSMUSG00000039252	5	-	52537864	52566303	C1
Ccbl2	10	ENSMUSG00000040213	3	+	142701051	142744910	H1
Fez2	10	ENSMUSG00000056121	17	-	78377885	78418131	E2
Ica1	10	ENSMUSG00000062995	6	-	8630527	8778488	A1
B3galt5	10	ENSMUSG00000074892	16	+	96235801	96319859	C4
Gm16759	10	ENSMUSG00000086539	9	+	63399381	63568691	C
Gm12153	10	ENSMUSG00000087172	11	+	43959089	44134987	B1.1
Gm17231	10	ENSMUSG00000091908	9	+	57777865	57834295	B
Zfp804b	10	ENSMUSG00000092094	5	-	6769030	6876523	A1
Th	9	ENSMUSG00000000214	7	-	142892752	142931128	F5
Rmnd5b	9	ENSMUSG00000001054	11	-	51623671	51635896	B1.3
Arid3b	9	ENSMUSG00000004661	9	-	57790353	57836793	B
Lbp	9	ENSMUSG00000016024	2	+	158306493	158332852	H1
Kremen1	9	ENSMUSG00000020393	11	-	5191552	5261558	A1
Qpct	9	ENSMUSG00000024084	17	+	79051906	79090243	E3
Inpp5a	9	ENSMUSG00000025477	7	+	139389109	139579652	F4
Fbxw7	9	ENSMUSG00000028086	3	+	84815268	84979198	F1
Slc6a9	9	ENSMUSG00000028542	4	+	117834506	117875198	D2.1
Scp2	9	ENSMUSG00000028603	4	-	108043839	108144998	C7
Glcci1	9	ENSMUSG00000029638	6	+	8509600	8597548	A1
Plxna1	9	ENSMUSG00000030084	6	-	89316316	89362613	D1
Gm498	9	ENSMUSG00000031085	7	+	143866871	143897506	F5
Aga	9	ENSMUSG00000031521	8	+	53511702	53523421	B1.3
Uaca	9	ENSMUSG00000034485	9	+	60794548	60880370	B
Zfp365	9	ENSMUSG00000037855	10	-	67886103	67912662	B5.1
Pogz	9	ENSMUSG00000038902	3	+	94837567	94882326	F2.1
Gm12169	9	ENSMUSG00000078924	11	+	46524212	46538156	B1.1

Table 3.2. con't

Gene	SNP score	Ensembl gene ID	Chr	Strand	Start (bp)	End (bp)	Band
Gm15866	9	ENSMUSG00000087290	5	-	43557285	43601730	B3
Gm12130	9	ENSMUSG00000087296	11	-	38493330	38520013	A5
Gm12680	9	ENSMUSG00000087349	4	+	85514327	85783127	C4
Pcp4	9	ENSMUSG00000090223	16	+	96467606	96525793	C4
Gm17114	9	ENSMUSG00000091237	4	-	117835299	117868558	D2.1
Xpo6	8	ENSMUSG00000000131	7	-	126101715	126200501	F3
Sod2	8	ENSMUSG00000006818	17	+	13007839	13018119	A1
Lrrc27	8	ENSMUSG00000015980	7	+	139212988	139242979	F4
Anxa6	8	ENSMUSG00000018340	11	-	54979108	55033445	B1.3
Slc36a2	8	ENSMUSG00000020264	11	-	55158470	55185077	B1.3
Cyfip2	8	ENSMUSG00000020340	11	-	46193850	46312859	B1.1
Zfp354a	8	ENSMUSG00000020364	11	+	51059257	51072799	B1.3
Ralgapb	8	ENSMUSG00000027652	2	+	158409848	158499253	H1
Ash1l	8	ENSMUSG00000028053	3	+	88965812	89079373	F1
Sh3d19	8	ENSMUSG00000028082	3	+	85971109	86130526	F1
Dnajc6	8	ENSMUSG00000028528	4	+	101496648	101642799	C6
Rnf220	8	ENSMUSG00000028677	4	-	117271463	117497052	D1
Sesn2	8	ENSMUSG00000028893	4	-	132492032	132510501	D2.3
Ctbp2	8	ENSMUSG00000030970	7	-	132987563	133124354	F3
Pstpip1	8	ENSMUSG00000032322	9	+	56089962	56128888	B
Tesk2	8	ENSMUSG00000033985	4	+	116720948	116805956	D1
Golim4	8	ENSMUSG00000034109	3	-	75876183	75956949	E3
Chst11	8	ENSMUSG00000034612	10	+	82985498	83195900	C1
Cdc42ep3	8	ENSMUSG00000036533	17	-	79334025	79355091	E3
Ccdc33	8	ENSMUSG00000037716	9	-	58028677	58118823	B
Sox5	8	ENSMUSG00000041540	6	-	143828425	144781977	G3
Rims1	8	ENSMUSG00000041670	1	-	22286251	22805994	A5
Tenm2	8	ENSMUSG00000049336	11	-	36006656	37235964	A5
Cdc42se2	8	ENSMUSG00000052298	11	-	54717456	54787675	B1.3
5830411N06Rik	8	ENSMUSG00000054672	7	+	140247301	140299791	F4
Alk	8	ENSMUSG00000055471	17	-	71869442	72603709	E1.3
Lepr	8	ENSMUSG00000057722	4	+	101717404	101815352	C6
Acat3	8	ENSMUSG00000062480	17	-	12923833	12940402	A1
Arhgap40	8	ENSMUSG00000074625	2	+	158512796	158550762	H1
Gm12147	8	ENSMUSG00000086791	11	-	43259791	43311088	A5
4930401O12Rik	8	ENSMUSG00000087460	13	-	31213410	31222096	A3.2
Gm16039	8	ENSMUSG00000089862	6	+	8259288	8597480	A1
Olfr1328	8	ENSMUSG00000096368	4	-	118933897	118934840	D2.1
1110019D14Rik	8	ENSMUSG00000097616	6	+	13871526	14044373	A1
Celf2	7	ENSMUSG00000002107	2	-	6539694	7509563	A1
Tpra1	7	ENSMUSG00000002871	6	+	88902251	88912238	D1
Pabpc4	7	ENSMUSG00000011257	4	+	123262351	123298925	D2.2
P4ha2	7	ENSMUSG00000018906	11	+	54100095	54131665	B1.3
Vdac1	7	ENSMUSG00000020402	11	+	52360860	52389397	B1.3
Eif4enif1	7	ENSMUSG00000020454	11	+	3202392	3244588	A1
Lrrc71	7	ENSMUSG00000023084	3	-	87736923	87748625	F1
Tubgcp2	7	ENSMUSG00000025474	7	-	139995955	140036350	F4
Serpini1	7	ENSMUSG00000027834	3	+	75557547	75643495	E3

Table 3.2. con't

Gene	SNP score	Ensembl gene ID	Chr	Strand	Start (bp)	End (bp)	Band
Glrb	7	ENSMUSG00000028020	3	-	80843599	80913660	E3
Dclk2	7	ENSMUSG00000028078	3	-	86786150	86920884	F1
Snx27	7	ENSMUSG00000028136	3	-	94497544	94582716	F2.1
Gtf2b	7	ENSMUSG00000028271	3	+	142765226	142783603	H1
Ndc1	7	ENSMUSG00000028614	4	+	107367784	107416346	C7
Ermap	7	ENSMUSG00000028644	4	-	119175457	119190011	D2.1
Ppt1	7	ENSMUSG00000028657	4	+	122836242	122859175	D2.2
Pik3r3	7	ENSMUSG00000028698	4	+	116221618	116303056	D1
Pi4k2b	7	ENSMUSG00000029186	5	+	52741587	52769344	C1
Zranb1	7	ENSMUSG00000030967	7	+	132931142	132986391	F3
Hcn4	7	ENSMUSG00000032338	9	+	58823512	58860955	B
Mgll	7	ENSMUSG00000033174	6	+	88724412	88828360	D1
Tie1	7	ENSMUSG00000033191	4	-	118471191	118490061	D2.1
Fgb	7	ENSMUSG00000033831	3	-	83042247	83049803	E3
Zbbx	7	ENSMUSG00000034151	3	-	75037907	75165034	E3
Glis1	7	ENSMUSG00000034762	4	+	107434591	107635061	C7
Ttc22	7	ENSMUSG00000034919	4	+	106622432	106640189	C7
Smad6	7	ENSMUSG00000036867	9	-	63953076	64022059	C
Btnl9	7	ENSMUSG00000040283	11	-	49165585	49187159	B1.2
Gsg1l	7	ENSMUSG00000046182	7	-	125878419	126082411	F3
Lrp1b	7	ENSMUSG00000049252	2	-	40595248	42653598	B
Aff4	7	ENSMUSG00000049470	11	+	53350833	53421830	B1.3
8030423F21Rik	7	ENSMUSG00000052295	5	-	52607550	52619011	C1
Fut9	7	ENSMUSG00000055373	4	-	25609332	25800244	A3
Dhcr7	7	ENSMUSG00000058454	7	+	143823145	143848410	F5
Slc22a21	7	ENSMUSG00000063652	11	-	53949965	53980332	B1.3
Cntnap5a	7	ENSMUSG00000070695	1	+	115684756	116582026	E2.3
Gm12649	7	ENSMUSG00000084833	4	-	93453258	93671070	C5
Gm12223	7	ENSMUSG00000085585	11	+	54247600	54254495	B1.3
4930564K09Rik	7	ENSMUSG00000086273	3	+	82876705	82943638	E3
3110021N24Rik	7	ENSMUSG00000094958	4	+	108719649	108781904	C7
Gm26551	7	ENSMUSG00000097219	11	-	51949882	52269514	B1.3
Wwox	6	ENSMUSG00000004637	8	+	114439655	115352708	E1
Ripk4	6	ENSMUSG00000005251	16	-	97741933	97763737	C4
Gabrb2	6	ENSMUSG00000007653	11	+	42419757	42629028	A5
Vps72	6	ENSMUSG00000008958	3	+	95111022	95123051	F2.1
Camta1	6	ENSMUSG00000014592	4	-	150917322	151861876	E2
Fcrls	6	ENSMUSG00000015852	3	-	87250758	87263738	F1
G3bp1	6	ENSMUSG00000018583	11	+	55469685	55504838	B1.3
Canx	6	ENSMUSG00000020368	11	-	50293961	50325673	B1.3
Drg1	6	ENSMUSG00000020457	11	-	3187360	3266415	A1
Bdkrb2	6	ENSMUSG00000021070	12	+	105563172	105593071	E
Plce1	6	ENSMUSG00000024998	19	+	38481109	38785030	C3
Paox	6	ENSMUSG00000025464	7	+	140125657	140134334	F4
Stmn3	6	ENSMUSG00000027581	2	-	181306459	181314500	H4
Lce1m	6	ENSMUSG00000027912	3	-	93017807	93019060	F1
Asic5	6	ENSMUSG00000028008	3	+	81982290	82021233	E3
Arhgef2	6	ENSMUSG00000028059	3	+	88607454	88648052	F1

Table 3.2. con't

Gene	SNP score	Ensembl gene ID	Chr	Strand	Start (bp)	End (bp)	Band
Caap1	6	ENSMUSG00000028578	4	-	94500081	94556796	C5
Cap1	6	ENSMUSG00000028656	4	-	122859047	122886056	D2.2
Dmbx1	6	ENSMUSG00000028707	4	-	115914544	115939926	D1
Chchd6	6	ENSMUSG00000030086	6	-	89383146	89595652	D1
Tenm3	6	ENSMUSG00000031561	8	-	48227682	48674690	B1.2
Hpgd	6	ENSMUSG00000031613	8	+	56294552	56321046	B2
Thoc5	6	ENSMUSG00000034274	11	+	4895320	4928867	A1
Uroc1	6	ENSMUSG00000034456	6	+	90333289	90364551	D1
Zcchc11	6	ENSMUSG00000034610	4	+	108459426	108559421	C7
Rims4	6	ENSMUSG00000035226	2	-	163859751	163918683	H3
Pml	6	ENSMUSG00000036986	9	-	58218076	58249786	B
Aff3	6	ENSMUSG00000037138	1	-	38177326	38664955	B
Acer2	6	ENSMUSG00000038007	4	+	86874396	86934822	C4
Sult6b1	6	ENSMUSG00000038045	17	-	78883938	78906992	E3
Neil3	6	ENSMUSG00000039396	8	-	53586867	53639065	B1.3
Cc2d2a	6	ENSMUSG00000039765	5	+	43662379	43740972	B3
Bace2	6	ENSMUSG00000040605	16	+	97356728	97439012	C4
Nme8	6	ENSMUSG00000041138	13	-	19645078	19697794	A2
Kirrel	6	ENSMUSG00000041734	3	-	87078593	87174747	F1
Mat2b	6	ENSMUSG00000042032	11	-	40679314	40695203	A5
Inpp5f	6	ENSMUSG00000042105	7	+	128611328	128696425	F3
Zfp536	6	ENSMUSG00000043456	7	-	37472135	37773641	B3
Tnfrsf26	6	ENSMUSG00000045362	7	-	143607685	143627845	F5
Spesp1	6	ENSMUSG00000046846	9	-	62270729	62282179	B
Urgcp	6	ENSMUSG00000049680	11	-	5713417	5762376	A1
Lrrc4c	6	ENSMUSG00000050587	2	+	96318169	97631666	E1
Gpatch11	6	ENSMUSG00000050668	17	+	78835516	78848299	E3
Camk2b	6	ENSMUSG00000057897	11	-	5969644	6066362	A1
R74862	6	ENSMUSG00000059277	7	-	143021784	143053686	F5
Olfr530	6	ENSMUSG00000060974	7	-	140372587	140373666	F4
Rapgef2	6	ENSMUSG00000062232	3	-	79062516	79181340	E3
Nlgn1	6	ENSMUSG00000063887	3	-	25431811	26133734	A3
Kndc1	6	ENSMUSG00000066129	7	+	139894696	139941537	F4
Gramd2	6	ENSMUSG00000074259	9	+	59680144	59718874	B
C230081A13Rik	6	ENSMUSG00000074305	9	-	56201131	56418050	B
Gm12856	6	ENSMUSG00000084133	4	-	118942060	118943352	D2.1
Gm14372	6	ENSMUSG00000085745	7	-	144368048	144406933	F5
Gm14342	6	ENSMUSG00000086166	2	-	180829490	180889660	H4
Gm26547	6	ENSMUSG00000097095	17	+	55557166	55563507	C
2510016G02Rik	6	ENSMUSG00000097595	7	-	132889489	132931375	F3
Tcf7	5	ENSMUSG00000000782	11	-	52252371	52283014	B1.3
Rrp15	5	ENSMUSG00000001305	1	-	186720978	186749358	H5
Mcm2	5	ENSMUSG00000002870	6	-	88883475	88898780	D1
Gpx5	5	ENSMUSG00000004344	13	-	21286429	21292731	A3.1
Mpl	5	ENSMUSG00000006389	4	-	118442415	118457513	D2.1
Zmat5	5	ENSMUSG00000009076	11	+	4704678	4737669	A1
Trpm5	5	ENSMUSG00000009246	7	-	143069153	143094642	F5
Cars	5	ENSMUSG00000010755	7	-	143557230	143600090	F5

Table 3.2. con't

Gene	SNP score	Ensembl gene ID	Chr	Strand	Start (bp)	End (bp)	Band
Kif3a	5	ENSMUSG00000018395	11	+	53567379	53601967	B1.3
Hcfc2	5	ENSMUSG00000020246	10	+	82696160	82742428	C1
Mgat1	5	ENSMUSG00000020346	11	+	49244191	49263030	B1.2
3010026O09Rik	5	ENSMUSG00000020381	11	+	50174444	50200115	B1.3
Itk	5	ENSMUSG00000020395	11	-	46325150	46389515	B1.1
Myo1g	5	ENSMUSG00000020437	11	-	6506548	6520965	A1
Polm	5	ENSMUSG00000020474	11	-	5827860	5838016	A1
Amph	5	ENSMUSG00000021314	13	+	18948371	19150913	A2
Zkscan3	5	ENSMUSG00000021327	13	-	21387013	21402755	A3.1
Exoc2	5	ENSMUSG00000021357	13	-	30813919	30974047	A3.2
Dapk1	5	ENSMUSG00000021559	13	+	60601947	60763185	B2
Marc1	5	ENSMUSG00000026621	1	-	184786776	184811313	H5
Fam198b	5	ENSMUSG00000027955	3	+	79884533	79946280	E3
Tmem144	5	ENSMUSG00000027956	3	-	79813148	79842662	E3
Npy2r	5	ENSMUSG00000028004	3	-	82538383	82548084	E3
Gucy1b3	5	ENSMUSG00000028005	3	-	82032004	82074711	E3
Sh2d2a	5	ENSMUSG00000028071	3	+	87846755	87855722	F1
Pdlim5	5	ENSMUSG00000028273	3	-	142239586	142395696	H1
Ptplad2	5	ENSMUSG00000028497	4	-	88396144	88438928	C4
B4galt2	5	ENSMUSG00000028541	4	-	117869260	117883487	D2.1
Col9a2	5	ENSMUSG00000028626	4	+	121039385	121055322	D2.2
Wdr65	5	ENSMUSG00000028730	4	-	118554551	118620777	D2.1
Rcc1	5	ENSMUSG00000028896	4	-	132331919	132353605	D2.3
Auts2	5	ENSMUSG00000029673	5	-	131437333	132543344	G2
Asb5	5	ENSMUSG00000031519	8	+	54550331	54587836	B1.3
Kirrel3	5	ENSMUSG00000032036	9	+	34486126	35036716	A4
Anp32a	5	ENSMUSG00000032249	9	+	62341293	62378812	B
1700017B05Rik	5	ENSMUSG00000032300	9	-	57252322	57262599	B
Dis3l	5	ENSMUSG00000032396	9	-	64306756	64341288	C
Smad3	5	ENSMUSG00000032402	9	-	63646767	63757994	C
Cspg4	5	ENSMUSG00000032911	9	+	56865104	56899870	B
Kbtbd12	5	ENSMUSG00000033182	6	-	88547340	88637950	D1
Gpbp1l1	5	ENSMUSG00000034042	4	+	116557658	116593882	D1
Tmem132d	5	ENSMUSG00000034310	5	-	127783491	128433077	G1.3
Morc2a	5	ENSMUSG00000034543	11	+	3649494	3690477	A1
Arhgap10	5	ENSMUSG00000037148	8	-	77250366	77517907	C1
Nmur2	5	ENSMUSG00000037393	11	-	56024987	56041010	B1.3
Dennd4c	5	ENSMUSG00000038024	4	+	86748555	86850603	C4
Slco4a1	5	ENSMUSG00000038963	2	+	180456245	180474867	H4
Cdk13	5	ENSMUSG00000041297	13	-	17715962	17805097	A2
Slc39a11	5	ENSMUSG00000041654	11	-	113244853	113650079	E2
Zfp62	5	ENSMUSG00000046311	11	+	49203292	49218816	B1.2
C1qtnf2	5	ENSMUSG00000046491	11	+	43474276	43491525	B1.1
Dlgap2	5	ENSMUSG00000047495	8	+	14095865	14847680	A1.1
Mroh7	5	ENSMUSG00000047502	4	-	106680417	106730925	C7
Olfr1396	5	ENSMUSG00000047511	11	-	49112777	49114874	B1.2
Dmbt1	5	ENSMUSG00000047517	7	+	131032076	131121626	F3
Lrrc49	5	ENSMUSG00000047766	9	-	60568859	60688158	B

Table 3.2. con't

Gene	SNP score	Ensembl gene ID	Chr	Strand	Start (bp)	End (bp)	Band
Fcrl5	5	ENSMUSG00000048031	3	+	87435885	87457836	F1
Tenm4	5	ENSMUSG00000048078	7	+	96171244	96911093	E1
Olfr1394	5	ENSMUSG00000048378	11	+	49160016	49160954	B1.2
Trpm3	5	ENSMUSG00000052387	19	+	22139119	22989884	B
Bpi	5	ENSMUSG00000052922	2	+	158258094	158284531	H1
Dnajc8	5	ENSMUSG00000054405	4	+	132535550	132553742	D2.3
Sec14l3	5	ENSMUSG00000054986	11	+	4064841	4077736	A1
Ubl7	5	ENSMUSG00000055720	9	+	57910986	57929968	B
Slit3	5	ENSMUSG00000056427	11	+	35121224	35708507	A4
Ptprn2	5	ENSMUSG00000056553	12	+	116485720	117278167	F2
Wtap	5	ENSMUSG00000060475	17	-	12966796	12992546	A1
Dcc	5	ENSMUSG00000060534	18	-	71258738	72351069	E2
Csmd1	5	ENSMUSG00000060924	8	-	15892537	17535586	A1.3
Agbl4	5	ENSMUSG00000061298	4	+	110397661	111664324	C7
Dpp6	5	ENSMUSG00000061576	5	+	26817203	27727505	B1
Tmem117	5	ENSMUSG00000063296	15	+	94629185	95096097	E3
Phactr4	5	ENSMUSG00000066043	4	-	132355923	132422489	D2.3
Mas1	5	ENSMUSG00000068037	17	-	12841079	12868143	A1
Trcg1	5	ENSMUSG00000070298	9	+	57236556	57249863	B
Ccdc24	5	ENSMUSG00000078588	4	-	117866524	117872557	D2.1
AY761185	5	ENSMUSG00000079120	8	-	20943693	20944748	A2
Gm14278	5	ENSMUSG00000080880	2	-	156888854	156915383	H1
Gm11980	5	ENSMUSG00000083075	11	+	6685824	6686809	A1
Gm12131	5	ENSMUSG00000083806	11	-	39727070	39727712	A5
4933416E03Rik	5	ENSMUSG00000085198	2	+	159947341	159981288	H2
Gm11958	5	ENSMUSG00000085512	11	+	4285460	4286939	A1
Gm12648	5	ENSMUSG00000085931	4	-	94089576	94425588	C5
Gm16144	5	ENSMUSG00000086399	9	-	69477029	69479598	C
Gm14204	5	ENSMUSG00000086496	2	-	158595472	158610723	H1
5133400J02Rik	5	ENSMUSG00000086646	11	-	51189833	51220418	B1.3
0610043K17Rik	5	ENSMUSG00000087361	4	+	101353783	101399181	C6
Gm17359	5	ENSMUSG00000091685	3	+	79345376	79464129	E3
Gm26561	5	ENSMUSG00000097625	17	+	70878078	71393284	E1.3
9530052C20Rik	5	ENSMUSG00000097858	3	+	142882495	142894644	H1

Table 3.3. Candidate loci underlying genetic sucsptibility to monoclonal gammopathy of undetermined signifiance

Chr	Gene	Ensembl gene ID	Strand	Start (bp)	End (bp)	Band	SNP	P-value	Position (bp)
1	SSBP3	ENSG00000157216	-	54691105	54879152	p32.3	rs3753405	0.0004368	54745708
	HSP90B3P	ENSG00000203914	+	92100568	92109639	p22.1	rs1887055	0.0002949	92113813
	RP11-433J22.3	ENSG00000234190	+	147249700	147261065	q21.2	rs1908628	0.0001312	147260568
	HMCN1	ENSG00000143341	+	185703683	186160085	q25.3	rs10911784	0.00005891	185915391
							rs7550425	0.0003429	186045280
	CSRP1	ENSG00000159176	-	201452658	201478584	q32.1	rs645390	0.0004114	201454923
	GPR37L1	ENSG00000170075	+	202091986	202102720	q32.1	rs11588918	0.0001055	202095560
							rs12737525	0.00006792	202095852
	RP11-400N13.1	ENSG00000236230	-	222262511	222560776	q41	rs4511115	0.0002854	222513180
	DNAH14	ENSG00000185842	+	225083964	225586996	q42.12	rs13376645	0.0004052	225551281
	EDARADD	ENSG00000186197	+	236511562	236648214	q42.3	rs16833652	0.0004461	236577350
	SMYD3	ENSG00000185420	-	245912642	246670614	q44	rs10924674	0.00006615	246452817
							rs12037567	0.00002431	246458746
							rs10802383	0.00008869	246459480
2	SH3YL1	ENSG00000035115	-	217730	266398	p25.3	rs6742278	0.00002812	226999
	AC012445.1	ENSG00000229550	-	4184234	4188321	p25.3	rs10178086	0.00001205	4187138
	LPIN1	ENSG00000134324	+	11817721	11967535	p25.1	rs7569901	0.0004234	11897225
							rs6726960	0.0003213	11898931
							rs6744695	0.000358	11899088
	ADCY3	ENSG00000138031	-	25042038	25142708	p23.3	rs17799872	0.0002614	25044957
	CENPO	ENSG00000138092	+	25016005	25045245	p23.3	rs17799872	0.0002614	25044957
	RP11-443B20.1	ENSG00000271936	+	25048479	25049586	p23.3	rs17799872	0.0002614	25044957
	CTNNA2	ENSG00000066032	+	79412357	80875905	p12	rs17017514	0.0004403	79903804
	KIAA1211L	ENSG00000196872	-	99410309	99552722	q11.2	rs13005148	0.0003975	99467538
							rs6757098	0.0001547	99471399
							rs11123756	0.0001437	99508012
							rs12464134	0.00004374	99540101
	CACNB4	ENSG00000182389	-	152689290	152955593	q23.3	rs13416880	0.0001254	152868683
							rs13421383	0.00009218	152879348
							rs7591461	0.0003871	152882123
							rs6722774	0.00005946	152916802
							rs12693235	0.0000739	152924481
							rs1806702	0.0004061	152930124
	UPP2	ENSG00000007001	+	158733214	158992666	q24.1	rs6731028	0.0004357	158890762
	AC104820.2	ENSG00000234663	+	181966659	182264286	q31.3	rs877226	0.0003604	182117625
	PTH2R	ENSG00000144407	+	209224438	209719227	q34	rs1598140	0.0003792	209471702
	SPAG16	ENSG00000144451	+	214149113	215275225	q34	rs1876837	0.0003171	215077766

Table 3.3. con't

Chr	Gene	Ensembl gene ID	Strand	Start (bp)	End (bp)	Band	SNP	P-value	Position (bp)
2	AC064853.2	ENSG00000236116	-	228481714	228482506	q36.3	rs16823719	0.00004776	228481316
	C2orf83	ENSG00000042304	-	228474806	228498036	q36.3	rs16823719	0.00004776	228481316
	AC009410.1	ENSG00000232023	-	229347977	229476111	q36.3	rs16825085	0.0001298	229390795
3	CCDC174	ENSG00000154781	+	14693271	14714166	p25.1	rs2276754	0.00001082	14702982
	AC133680.1	ENSG00000237838	+	24729410	25215796	p24.2	rs17576864	0.0002854	25192389
							rs17517875	0.0002831	25208270
							rs17577191	0.0002344	25208341
							rs12152294	0.0002837	25215670
	RARB	ENSG00000077092	+	25215823	25639423	p24.2	rs12152294	0.0002837	25215670
							rs17518622	0.0002824	25227079
	SLC4A7	ENSG00000033867	-	27414214	27525911	p24.1	rs3755652	0.0003041	27472936
	CMTM8	ENSG00000170293	+	32280171	32411817	p22.3	rs3853711	0.0003912	32395577
	CCDC13	ENSG00000244607	-	42734155	42814745	p22.1	rs9836162	0.0002569	42747548
	HHATL	ENSG00000010282	-	42734155	42744319	p22.1	rs9836162	0.0002569	42747548
	HHATL-AS1	ENSG00000230970	+	42744145	42748154	p22.1	rs9836162	0.0002569	42747548
		ENSG00000244607	-	42734155	42814745	p22.1	rs2240861	0.0003139	42750324
		ENSG00000230970	+	42744145	42748154	p22.1	rs2240861	0.0003139	42750324
		ENSG00000244607	-	42734155	42814745	p22.1	rs17238798	0.0003606	42799765
	HIGD1A	ENSG00000181061	-	42798669	42846023	p22.1	rs17238798	0.0003606	42799765
		ENSG00000244607	-	42734155	42814745	p22.1	rs11915803	0.0003606	42800291
		ENSG00000181061	-	42798669	42846023	p22.1	rs11915803	0.0003606	42800291
	LINC00971	ENSG00000242641	-	84687557	84930830	p12.1	rs2326227	0.0003381	84755963
	CLDND1	ENSG00000080822	-	98216756	98241910	q11.2	rs9819403	0.0003452	98245718
	CPOX	ENSG00000080819	-	98239976	98312567	q12.1	rs9819403	0.0003452	98245718
	RP11-227H4.5	ENSG00000248839	+	98241414	98244178	q11.2	rs9819403	0.0003452	98245718
	RPL38P4	ENSG00000250562	-	98243905	98244118	q11.2	rs9819403	0.0003452	98245718
	TMCC1	ENSG00000172765	-	129366635	129612419	q22.1	rs4306849	0.0004246	129384180
	RP11-23D24.2	ENSG00000238755	-	153102723	153697975	q25.2	rs17745929	0.000283	153506050
	KCNAB1	ENSG00000169282	+	155755490	156256545	q25.31	rs1474024	0.0000279	155775874
	RP11-85M11.2	ENSG00000244128	+	164924748	165373211	q26.1	rs9839370	0.00007675	165200881
							rs3106448	0.0003237	165343107
	B3GNT5	ENSG00000176597	+	182971032	183016292	q27.1	rs6803209	0.0000113	182968709
	MCF2L2	ENSG00000053524	-	182895831	183146566	q27.1	rs6803209	0.0000113	182968709
	RP11-430L16.1	ENSG00000234238	+	187824884	187864808	q27.3	rs9852144	0.0004035	187842721
	RP11-513G11.4	ENSG00000225742	-	193920805	193967942	q29	rs6800138	0.0003418	193937606
4	STK32B	ENSG00000152953	+	5053169	5502725	p16.2	rs1838973	0.0004397	5157262
	MUC7	ENSG00000171195	+	71296209	71348714	q13.3	rs11249502	0.0001027	71341161

Table 3.3. con't

Chr	Gene	Ensembl gene ID	Strand	Start (bp)	End (bp)	Band	SNP	P-value	Position (bp)
4	AC107072.2	ENSG00000231335	+	77558776	77565521	q21.1	rs1986966	0.0003857	77558777
	SHROOM3	ENSG00000138771	+	77356253	77704406	q21.1	rs1986966	0.0003857	77558777
							rs17002148	0.0001498	77580240
							rs6817407	0.0003579	77616338
	CCNG2	ENSG00000138764	+	78078304	78354542	q21.1	rs12649862	0.000331	78343820
	RP11-625I7.1	ENSG00000249036	-	78315645	78415440	q21.1	rs12649862	0.000331	78343820
		ENSG00000138764	+	78078304	78354542	q21.1	rs41476645	0.0001599	78344385
		ENSG00000249036	-	78315645	78415440	q21.1	rs41476645	0.0001599	78344385
		ENSG00000138764	+	78078304	78354542	q21.1	rs12644936	0.0001599	78345120
		ENSG00000249036	-	78315645	78415440	q21.1	rs12644936	0.0001599	78345120
							rs12501028	0.0001656	78391533
							rs7689830	0.00003848	78416791
	RASGEF1B	ENSG00000138670	-	82347547	82965397	q21.22	rs17005163	0.00006777	82483468
	PLAC8	ENSG00000145287	-	84011201	84058228	q21.22	rs17006484	0.00006746	84035969
	CCSER1	ENSG00000184305	+	91048686	92523064	q22.1	rs1849809	0.0002955	91596240
	RP11-255I10.2	ENSG00000248656	+	112561651	112569964	q25	rs17043540	0.000003519	112558571
	ZNF827	ENSG00000151612	-	146678779	146859787	q31.22	rs6814298	0.0000153	146780732
	AC108142.1	ENSG00000177822	-	182795591	183066402	q34.3	rs10009617	0.0004117	182874271
	MIR1305	ENSG00000221227	+	183090446	183090531	q34.3	rs12504374	0.000003003	183086701
	RP11-402C9.1	ENSG00000248266	+	183066005	183111535	q34.3	rs12504374	0.000003003	183086701
	TENM3	ENSG00000218336	+	183065140	183724177	q34.3	rs12504374	0.000003003	183086701
5	FSTL4	ENSG00000053108	-	132532147	132948255	q31.1	rs11242158	0.0004328	132835992
	ARHGAP26	ENSG00000145819	+	142149949	142608576	q31.3	rs10875602	0.0001677	142599713
	CTD-2270F17.1	ENSG00000253647	+	169816497	169849848	q35.1	rs314120	0.00006844	169823196
	KCNIP1	ENSG00000182132	+	169780491	170163636	q35.1	rs314120	0.00006844	169823196
	RNA5SP200	ENSG00000252169	-	172719520	172719622	q35.1	rs7714152	0.00005878	172715409
							rs10061599	0.00004471	172723332
							rs17675787	0.00002048	172724246
6	GMDS	ENSG00000112699	-	1624041	2245926	p25.3	rs3800125	0.00001667	1906861
	B3GALT4	ENSG00000226936	+	33166523	33168208	p21.32	rs458679	0.0001654	33164098
	RPS18	ENSG00000235650	+	33161393	33165893	p21.32	rs458679	0.0001654	33164098
	VPS52	ENSG00000225590	-	33139671	33161430	p21.32	rs458679	0.0001654	33164098
	WDR46	ENSG00000204221	-	33168491	33178914	p21.32	rs458679	0.0001654	33164098
		ENSG00000206285	+	33173759	33175444	p21.32			33171335
		ENSG00000096150	+	33168626	33173129	p21.32			33171335
		ENSG00000206286	-	33146871	33168663	p21.32	rs458679	0.0001654	33171335
		ENSG00000206284	-	33175727	33186150	p21.32			33171335

Table 3.3. con't

Chr	Gene	Ensembl gene ID	Strand	Start (bp)	End (bp)	Band	SNP	P-value	Position (bp)
6		ENSG00000235155	+	33222842	33224527	p21.32			33220417
		ENSG00000223367	+	33217712	33222212	p21.32			33220417
		ENSG00000228425	-	33195972	33217749	p21.32	rs458679	0.0001654	33220417
		ENSG00000226916	-	33224810	33235233	p21.32			33220417
		ENSG00000235863	+	33244917	33252609	p21.32			33242492
		ENSG00000231500	+	33239787	33244287	p21.32			33242492
		ENSG00000223501	-	33218049	33239824	p21.32	rs458679	0.0001654	33242492
		ENSG00000227057	-	33246885	33257304	p21.32			33242492
		ENSG00000227794	+	33379131	33382651	p21.32			33381840
		ENSG00000236014	-	33357416	33379168	p21.32	rs458679	0.0001654	33381840
		ENSG00000236802	+	33415294	33416979	p21.32			33412869
		ENSG00000226225	+	33410160	33414664	p21.32			33412869
		ENSG00000224455	-	33388442	33410197	p21.32	rs458679	0.0001654	33412869
		ENSG00000236222	-	33417262	33427651	p21.32			33412869
	KLHL31	ENSG00000124743	-	53512699	53530506	p12.1	rs6942249	0.0003955	53515483
							rs2478352	0.0003203	53533265
	RP11-304C16.3	ENSG00000217331	-	97120005	97120845	q16.1	rs17797978	0.0003369	97115085
	ADGB	ENSG00000118492	+	146920101	147136598	q24.3	rs1572902	0.0004276	146979589
							rs1340996	0.0004072	146988978
	RP1-125N5.2	ENSG00000235815	+	169116745	169123604	q27	rs196469	0.0000181	169123297
							rs196479	0.00004366	169127361
7	ITGB8	ENSG00000105855	+	20370325	20455377	p21.1	rs6461490	0.000337	20381806
							rs7793190	0.00006727	20407356
	RAPGEF5	ENSG00000136237	-	22157856	22396763	p15.3	rs17507	0.0003288	22175235
							rs3901281	0.0001779	22175472
							rs3807531	0.0003865	22187744
	STEAP1B	ENSG00000105889	-	22459063	22672544	p15.3	rs740295	0.0002376	22473288
							rs10250954	0.0002395	22474949
							rs4318962	0.00009263	22475742
	GLI3	ENSG00000106571	-	42000548	42277469	p14.1	rs846394	0.0001328	42162825
							rs846393	0.0001339	42163860
							rs846385	0.0001009	42168935
	CCM2	ENSG00000136280	+	45039074	45116068	p13	rs10951785	0.0002309	45047791
	CCDC146	ENSG00000135205	+	76751751	76958850	q11.23	rs3108440	0.0003706	76896701
							rs3108442	0.0003706	76901907
							rs7780929	0.0001147	76914712
							rs7786334	0.0001152	76915253

Table 3.3. con't

Chr	Gene	Ensembl gene ID	Strand	Start (bp)	End (bp)	Band	SNP	P-value	Position (bp)
7							rs17151066	0.0001152	76917303
							rs17151097	0.0001152	76918307
							rs17151110	0.00006989	76918782
	DBF4	ENSG00000006634	+	87505531	87538856	q21.12	rs11982729	0.0003455	87516527
8	CSMD1	ENSG00000183117	-	2792875	4852494	p23.2	rs17414486	0.0004013	4283673
	RP11-1080G15.1	ENSG00000253557	-	18942502	19116979	p21.3	rs2672282	0.0002106	19055204
	RP11-624C23.1	ENSG00000253535	-	24153327	24769586	p21.2	rs17052236	0.0002338	24462582
	AC012215.1	ENSG00000233863	+	35649365	35653384	p12	rs16884444	0.0001357	35648980
	UNC5D	ENSG00000156687	+	35092975	35654068	p12	rs16884444	0.0001357	35648980
	ASPH	ENSG00000198363	-	62413116	62627155	q12.3	rs16927431	0.00009409	62424008
	RP11-6I2.3	ENSG00000254288	+	74964575	75012088	q21.11	rs6988353	0.0003492	74997242
	KB-1184D12.1	ENSG00000253585	-	95109992	95116550	q22.1	rs2446833	0.000418	95111326
	FSBP	ENSG00000265817	-	95390605	95449180	q22.1	rs2470737	0.0002017	95407427
	RAD54B	ENSG00000197275	-	95384188	95487337	q22.1	rs2470737	0.0002017	95407427
	AF216667.1	ENSG00000222570	-	133693146	133693248	q24.22	rs7827081	0.0002315	133696552
	TMEM71	ENSG00000165071	-	133697253	133772958	q24.22	rs7827081	0.0002315	133696552
							rs10956677	0.000438	133708897
9	HAUS6	ENSG00000147874	-	19053141	19103117	p22.1	rs7869414	0.0003545	19082832
	NOL8	ENSG00000198000	-	95059640	95087918	q22.31	rs16908281	0.0002286	95072094
	CDC26	ENSG00000176386	-	116018115	116037869	q32	rs17831256	0.0001976	116042867
	PRPF4	ENSG00000136875	+	116037623	116055185	q32	rs17831256	0.0001976	116042867
							rs12352784	0.0001976	116045074
	GSN	ENSG00000148180	+	123970072	124095121	q33.2	rs4837817	0.0004299	123995163
10	CACNB2	ENSG00000165995	+	18429606	18830798	p12.33	rs2482100	0.00009705	18481080
							rs1277768	0.0003153	18499676
	VSTM4	ENSG00000165633	-	50222290	50323554	q11.23	rs4488117	0.0002074	50309905
	TSPAN15	ENSG00000099282	+	71211229	71267425	q22.1	rs7078095	0.00001963	71263424
	SEC23IP	ENSG00000107651	+	121652223	121702014	q26.11	rs2279939	0.0001692	121693020
	RPS27P18	ENSG00000233135	-	127162255	127162501	q26.13	rs3813859	0.000005007	127166793
11	SCUBE2	ENSG00000175356	-	9041071	9159661	p15.4	rs2647537	0.0001835	9125301
							rs7931872	0.0001388	9142062
							rs10840175	0.0002378	9143548
	DENND5A	ENSG00000184014	-	9160372	9286937	p15.4	rs10840176	0.0001697	9155570
		ENSG00000175356	-	9041071	9159661	p15.4	rs10840176	0.0001697	9155570
		ENSG00000184014	-	9160372	9286937	p15.4	rs2133217	0.0003779	9177012
							rs7394878	0.0003604	9198276
	NELL1	ENSG00000165973	+	20691117	21597227	p15.1	rs12791900	0.0002738	21022007

Table 3.3. con't

Chr	Gene	Ensembl gene ID	Strand	Start (bp)	End (bp)	Band	SNP	P-value	Position (bp)
11	RNA5SP336	ENSG00000201059	-	21022427	21022543	p15.1	rs12791900	0.0002738	21022007
		ENSG00000165973	+	20691117	21597227	p15.1	rs7122556	0.0004212	21045022
	SLC1A2	ENSG00000110436	-	35272753	35441610	p13	rs3847613	0.000157	35338345
							rs11033071	0.00032	35347685
							rs7114383	0.0003204	35356793
							rs11033080	0.0003811	35362357
							rs7934047	0.0004051	35367925
							rs4756221	0.0001532	35378069
	INCENP	ENSG00000149503	+	61891445	61920635	q12.3	rs1675126	0.000403	61906374
	RP11-691L4.2	ENSG00000236607	+	61936765	61937300	q12.3	rs1792908	0.0001881	61941265
							rs11230950	0.000106	61941816
	ACY3	ENSG00000132744	-	67410026	67418130	q13.2	rs12288023	0.0003361	67421341
	AP003385.2	ENSG00000227834	-	67419047	67420875	q13.2	rs12288023	0.0003361	67421341
	MAML2	ENSG00000184384	-	95709762	96076344	q21	rs12286219	0.0001786	95770904
	CNTN5	ENSG00000149972	+	98891683	100229616	q22.1	rs614096	0.0003917	99577390
							rs2010803	0.00009028	99600358
	RP11-94P11.4	ENSG00000254998	-	105028654	105402424	q22.3	rs7947277	0.0002016	105301479
	USP2-AS1	ENSG00000245248	+	119252488	119397374	q23.3	rs7949052	0.0001409	119400127
12	PTPRB	ENSG00000127329	-	70910630	71031220	q15	rs17108396	0.00008915	71009354
	LGR5	ENSG00000139292	+	71833550	71980090	q21.1	rs4486718	0.00006204	71899966
13	HNF4GP1	ENSG00000228611	-	56573334	56574582	q21.1	rs9316831	0.0002368	56574936
	MYO16	ENSG00000041515	+	109248500	109860355	q33.3	rs651270	0.0002752	109629324
14	OR4U1P	ENSG00000258899	+	20512075	20512986	q11.2	rs1952805	0.0001053	20516355
	RP11-116N8.1	ENSG00000258342	+	36367188	36532949	q13.2	rs7401172	0.0003348	36451285
	SEC23A	ENSG00000100934	-	39501123	39578850	q21.1	rs4902308	0.0003054	39499158
	FRMD6	ENSG00000139926	+	51955818	52197445	q22.1	rs4898705	0.0003329	52109999
							rs8019441	0.0002757	52110329
	BMP4	ENSG00000125378	-	54416454	54425479	q22.2	rs12434228	0.0001107	54427602
15	FAM189A1	ENSG00000104059	-	29412457	29862927	q13.1	rs511092	0.0004207	29733674
	AGBL1	ENSG00000166748	+	86685227	87572283	q25.3	rs11073666	0.00008602	87299209
	RP11-266O8.1	ENSG00000257060	+	93855786	94112712	q26.1	rs8037879	0.0001737	93900397
							rs735912	0.00008711	93900938
	CERS3	ENSG00000154227	-	100940600	101085200	q26.3	rs4965668	0.0003708	101077349
16	CASC16	ENSG00000249231	-	52586002	52686017	q12.2	rs4784227	0.0003197	52599188
	CDH11	ENSG00000140937	-	64977656	65160015	q21	rs7203623	0.0002642	65138590
	RP11-95H3.1	ENSG00000259847	-	65175659	65210616	q21	rs7206260	0.0003446	65211408
	C16orf95	ENSG00000260456	-	87117168	87351022	q24.2	rs7498934	0.0003701	87313604

Table 3.3. con't

Chr	Gene	Ensembl gene ID	Strand	Start (bp)	End (bp)	Band	SNP	P-value	Position (bp)
16	RP11-178L8.5	ENSG00000261697	-	87296365	87326044	q24.2	rs7498934	0.0003701	87313604
17	WDR16	ENSG00000166596	+	9479944	9546776	p13.1	rs6503235	0.000431	9515777
	AC005772.2	ENSG00000232058	+	14918122	14955593	p12	rs2323554	0.00002671	14927112
	IGF2BP1	ENSG00000159217	+	47074774	47133012	q21.32	rs1495274	0.000006974	47077648
	RP11-501C14.5	ENSG00000250838	-	47072628	47074854	q21.32	rs1495274	0.000006974	47077648
	RP11-501C14.6	ENSG00000251461	-	47082093	47091087	q21.32	rs1495274	0.000006974	47077648
	RP11-120M18.2	ENSG00000267009	+	66409764	66521090	q24.2	rs6501468	0.00005995	66427696
	WIPI1	ENSG00000070540	-	66417089	66453654	q24.2	rs6501468	0.00005995	66427696
		ENSG00000267009	+	66409764	66521090	q24.2	rs2909207	0.00007614	66439605
		ENSG00000070540	-	66417089	66453654	q24.2	rs2909207	0.00007614	66439605
		ENSG00000267009	+	66409764	66521090	q24.2	rs883541	0.00008579	66449122
		ENSG00000070540	-	66417089	66453654	q24.2	rs883541	0.00008579	66449122
	RBFOX3	ENSG00000167281	-	77085427	77613550	q25.3	rs8073623	0.0001163	77209928
		ENSG00000267483	-	77085427	77512230	q25.3	rs8073623	0.0001163	77209928
	CARD14	ENSG00000141527	+	78143791	78183130	q25.3	rs3829611	0.0003766	78161815
18	CABLES1	ENSG00000134508	+	20714528	20840431	q11.2	rs4800149	0.00007593	20744254
							rs8094261	0.0001353	20746728
							rs7244739	0.00004108	20747874
	RNF125	ENSG00000101695	+	29598335	29653176	q12.1	rs17718931	0.000376	29595943
	RP11-53I6.2	ENSG00000263917	+	29598792	29691742	q12.1	rs17718931	0.000376	29595943
	LINC00907	ENSG00000267586	+	39739247	40271387	q12.3	rs7233167	0.0004234	39905099
	RNF165	ENSG00000141622	+	43906772	44043103	q21.1	rs4890643	0.00005549	43913125
							rs9958625	0.00005135	43914787
	RP11-146N18.1	ENSG00000267134	+	61771325	62090836	q22.1	rs11877311	0.00008493	62032809
19	TJP3	ENSG00000105289	+	3708107	3750811	p13.3	rs475112	0.0001404	3745546
	MRPL54	ENSG00000183617	+	3762662	3768573	p13.3	rs917546	0.000003929	3769834
	RAX2	ENSG00000173976	-	3769087	3772233	p13.3	rs917546	0.000003929	3769834
	AC005307.3	ENSG00000267243	-	28926295	29218684	q12	rs1476739	0.000003327	29083380
	AC005616.1	ENSG00000266893	-	28982771	29123635	q12	rs1476739	0.000003327	29083380
		ENSG00000267243	-	28926295	29218684	q12	rs9653109	0.000228	29090291
	AC005394.1	ENSG00000267537	-	29093286	29139210	q12	rs9653109	0.000228	29090291
		ENSG00000266893	-	28982771	29123635	q12	rs9653109	0.000228	29090291
	CD22	ENSG00000012124	+	35810164	35838258	q13.12	rs11673522	0.00009619	35807727
	MAG	ENSG00000105695	+	35783028	35804707	q13.12	rs11673522	0.00009619	35807727
	ZNF321P	ENSG00000221874	-	53431728	53466076	q13.41	rs8110394	0.0003313	53439481
	ZNF816	ENSG00000180257	-	53430388	53466164	q13.41	rs8110394	0.0003313	53439481
	ZNF816-ZNF321P	ENSG00000213801	-	53430388	53445854	q13.41	rs8110394	0.0003313	53439481

Table 3.3. con't

Chr	Gene	Ensembl gene ID	Strand	Start (bp)	End (bp)	Band	SNP	P-value	Position (bp)
20	MACROD2	ENSG00000172264	+	13976015	16033842	p12.1	rs6131652	0.0003937	15211513
							rs1304179	0.0004005	15296031
	RPL7AL3	ENSG00000235208	-	16664753	16665049	p12.1	rs6044230	0.0001602	16665232
	EYA2	ENSG00000064655	+	45523263	45817492	q13.12	rs1541256	0.00001494	45784212
	GNAS-AS1	ENSG00000235590	-	57393974	57425958	q13.32	rs6128441	0.0003562	57402992
	GNAS	ENSG00000087460	+	57414773	57486247	q13.32	rs35113254	0.000007265	57435532
	RP1-309F20.3	ENSG00000225806	-	57438583	57463864	q13.32	rs35113254	0.000007265	57435532
21	SAMSN1	ENSG00000155307	-	15857549	15955723	q11.2	rs12626593	0.0004051	15857846
	ABCG1	ENSG00000160179	+	43619799	43717354	q22.3	rs225401	0.0003771	43693693
	UBASH3A	ENSG00000160185	+	43824008	43867791	q22.3	rs884339	0.0003464	43866505
	PCBP3	ENSG00000183570	+	47063608	47362368	q22.3	rs17004793	0.0002008	47119273
22	LL22NC03-30E12.13	ENSG00000227710	+	22522682	22523027	q11.22	rs5995601	0.00006649	22524871
	SOCS2P2	ENSG00000224465	-	22525369	22525942	q11.22	rs5995601	0.00006649	22524871
	LARGE	ENSG00000133424	-	33558212	34318829	q12.3	rs16992029	0.0002015	33668879
	RP1-41P2.7	ENSG00000228587	+	36081987	36085420	q12.3	rs16995953	0.00007196	36084258

Table 3.4. Differentially expressed genes in KaLwRij bone marrow macrophages

	Gene	Fold change	P-value
*	Tnfrsf26	-29.9811	2.65E-09
	Tnfrsf23	-14.6596	1.89E-07
*	Samsn1	-14.4329	1.14E-07
	2210012G02Rik	-9.58558	4.43E-07
	Mpo	6.93897	1.54E-06
	Ctsg	5.64399	2.33E-05
	Pdlim4	-5.33088	3.23E-05
	Tspan32	-5.15177	6.34E-07
	Ms4a3	4.77849	2.22E-05
	Elane	4.51361	1.21E-07
	2210012G02Rik	-4.36785	2.98E-05
	Timp3	4.17675	4.94E-07
	Ly6g	4.09308	3.00E-05
	Ada	3.75752	5.59E-05
	Bgn	3.33172	1.19E-07
	Igfbp7	2.95073	3.30E-06
*	Qpct	-2.89029	5.46E-05
	Chi3l1	2.8762	8.41E-06
*	Lrrc27	-2.87336	1.43E-05
*	Lyrm7	2.82725	1.19E-06
	Ceacam10	2.76395	3.59E-05
	Cd81	-2.62216	8.44E-06
	Wdfy1	2.60413	3.57E-06
*	Sparc	2.52091	1.38E-06
	Cd276	2.23131	1.09E-05
	Fcnb	2.00202	6.59E-06
	Scnm1	-1.6946	7.08E-07
	Mtg1	1.67805	4.04E-05
	ND3	-1.64285	1.77E-05
	Alad	1.60752	4.37E-05
	Dmwd	1.53818	1.33E-05
	2410091C18Rik	-1.5002	3.72E-05

Fold change is expression in KaLwRij bone marrow macropchages compared to B6
* gene is present on KaLwRij BIP susceptibility candidate gene list

Table 3.5. Differentially expressed genes in KaLwRij bone marrow stromal cells

	Gene	Fold change	P-value
*	Tnfrsf26	-11.3288	3.81E-08
*	Tnfrsf23	-21.709	6.49E-08
	Wdfy1	3.27725	6.87E-07
	Tceanc2	-6.67305	1.05E-05
*	Lyrm7	2.21795	8.92E-06
	Mtg1	1.90874	7.88E-06
	ND3	-1.75834	6.83E-06
	5830417I10Rik	-6.2556	1.73E-05

Fold change is expression in KaLwRij compared to B6

* gene is present on KaLwRij BIP susceptibility candidate gene list

Table 3.6. *SAMSN1* variant frequencies in MM patients

Position Chr21	SNP	Allele (Ref/Alt)	Consequence	MM patients			Controls			odds ratio	P-value
				N	variant alleles	%	N	variant alleles	%		
15830578	rs2822669	C/T		366	44	12.02	210	38	18.10	0.6421	0.0593
15857533		A/G		366	1	0.27	210	0	0	private variant	
15857592	rs76251857	G/A	3' UTR variant	366	3	0.82	210	2	0.95	0.8583	0.8683
15857846	rs12626593	C/G	3' UTR variant	366	34	9.29	210	19	9.05	1.0276	0.9245
15858171	rs28470776	G/A	3' UTR variant	366	1	0.27	210	0	0	private variant	
15858207	rs80062901	G/A	3' UTR variant	366	3	0.82	210	4	1.90	0.4209	0.2634
15858228	rs373757186	C/T	3' UTR variant	366	1	0.27	210	0	0	private variant	
15858229	rs149543089	G/A	3' UTR variant	366	1	0.27	210	0	0	private variant	
15858302		T/C		366	1	0.27	210	0	0	private variant	
15872961		C/T		366	1	0.27	210	0	0	private variant	
15873026	rs62227165	T/C	missense variant	366	8	2.19	210	3	1.43	1.5540	0.5217
15882622	rs118173592	T/C		366	0	0	210	1	0.48	private variant	
15884758	s376866016	G/A		366	0	0	210	1	0.48	private variant	
15884899	rs73344160	A/G	splice region variant	366	4	1.09	210	3	1.43	0.8090	0.7533
15889304	rs34607574	C/G	missense variant	366	6	1.64	210	3	1.43	1.1525	0.8432
15889359	rs368475908	G/A	missense variant	366	0	0.00	210	1	0.48	private variant	
15893545	rs150644782	A/T		366	1	0.27	210	0	0	private variant	
15893567	rs760344	A/T		366	54	14.75	210	28	13.33	1.1323	0.6360
15893594	rs760345	T/C		366	165	45.08	210	87	41.43	1.1476	0.4214
15893619	rs139733326	A/G		366	1	0.27	210	0	0	private variant	
15918508		T/C		366	1	0.27	210	0	0	private variant	
15918577	rs7281104	G/C		366	88	24.04	210	57	27.14	0.8651	0.4360
15918601	rs118133999	C/T		366	10	2.73	210	5	2.38	1.1359	0.8017
15918714	rs12329657	A/G		364	169	46.43	210	107	50.95	0.8571	0.3396
15954440		G/A		366	1	0.27	210	0	0	private variant	
15954528	rs2822785	G/A	missense variant	352	145	41.19	210	87	41.43	0.9902	0.9564

Table 3.6. con't

Position	SNP	Allele (Ref/Alt)	Consequence	MM patients			Controls			odds ratio	P-value
				N	variant alleles	%	N	variant alleles	%		
15954593	rs2822786	G/A	missense variant	366	104	28.42	210	50	23.81	1.3256	0.1707
15954601	rs139465416	G/T	missense variant	366	2	0.55	210	1	0.48	1.1492	0.9101
15954660	rs2822787	T/C	missense variant	366	301	82.24	210	163	77.62	1.3270	0.1834
15954748		C/A		366	0	0	210	1	0.48	private variant	
15954849	rs2822788	T/C		366	17	4.64	210	17	8.10	0.5710	0.0921
15954862	rs34228133	G/A		366	5	1.37	210	4	1.90	0.7093	0.6146
15955575	rs2822790	C/T		364	15	4.12	210	17	8.10	0.5098	0.0472
15955633	rs2822791	G/A	splice region variant	364	15	4.12	210	17	8.10	0.5098	0.0472
15955648	rs2822792	T/C	5' UTR variant	350	273	78.00	210	156	74.29	1.2195	0.3184
15955691	rs144975197	A/T	5' UTR variant	366	1	0.27	210	1	0.48	0.5714	0.6934
15955693	rs17240787	G/A	5' UTR variant	366	0	0	210	1	0.48	private variant	
15955779	rs9980152	G/A		366	17	4.64	210	17	8.10	0.5710	0.0921

Odds ratio and P-value were calculated by logistic regression analysis.

References

Alici, E., Konstantinidis, K.V., Aints, A., Dilber, M.S., and Abedi-Valugerdi, M. (2004). Visualization of 5T33 myeloma cells in the C57BL/KaLwRij mouse: establishment of a new syngeneic murine model of multiple myeloma. Experimental hematology *32*, 1064-1072.

Asimakopoulos, F., Kim, J., Denu, R.A., Hope, C., Jensen, J.L., Ollar, S.J., Hebron, E., Flanagan, C., Callander, N., and Hematti, P. (2013). Macrophages in multiple myeloma: emerging concepts and therapeutic implications. Leukemia & lymphoma *54*, 2112-2121.

Asosingh, K., Radl, J., Van Riet, I., Van Camp, B., and Vanderkerken, K. (2000). The 5TMM series: a useful in vivo mouse model of human multiple myeloma. The hematology journal : the official journal of the European Haematology Association / EHA *1*, 351-356.

Berardi, S., Ria, R., Reale, A., De Luisi, A., Catacchio, I., Moschetta, M., and Vacca, A. (2013). Multiple myeloma macrophages: pivotal players in the tumor microenvironment. J Oncol *2013*, 183602.

Brenner, S., Whiting-Theobald, N., Kawai, T., Linton, G.F., Rudikoff, A.G., Choi, U., Ryser, M.F., Murphy, P.M., Sechler, J.M., and Malech, H.L. (2004). CXCR4-transgene expression significantly improves marrow engraftment of cultured hematopoietic stem cells. Stem Cells *22*, 1128-1133.

Broderick, P., Chubb, D., Johnson, D.C., Weinhold, N., Forsti, A., Lloyd, A., Olver, B., Ma, Y.P., Dobbins, S.E., Walker, B.A.*, et al.* (2012). Common variation at 3p22.1 and 7p15.3 influences multiple myeloma risk. Nature genetics *44*, 58-61.

Burgess-Herbert, S.L., Cox, A., Tsaih, S.W., and Paigen, B. (2008). Practical applications of the bioinformatics toolbox for narrowing quantitative trait loci. Genetics *180*, 2227-2235.

Chu, L., Su, M.Y., Maggi, L.B., Jr., Lu, L., Mullins, C., Crosby, S., Huang, G., Chng, W.J., Vij, R., and Tomasson, M.H. (2012). Multiple myeloma-associated chromosomal translocation activates orphan snoRNA ACA11 to suppress oxidative stress. J Clin Invest *122*, 2793-2806.

Chubb, D., Weinhold, N., Broderick, P., Chen, B., Johnson, D.C., Forsti, A., Vijayakrishnan, J., Migliorini, G., Dobbins, S.E., Holroyd, A.*, et al.* (2013). Common variation at 3q26.2, 6p21.33, 17p11.2 and 22q13.1 influences multiple myeloma risk. Nature genetics *45*, 1221-1225.

Claudio, J.O., Zhu, Y.X., Benn, S.J., Shukla, A.H., McGlade, C.J., Falcioni, N., and Stewart, A.K. (2001). HACS1 encodes a novel SH3-SAM adaptor protein differentially expressed in normal and malignant hematopoietic cells. Oncogene *20*, 5373-5377.

Davies, F.E., Dring, A.M., Li, C., Rawstron, A.C., Shammas, M.A., O'Connor, S.M., Fenton, J.A., Hideshima, T., Chauhan, D., Tai, I.T.*, et al.* (2003). Insights into the multistep transformation of MGUS to myeloma using microarray expression analysis. Blood *102*, 4504-4511.

Didion, J.P., Yang, H., Sheppard, K., Fu, C.P., McMillan, L., de Villena, F.P., and Churchill, G.A. (2012). Discovery of novel variants in genotyping arrays improves genotype retention and reduces ascertainment bias. BMC genomics *13*, 34.

Fowler, J.A., Lwin, S.T., Drake, M.T., Edwards, J.R., Kyle, R.A., Mundy, G.R., and Edwards, C.M. (2011). Host-derived adiponectin is tumor-suppressive and a novel therapeutic target for multiple myeloma and the associated bone disease. Blood *118*, 5872-5882.

Jain, M., Ascensao, J., and Schechter, G.P. (2009). Familial myeloma and monoclonal gammopathy: a report of eight African American families. American journal of hematology *84*, 34-38.

Kim, J., Denu, R.A., Dollar, B.A., Escalante, L.E., Kuether, J.P., Callander, N.S., Asimakopoulos, F., and Hematti, P. (2012). Macrophages and mesenchymal stromal cells support survival and proliferation of multiple myeloma cells. British journal of haematology *158*, 336-346.

Kuehl, W.M., and Bergsagel, P.L. (2002). Multiple myeloma: evolving genetic events and host interactions. Nat Rev Cancer *2*, 175-187.

Kumar, S.K., Dispenzieri, A., Lacy, M.Q., Gertz, M.A., Buadi, F.K., Pandey, S., Kapoor, P., Dingli, D., Hayman, S.R., Leung, N.*, et al.* (2013). Continued improvement in survival in multiple myeloma: changes in early mortality and outcomes in older patients. Leukemia.

Kyle, R.A., Durie, B.G., Rajkumar, S.V., Landgren, O., Blade, J., Merlini, G., Kroger, N., Einsele, H., Vesole, D.H., Dimopoulos, M.*, et al.* (2010). Monoclonal gammopathy of undetermined significance (MGUS) and smoldering (asymptomatic) multiple myeloma: IMWG consensus perspectives risk factors for progression and guidelines for monitoring and management. Leukemia *24*, 1121-1127.

Kyle, R.A., Therneau, T.M., Rajkumar, S.V., Larson, D.R., Plevak, M.F., and Melton, L.J., 3rd (2004). Long-term follow-up of 241 patients with monoclonal gammopathy of undetermined significance: the original Mayo Clinic series 25 years later. Mayo Clinic proceedings *79*, 859-866.

Kyle, R.A., Therneau, T.M., Rajkumar, S.V., Larson, D.R., Plevak, M.F., Offord, J.R., Dispenzieri, A., Katzmann, J.A., and Melton, L.J., 3rd (2006). Prevalence of monoclonal gammopathy of undetermined significance. N Engl J Med *354*, 1362-1369.

Landgren, O., Gridley, G., Turesson, I., Caporaso, N.E., Goldin, L.R., Baris, D., Fears, T.R., Hoover, R.N., and Linet, M.S. (2006). Risk of monoclonal gammopathy of undetermined significance (MGUS) and subsequent multiple myeloma among African American and white veterans in the United States. Blood *107*, 904-906.

Landgren, O., Kyle, R.A., Pfeiffer, R.M., Katzmann, J.A., Caporaso, N.E., Hayes, R.B., Dispenzieri, A., Kumar, S., Clark, R.J., Baris, D.*, et al.* (2009). Monoclonal gammopathy of undetermined significance (MGUS) consistently precedes multiple myeloma: a prospective study. Blood *113*, 5412-5417.

Melton, L.J., 3rd, Kyle, R.A., Achenbach, S.J., Oberg, A.L., and Rajkumar, S.V. (2005). Fracture risk with multiple myeloma: a population-based study. J Bone Miner Res *20*, 487-493.

Munitz, A., Cole, E.T., Beichler, A., Groschwitz, K., Ahrens, R., Steinbrecher, K., Willson, T., Han, X., Denson, L., Rothenberg, M.E.*, et al.* (2010). Paired immunoglobulin-like receptor B (PIR-B) negatively regulates macrophage activation in experimental colitis. Gastroenterology *139*, 530-541.

Ogawa, K., Funaba, M., and Tsujimoto, M. (2008). A dual role of activin A in regulating immunoglobulin production of B cells. Journal of leukocyte biology *83*, 1451-1458.

Purcell, S., Neale, B., Todd-Brown, K., Thomas, L., Ferreira, M.A., Bender, D., Maller, J., Sklar, P., de Bakker, P.I., Daly, M.J.*, et al.* (2007). PLINK: a tool set for whole-genome association and population-based linkage analyses. American journal of human genetics *81*, 559-575.

Radl, J., De Glopper, E.D., Schuit, H.R., and Zurcher, C. (1979). Idiopathic paraproteinemia. II. Transplantation of the paraprotein-producing clone from old to young C57BL/KaLwRij mice. J Immunol *122*, 609-613.

Radl, J., and Hollander, C.F. (1974). Homogeneous immunoglobulins in sera of mice during aging. J Immunol *112*, 2271-2273.

Radl, J., Hollander, C.F., van den Berg, P., and de Glopper, E. (1978). Idiopathic paraproteinaemia. I. Studies in an animal model--the ageing C57BL/KaLwRij mouse. Clinical and experimental immunology *33*, 395-402.

Ribatti, D., Moschetta, M., and Vacca, A. (2013). Macrophages in multiple myeloma. Immunology letters.

Ribatti, D., Nico, B., and Vacca, A. (2006). Importance of the bone marrow microenvironment in inducing the angiogenic response in multiple myeloma. Oncogene *25*, 4257-4266.

Scavelli, C., Nico, B., Cirulli, T., Ria, R., Di Pietro, G., Mangieri, D., Bacigalupo, A., Mangialardi, G., Coluccia, A.M., Caravita, T.*, et al.* (2008). Vasculogenic mimicry by bone marrow macrophages in patients with multiple myeloma. Oncogene *27*, 663-674.

Sierra-Filardi, E., Puig-Kroger, A., Blanco, F.J., Nieto, C., Bragado, R., Palomero, M.I., Bernabeu, C., Vega, M.A., and Corbi, A.L. (2011). Activin A skews macrophage polarization by promoting a proinflammatory phenotype and inhibiting the acquisition of anti-inflammatory macrophage markers. Blood *117*, 5092-5101.

Sirohi, B., and Powles, R. (2006). Epidemiology and outcomes research for MGUS, myeloma and amyloidosis. Eur J Cancer *42*, 1671-1683.

Vacca, A., and Ribatti, D. (2011). Angiogenesis and vasculogenesis in multiple myeloma: role of inflammatory cells. Recent results in cancer research Fortschritte der Krebsforschung Progres dans les recherches sur le cancer *183*, 87-95.

Vachon, C.M., Kyle, R.A., Therneau, T.M., Foreman, B.J., Larson, D.R., Colby, C.L., Phelps, T.K., Dispenzieri, A., Kumar, S.K., Katzmann, J.A.*, et al.* (2009). Increased risk of monoclonal gammopathy in first-degree relatives of patients with multiple myeloma or monoclonal gammopathy of undetermined significance. Blood *114*, 785-790.

Vanderkerken, K., Asosingh, K., Croucher, P., and Van Camp, B. (2003). Multiple myeloma biology: lessons from the 5TMM models. Immunol Rev *194*, 196-206.

Wang, C., Yu, X., Cao, Q., Wang, Y., Zheng, G., Tan, T.K., Zhao, H., Zhao, Y., Wang, Y., and Harris, D. (2013). Characterization of murine macrophages from bone marrow, spleen and peritoneum. BMC immunology *14*, 6.

Wang, D., Stewart, A.K., Zhuang, L., Zhu, Y., Wang, Y., Shi, C., Keating, A., Slutsky, A., Zhang, H., and Wen, X.Y. (2010). Enhanced adaptive immunity in mice lacking the immunoinhibitory adaptor Hacs1. FASEB J *24*, 947-956.

Weinhold, N., Johnson, D.C., Rawstron, A.C., Forsti, A., Doughty, C., Vijayakrishnan, J., Broderick, P., Dahir, N.B., Begum, D.B., Hosking, F.J.*, et al.* (2014). Inherited genetic susceptibility to monoclonal gammopathy of unknown significance. Blood *123*, 2513-2517.

Xie, S., Chen, M., Yan, B., He, X., Chen, X., and Li, D. (2014). Identification of a Role for the PI3K/AKT/mTOR Signaling Pathway in Innate Immune Cells. PloS one *9*, e94496.

Yang, H., Ding, Y., Hutchins, L.N., Szatkiewicz, J., Bell, T.A., Paigen, B.J., Graber, J.H., de Villena, F.P., and Churchill, G.A. (2009). A customized and versatile high-density genotyping array for the mouse. Nature methods *6*, 663-666.

Zheng, Y., Cai, Z., Wang, S., Zhang, X., Qian, J., Hong, S., Li, H., Wang, M., Yang, J., and Yi, Q. (2009). Macrophages are an abundant component of myeloma microenvironment and protect myeloma cells from chemotherapy drug-induced apoptosis. Blood *114*, 3625-3628.

Zhu, Y.X., Benn, S., Li, Z.H., Wei, E., Masih-Khan, E., Trieu, Y., Bali, M., McGlade, C.J., Claudio, J.O., and Stewart, A.K. (2004). The SH3-SAM adaptor HACS1 is up-regulated in B cell activation signaling cascades. The Journal of experimental medicine *200*, 737-747.

Zingone, A., and Kuehl, W.M. (2011). Pathogenesis of monoclonal gammopathy of undetermined significance and progression to multiple myeloma. Seminars in hematology *48*, 4-12.

Chapter 4

Summary of work, future directions, and clinical relevancy

Part I: Summary of work

Contributions to the understanding of Paget's "congenial soil"

The "seed and soil" hypothesis has been accepted as a model for cancer cell metastasis for decades, but, despite advances in the field's knowledge of cancer cell biology and the bone microenvironment, the definition of a "congenial soil" remains incomplete. This dissertation is focused on elucidation of this question, addressing both the composition of the bone microenvironment "soil" and whole-host "congeniality" to disease progression.

We demonstrated a novel role for anti-angiogenic and therapeutic target TSP1 in bone homeostasis in **Chapter 2**. We found that TSP1 played important roles in maintaining bone matrix integrity through effects on materials properties and overall morphology. Further, we identified TSP1 as a necessary ligand in OC formation, inhibiting iNOS and thus permitting osteoclastogenesis. Finally, we demonstrated that TSP1-deficient bone failed to inhibit iNOS in OC, leading to a model of TSP1 as a paracrine signaling molecule, coupling OB activity to OC formation. These findings have implications for TSP1-pathway directed therapeutics in trial and in clinical use to have effects on bone that will be discussed in **Part II.**

In **Chapter 3**, we focused on identifying genetic risk loci contributing to bone marrow-dependent MGUS and MM susceptibility. Using a non-biased approach, we identified large candidate gene lists that may underlie susceptibility to MGUS and/or MM in humans and BIP, the analogous disorder in mice. Combining these two datasets, we identified a candidate gene list of five genes that may contribute to both murine BIP and human MGUS. One of these genes, *Samsn1*, drew our particular attention because it is a negative regulator of B-cell activation (Zhu

et al., 2004). Importantly, we found that BIP-prone KaLwRij mice have complete germline deletion of *Samsn1*, the first germline lesion identified in these mice. KaLwRij mouse plasma B-cells had enhanced activity in vitro and vivo, consistent with the published role for Samsn1 as a negative regulator in B-cells. KaLwRij mice have increased pro-tumorigenic M2-macrophage activation under basal conditions, and macrophages polarized to M2 have increased ability to promote tumor growth in vivo. These findings suggest a novel role for *Samsn1* in macrophages, fulfilling a similar inhibitory role as in B-cells. Finally, we demonstrated that restoration of *Samsn1* expression in KaLwRij-derived 5TGM1 myeloma cells reduced proliferation, indicating that *Samsn1* also contributes to cell-autonomous myeloma cell regulation. Thus, we demonstrated a single risk allele that participates in the negative regulation of both pre-malignant plasma B-cells and host MGUS- and MM-supportive macrophages.

While our studies focused on the role of *Samsn1* in conferring risk to murine BIP, it is likely not the only susceptibility gene contributing to the KaLwRij BIP phenotype. We will discuss the utility of further characterization of the KaLwRij mouse strain in **Part III**.

Collectively, the data presented in **Chapter 2** and **Chapter 3** contribute to our understanding of Paget's "congenial soil," providing important rationale for studying genes and proteins with pleiotropic roles in multiple cell types, locations, and pathologic states.

Part II: Future directions and clinical significance of Chapter 2

The work described in **Chapter 2** more fully characterized the role of TSP1 in bone homeostasis, but several questions regarding TSP1 function remain. As in other cell types and processes, it is likely that TSP1 plays pleiotropic, and perhaps contradictory, roles in bone.

What are the effects of bone-resident TSP1 on matrix composition and osteoclast activity?

We found that TSP1 contributes to bone quality, in part through maintenance of bone material properties. It is unclear, however, whether this phenotype is due to presence of the TSP1 ligand itself or TSP1 regulation of the stoichiometry and physical organization of other components of the bone matrix. TSP1 binds many proteins essential for bone quality, including hydroxyapatite, collagen, and numerous non-collagenous proteins including osteonectin, fibronectin, osteopontin, and proteoglycans. To determine whether presence of TSP1 influences the protein stoichiometry of bone, it would be useful to perform mass spectroscopy on devitalized bone from wild type and TSP1-/- mice. Unfortunately, the technology to perform mass spectroscopy in rigid calcified bone tissue is currently unavailable. As part of an effort to map the proteins of the extracellular matrisome, however, methods are being developed to digest bone lysate while maintaining protein structure with promising preliminary results (Alexandra Naba, 2013; Hynes and Naba, 2012). As these technologies become available, it will be important to evaluate mice deficient for TSP1 and other non-collagenous proteins to determine how they influence each other and, in turn, the bone extra cellular matrix to effect bone strength and osteoclast function.

A conditional TSP1 knock out in OBs would be a useful model to further evaluate the role of OB-deposited TSP1 in bone strength and quality. These mice presumably would not express TSP1 in the bone matrix or in OBs, but would have active TSP1 signaling elsewhere. While it has been shown that OBs secrete TSP1 during bone formation (Clezardin et al., 1989; Robey et al., 1989), it is possible that other cell types also produce TSP1 for deposition in the bone matrix. If we observed TSP1 in the bone of OB-conditional TSP1-/- mice, we could use the floxed TSP1 mouse crossed to cell-specific cre mice to isolate the secretory cells contributing bone matrix TSP1. To achieve a similar mouse model, we would typically create bone marrow chimeras by lethally irradiating TSP1-/- mice and transplanting wild type bone marrow to measure normal osteoclast resorption of TSP1-/- bone. TSP1-/- mice, however, are protected from sub-lethal irradiation (Isenberg et al., 2008) and partially protected from lethal irradiation. Attempts to engraft wild type donor bone marrow have failed, resulting in a chimeric hematopoietic compartment containing both wild type and TSP1-/- cells.

In **Chapter 2**, we identify that loss of TSP1 influences both bone morphology and bone matrix materials properties, and it is likely that OB expression and secretion of TSP1 plays a role in these phenotypes. While it has been established that OB secrete TSP1, it is unclear at what maturation stage OB contribute to TSP1 deposition in bone. It may be interesting to use multiple OB-lineage cre mice (osterix-cre to target early OBs, osteocalcin-cre to target mature OB, and DMP1-cre to target osteocytes) to identify the temporal requirement of TSP1 expression and secretion for matrix deposition during OB maturation. Using this OB-conditional TSP1-/- model, we could evaluate bone morphology, bone strength parameters, and bone material properties as in **Chapter 2** to determine if bone strength phenotype in TSP1-/- is solely contributed to osteoblastic secretion of TSP1. Moreover, beyond the scope of our work

described here, further work is necessary to understand the role of TSP1 in bone strength and fracture healing, especially given established roles for TSP1 in wound healing and angiogenesis.

In addition to its role in promoting bone quality, we hypothesize in **Chapter 2** that TSP1 deposited in the bone matrix by OB is responsible for inhibiting iNOS transcription in OC progenitors. If OB-deposited TSP1 is necessary for OC formation, we would observe a similar OC phenotype in conditional TSP1-/- in OB mice as in the global TSP1-/- mouse: decreased serum CTX that is rescued upon inhibition of nitric oxide synthase. These experiments would also further elucidate the role of TSP1 as a paracrine signaling molecule, coupling OB activity to OC formation via the bone matrix.

What receptors does TSP1 bind to modulate OC activity?

While we demonstrated that TSP1 is a negative regulator of iNOS in pre-OC, it remains unclear what receptor(s) it binds to exert this effect. In other cell types, both CD47 and CD36 have been implicated in TSP1-mediated inhibition of NO signaling (Isenberg et al., 2006; Isenberg et al., 2005). Importantly, TSP1 has not previously been described to modulate iNOS, though effects on eNOS and downstream molecules have been reported. Our lab previously demonstrated that CD47 negatively regulates iNOS in OC (Uluckan et al., 2009), leading us to hypothesize that it is likely a requisite receptor for TSP1-mediated NO effects. TSP1-/- mice had a more severe OC phenotype in vivo than any TSP1-receptor knock out mouse models, including CD47-/- and CD36-/-, suggesting that TSP1 exerts its effects on OC via multiple different receptors. To test whether TSP1 binds both CD47 and CD36 to inhibit NO signaling in early OC, we could evaluate iNOS in OC from double knock-out CD47-/-, CD36-/- mice. If both receptors

contribute to TSP1-mediated NOS inhibition, treating OC with TSP1 neutralizing antibody should have no additional effect beyond the null phenotype.

Does TSP1 promote or inhibit metastatic tumor growth in bone?

In addition to understanding its role in homeostasis, it is important to investigate the role of TSP1 in bone during pathologic states such as bone metastasis. TSP1 was the first identified endogenous anti-angiogenic, and TSP1-/- mice have increased primary tumor burden and tumor-associated vasculature (Rodriguez-Manzaneque et al., 2001). In some bone metastatic prostate cancer models however, increased TSP1 promotes tumor progression through effects on cancer cell migration (Dias et al., 2012; Firlej et al., 2011; John et al., 2010; Tuszynski et al., 1987). Interestingly, high tumor-derived TSP1 levels are a prognostic marker for cancer progression and relapse (Firlej et al., 2011). We found that the bone metastatic C42b prostate cancer cell line expressed significantly higher levels of TSP1 compared to its parental non-metastatic LnCaP cell line by RNA-seq (Li Jia, unpublished data). Similarly, but to a lesser magnitude, TSP1 expression is also elevated in bone metastatic melanoma cell line subclone B16-F10 compared to its parental non-metastatic cell line, B16-F0. We would hypothesize that high TSP1-expressing bone metastatic tumors overcome TSP1's anti-angiogenic functions and take advantage of other TSP1 functions such as mediating migration and adhesion. Once in the bone microenvironment, tumoral secretion of TSP1 will stimulate OC and initiate the vicious cycle of bone metastasis, leading to increased tumor growth. We would anticipate, therefore, that injection of TSP1-low primary tumor cell line and TSP1-high bone metastatic subclone into the mammary fat pad of mice would show similar primary tumor growth, but that the TSP1-high tumor would have

141

increased bone metastasis. In an intratibial model, we would anticipate that TSP1-high expressing tumors would have increased bone lesions and increased tumor burden. Subsequent overexpression and knock-down experiments in these cell lines would demonstrate sufficiency and necessity of tumor-derived TSP1 in mediating migration to and growth in bone.

While the experiments outlined address the role of tumor-derived TSP1 in tumor growth in bone, it is still unclear what role bone microenvironment TSP1 plays in bone metastasis. We hypothesized that TSP1 would promote tumor growth in bone by promoting OC activity and stimulating the vicious cycle. Our studies of bone metastasis in TSP1-/- mice, however, have been largely inconclusive with TSP1-/- mice having modest but non-statistically significant increases in tumor burden in aggressive intratibial models (B16-F10 melanoma and PyMMT-LV1) and an intracardiac model (B16-F10) of bone metastases, but no increases in tumor-associated osteolysis. Though we are unable to make any definitive conclusions, these data are consistent with the hypothesis that host-derived TSP1 may play different roles in tumor progression based on location and severity of malignancy. To investigate the role of TSP1 in bone metastasis, it will be necessary to use a less aggressive model, such as a orthotopic injection of PyMMT cells into the mammary fat pad of TSP1-/- mice, performing tumor resection, and monitoring bone metastasis. A slower-growing tumor may allow the time necessary to uncover subtle effects of TSP1 on metastatic bone tumor burden.

Subtle effects of host TSP1 on bone metastasis may be due in part to the role of TSP1 in angiogenesis. TSP1 is largely recognized an anti-angiogenic through its interactions with CD47 and $\alpha v \beta 3$, but there are also reports that TSP1 interacts with $\alpha 6$ to promote angiogenesis. Moreover, TSP1's angiogenic properties have not been evaluated in the sinusoidal blood vessels

of the bone microenvironment. It would be useful to evaluate the effects of tumor- and host-

TSP1 on angiogenesis in the experiments described above.

Clinical significance

Will pharmacologic modulation of the TSP1 pathway have effects on bone?

It will be interesting to evaluate the bone effects of TSP1-pathway directed therapeutics under development and in clinical use as anti-cancer therapeutics (TSP1 mimetics and CD47 antibodies) and to modulate blood pressure (NO donors and NOS inhibitors). We anticipate that agents that mimic TSP1 signaling (TSP1 mimetics, CD47 antagonists, and NOS inhibitors such as L-NAME used in our study) will stimulate osteoclastic bone resorption. While this increase in bone remodeling may be of minimal concern in the general population, it will be important to monitor patients at increased risk of skeletal related events such as cardiovascular disease patients presenting with osteoporosis and cancer patients at risk for bone metastasis. Our data provide rationale for TSP1-pathway inhibitory therapeutics (NO donors such as Isordil and TSP1-blocking CD47 antibodies) to reduce OC activity, especially in comorbidities such as osteoporosis and bone metastasis. As these TSP1-pathway directed therapeutics become standard-of-care, it will be important to identify and monitor both harmful and positive bone effects, including effects on bone mineral density as well as bone quality.

Part III: Future directions and clinical significance of Chapter 3

The major finding presented in **Chapter 3** is that *Samsn1* is deleted in the germline of BIP-resistant KaLwRij mice. KaLwRij have enhanced B-cell and macrophage activation, and re-expression of *Samsn1* in myeloma cells reduces proliferation. Therefore, we hypothesize that *Samsn1* contributes to genetic susceptibility of murine BIP through independent effects on multiple cell types, and that the SAMSN1 pathway likely participates in human genetic risk to MGUS and MM.

Is *Samsn1* deficiency sufficient to confer increased risk of BIP in mice?

To determine whether *Samsn1* deletion is sufficient to confer BIP-susceptibility in mice, we could use a targeted Samsn1-/- mouse model (Wang et al., 2010). To determine effects on BIP-susceptibility, we could immunize Samsn1-/- mice and monitor SPEP response as in **Figure 3.1b**. In addition, to determine whether loss of Samsn1 creates a myeloma-permissive microenvironment, we could inoculate Samsn1-/- mice with 5TGM1 myeloma cells and monitor tumor growth. If *Samsn1* contributes to host BIP susceptibility and microenvironment support of myeloma, we would predict that SPEP response and tumor burden in Samsn1-/- mice would be similar to KaLwRij.

What role do *Samsn1*-null macrophages play in BIP and myeloma?

The only published role for *Samsn1* is in B-cell activation ((Wang et al., 2010; Zhu et al., 2004)), but many cells of the hematopoietic lineage, including macrophages, are *Samsn1* expressors (BioGPS, (Claudio et al., 2001)). In B-cells, SAMSN1 is a proposed adaptor protein

that interacts with the ITIM domain of PIR-B and phosphorylated SHP-1/2 to inhibit B-cell activation, likely through modulation of Lyn phosphorylation and subsequent effects on B-cell receptor (BCR) and its binding partners, including Syk, PI3 kinase, and PLCγ ((Wang et al., 2010; Zhu et al., 2004)) (**Figure 4.1**). Notably, many of these proteins participate in regulation of other hematopoietic cells, with reports of BCR complex proteins to promote and PIR-B complex proteins to inhibit macrophage activation and function (Brenner et al., 2004; Munitz et al., 2010; Xie et al., 2014). We found that KaLwRij mice have increased macrophage activation in vitro and increased pro-tumor effects in vivo, and we hypothesize that these effects are due to *Samsn1* deletion. Repeating these macrophage experiments in Samsn1-/- mice would determine whether *Samsn1* deletion is the causal variant of the KaLwRij macrophage phenotype. Furthermore, it will also important to identify the macrophage-autonomous role of *Samsn1*, including regulatory factors, binding partners, and downstream effects, to identify manipulatable pathways for modulating MGUS and myeloma microenvironment in a preventative setting.

Increased macrophage activation has been implicated in human MM pathogenesis (Asimakopoulos et al., 2013; Berardi et al., 2013; Ribatti et al., 2013). We found that KaLwRij mice have macrophage activation that precedes the onset of detectable BIP. We hypothesize that the increased KaLwRij macrophage activation increases BIP development, and subsequently contributes to transformation to overt myeloma. Notably, however, it is unclear both in mice and in humans whether the microenvironment promotes MGUS and myeloma development or whether microenvironment changes are a result of increased B-cell activation, representing "low-level" MGUS undetectable by current methods. It will be difficult to answer this question using current mouse models of MGUS, with the KaLwRij mouse only presenting with BIP at 2 years of age. Vitamin D deficiency and irradiation can accelerate BIP development in KaLwRij mice

(Michael Tomasson, unpublished data). We predict that chronic activation of macrophages by LPS treatment or transplant of in vitro activated macrophages may also accelerate BIP development via increased support of pre-malignant plasma B-cells. In addition, as the field identifies susceptibility loci contributing to MGUS and MM susceptibility in humans and in mice, more precise genetic models can be developed to study the pre-malignant microenvironment and evaluate the contribution of individual microenvironment cell types to disease progression, including macrophages as well as osteoclasts and bone marrow stromal cells.

What genetic variation contributes to stepwise progression of myeloma in KaLwRij mice?

We found that KaLwRij mice have homozygous germline deletion of *Samsn1*, but, while *Samsn1* likely contributes to the increased penetrance of BIP in KaLwRij, it is unlikely to be the only participating locus. Our SNP analysis identified several thousand variants between BIP-resistant B6 mice and BIP-susceptible KaLwRij mice, providing a wealth of information of genes that may contribute to BIP in mice. Particularly compelling are genes with dramatically high variation between B6 and KaLwRij, in some cases with more than 100 variant SNPs. In addition to the germline variants, we also identified differential gene expression between B6 and KaLwRij in macrophages and bone marrow stromal cells, both known to support MGUS and MM cells. Interestingly, several differentially expressed genes have genetic variation between B6 and KaLwRij, suggesting that those alleles confer risk via impacts on the microenvironment. Importantly, however, we did not identify germline genetic variation in many of the differentially expressed genes, indicating that their gene expression is dependent on non-cell autonomous effects or due to downstream effects of KaLwRij genetic variants. It is likely that

causal gene variants lie in shared or cooperative pathways to modulate B-cells and microenvironment cells to confer increased BIP risk. Bioinformatics pathway analysis of all candidate genes would be useful to identify pathways of interest for further investigation.

What role do the other candidate genes (*Fstl4, Ccm2, Tenm3,* and *Csmd1*) play in BIP risk?

In addition to whole gene-set analysis, focused examination and verification of the other four candidate genes identified in the mouse and human integrative analysis would be useful to further characterize the genetic contributions to BIP-risk in KaLwRij mice and MM-risk in humans. None of the remaining four candidate genes have been reported to play roles in plasma B-cells, myeloma cells, or host supportive cells. Based on the success of *Samsn1*, however, we anticipate that further investigation of *Fstl4, Ccm2, Tenm3,* and *Csmd1* will identify new roles for the genes in cells contributing to MM progression.

While most of the research of Ccm2 has focused on its effects in cerebral cavernous malformations, there is evidence that it is involved in p38 MAP kinase signaling (Zawistowski et al., 2005), known to promote MM growth and a target for therapeutic intervention (Campbell et al., 2014). Csmd may also be a good candidate as it exerts anti-tumor effects in solid tumors, and loss of *Csmd1* is associated with poor prognosis in colorectal cancer patients (Tang et al., 2012; Zhang and Song, 2014). Relatively little is known about the function of Tenm3, with most of the published research focused on its role in vision. It is possible that *Tenm3* underlies a trait other than BIP-susceptibility present in KaLwRij that has not yet been characterized.

The most intriguing gene for subsequent follow-up studies is *Fstl4*. While there are no reports of Fstl4 directly influencing cells contributing to myeloma pathogenesis, there is evidence for a downstream molecule, activin A, in multiple cell types participating in MM

progression. Follistatin inhibits the activity of activin A to promote B-cell immunoglobulin secretion (Ogawa et al., 2008), MM bone disease (Vallet et al., 2010), and pro-tumor M2 macrophage polarization (Sierra-Filardi et al., 2011). Further, the actvin A pathway has direct clinical implications with increased circulating activin A correlated with increased bone disease and decreased survival in MM patients (Terpos et al., 2012). With potential roles in multiple cell types, it will be interesting to characterize the role of Fstl4 in mediating the activin A pathway in BIP-prone mice and in MGUS patients.

Sequencing of KaLwRij to identify genetic events during myeloma progression

While SNP mapping was successful in our approach described in **Chapter 3**, the approach has substantial shortcomings. SNP mapping takes advantage of "marker" SNPs that are likely in linkage with causal variants, but are not necessarily causal themselves. Moreover, SNP mapping will not identify small but biologically significant genetic lesions that may contribute to disease, especially when used to compare two closely related strains. To fully characterize the KaLwRij mouse strain, whole genome sequencing is necessary to identify all variants, including protein coding genes, non-coding RNAs, and regulatory regions. Logistically important, the closely related but BIP-resistant B6 strain is the mouse reference genome and is complete, well annotated, and publically available.

It is likely that much of the variation between B6 and KaLwRij is unrelated to inherited BIP risk. To reduce follow-up studies of non-BIP related variation, we could compare the sequence of the locus of interest from our KaLwRij colony to other isolated BIP-susceptible KaLwRij colonies. Because of the limited commercial availability, individual laboratories maintain independent KaLwRij colonies, all of which have been inbred independently for more

than 20 generations, the requisite for defining a substrain (2013). Comparing our KaLwRij substrain sequence to the sequences of other sub-strains (e.g. Croucher colony and Zannettino colony at the Garvan Institute, Mundy colony at Vanderbilt University, etc.) will help to filter variation due to genetic drift. We anticipate that all BIP-susceptible KaLwRij colonies would share alleles contributing to increased BIP risk.

While the work presented in **Chapter 3** explored the transition from a normal state to BIP, it does not address the transition to overt myeloma. The KaLwRij 5T myeloma model is the ideal system to identify plasma-cell intrinsic genetic changes between BIP and myeloma. The 5T myeloma cell lines were isolated from spontaneous myelomas arising in KaLwRij mice, and can be transplanted into syngeneic KaLwRij mice to propagate the myeloma (Alici et al., 2004; Asosingh et al., 2000; Vanderkerken et al., 2003). In this work, we utilized 5TGM1 myeloma cells to determine the role of *Samsn1* in myeloma cell proliferation. Whole genome sequencing of the 5TGM1 cell line and comparing the variation to the KaLwRij sequence would identify genes that are mutated during the BIP-to-myeloma transition in mice. Similar to comparing our KaLwRij colony sequence to other KaLwRij substrains, it would be useful to compare the 5TGM1 sequence to other available 5T cell lines (e.g. 5T33vv, 5T33vt, etc.) to filter any variation due to genetic drift. At the conclusion of these sequencing efforts, therefore, we would have a genetic model for the plasma-cell intrinsic variation that participates in the step-wise progression of myeloma: normal (B6), "MGUS" (BIP – KaLwRij), and myeloma (5T cell line).

Clinical significance:

Genetic screening and treatment strategies for high-risk MGUS patients

Despite advances in treatment, including chemotherapy, proteasome inhibitors, and bisphosphonates, that target both the malignant plasma cell as well as host supportive cells, MM remains an invariably fatal disease with a short median survival of only 6 years. MM has a requisite precursor, MGUS, that represents a unique opportunity for preventative treatment of malignancy. Despite the rapid progression of MM, however, MGUS remains non-malignant for decades, and often never transforms to overt myeloma. Because of low rates of progression, MGUS patients are not clinically treated.

Inherited risk of MM is due to increased risk of MGUS, not increased rate of transformation from MGUS to myeloma. Notably, plasma-cell autonomous genetic changes occur during the transition from normal to MGUS, with few variations between MGUS and MM affected cells (Davies et al., 2003), implicating B-cell extrinsic events in promoting malignancy. Identifying susceptibility loci to MGUS, specifically in genes that participate in microenvironment cells, will provide important data for the development of screening strategies to identify high-risk MGUS patients. Moreover, understanding malignant-cell extrinsic mechanisms that promote the progression of MGUS to MM will help to identify preventative strategies to prevent or delay onset of MM.

In our work presented here, we used a strategy to identify inherited genetic variation in MM patients compared to controls. Our analysis yielded gene candidates that act in multiple cell types, both B-cells, the current focus of the myeloma field, and in host supportive microenvironment cells. We focused our efforts on the candidate gene *Samsn1* and evaluated its

biologic function in murine myeloma cells, BIP-susceptible B-cells, and supportive macrophages. Importantly, we identified two SNPs in *Samsn1* that are underrepresented in a MM patient population. These data provide important rationale for pursuing *Samsn1* pathway genes for both screening of MGUS patients and development of preventative strategies targeted to both B-cells and macrophages.
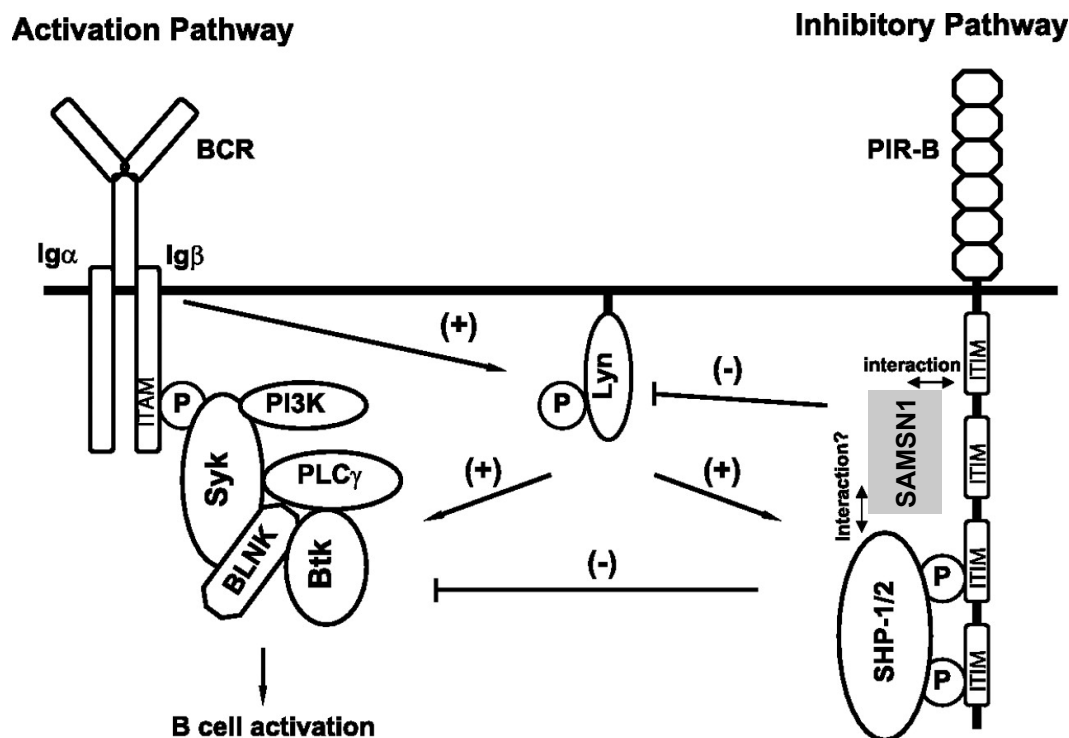
Figure 4.1.
SAMSN1 is member of the PIR-B / SHP-1/2 B-cell inhibitory complex
Following activation of the B-cell receptor (BCR), Lyn phosphorylates the ITAM for recruitment of the positive regulatory signaling complex. Lyn also phosphorylates the ITIM domain of PIR-B for recruitment of SHP-1/2 for negative regulation of B-cells. SAMSN1 is likely a component of this inhibitory complex, with interactions with the PIR-B ITIM domains and SHP-1/2.
Modified from (Wang et al., 2010).

References

(2013). Guidelines for Nomenclature of Mouse and Rat Strains. Paper presented at: International Committee on Standardized Genetic Nomenclature for Mice.

Alexandra Naba, R.H. (2013). Exploring the role of the extracellular matrix in tumor progression. Paper presented at: 13th International Conference on Cancer-Induced Bone Disease (Miami, FL).

Alici, E., Konstantinidis, K.V., Aints, A., Dilber, M.S., and Abedi-Valugerdi, M. (2004). Visualization of 5T33 myeloma cells in the C57BL/KaLwRij mouse: establishment of a new syngeneic murine model of multiple myeloma. Experimental hematology *32*, 1064-1072.

Asimakopoulos, F., Kim, J., Denu, R.A., Hope, C., Jensen, J.L., Ollar, S.J., Hebron, E., Flanagan, C., Callander, N., and Hematti, P. (2013). Macrophages in multiple myeloma: emerging concepts and therapeutic implications. Leukemia & lymphoma *54*, 2112-2121.

Asosingh, K., Radl, J., Van Riet, I., Van Camp, B., and Vanderkerken, K. (2000). The 5TMM series: a useful in vivo mouse model of human multiple myeloma. The hematology journal : the official journal of the European Haematology Association / EHA *1*, 351-356.

Berardi, S., Ria, R., Reale, A., De Luisi, A., Catacchio, I., Moschetta, M., and Vacca, A. (2013). Multiple myeloma macrophages: pivotal players in the tumor microenvironment. J Oncol *2013*, 183602.

Brenner, S., Whiting-Theobald, N., Kawai, T., Linton, G.F., Rudikoff, A.G., Choi, U., Ryser, M.F., Murphy, P.M., Sechler, J.M., and Malech, H.L. (2004). CXCR4-transgene expression significantly improves marrow engraftment of cultured hematopoietic stem cells. Stem Cells *22*, 1128-1133.

Campbell, R.M., Anderson, B.D., Brooks, N.A., Brooks, H.B., Chan, E.M., De Dios, A., Gilmour, R., Graff, J.R., Jambrina, E., Mader, M.*, et al.* (2014). Characterization of LY2228820 dimesylate, a potent and selective inhibitor of p38 MAPK with antitumor activity. Mol Cancer Ther *13*, 364-374.

Claudio, J.O., Zhu, Y.X., Benn, S.J., Shukla, A.H., McGlade, C.J., Falcioni, N., and Stewart, A.K. (2001). HACS1 encodes a novel SH3-SAM adaptor protein differentially expressed in normal and malignant hematopoietic cells. Oncogene *20*, 5373-5377.

Clezardin, P., Jouishomme, H., Chavassieux, P., and Marie, P.J. (1989). Thrombospondin is synthesized and secreted by human osteoblasts and osteosarcoma cells. A model to study the different effects of thrombospondin in cell adhesion. European journal of biochemistry / FEBS *181*, 721-726.

Davies, F.E., Dring, A.M., Li, C., Rawstron, A.C., Shammas, M.A., O'Connor, S.M., Fenton, J.A., Hideshima, T., Chauhan, D., Tai, I.T.*, et al.* (2003). Insights into the multistep transformation of MGUS to myeloma using microarray expression analysis. Blood *102*, 4504-4511.

Dias, J.V., Benslimane-Ahmim, Z., Egot, M., Lokajczyk, A., Grelac, F., Galy-Fauroux, I., Juliano, L., Le-Bonniec, B., Takiya, C.M., Fischer, A.M.*, et al.* (2012). A motif within the N-terminal domain of TSP-1 specifically promotes the proangiogenic activity of endothelial colony-forming cells. Biochem Pharmacol *84*, 1014-1023.

Firlej, V., Mathieu, J.R., Gilbert, C., Lemonnier, L., Nakhle, J., Gallou-Kabani, C., Guarmit, B., Morin, A., Prevarskaya, N., Delongchamps, N.B.*, et al.* (2011). Thrombospondin-1 Triggers Cell Migration and Development of Advanced Prostate Tumors. Cancer Res.

Hynes, R.O., and Naba, A. (2012). Overview of the matrisome--an inventory of extracellular matrix constituents and functions. Cold Spring Harbor perspectives in biology *4*, a004903.

Isenberg, J.S., Maxhimer, J.B., Hyodo, F., Pendrak, M.L., Ridnour, L.A., DeGraff, W.G., Tsokos, M., Wink, D.A., and Roberts, D.D. (2008). Thrombospondin-1 and CD47 limit cell and tissue survival of radiation injury. Am J Pathol *173*, 1100-1112.

Isenberg, J.S., Ridnour, L.A., Dimitry, J., Frazier, W.A., Wink, D.A., and Roberts, D.D. (2006). CD47 is necessary for inhibition of nitric oxide-stimulated vascular cell responses by thrombospondin-1. J Biol Chem *281*, 26069-26080.

Isenberg, J.S., Ridnour, L.A., Perruccio, E.M., Espey, M.G., Wink, D.A., and Roberts, D.D. (2005). Thrombospondin-1 inhibits endothelial cell responses to nitric oxide in a cGMP-dependent manner. Proc Natl Acad Sci U S A *102*, 13141-13146.

John, A.S., Rothman, V.L., and Tuszynski, G.P. (2010). Thrombospondin-1 (TSP-1) Stimulates Expression of Integrin alpha6 in Human Breast Carcinoma Cells: A Downstream Modulator of TSP-1-Induced Cellular Adhesion. J Oncol *2010*, 645376.

Munitz, A., Cole, E.T., Beichler, A., Groschwitz, K., Ahrens, R., Steinbrecher, K., Willson, T., Han, X., Denson, L., Rothenberg, M.E.*, et al.* (2010). Paired immunoglobulin-like receptor B (PIR-B) negatively regulates macrophage activation in experimental colitis. Gastroenterology *139*, 530-541.

Ogawa, K., Funaba, M., and Tsujimoto, M. (2008). A dual role of activin A in regulating immunoglobulin production of B cells. Journal of leukocyte biology *83*, 1451-1458.

Ribatti, D., Moschetta, M., and Vacca, A. (2013). Macrophages in multiple myeloma. Immunology letters.

Robey, P.G., Young, M.F., Fisher, L.W., and McClain, T.D. (1989). Thrombospondin is an osteoblast-derived component of mineralized extracellular matrix. J Cell Biol *108*, 719-727.

Rodriguez-Manzaneque, J.C., Lane, T.F., Ortega, M.A., Hynes, R.O., Lawler, J., and Iruela-Arispe, M.L. (2001). Thrombospondin-1 suppresses spontaneous tumor growth and inhibits activation of matrix metalloproteinase-9 and mobilization of vascular endothelial growth factor. Proc Natl Acad Sci U S A *98*, 12485-12490.

Sierra-Filardi, E., Puig-Kroger, A., Blanco, F.J., Nieto, C., Bragado, R., Palomero, M.I., Bernabeu, C., Vega, M.A., and Corbi, A.L. (2011). Activin A skews macrophage polarization by promoting a proinflammatory phenotype and inhibiting the acquisition of anti-inflammatory macrophage markers. Blood *117*, 5092-5101.

Tang, M.R., Wang, Y.X., Guo, S., Han, S.Y., and Wang, D. (2012). CSMD1 exhibits antitumor activity in A375 melanoma cells through activation of the Smad pathway. Apoptosis : an international journal on programmed cell death *17*, 927-937.

Terpos, E., Kastritis, E., Christoulas, D., Gkotzamanidou, M., Eleutherakis-Papaiakovou, E., Kanellias, N., Papatheodorou, A., and Dimopoulos, M.A. (2012). Circulating activin-A is elevated in patients with advanced multiple myeloma and correlates with extensive bone involvement and inferior survival; no alterations post-lenalidomide and dexamethasone therapy. Annals of oncology : official journal of the European Society for Medical Oncology / ESMO *23*, 2681-2686.

Tuszynski, G.P., Gasic, T.B., Rothman, V.L., Knudsen, K.A., and Gasic, G.J. (1987). Thrombospondin, a potentiator of tumor cell metastasis. Cancer Res *47*, 4130-4133.

Uluckan, O., Becker, S.N., Deng, H., Zou, W., Prior, J.L., Piwnica-Worms, D., Frazier, W.A., and Weilbaecher, K.N. (2009). CD47 regulates bone mass and tumor metastasis to bone. Cancer Res *69*, 3196-3204.

Vallet, S., Mukherjee, S., Vaghela, N., Hideshima, T., Fulciniti, M., Pozzi, S., Santo, L., Cirstea, D., Patel, K., Sohani, A.R.*, et al.* (2010). Activin A promotes multiple myeloma-induced osteolysis and is a promising target for myeloma bone disease. Proc Natl Acad Sci U S A *107*, 5124-5129.

Vanderkerken, K., Asosingh, K., Croucher, P., and Van Camp, B. (2003). Multiple myeloma biology: lessons from the 5TMM models. Immunol Rev *194*, 196-206.

Wang, D., Stewart, A.K., Zhuang, L., Zhu, Y., Wang, Y., Shi, C., Keating, A., Slutsky, A., Zhang, H., and Wen, X.Y. (2010). Enhanced adaptive immunity in mice lacking the immunoinhibitory adaptor Hacs1. FASEB J *24*, 947-956.

Xie, S., Chen, M., Yan, B., He, X., Chen, X., and Li, D. (2014). Identification of a Role for the PI3K/AKT/mTOR Signaling Pathway in Innate Immune Cells. PloS one *9*, e94496.

Zawistowski, J.S., Stalheim, L., Uhlik, M.T., Abell, A.N., Ancrile, B.B., Johnson, G.L., and Marchuk, D.A. (2005). CCM1 and CCM2 protein interactions in cell signaling: implications for cerebral cavernous malformations pathogenesis. Human molecular genetics *14*, 2521-2531.

Zhang, R., and Song, C. (2014). Loss of CSMD1 or 2 may contribute to the poor prognosis of colorectal cancer patients. Tumour biology : the journal of the International Society for Oncodevelopmental Biology and Medicine *35*, 4419-4423.

Zhu, Y.X., Benn, S., Li, Z.H., Wei, E., Masih-Khan, E., Trieu, Y., Bali, M., McGlade, C.J., Claudio, J.O., and Stewart, A.K. (2004). The SH3-SAM adaptor HACS1 is up-regulated in B cell activation signaling cascades. The Journal of experimental medicine *200*, 737-747.
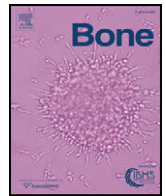
Review

Integrins and bone metastasis: Integrating tumor cell and stromal cell interactions

Jochen G. Schneider [b,c], Sarah R. Amend [a], Katherine N. Weilbaecher [a,*]

[a] Department of Medicine and Division of Oncology, Washington University, School of Medicine, St. Louis, MO, USA
[b] Institute for Clinical Biochemistry and Pathobiochemistry, University of Wuerzburg, Germany
[c] Luxembourg Centre for Systems Biomedicine (LCSB), University of Luxembourg, Luxembourg

ARTICLE INFO

ABSTRACT

Integrins on both tumor cells and the supporting host stromal cells in bone (osteoclasts, new blood vessels, inflammatory cells, platelets and bone marrow stromal cells) play key roles in enhancing bone metastasis. Tumor cells localize to specific tissues through integrin-mediated contacts with extracellular matrix and stromal cells. Integrin expression and signaling are perturbed in cancer cells, allowing them to "escape" from cell–cell and cell–matrix tethers, invade, migrate and colonize within new tissues and matrices. Integrin signaling through $\alpha v\beta 3$ and VLA-4 on tumor cells can promote tumor metastasis to and proliferation in the bone microenvironment. Osteoclast (OC) mediated bone resorption is a critical component of bone metastasis and can promote tumor growth in bone and $\alpha v\beta 3$ integrins are critical to OC function and development. Tumors in the bone microenvironment can recruit new blood vessel formation, platelets, pro-tumor immune cells and bone marrow stromal cells that promote tumor growth and invasion in bone. Integrins and their ligands play critical roles in platelet aggregation ($\alpha v\beta 3$ and $\alpha IIb\beta 3$), hematopoietic cell mobilization (VLA-4 and osteopontin), neoangiogenesis ($\alpha v\beta 3$, $\alpha v\beta 5$, $\alpha 6\beta 4$, and $\beta 1$ integrin) and stromal function (osteopontin and VLA-4). Integrins are involved in the pathogenesis of bone metastasis at many levels and further study to define integrin dysregulation by cancer will yield new therapeutic targets for the prevention and treatment of bone metastasis.

© 2010 Elsevier Inc. All rights reserved.

Contents

Introduction

The development of bone metastasis is common in many cancers, occurring in virtually all patients with multiple myeloma, in 65%–75% of patients with advanced breast and prostate cancers, and in 30%–40% of patients with lung cancer [1–3]. The consequences of bone metastases are often devastating and can cause pain, pathologic

* Corresponding author. Department of Medicine and Cell Biology and Physiology, Division of Oncology, Washington University, School of Medicine, 660 S. Euclid Ave, PO Box 8069, St. Louis, MO, 63110, USA.
E-mail address: kweilbae@wustl.edu (K.N. Weilbaecher).

fractures, spinal cord and other nerve-compression syndromes and life-threatening hypercalcemia [4]. Both osteolytic lesions and osteoblastic bone metastases are associated with increased OC activity and disrupted bone micro-architecture [5,6]. In the bone microenvironment, tumor cells secrete soluble factors that promote bone remodeling resulting in the release of additional bone matrix-bound growth factors which further activate OCs and osteoblasts (OB) and promote tumor growth [3,4,7–16]. Anti-resorptive therapy, e.g. with bisphosphonates or denosumab, significantly decreases skeletal complications of cancer and is a standard of care for patients with bone metastases [4,8,17–19]. In addition to their effects on bone, tumors in the bone microenvironment recruit blood vessel formation, platelets, immune cells and stromal cells that promote tumor growth and invasion in bone. Integrin-mediated cell signaling plays a critical role in many of these processes during bone metastasis, including platelet aggregation (αIIbβ3), hematopoietic/immune cell mobilization (VLA-4 and osteopontin), neoangiogenesis (αvβ3, αvβ5, α6β4, and β1 integrin) and stromal function (osteopontin and VLA-4) (see Fig. 1). For these reasons, the mechanisms by which integrin signaling mediates the pathogenesis of bone metastasis have been an area of active research.

Integrin structure, activation and signaling

Integrins are heterodimeric transmembrane glycoproteins that facilitate cell–cell and cell–extracellular matrix (ECM) adhesion and cell migration [20]. Integrins recruit many intracellular signaling molecules and can activate survival, proliferation, and motility signaling pathways [21]. There are 8 beta and 18 alpha integrin subunits that assemble into 24 unique known combinations in different cell types, each characterized by distinct ligand binding specificities (including collagen, osteopontin, fibronectin, laminin, and others, depending on the integrin family), signaling abilities, and regulatory mechanisms [22]. Integrins are activated by conformational changes in the integrin extracellular domains. When the integrin α and β subunit cytoplasmic and transmembrane domains remain closely juxtaposed, the extracellular domains are held in a closed conformation. Activation by intracellular signals to the cytoplasmic tails results in separation of the α and β cytoplasmic and transmembrane domains and exposure of the extracellular ligand binding domain [23] (inside-out signaling). The

open conformation, facilitates high affinity ligand binding and triggers integrin-mediated cell signaling cascades (outside-in signaling) [24,25].

Many proteins play critical roles in the activation of specific integrins, but two cytoplasmic proteins, talin and kindlin, are necessary for inside-out signaling required for the activation of all integrin subtypes [23,26–29]. Talin binds to the proximal end of the beta cytoplasmic tail via a phosphotyrosine-binding (PTB) domain within its FERM domain [27] and links the integrin to the actin cytoskeleton [23]. Kindlin 1, 2, or 3, is necessary for talin-induced integrin activation [26,30,31]. Kindlin, like talin, also interacts with intracellular proteins resulting in cytoskeleton reorganization and adhesion [32]. G-protein coupled receptors such as the ADP receptor P2Y12, also play critical roles in the inside-out signaling required for integrin activation [25,33,34]. Structure–function analyses on β3 integrins have shown that a membrane-proximal region is important for inside-out signaling [28,35–40].

In addition to activation by inside-out signaling, ligand binding and integrin clustering can be significantly modulated by growth factor receptor interactions and other integrin interacting proteins, as reviewed in [22,23,41]. For example, integrin associated protein, CD47, augments integrin activation and affects the ability of αvβ3 integrin to cluster upon ligand binding [42]. Ligation of the integrin then stimulates outside-in signaling that leads to the activation of numerous signals critical for growth, migration, survival and other functions, including FAK phosphorylation, ERK signaling, and NF-κB activation. Thus, integrin signaling in cancer cells and in associated stromal, endothelial and hematopoietic cells can be influenced by intracellular signaling proteins, growth factors, chemokines and other receptors that participate in regulating integrin function through effects on integrin activation, ligand binding, ligand affinity and integrin clustering.

Maintaining adhesion to the ECM, in part through integrin signaling, is critical to cell survival [43]. Altered cell–cell or cell–ECM interactions results in disruption of downstream survival signaling and anchorage-dependent non-transformed cells undergo anoikis [43]. Under normal conditions, because each cell type expresses a unique set of integrins that recognize underlying ECM ligands, this form of apoptosis ensures that detached cells do not colonize inappropriate locations [43]. Cells that resist anoikis, such as metastatic cells, take advantage of several different mechanisms so
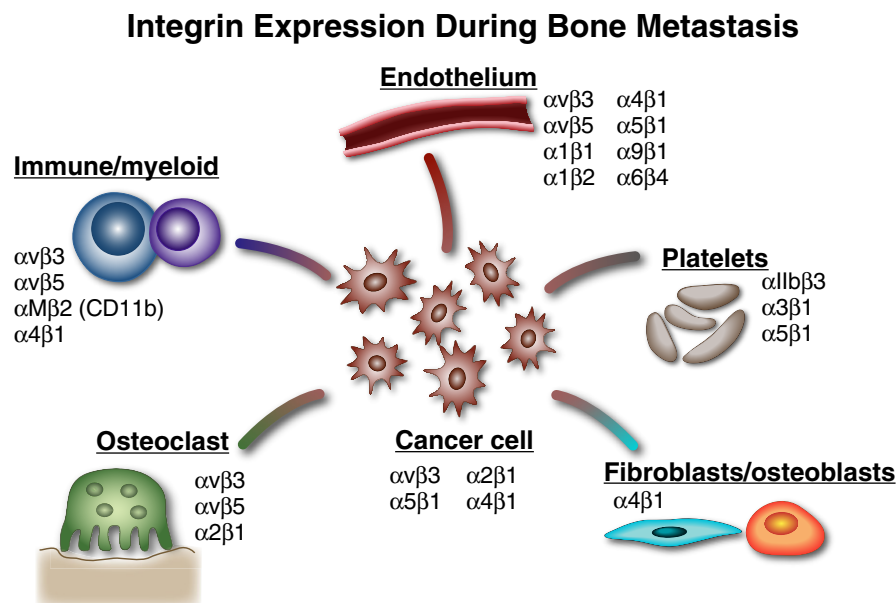

Fig. 1. Integrin Expression During Bone Metastasis: Numerous host stromal cells types interact with tumor cells to facilitate tumor cell homing, colonization and invasion in bone. Preclinical and clinical evidence demonstrate that specific integrin expression and signaling on both tumor cells and host cells are central to facilitating bone metastasis.

that the cell can adhere to a novel ECM, including aberrant integrin expression [44], constitutive activation of molecules usually activated via integrin signaling including FAK [45], EGFR [46] and SRC [47], and lack of activation of pro-apoptotic pathways [48], among others.

The integrin family of adhesion receptors links ECM to the cytoskeleton through a complex and regulated network of activation, interaction with numerous growth factor, GPCR, chemokine and cytokine receptors and induction of complex signaling cascades.

Integrin expression and signaling on tumor cells that metastasize to bone

Tumor progression, invasion and eventual metastasis require the activity of many adhesion proteins, including the integrin superfamily. At each stage of cancer progression, subsets of integrin heterodimers are activated, providing the necessary signaling pathways for adhesion, migration and cell survival. Metastatic tumor cells show differential integrin heterodimerization and activation compared to non-metastatic tumor cells that enable the cell to home to and colonize in a metastatic site, such as the bone marrow cavity [49,50]. In order for primary epithelial cancers to metastasize, the tumor cells must become resistant to anoikis and detach from the primary tumor site ECM, enter the vasculature, and eventually colonize a distant site. Upon reaching a successful metastatic site, however, tumor cells use both anoikis and anoikis-resistance to their advantage, in some cases forming micro-metastases that are resistant to cancer treatment via integrin binding to the underlying bone ECM as reviewed in [51]. Tumor cells must also form interactions between the tumor cell and bone stroma to establish and maintain skeletal metastasis. Many integrins have been implicated in tumor cell–host bone stroma interactions during bone metastasis and tumor growth in bone (Fig. 1, Table 1), including the β1 and β3 integrin family members.

αvβ3 is a receptor for osteopontin, fibronectin, and vitronectin, ECM proteins that are important bone matrix proteins, and αvβ3 has been identified as a critical integrin in breast cancer and prostate cancer skeletal metastasis [50,52–56]. Interestingly, although αvβ3 has been shown to bind to fibronectin in other locations with high affinity, tumor αvβ3 integrins do not bind fibronectin in bone marrow stroma, indicating that αvβ3-expressing tumor cells bind to the bone stromal ligands vitronectin and osteopontin [57]. In breast cancer, αvβ3 binding of host osteopontin is necessary for tumor cell colonization to bone [58]. Bone metastatic cells have a higher expression of αvβ3 than the primary tumor [53], promoting adherence to the bone matrix by binding osteopontin expressed by bone stromal cells [58]. Breast cancer cells that overexpress αvβ3 have increased levels of bone metastasis and associated tumor burden and osteolysis [52,59–62]. This overexpression of αvβ3 in the tumor cells leads to increased tumor cell adhesion, migration and invasion to bone as well as enhanced OC recruitment within the bone microenvironment [60,61], implicating a role of tumor-specific αvβ3 expression in breast cancer metastasis to bone as well as tumor-associated osteolysis. Likewise, in prostate cancer cells, active αvβ3 is necessary for the adherence and migration to bone matrix proteins at early stages of skeletal metastasis. This tumor cell αvβ3 integrin expression allows cancer cells to adhere to the bone matrix and interact directly with the native bone cells, OBs and OCs, as well as with the bone matrix itself [59].

The β1 family member, α5β1, has been identified as the primary integrin receptor for fibronectin on human bone marrow stroma [57]. α5β1 expression on leukemia, prostate and breast cancer cells facilitates interaction with bone stroma [57,63–65]. Antibody inhibition of α5, β1 or fibronectin blocks prostate cancer tumor cell binding to bone stroma, indicating necessary roles for both integrin α5β1 on tumor cells and fibronectin on bone marrow stromal cells [57]. In breast cancer skeletal metastasis, the interaction between malignant cell α5β1 and host stromal cell fibronectin contributes to the survival of growth-arrested tumor cells, a potential mechanism through which tumor cells can become sequestered and "dormant" within the bone marrow cavity and may later begin to proliferate to establish a skeletal metastasis [64]. Upon FGF-2 growth factor stimulation, breast cancer cells undergo growth arrest and up-regulate α5β1 expression. In most cases, these cells die, but cells that bind fibronectin via α5β1 and initiate cell survival signaling cascades survive [64].

Another β1 family member, α2β1, a collagen type I receptor, is expressed by prostate tumor cells, and its activity promotes invasion and adherence to the bone stroma. The presence of collagen I, the most abundant protein in bone, significantly increases prostate epithelial cell adhesion in culture, and antibody inhibition of integrin subunits α2 and β1 significantly inhibits tumor cell binding to stroma [66]. Hall et al. showed that a skeletal metastatic prostate cancer cell line, but not cell lines that are metastatic to other organs, binds to collagen I and that this collagen I binding is α2β1 dependent in vivo [67]. Interestingly, stromal expression of collagen I does not increase tumor growth, but instead promotes tumor cell migration [67]. Tumor cell α2β1 binding of host bone marrow stromal collagen I activates RhoC GTPase which instigates a signaling cascade responsible for cytoskeleton reorganization, migration, and, eventually, collagen-stimulated invasion and preferential skeletal metastasis [68].

α4β1/vascular cell adhesion molecule-1 (VCAM-1) binding has been identified as important for cell–cell contact between α4β1 expressing myeloma cells and VCAM-1 expressing bone marrow stroma [69]. This interaction contributes to bone tumor growth, OC stimulation and resultant osteolysis [69,70]. Likewise, epithelial tumor cells (CHO) that overexpress α4β1 developed significantly more bone metastases than mice inoculated with CHO cells alone [71]. Bone metastases, but not other metastases, were inhibited by antibodies against α4 and/or VCAM-1, suggesting a role for α4β1/ VCAM-1 binding in the skeletal metastases of solid tumors [71]. The role of integrins and chemokine cross talk in tumor cell homing to bone will be discussed later. While many aspects of tumor–bone stromal interactions remain unknown, it is clear that specific interactions between tumor cell integrins and bone stromal cell ligands are essential for successful homing and metastasis to bone.

Integrin expression and signaling in osteoclast function and bone metastasis

Bone invading metastatic tumor cells co-opt integrin signaling pathways that enhance OC function and recruitment. As part of bone remodeling, OCs bind to the bone matrix, form an actin ring mediated sealing zone, secrete enzymes and acid to degrade bone, and then migrate to a new site. Each of these functions is regulated in part by integrins located on the membrane surface of the OC, interacting with neighboring cells and with the ECM [72].

Table 1
Extracellular matrix proteins and the main integrins that participate in bone metastasis and tumor growth in bone.

Integrin	ECM ligands
αvβ3	Vitronectin, osteopontin, bone sialoprotein, fibronectin, TSP-1
α2β1	Collagen I, laminin
α4β1 (VLA-4)	VCAM-1 fibronectin, osteopontin
αvβ1	Fibronectin, vitronectin
αvβ5	Vitronectin, osteonectin, bone sialoprotein, fibronectin
αIIbβ3	Fibrinogen
β2	VCAM-1, ICAM-1, fibrinogen
α1β1	Collagen
α5β1	Fibronectin
α9β1	TSP1
α6β4	Laminin, TSP-1

Several integrins are involved in OC binding to bone, including αvβ3 (osteopontin, vitronectin, bone sialoprotein), αvβ5 (fibronectin), and α2β1 (collagen) [73,74]. Of these, αvβ3 is the predominant integrin found on OCs, and antibody inhibition of αvβ3 inhibits OC attachment to the bone matrix as well as OC mediated bone resorption [75]. In addition, mice with targeted disruption of β3 integrin (β3−/−) have defective OC function [76] and are protected from tumor-associated osteolysis [77]. αvβ3 is responsible for mediating OC-bone recognition [53,75,78,79] and subsequent attachment to the bone matrix [75,80], signaling to create the characteristic resorptive ruffled membrane, regulation of OC spreading, and overall organization of the cytoskeleton [76,81]. Activation of αvβ3 regulates OC adhesion and migration on osteopontin, important for OC polarization and bone resorption [82]. Osteopontin ligand binding of αvβ3 causes a reduction of OC cytosolic calcium, inducing podosome formation and subsequent resorption [83]. In addition, αvβ3 is critical for the activation of c-Src, c-Cbl, and GTPases Rho and Rac, signaling that is necessary for the cytoskeletal reorganization important in OC function [81,84,85].

OC targeted therapy is a standard of care for the treatment of bone metastasis and myeloma bone disease. Tumor cells recruit OCs resulting in bone destruction and pain [3,86,87]. Because of its known role in OC function and its high expression in skeletal metastatic tumors much research has focused on αvβ3 integrin and its ligands. An important characteristic of αvβ3 mediated cell adhesion, both in OCs and tumor cells, is the requirement of osteopontin, an αvβ3 ligand [58]. Osteopontin is a non-collagenous bone matrix protein that is produced by OBs, OCs, and macrophages and is found in the ECM adjacent to calcified bone [88–90]. Expression of osteopontin in both the tumor cell and in the bone microenvironment can promote skeletal metastasis [91,92]. Osteopontin-deficient mice have reduced bone metastasis and tumor-induced osteolysis than wild type controls in a mouse model of tumor metastasis using syngeneic B16 melanoma cells [93,94], confirming a role for host cell osteopontin expression during bone metastasis. Recombinant osteopontin induces cell migration of B16 cells that is inhibited by repressing the ERK/MAPK pathway, suggesting that the ERK/MAPK pathway regulates bone microenvironment osteopontin levels [91]. Overexpression of osteopontin in B16 melanoma cells increases cell proliferation and migration, indicating that the ligand also plays an important role in the tumor cell itself [91]. It has been demonstrated using a prostate cancer cell line overexpressing osteopontin that tumor cell osteopontin regulates MMP-9 secretion and the subsequent CD44/MMP-9 interaction, important for the migration of prostate cancer cells, contributing to metastatic potential [95]. Osteopontin-producing tumor cells enhance osteopontin production by OBs [96] and OCs [97], stimulating osteoclastogenesis, OC adherence, migration, and bone resorption via host αvβ3 binding [88,98]. Osteopontin activation of αvβ3 integrin leads to downstream activation of FAK, c-Src kinase, and Ras-ERK, among other signaling molecules, resulting in cytoskeletal reorganization, focal adhesion formation, basolateral membrane differentiation, and osteoclastic resorption [59,99].

CD47, integrin associated protein, is expressed constitutively and interacts with integrins, including αvβ3, as part of inside-out signaling cascades and also operates in an integrin-independent manner. CD47 plays a role in OC and macrophage biology and CD47−/− mice have decreased OC number and function [100,101] which can be rescued in vitro by inhibiting nitric oxide synthase [101]. CD47−/− mice have decreased bone metastases and tumor-associated osteolysis compared to wild type [101]. During the early stages of osteoclastogenesis, namely, macrophage fusion, CD47 binds with SIRP1α, a molecule that is transiently induced in myeloid cells and that likely participates in early fusion events [102]. In the event of tumor cell metastasis to bone, however, it has been reported that cancer cells may utilize this macrophage self-recognition signaling to fuse with macrophages [103], leading to mature OCs with tumor cell nuclei and subsequent over-expression of OC stimulation factors, thus leading to increased OC function [104].

These data underscore the importance of integrins, especially αvβ3, and its adaptor proteins in OC biology and bone metabolism and point to the role of OC integrins in regulating growth of cancer cells in the bone.

Integrins and tumor neovasculature and bone metastasis

Tumor neovascularization is essential for tumor cell invasion and metastasis. Access to the host blood supply provides the tumor cells with nutrients and connects the tumor to the circulation, facilitating the dissemination of metastatic cells. The angiogenic process begins with the de-stabilization and de-differentiation of local vessels, followed by activation of endothelial cells (EC), EC migration and proliferation into the tumor ECM, and finally organization of ECs into functional vessels. The ability of tumor cells to activate the normally quiescent vasculature is proposed to be controlled by an "angiogenic switch" mechanism, whereby tumor or stromal cells induce changes in the relative balance of inducers (e.g. vascular endothelial growth factor (VEGF) or TGFβ, PDGF, TNFα, bFGF) and inhibitors (e.g. thrombospondin-1 [TSP-1]) of angiogenesis reviewed in [41,105–109]. Activated platelets, tumor cells, and fibroblasts secrete many of these pro-angiogenic factors. It has recently been appreciated that macrophage lineage cells play important roles in promoting tumor-associated angiogenesis [110–113]. Bone metastasis and bone residing tumors like myeloma also modify and recruit ECs to enhance neoangiogenesis [114,115].

Many integrin heterodimers have been implicated in tumor-associated angiogenesis [41,105–109,116]. The first integrin found to regulate angiogenesis, αvβ3, is expressed at high levels on tumor-associated vasculature [117,118] and tumor-associated angiogenesis can be inhibited by β3 integrin neutralizing antibodies [119–122]. αvβ3 has been specifically implicated in the angiogenesis associated with prostate cancer bone metastases; antibody inhibition of αvβ3 decreases tumor-associated blood vessels in mice [123]. Interestingly, Reynolds et al. demonstrated enhanced (not reduced) tumor-associated angiogenesis in subcutaneous tumors in β3−/− mice [124]. Elevated levels of VEGFR2 were found on tumor-associated blood vessels in β3−/− mice, and a VEGFR2 inhibitor could block the enhanced blood vessel formation [125]. It should be noted that an inhibitor of integrin binding and signaling might have different consequences than loss of integrin expression. For example, apoptotic machinery is activated in certain cells expressing integrins that are not ligand-bound [126–129]. Recent reports that low dose integrin antagonists can increase tumor growth and angiogenesis while higher doses suppress tumor growth and angiogenesis [130] underscore the complexity of targeting β3 integrins for angiogenesis and cancer therapy.

Another αv integrin, αvβ5, also shows increased expression on tumor-associated vasculature, and αvβ5 antibodies inhibit VEGF-induced tumor-associated angiogenesis [131]. In contrast, the β3/β5−/− double knockout mice show enhanced tumor-associated angiogenesis, as was seen in β3−/− mice [125]. Several hypotheses have been proposed that reconcile the contradictory results involving the αv integrin family that outline the roles of the integrins as pro-angiogenic, anti-angiogenic, and/or working through different pathways as reviewed in [41,108]. It is clear, however, that αvβ3 and αvβ5 have distinct roles in regulation of tumor-associated angiogenesis and associated metastasis. The bone targeted bisphosphonate, zoledronic acid, alters EC integrin-mediated adhesion by reduced expression of αvβ3 and αvβ5 integrin on ECs in vitro in one observation [132]. This observation provides a possible mechanism for OC-independent anti-tumor

actions for bisphosphonates that have been reported in animal models [133–135] and clinically [136–139]. Evaluation of the effects of bisphosphonates on integrin signaling in the tumor–bone microenvironment is underway.

While much of the research in integrin-mediated angiogenesis has been focused on the αv integrins, there is evidence that other heterodimers play a role in angiogenic regulation, particularly the β1 and β4 families. The β1 integrin family (α1β1, α2β1, α5β1, and α4β1) has a critical role in angiogenesis with β1−/− mice having severe vascular defects. α1β1 (a collagen receptor) and α2β1 (a laminin receptor) have been shown to be important for mediating cell adhesion in VEGF-stimulated ECs [140]. In vivo, function-blocking antibodies to α1 and α2 significantly inhibited VEGF-induced angiogenesis, indicating a positive regulatory role for α1β1 and α2β1 expression in tumor-associated angiogenesis [141]. Genetic data further support a role for the integrin α1β1 as a positive regulator of angiogenesis as α1-deficient mice show reduced angiogenesis [142].

Fibronectin receptor α5β1 has also been implicated as a positive regulator of angiogenesis: α5β1 antagonists inhibit tumor-associated angiogenesis in mice by inhibition of EC migration and regulating proliferation and apoptosis [143,144]. Importantly, the α5β1 antagonists did not inhibit angiogenesis induced by VEGF, indicating that the integrin α5β1 (together with αvβ3) may act in a VEGF-independent pathway [144]. α4β1, together with its ligand, VCAM-1, expressed in vessel mural cells, plays an important role in adhesion of ECs and vascular smooth muscle cells during blood vessel formation [145]. Both anti-α4β1 antibodies and anti-VCAM-1 antibodies inhibit angiogenesis in vivo. Another integrin, laminin receptor α6β4 is reported to regulate several aspects of tumor angiogenesis. Genetic studies revealed that α6β4 promotes endothelial cell migration in culture; in addition, the integrin is involved in the translational regulation of VEGF, having a pro-angiogenic effect [146,147].

In many cases, integrins influence angiogenesis through their interaction with the integrin ligand thrombospondin 1 (TSP-1). Mice with a TSP-1 deficiency have increased tumor burden and tumor-associated vasculature, both in capillary size and number, while mice that overexpress TSP-1 have delayed or absent tumor growth and reduced tumor-associated vasculature [148]. These data indicate that TSP-1 can contribute to tumor burden via negative regulation of angiogenesis. In contrast, in a human breast cancer cell line, TSP-1 stimulation up-regulates both integrin subunit α6 mRNA levels and protein levels which leads to increased adhesion to ECM protein laminin in vitro, suggesting that TSP-1 facilitates pathogenic angiogenesis [149]. TSP-1 also interacts with α9β1 via its N-terminal domain and has a positive effect on proliferation and motility in culture and on angiogenesis in vivo that can be reduced by α9β1 inhibitors. This binding of the microvasculature-associated integrin in ECs with TSP-1 activates signaling cascades including ERK and paxillin. Thus, TSP-1 can play both pro- and anti-angiogenic roles, depending on its specific integrin interaction.

The roles of integrins in tumor-associated angiogenesis are complex, not only involving integrin ligand interactions and associated signaling pathways, but also specific temporal regulation and indirect effects through proteins such as TSP-1, and are important for the progression of angiogenesis and eventual metastasis.

Integrin-hematopoietic cell interactions: tumor-induced mobilization and modulation of bone marrow cells

The bone marrow is the primary site of hematopoiesis in the adult. OBs and bone marrow stromal cells regulate hematopoietic stem cell (HSC) growth, differentiation and bone marrow retention through numerous signaling pathways including integrin VLA-4/VCAM [150], chemokine SDF-1/CXCR4, BMPs and Notch [151–156]. Hematopoietic progenitors and stem cells express the integrin VLA-4 and the

chemokine receptor CXCR4. OB and bone marrow stromal cells produce VCAM-1, SDF-1 and osteopontin, all important components of the "HSC niche" [157–159]. Integrin and chemokine signaling work in concert to promote HSC and progenitor cell homing and mobilization in the bone marrow [160]. Disruption of VLA-4/VCAM-1 and SDF-1/CXCR4 interactions results in mobilization of HSC into the circulation [159]. G-CSF mobilization of HSC acts in part through disruption of VLA-4/VCAM-1 and CXCR4/SDF1 interactions [158,161]. OC resorption can also regulate HSC mobilization and the stem cell niche [162].

Diverse integrins are expressed on hematopoietic progenitor cells in specific patterns and at distinct time points [163]. Integrins not only mediate the binding of normal progenitor cells to stroma and matrix molecules, but may also regulate expansion, maturation and differentiation of those cells [164,165]. For example, α4β1 integrin regulates hematopoietic progenitor cell fate through changes in integrin expression and activity levels during cell maturation and differentiation into erythrocytes and neutrophils [165–167]. α4 containing integrins mediate adhesion of hematopoietic progenitors to stromal cells likely through binding to matrix components such as fibronectin [168] or cellular receptors such as VCAM-1 [169]. The integrin subunits α5, α6 and α9 have also been shown to be expressed by progenitor cells [170–172]. Studies using blocking antibodies demonstrated that α6 subunit cooperates in collaboration with the α4 subunit in regulating the homing of progenitor cells [171]. α9β1 integrin is also important for adhesion of progenitor cells to OBs in the bone marrow [172], illustrating the fact that hematopoiesis takes place in three dimensional matrices, the so-called bone marrow niches. These niches are located at the endosteum near OBs and in the vascular niche close to marrow blood vessels [173].

Tumor cells both in the bone microenvironment and at distant sites can modulate and mobilize hematopoietic progenitor and immune cells to promote bone and visceral metastasis and local tumor growth. Tumor-induced mobilization of VEGFR+ and Sca+kit-bone marrow derived cells has been implicated in enhancing distant tumor and metastatic growth [174]. These mobilized VEGFR+ cells also express α4β1 and can migrate to sites of increased synthesis of matrix components such as fibronectin and establish a "pre-metastatic niche" that can favor tumor metastasis and growth [174]. β2 integrins on bone marrow derived endothelial progenitors can also mediate the adhesion and VEGF-induced migration of the progenitors to the mature endothelium of actively remodeling vasculature [175].

Tumor cells from a primary lesion can act at a distance to influence bone marrow hematopoiesis through secreted factors such as the integrin ligand, osteopontin [176]. Primary epithelial tumors can instigate growth of indolent tumors through modulation of the bone marrow microenvironment and mobilization and recruitment of bone marrow cells to distant tumor sites [176,177]. McAllister et al. found that tumor secretion of osteopontin is necessary but not sufficient in xenograft models to modulate the bone microenvironment and promote bone marrow cell recruitment to tumor metastasis [176]. Pazolli et al. found that osteopontin secreted by senescent fibroblasts promoted tumorigenesis in animal models of skin cancer [178].

Thus tumors cells both in bone and at distant sites can modulate hematopoiesis in part through osteopontin and bone marrow cell integrins resulting in the mobilization and recruitment of bone marrow derived cells that will enhance local and metastatic tumor growth.

Integrins and tumor cell homing/colonization of bone

The site of metastasis is tumor cell specific depending on their integrin, chemokine receptor and cytokine/receptor expression profiles [50,179–181]. At the metastatic site, normal physiology is changed towards increased secretion of cytokines and activation of integrins to support recruitment, survival and growth of tumor cells.

Metastasizing cancer cells can co-opt the same mechanisms used in physiological hematopoietic progenitor cell homing to bone through expression of integrins and chemokines [150,152,153]. CXCR4 expressed on cancer cells can direct those cells to bone [181–186]. The migration of myeloma cells to and across bone marrow stromal cells is in part regulated by SDF-1α/CXCR4 ligation and up-regulation of α4β1 (VLA-4) results in adhesion of myeloma cells to the underlying bone marrow stroma [187]. Likewise, CXCR4 ligation can increase αvβ3 expression and aggressiveness of metastatic prostate cancer cells, and disruption of CXCR4 can inhibit prostate cancer bone metastases [183–185].

It has recently been shown that β3 integrin activity on circulating CXCR4-positive bone marrow derived cells is important for their migration and recruitment to sites of angiogenesis. In mice with mutated tyrosine residues "knocked in" to the β3 integrin locus to inhibit proper phosphorylation (DiYF mice) [188], CXCR4-positive bone marrow derived cells were higher in number and defective in recruitment to subcutaneously implanted tumors or wounds, where SDF-1 levels were also lower [189]. These data demonstrate that β3 integrin on bone marrow derived cells may be critical for the CXCR4/SDF-1 gradient, and thus may be important for localization of tumor cells to the bone microenvironment and also localization of myeloid/ECs to tumors. Interestingly, CXCR4 deletion on bone marrow cells can enhance OC activity which could counteract some of the beneficial effects of CXCR4 inhibition on bone metastases [9].

Integrins expressed by tumor cells, in concert with bone microenvironment chemokine secretion and further integrin activation, determine the osteotropic characteristics of metastasizing cancer cells and represent an ideal target for skeletal metastatic cancer therapy.

Integrins and myeloid/immune cell function during tumor growth in bone

Myeloid cell integrins are involved in tumor escape from immune responses and tumor-induced angiogenesis. Bone marrow derived myeloid cells (macrophages, monocytes, myeloid derived suppressor cells, and myeloid dendritic cells) migrate to tumors and contribute to tumor growth, invasion and angiogenesis [190–194]. Macrophages within tumors, called tumor-associated-macrophages (TAM) [127], are recruited by chemoattractants such as MCP-1 [195] secreted by the tumor and then differentiate into tissue macrophages [196]. The anti-tumor M1 phenotype represents a classical activation that is induced by pathogens, lipopolysaccharides (LPS) or interferon gamma resulting in secretion of proinflammatory cytokines such as tumor necrosis factor α (TNFα), interleukin 1β (IL-1 β) and others. M1 macrophages can act in an anti-tumor fashion by secretion of cytotoxic cytokines and antigen presentation to lymphocytes [197]. The pro-tumor M2 phenotype, represents alternative activation induced by IL-4 or IL-10 [198]. M2 polarized macrophages promote tumor cell proliferation and survival, suppress immune responses and drive tumor neoangiogenesis [197,199–201]. Studies have shown that the TAM content of tumors and prognosis of patients are inversely correlated [192,202,203].

β2 integrins are involved in monocyte/myeloid cell migration through endothelium and in phagocytosis, while β1 integrins mediate adhesion to matrix proteins and the induction of inflammatory genes [204]. α4β1 and αvβ3 integrins have been implicated in myeloid cell homing, adhesion and migration to tumors. α4β1 promotes endothelial progenitor cells and monocyte homing and adhesion to sites of active pathological angiogenesis [205]. Inhibition of α4β1 leads to suppressed monocyte and macrophage colonization of tumors and associated vasculature and decreased angiogenesis [194].

The αvβ3 integrin is down-regulated during differentiation of bone marrow myeloid progenitor cells to monocytes but induced in macrophages during inflammation [206,207]. αvβ3 promotes myeloid homing, adhesion and migration of bone marrow derived cells through the endothelium to sites of tumor angiogenesis [189]. β3 integrins are involved in phagocytosis of apoptotic cells [208,209] and limit the secretion of inflammatory mediators [207]. Defective macrophage tumor infiltration is observed in TAM from β3−/− bone marrow, myeloid specific β3KOM−/− mice and in the signaling defective *DiYF β3* mice (mice with two mutated tyrosine residues) [111,189,210–213], suggesting that defective cytoskeletal reorganization or lack of appropriately polarized macrophages [212] within tumors may be due to β3 integrin deficiency.

Myeloid derived suppressor cells (MDSC) [214] represent a subpopulation of immature myeloid cells that are roughly characterized by GR1+ and by the αMβ2(CD11b) integrin adhesion marker [214]. The MDSC suppress T-cell antigen receptor mediated immune responses [190] and can promote TAM M2 polarization [215]. MDSC from myeloma bearing mice had a greater capacity to become bone resorbing cells compared to MDSC from control mice [191]. The role of integrins in MDSC differentiation, recruitment and function is under investigation. Integrins are involved in monocyte/macrophage differentiation and recruitment to tumors and can influence local and metastatic tumor growth.

Integrins and tumor recruited platelets and bone metastasis

Cancer cells co-exist with platelets and mononuclear hematopoietic cells in thrombi located throughout the organs of patients with metastatic cancer [216–218]. Platelet aggregation and activation enhances tumor growth and metastasis to bone [77,219]. Platelets are anuclear metabolically active cells that are formed from bone marrow megakaryocytes. Platelet aggregation is stimulated by soluble factors such as ADP and thromboxane (TXA$_2$), membrane proteins, collagen or von Willebrand factor that are produced by injured endothelial, inflammatory and tumor cells. αIIbβ3 plays a central role in the initiation of arterial thrombosis and platelet aggregation [220,221]. αIIbβ3 integrins are expressed on the surface of megakaryocytes and platelets and are undetectable on any other non-cancerous cell type. Mice globally deficient for the β3 integrin have prolonged bleeding times, defects in platelet aggregation and clot retraction and cutaneous and gastrointestinal bleeding, all characteristics of Glanzmann's thrombasthenia, [222] a disease characterized by functional reduction or absence of αIIbβ3 in humans. Targeting β3 integrins by monoclonal antibodies to the receptor (abciximab/Reopro) or by inhibiting the binding of the ligand fibrinogen to the receptor (tirofiban/Integrilin) are used in patients with acute coronary and cerebral vascular syndromes but have significant bleeding risks that prevent their usefulness for chronic uses such as cancer.

Tumor cell lines have been shown to induce platelet aggregation and adhesion in vitro through mechanisms involving αIIbβ3 integrin, ADP, thrombin, von Willebrand factor and selectins [77,223–229]. The metastatic potential of tumor cell lines is markedly diminished in mice with defective platelet aggregation (*β3 integrin−/−, Gaq−/−, Par4−/−, NFE2−/−* and *fibrinogen−/−*) [77,219,223,226,228–244]. β3−/− mice are protected from bone metastasis in part through a mechanism involving defective platelet aggregation [77]. Additionally, tumor cells engineered to respond to platelet-derived lysophosphatidic acid (LPA) have enhanced bone metastatic potential in mice [219]. Platelets also represent a significant source of pro-angiogenic (VEGF) and anti-angiogenic factors (TSP-1) and are recruited to tumor sites where their aggregation could affect local tumor growth [245]. Platelet-specific integrin targeting is a promising therapeutic approach for inhibiting bone metastasis, especially to prevent or slow metastasis.

In contrast to platelets, bone marrow megakaryocytes can inhibit prostate cancer tumor growth in bone [246]. Megakaryocytes can indirectly inhibit bone resorption by inhibiting OC formation [247]. The negative effect of megakaryocytes on bone resorption is likely

mediated in part through the OC inhibitory factor osteoprotegrin that is contained in secretory granules of platelets and megakaryocytes [248,249]. Adhesion of mature polyploid megakaryocytes to fibronectin is also mediated by β1 subunit containing integrins [250,251]. Megakaryocytes may also influence bone remodeling and resorption through effects on OB proliferation that are mediated by the α3β1, α5β1 and glycoprotein IIb integrins [252]. Given the location of mature megakaryocytes at vascular sinusoids, they are also among the first cells to physically encounter cancer cells as they enter the bone marrow, so a direct mechanism of action involving integrin-mediated signal transduction could be involved. Interestingly, bisphosphonates (BP) increase megakaryocyte proliferation and increase the platelet concentration of the anti-angiogenic integrin ligand TSP-1 [253–255] which suggests non-OC mechanisms of BPs' action in decreasing tumor growth in bone. Thus, platelets and their megakaryocytic precursors interact with cancer cells before, during and after metastasis to bone through interactions mainly determined by integrins and their ligands.

Integrins and bone metastasis: Therapeutic aspects

Because of the wide range of functions in physiological and pathological processes, the integrin family of adhesion receptors has been adopted as a promising target for metastatic bone diseases. Several tumor cell types express an abnormal integrin profile compared to non-tumor cells [41,51,256], providing an opportunity for specific targeting. Targeting integrins on both tumor and/or host cells has proven to be effective not only in blocking local cancer progression, but also in reducing tumor cell detachment from their primary site in preclinical models [257–259].

In recent years, integrins on the tumor cells and the endothelium have been targeted by monoclonal antibodies and RGD peptides in order to reduce tumor angiogenesis [109,260]. Integrin antagonists, including humanized monoclonal antibodies, small molecule antagonists and cyclic peptides, have been developed based on the recognition sequences of integrin physiological ligands [261]. Several compounds are already in clinical use or undergoing their clinical evaluation for various diseases.

For the future treatment of skeletal metastasis, the αvβ3 integrin has become an attractive target because of its expression in tumor and angiogenic cells, its role in OC differentiation and function and its role in tumor cell homing to bone [53,60,61,183,262–267]. The multiple expected beneficial effects on endothelial, cancer and osteoclastic cells instigated a significant effort to develop drug candidates that target the αvβ3 integrin for therapy of skeletal complications of cancer. These strategies resulted predominantly in antagonists of αvβ3, αvβ5 and αIIβ3 integrins that showed efficacy in animal models. Peptidomimentic antagonists of the αvβ3 and αvβ5 integrins were successfully used to inhibit OC in vitro and to reduce bone loss in a rat osteoporosis model [268]. An active nonpeptide αvβ3 integrin antagonist and anti-αvβ3 antibodies were shown to hinder cancer induced bone loss [79,268–270]. It is possible that the current treatment for bone metastasis, BPs, may also exert an effect on αvβ3 on both ECs [132] as well as OCs in a similar manner.

Many drugs candidates targeting integrin αvβ3 have advanced to the clinic for the treatment of osteoporosis and cancer, though none have specifically targeted patients with bone metastases. A lipophilic isoester of RGD (L000845704), developed by Merck, is effective in increasing bone mineral density (BMD) in postmenopausal women [271]. Another inhibitor, RGD-mimetic cyclic peptide Cilengitide (EMD-1219974) directed at both αvβ3 and αvβ5 [272] and currently investigated by MerckSerono, is in advanced stages of clinical testing for the treatment of glioblastoma multiforme and is under investigation for the treatment of squamous cell carcinoma, prostate cancer, and lung cancer (Phase II).

Clinical trials of function-blocking antibodies are also ongoing, including Vitaxin (LM609), a humanized monoclonal IgG$_1$ antibody against the extracellular domain of the αvβ3 integrin heterodimer. Vitaxin had substantial anti-angiogenic effects in preclinical models [119,262] and has shown direct anti-tumor effects as well as impaired bone resorption by inhibiting OC attachment to the bone surface [273]. Another monoclonal antibody (CNTO95), directed against the αv subunit, is under development by Centocor and is in phases I–II testing for solid tumors. Two other additions to this therapeutic family are planned to be more specifically evaluated for their effects on bone metastasis [62], organic small molecule GLPG0187 [62] and peptide antagonist S247 [257].

Given the participation of the OCs, blood vessels and platelets in bone metastases, it may be beneficial to block both αvβ3 and αIIβ3 integrins on host cells. This concept of combination inhibition relies on the common RGD ligand binding domains of αvβ3, αvβ5 and αIIbβ3. In fact, many of the synthetically designed αvβ3 integrin inhibitors display some selectivity towards αvβ5 integrin, and, in the case of Cilengitide, this dual antagonism is part of the mechanism to treat cancer by inhibiting neoangiogenesis as well as invasion [274,275]. The strategy to combine multiple targets also bears some risks with regards to the desired high therapeutic specificity and low off-target toxicity. This issue is further complicated by the differential function of the integrins as determined by their location, expression level, activation status and ligand binding. Studies in animal models and xenograft tumor models have demonstrated that low concentrations of αvβ3 integrin antagonists can act as integrin agonists [130,276,277]. Further research is necessary to identify optimal drug dosing and targeting that overcome the problem of generalized integrin inhibition to reduce or prevent skeletal metastasis.

Another area of active research in bone metastasis therapeutics is the specific targeting of integrins on HSCs or progenitors that prepare the metastatic niche and enhance bone marrow colonization by cancer cells which then instigate the vicious cycle of bone metastasis [278,279]. Interfering with integrin-mediated homing of cancer cells to the cells to the bone represents an early option for intervention. siRNA against the αv integrin subunit was used to prevent the progression of prostate cancer to bone by interfering with the ECM–integrin interaction [280]. In another approach, a disintegrin and a neutralizing antibody to VCAM-1 or its receptor α4β1 integrin reduced metastasis of melanoma cells and diminished osteolysis by decreasing OC activity in a myeloma in vitro model [69,281]. These strategies, however, are not yet in clinical trials. An exciting new approach to cancer therapy takes advantage of the fact that cancer cells use CXCR4 and VLA-4 to home to and engraft in the marrow. HSC mobilizing agents such as AMD3100 and anti-VLA-4 targeted agents can be used to mobilize leukemia and myeloma cells into the blood from the bone marrow leading to increased sensitivity to chemotherapy [282–284] in mice. This approach is now being tested in clinical trials.

Future perspectives

Despite the high level of complexity of the integrin family, the β3 integrin remains a major target in the search for effective therapies for skeletal metastasis. In recent years, a steady increase in knowledge has led to clinical testing of several interesting compounds. There remains, however, a lack of clarity concerning the exact roles of the integrins in different cell types. In the initiated clinical studies using αvβ3 integrin antagonists, the overall effect in reducing tumor growth and pathological angiogenesis in fast progressing deadly tumors may outweigh potential undesired effects in tissues or cells other than tumor or endothelial origin. Drugs designed to tackle skeletal complications of cancer must be targeted to the bone microenvironment. This fact is underscored by

the clinical successes of the bone matrix targeted bisphosphonates and the OC targeted denosumab in treating and preventing skeletal complications of bone metastases and myeloma. A detailed understanding of the role of integrin regulation in both the metastatic tumor cells and the tumor-associated stroma will allow for a more targeted and focused approach to treat bone metastases.

Acknowledgments

References

[1] Lipton A. Pathophysiology of bone metastases: how this knowledge may lead to therapeutic intervention. J Support Oncol 2004;2:205–13 [discussion 213–4, 216–7, 219–20].

[2] Coleman RE. Metastatic bone disease: clinical features, pathophysiology and treatment strategies. Cancer Treat Rev 2001;27:165–76.

[3] Mundy GR. Metastasis to bone: causes, consequences and therapeutic opportunities. Nat Rev Cancer 2002;2:584–93.

[4] Roodman GD. Mechanisms of bone metastasis. N Engl J Med 2004;350:1655–64.

[5] Lipton A, Costa L, Ali S, Demers L. Use of markers of bone turnover for monitoring bone metastases and the response to therapy. Semin Oncol 2001;28:54–9.

[6] Coleman RE, Major P, Lipton A, Brown JE, Lee KA, Smith M, et al. Predictive value of bone resorption and formation markers in cancer patients with bone metastases receiving the bisphosphonate zoledronic acid. J Clin Oncol 2005;23: 4925–35.

[7] Guise TA, Mohammad KS, Clines G, Stebbins EG, Wong DH, Higgins LS, et al. Basic mechanisms responsible for osteolytic and osteoblastic bone metastases. Clin Cancer Res 2006;12:6213s–6s.

[8] Hirbe A, Morgan EA, Uluckan O, Weilbaecher K. Skeletal complications of breast cancer therapies. Clin Cancer Res 2006;12:6309s–14s.

[9] Hirbe AC, Rubin J, Uluckan O, Morgan EA, Eagleton MC, Prior JL, et al. Disruption of CXCR4 enhances osteoclastogenesis and tumor growth in bone. Proc Natl Acad Sci U S A 2007;104:14062–7.

[10] Bendre MS, Montague DC, Peery T, Akel NS, Gaddy D, Suva LJ. Interleukin-8 stimulation of osteoclastogenesis and bone resorption is a mechanism for the increased osteolysis of metastatic bone disease. Bone 2003;33:28–37.

[11] Pfeilschifter J, D'Souza SM, Mundy GR. Effects of transforming growth factor-beta on osteoblastic osteosarcoma cells. Endocrinology 1987;121:212–8.

[12] Kozlow W, Guise TA. Breast cancer metastasis to bone: mechanisms of osteolysis and implications for therapy. J Mammary Gland Biol Neoplasia 2005;10:169–80.

[13] Kingsley LA, Fournier PG, Chirgwin JM, Guise TA. Molecular biology of bone metastasis. Mol Cancer Ther 2007;6:2609–17.

[14] Clines GA, Guise TA. Molecular mechanisms and treatment of bone metastasis. Expert Rev Mol Med 2008;10:e7.

[15] Yin JJ, Selander K, Chirgwin JM, Dallas M, Grubbs BG, Wieser R, et al. TGF-beta signaling blockade inhibits PTHrP secretion by breast cancer cells and bone metastases development. J Clin Invest 1999;103:197–206.

[16] Kakonen SM, Selander KS, Chirgwin JM, Yin JJ, Burns S, Rankin WA, et al. Transforming growth factor-beta stimulates parathyroid hormone-related protein and osteolytic metastases via Smad and mitogen-activated protein kinase signaling pathways. J Biol Chem 2002;277:24571–8.

[17] Hamdy NA. Denosumab: RANKL inhibition in the management of bone loss. Drugs Today (Barc) 2008;44:7–21.

[18] Body JJ, Lipton A, Gralow J, Steger GG, Gao G, Yeh H, et al. Effects of denosumab in patients with bone metastases, with and without previous bisphosphonate exposure. J Bone Miner Res 2009.

[19] Fizazi K, Lipton A, Mariette X, Body JJ, Rahim Y, Gralow JR, et al. Randomized phase II trial of denosumab in patients with bone metastases from prostate cancer, breast cancer, or other neoplasms after intravenous bisphosphonates. J Clin Oncol 2009;27:1564–71.

[20] Schwartz MA, Schaller MD, Ginsberg MH. Integrins: emerging paradigms of signal transduction. Annu Rev Cell Dev Biol 1995;11:549–99.

[21] Hynes RO. Integrins: versatility, modulation, and signaling in cell adhesion. Cell 1992;69:11–25.

[22] Hynes RO. Integrins: bidirectional, allosteric signaling machines. Cell 2002;110: 673–87.

[23] Shattil SJ, Kim C, Ginsberg MH. The final steps of integrin activation: the end game. Nat Rev Mol Cell Biol 2010;11:288–300.

[24] Qin J, Vinogradova O, Plow EF. Integrin bidirectional signaling: a molecular view. PLoS Biol 2004;2:e169.

[25] Offermanns S. Activation of platelet function through G protein-coupled receptors. Circ Res 2006;99:1293–304.

[26] Ma YQ, Qin J, Wu C, Plow EF. Kindlin-2 (Mig-2): a co-activator of beta3 integrins. J Cell Biol 2008;181:439–46.

[27] Tadokoro S, Shattil SJ, Eto K, Tai V, Liddington RC, de Pereda JM, et al. Talin binding to integrin beta tails: a final common step in integrin activation. Science 2003;302:103–6.

[28] Vinogradova O, Velyvis A, Velyviene A, Hu B, Haas T, Plow E, et al. A structural mechanism of integrin alpha(IIb)beta(3) "inside-out" activation as regulated by its cytoplasmic face. Cell 2002;110:587–97.

[29] Harburger DS, Calderwood DA. Integrin signalling at a glance. J Cell Sci 2009;122: 159–63.

[30] Montanez E, Ussar S, Schifferer M, Bosl M, Zent R, Moser M, et al. Kindlin-2 controls bidirectional signaling of integrins. Genes Dev 2008;22:1325–30.

[31] Moser M, Nieswandt B, Ussar S, Pozgajova M, Fassler R. Kindlin-3 is essential for integrin activation and platelet aggregation. Nat Med 2008;14:325–30.

[32] Lai-Cheong JE, Parsons M, McGrath JA. The role of kindlins in cell biology and relevance to human disease. Int J Biochem Cell Biol 2010;42:595–603.

[33] Kamae T, Shiraga M, Kashiwagi H, Kato H, Tadokoro S, Kurata Y, et al. Critical role of ADP interaction with P2Y12 receptor in the maintenance of alpha(IIb)beta3 activation: association with Rap1B activation. J Thromb Haemost 2006;4:1379–87.

[34] Woulfe D, Jiang H, Mortensen R, Yang J, Brass LF. Activation of Rap1B by G(i) family members in platelets. J Biol Chem 2002;277:23382–90.

[35] Chen YP, O'Toole TE, Ylanne J, Rosa JP, Ginsberg MH. A point mutation in the integrin beta 3 cytoplasmic domain (S752–>P) impairs bidirectional signaling through alpha IIb beta 3 (platelet glycoprotein IIb–IIIa). Blood 1994;84:1857–65.

[36] Hughes PE, Diaz-Gonzalez F, Leong L, Wu C, McDonald JA, Shattil SJ, et al. Breaking the integrin hinge. A defined structural constraint regulates integrin signaling. J Biol Chem 1996;271:6571–4.

[37] O'Toole TE, Katagiri Y, Faull RJ, Peter K, Tamura R, Quaranta V, et al. Integrin cytoplasmic domains mediate inside-out signal transduction. J Cell Biol 1994;124:1047–59.

[38] Vinogradova O, Haas T, Plow EF, Qin J. A structural basis for integrin activation by the cytoplasmic tail of the alpha IIb-subunit. Proc Natl Acad Sci U S A 2000;97: 1450–5.

[39] Vinogradova O, Vaynberg J, Kong X, Haas TA, Plow EF, Qin J. Membrane-mediated structural transitions at the cytoplasmic face during integrin activation. Proc Natl Acad Sci U S A 2004;101:4094–9.

[40] Ylanne J, Huuskonen J, O'Toole TE, Ginsberg MH, Virtanen I, Gahmberg CG. Mutation of the cytoplasmic domain of the integrin beta 3 subunit. Differential effects on cell spreading, recruitment to adhesion plaques, endocytosis, and phagocytosis. J Biol Chem 1995;270:9550–7.

[41] Desgrosellier JS, Cheresh DA. Integrins in cancer: biological implications and therapeutic opportunities. Nat Rev Cancer 2010: 9–22. [Review]

[42] Brown EJ, Frazier WA. Integrin-associated protein (CD47) and its ligands. Trends Cell Biol 2001;11:130–5.

[43] Frisch SM, Screaton RA. Anoikis mechanisms. Curr Opin Cell Biol 2001;13: 555–62.

[44] Bissell MJ, Radisky D. Putting tumours in context. Nat Rev Cancer 2001;1:46–54.

[45] Frisch SM, Vuori K, Ruoslahti E, Chan-Hui PY. Control of adhesion-dependent cell survival by focal adhesion kinase. J Cell Biol 1996;134:793–9.

[46] Demers MJ, Thibodeau S, Noel D, Fujita N, Tsuruo T, Gauthier R, et al. Intestinal epithelial cancer cell anoikis resistance: EGFR-mediated sustained activation of Src overrides Fak-dependent signaling to MEK/Erk and/or PI3-K/Akt-1. J Cell Biochem 2009;107:639–54.

[47] Shain KH, Landowski TH, Dalton WS. Adhesion-mediated intracellular redistribution of c-Fas-associated death domain-like IL-1-converting enzyme-like inhibitory protein-long confers resistance to CD95-induced apoptosis in hematopoietic cancer cell lines. J Immunol 2002;168:2544–53.

[48] Simpson KJ, Selfors LM, Bui J, Reynolds A, Leake D, Khvorova A, et al. Identification of genes that regulate epithelial cell migration using an siRNA screening approach. Nat Cell Biol 2008;10:1027–38.

[49] Edlund M, Miyamoto T, Sikes RA, Ogle R, Laurie GW, Farach-Carson MC, et al. Integrin expression and usage by prostate cancer cell lines on laminin substrata. Cell Growth Differ 2001;12:99–107.

[50] Yoneda T. Cellular and molecular basis of preferential metastasis of breast cancer to bone. J Orthop Sci 2000;5:75–81.

[51] Clezardin P. Integrins in bone metastasis formation and potential therapeutic implications. Curr Cancer Drug Targets 2009;9:801–6.

[52] van der P, Vloedgraven H, Papapoulos S, Lowick C, Grzesik W, Kerr J, et al. Attachment characteristics and involvement of integrins in adhesion of breast cancer cell lines to extracellular bone matrix components. Lab Invest 1997;77: 665–75.

[53] Liapis H, Flath A, Kitazawa S. Integrin alpha V beta 3 expression by bone-residing breast cancer metastases. Diagn Mol Pathol 1996;5:127–35.

[54] McCabe NP, De S, Vasanji A, Brainard J, Byzova TV. Prostate cancer specific integrin alphavbeta3 modulates bone metastatic growth and tissue remodeling. Oncogene 2007;26:6238–43.

[55] Townsend PA, Villanova I, Uhlmann E, Peyman A, Knolle J, Baron R, et al. An antisense oligonucleotide targeting the alphaV integrin gene inhibits adhesion and induces apoptosis in breast cancer cells. Eur J Cancer 2000;36:397–409.

[56] Gillespie MT, Thomas RJ, Pu ZY, Zhou H, Martin TJ, Findlay DM. Calcitonin receptors, bone sialoprotein and osteopontin are expressed in primary breast cancers. Int J Cancer 1997;73:812–5.

[57] Van der Velde-Zimmermann D, Verdaasdonk MA, Rademakers LH, De Weger RA, Van den Tweel JG, Joling P. Fibronectin distribution in human bone marrow stroma: matrix assembly and tumor cell adhesion via alpha5 beta1 integrin. Exp Cell Res 1997;230:111–20.

[58] Takayama S, Ishii S, Ikeda T, Masamura S, Doi M, Kitajima M. The relationship between bone metastasis from human breast cancer and integrin alpha(v)beta3 expression. Anticancer Res 2005;25:79–83.

[59] Nakamura I, Duong le T, Rodan SB, Rodan GA. Involvement of alpha(v)beta3 integrins in osteoclast function. J Bone Miner Metab 2007;25:337–44.

[60] Pecheur I, Peyruchaud O, Serre CM, Guglielmi J, Voland C, Bourre F, et al. Integrin alpha(v)beta3 expression confers on tumor cells a greater propensity to metastasize to bone. FASEB J 2002;16:1266–8.

[61] Sloan EK, Pouliot N, Stanley KL, Chia J, Moseley JM, Hards DK, et al. Tumor-specific expression of alphavbeta3 integrin promotes spontaneous metastasis of breast cancer to bone. Breast Cancer Res 2006;8:R20.

[62] Zhao Y, Bachelier R, Treilleux I, Pujuguet P, Peyruchaud O, Baron R, et al. Tumor alphavbeta3 integrin is a therapeutic target for breast cancer bone metastases. Cancer Res 2007;67:5821–30.

[63] Martin-Thouvenin V, Gendron MC, Hogervorst F, Figdor CG, Lanotte M. Phorbol ester-induced promyelocytic leukemia cell adhesion to marrow stromal cells involves fibronectin specific alpha 5 beta 1 integrin receptors. J Cell Physiol 1992;153:95–102.

[64] Korah R, Boots M, Wieder R. Integrin alpha5beta1 promotes survival of growth-arrested breast cancer cells: an in vitro paradigm for breast cancer dormancy in bone marrow. Cancer Res 2004;64:4514–22.

[65] Liesveld JL, Dipersio JF, Abboud CN. Integrins and adhesive receptors in normal and leukemic CD34+ progenitor cells: potential regulatory checkpoints for cellular traffic. Leuk Lymphoma 1994;14:19–28.

[66] Lang SH, Clarke NW, George NJ, Testa NG. Primary prostatic epithelial cell binding to human bone marrow stroma and the role of alpha2beta1 integrin. Clin Exp Metastasis 1997;15:218–27.

[67] Hall CL, Dai J, van Golen KL, Keller ET, Long MW. Type I collagen receptor (alpha 2 beta 1) signaling promotes the growth of human prostate cancer cells within the bone. Cancer Res 2006;66:8648–54.

[68] Hall CL, Dubyk CW, Riesenberger TA, Shein D, Keller ET, van Golen KL. Type I collagen receptor (alpha2beta1) signaling promotes prostate cancer invasion through RhoC GTPase. Neoplasia 2008;10:797–803.

[69] Mori Y, Shimizu N, Dallas M, Niewolna M, Story B, Williams PJ, et al. Anti-alpha4 integrin antibody suppresses the development of multiple myeloma and associated osteoclastic osteolysis. Blood 2004;104:2149–54.

[70] Michigami T, Shimizu N, Williams PJ, Niewolna M, Dallas SL, Mundy GR, et al. Cell–cell contact between marrow stromal cells and myeloma cells via VCAM-1 and alpha(4)beta(1)-integrin enhances production of osteoclast-stimulating activity. Blood 2000;96:1953–60.

[71] Matsuura N, Puzon-McLaughlin W, Irie A, Morikawa Y, Kakudo K, Takada Y. Induction of experimental bone metastasis in mice by transfection of integrin alpha 4 beta 1 into tumor cells. Am J Pathol 1996;148:55–61.

[72] Teitelbaum SL, Ross FP. Genetic regulation of osteoclast development and function. Nat Rev Genet 2003;4:638–49.

[73] Ross FP, Teitelbaum SL. alphavbeta3 and macrophage colony-stimulating factor: partners in osteoclast biology. Immunol Rev 2005;208:88–105.

[74] Novack DV, Teitelbaum SL. The osteoclast: friend or foe? Annu Rev Pathol 2008;3:457–84.

[75] Ross FP, Chappel J, Alvarez JI, Sander D, Butler WT, Farach-Carson MC, et al. Interactions between the bone matrix proteins osteopontin and bone sialoprotein and the osteoclast integrin alpha v beta 3 potentiate bone resorption. J Biol Chem 1993;268:9901–7.

[76] McHugh KP. Mice lacking b3 integrins are osteosclerotic because of dysfunctional osteoclasts. J Clin Invest 2000;105:433–40.

[77] Bakewell SJ, Nestor P, Prasad S, Tomasson MH, Dowland N, Mehrotra M, et al. Platelet and osteoclast beta3 integrins are critical for bone metastasis. Proc Natl Acad Sci U S A 2003;100:14205–10.

[78] Zambonin Zallone A, Teti A, Gaboli M, Marchisio PC. Beta 3 subunit of vitronectin receptor is present in osteoclast adhesion structures and not in other monocyte-macrophage derived cells. Connect Tissue Res 1989;20:143–9.

[79] Crippes BA, Engleman VW, Settle SL, Delarco J, Ornberg RL, Helfrich MH, et al. Antibody to beta3 integrin inhibits osteoclast-mediated bone resorption in the thyroparathyroidectomized rat. Endocrinology 1996;137:918–24.

[80] Chellaiah MA. Regulation of podosomes by integrin alphavbeta3 and Rho GTPase-facilitated phosphoinositide signaling. Eur J Cell Biol 2006;85:311–7.

[81] Faccio R, Takeshita S, Zallone A, Ross FP, Teitelbaum SL. c-Fms and the alphavbeta3 integrin collaborate during osteoclast differentiation. J Clin Invest 2003;111:749–58.

[82] Faccio R, Grano M, Colucci S, Zallone AZ, Quaranta V, Pelletier AJ. Activation of alphav beta3 integrin on human osteoclast-like cells stimulates adhesion and migration in response to osteopontin. Biochem Biophys Res Commun 1998;249: 522–5.

[83] Miyauchi A, Alvarez J, Greenfield EM, Teti A, Grano M, Colucci S, et al. Recognition of osteopontin and related peptides by an alpha v beta 3 integrin stimulates immediate cell signals in osteoclasts. J Biol Chem 1991;266:20369–74.

[84] Rucci N, DiGiacinto C, Orru L, Millimaggi D, Baron R, Teti A. A novel protein kinase C alpha-dependent signal to ERK1/2 activated by alphaVbeta3 integrin in osteoclasts and in Chinese hamster ovary (CHO) cells. J Cell Sci 2005;118: 3263–75.

[85] Zhang Z, Baron R, Horne WC. Integrin engagement, the actin cytoskeleton, and c-Src are required for the calcitonin-induced tyrosine phosphorylation of paxillin and HEF1, but not for calcitonin-induced Erk1/2 phosphorylation. J Biol Chem 2000;275:37219–23.

[86] Clohisy DR, Ramnaraine ML. Osteoclasts are required for bone tumors to grow and destroy bone. J Orthop Res 1998;16:660–6.

[87] Honore P, Luger NM, Sabino MA, Schwei MJ, Rogers SD, Mach DB, et al. Osteoprotegerin blocks bone cancer-induced skeletal destruction, skeletal pain and pain-related neurochemical reorganization of the spinal cord. Nat Med 2000;6:521–8.

[88] Carlinfante G, Vassiliou D, Svensson O, Wendel M, Heinegard D, Andersson G. Differential expression of osteopontin and bone sialoprotein in bone metastasis of breast and prostate carcinoma. Clin Exp Metastasis 2003;20:437–44.

[89] Heinegard D, Andersson G, Reinholt FP. Roles of osteopontin in bone remodeling. Ann N Y Acad Sci 1995;760:213–22.

[90] Katayama Y, House CM, Udagawa N, Kazama JJ, McFarland RJ, Martin TJ, et al. Casein kinase 2 phosphorylation of recombinant rat osteopontin enhances adhesion of osteoclasts but not osteoblasts. J Cell Physiol 1998;176:179–87.

[91] Hayashi C, Rittling S, Hayata T, Amagasa T, Denhardt D, Ezura Y, et al. Serum osteopontin, an enhancer of tumor metastasis to bone, promotes B16 melanoma cell migration. J Cell Biochem 2007;101:979–86.

[92] Denhardt DT, Chambers AF. Overcoming obstacles to metastasis—defenses against host defenses: osteopontin (OPN) as a shield against attack by cytotoxic host cells. J Cell Biochem 1994;56:48–51.

[93] Nemoto H, Rittling SR, Yoshitake H, Furuya K, Amagasa T, Tsuji K, et al. Osteopontin deficiency reduces experimental tumor cell metastasis to bone and soft tissues. J Bone Miner Res 2001;16:652–9.

[94] Ohyama Y, Nemoto H, Rittling S, Tsuji K, Amagasa T, Denhardt DT, et al. Osteopontin-deficiency suppresses growth of B16 melanoma cells implanted in bone and osteoclastogenesis in co-cultures. J Bone Miner Res 2004;19: 1706–11.

[95] Desai B, Rogers MJ, Chellaiah MA. Mechanisms of osteopontin and CD44 as metastatic principles in prostate cancer cells. Mol Cancer 2007;6:18.

[96] Hullinger TG, Taichman RS, Linseman DA, Somerman MJ. Secretory products from PC-3 and MCF-7 tumor cell lines upregulate osteopontin in MC3T3-E1 cells. J Cell Biochem 2000;78:607–16.

[97] Abe M, Hiura K, Wilde J, Shioyasono A, Moriyama K, Hashimoto T, et al. Osteoclasts enhance myeloma cell growth and survival via cell–cell contact: a vicious cycle between bone destruction and myeloma expansion. Blood 2004;104:2484–91.

[98] Standal T, Borset M, Sundan A. Role of osteopontin in adhesion, migration, cell survival and bone remodeling. Exp Oncol 2004;26:179–84.

[99] Chen YJ, Wei YY, Chen HT, Fong YC, Hsu CJ, Tsai CH, et al. Osteopontin increases migration and MMP-9 up-regulation via alphavbeta3 integrin, FAK, ERK, and NF-kappaB-dependent pathway in human chondrosarcoma cells. J Cell Physiol 2009;221:98–108.

[100] Lundberg P, Koskinen C, Baldock PA, Lothgren H, Stenberg A, Lerner UH, et al. Osteoclast formation is strongly reduced both in vivo and in vitro in the absence of CD47/SIRPalpha-interaction. Biochem Biophys Res Commun 2007;352:444–8.

[101] Uluckan O, Becker SN, Deng H, Zou W, Prior JL, Piwnica-Worms D, et al. CD47 regulates bone mass and tumor metastasis to bone. Cancer Res 2009;69: 3196–204.

[102] Han X, Sterling H, Chen Y, Saginario C, Brown EJ, Frazier WA, et al. CD47, a ligand for the macrophage fusion receptor, participates in macrophage multinucleation. J Biol Chem 2000;275:37984–92.

[103] Rachkovsky M, Sodi S, Chakraborty A, Avissar Y, Bolognia J, McNiff JM, et al. Melanoma x macrophage hybrids with enhanced metastatic potential. Clin Exp Metastasis 1998;16:299–312.

[104] Vignery A. Macrophage fusion: are somatic and cancer cells possible partners? Trends Cell Biol 2005;15:188–93.

[105] Hanahan D, Weinberg RA. The hallmarks of cancer. Cell 2000;100:57–70.

[106] Stupack DG, Cheresh DA. Integrins and angiogenesis. Curr Top Dev Biol 2004;64: 207–38.

[107] Hood JD, Cheresh DA. Role of integrins in cell invasion and migration. Nat Rev Cancer 2002;2:91–100.

[108] Hodivala-Dilke K. alphavbeta3 integrin and angiogenesis: a moody integrin in a changing environment. Curr Opin Cell Biol 2008;20:514–9.

[109] Silva R, D'Amico G, Hodivala-Dilke KM, Reynolds LE. Integrins: the keys to unlocking angiogenesis. Arterioscler Thromb Vasc Biol 2008;28:1703–13.

[110] Stockmann C, Doedens A, Weidemann A, Zhang N, Takeda N, Greenberg JI, et al. Deletion of vascular endothelial growth factor in myeloid cells accelerates tumorigenesis. Nature 2008;456:814–8.

[111] Morga EA, Schneider J, Uluckan TB, Heller EA, Hurchla MA, et al. Dissection of platelet and myeloid cell defects by conditional targeting of the β3 integrin subunit. FASEB J 2010;24:1117–27.

[112] Cackowski FC, Anderson JL, Patrene KD, Choksi RJ, Shapiro SD, Windle JJ, et al. Osteoclasts are important for bone angiogenesis. Blood 2010;115:140–9.

[113] Capoccia BJ, Shepherd RM, Link DC. G-CSF and AMD3100 mobilize monocytes into the blood that stimulate angiogenesis in vivo through a paracrine mechanism. Blood 2006;108:2438–45.

[114] De Palma M, Naldini L. Role of haematopoietic cells and endothelial progenitors in tumour angiogenesis. Biochim Biophys Acta 2006;1766:159–66.

[115] Papaspyridonos M, Lyden D. Chapter 11. The role of bone marrow-derived cells in tumor angiogenesis and metastatic progression. Methods Enzymol 2008;444: 255–69.

[116] Ramjaun AR, Hodivala-Dilke K. The role of cell adhesion pathways in angiogenesis. Int J Biochem Cell Biol 2009;41:521–30.

[117] Brooks PC, Clark RA, Cheresh DA. Requirement of vascular integrin alpha v beta 3 for angiogenesis. Science 1994;264:569–71.

[118] Mahabeleshwar GH, Byzova TV. Vascular integrin signaling. Methods Enzymol 2008;443:199–226.

[119] Brooks PC, Montgomery AM, Rosenfeld M, Reisfeld RA, Hu T, Klier G, et al. Integrin alpha v beta 3 antagonists promote tumor regression by inducing apoptosis of angiogenic blood vessels. Cell 1994;79:1157–64.

[120] Brooks PC, Silletti S, von Schalscha TL, Friedlander M, Cheresh DA. Disruption of angiogenesis by PEX, a noncatalytic metalloproteinase fragment with integrin binding activity. Cell 1998;92:391–400.

[121] Silletti S, Kessler T, Goldberg J, Boger DL, Cheresh DA. Disruption of matrix metalloproteinase 2 binding to integrin alpha vbeta 3 by an organic molecule inhibits angiogenesis and tumor growth in vivo. Proc Natl Acad Sci U S A 2001;98:119–24.

[122] Maeshima Y, Yerramalla UL, Dhanabal M, Holthaus KA, Barbashov S, Kharbanda S, et al. Extracellular matrix-derived peptide binds to alpha(v)beta(3) integrin and inhibits angiogenesis. J Biol Chem 2001;276:31959–68.

[123] Nemeth JA, Cher ML, Zhou Z, Mullins C, Bhagat S, Trikha M. Inhibition of alpha(v) beta3 integrin reduces angiogenesis, bone turnover, and tumor cell proliferation in experimental prostate cancer bone metastases. Clin Exp Metastasis 2003;20: 413–20.

[124] Reynolds LE, Wyder L, Lively JC, Taverna D, Robinson SD, Huang X, et al. Enhanced pathological angiogenesis in mice lacking beta3 integrin or beta3 and beta5 integrins. Nat Med 2002;8:27–34.

[125] Reynolds AR, Reynolds LE, Nagel TE, Lively JC, Robinson SD, Hicklin DJ, et al. Elevated Flk1 (vascular endothelial growth factor receptor 2) signaling mediates enhanced angiogenesis in beta3-integrin-deficient mice. Cancer Res 2004;64: 8643–50.

[126] Carmeliet P. Integrin indecision. Nat Med 2002;8:14–6.

[127] Martin KH, Slack JK, Boerner SA, Martin CC, Parsons JT. Integrin connections map: to infinity and beyond. Science 2002;296:1652–3.

[128] Wang XQ, Sun P, Paller AS. Inhibition of integrin-linked kinase/protein kinase B/ Akt signaling: mechanism for ganglioside-induced apoptosis. J Biol Chem 2001;276:44504–11.

[129] Zhao H, Ross FP, Teitelbaum SL. Unoccupied alpha(v)beta3 integrin regulates osteoclast apoptosis by transmitting a positive death signal. Mol Endocrinol 2005;19:771–80.

[130] Reynolds AR, Hart IR, Watson AR, Welti JC, Silva RG, Robinson SD, et al. Stimulation of tumor growth and angiogenesis by low concentrations of RGD-mimetic integrin inhibitors. Nat Med 2009;15:392–400.

[131] Friedlander M, Brooks PC, Shaffer RW, Kincaid CM, Varner JA, Cheresh DA. Definition of two angiogenic pathways by distinct alpha v integrins. Science 1995;270:1500–2.

[132] Bellahcene A, Chaplet M, Bonjean K, Castronovo V. Zoledronate inhibits alphavbeta3 and alphavbeta5 integrin cell surface expression in endothelial cells. Endothelium 2007;14:123–30.

[133] Hirbe AC, Roelofs AJ, Floyd DH, Deng H, Becker SN, Lanigan LG, et al. The bisphosphonate zoledronic acid decreases tumor growth in bone in mice with defective osteoclasts. Bone 2009;44:908–16.

[134] Ottewell PD, Monkkonen H, Jones M, Lefley DV, Coleman RE, Holen I. Antitumor effects of doxorubicin followed by zoledronic acid in a mouse model of breast cancer. J Natl Cancer Inst 2008;100:1167–78.

[135] Gao L, Deng H, Zhao H, Hirbe A, Harding J, Ratner L, et al. HTLV-1 Tax transgenic mice develop spontaneous osteolytic bone metastases prevented by osteoclast inhibition. Blood 2005;106:4294–302.

[136] Coleman RE, Guise TA, Lipton A, Roodman GD, Berenson JR, Body JJ, et al. Advancing treatment for metastatic bone cancer: consensus recommendations from the Second Cambridge Conference. Clin Cancer Res 2008;14:6387–95.

[137] Gnant M, Mlineritsch B, Schippinger W, Luschin-Ebengreuth G, Postlberger S, Menzel C, et al. Endocrine therapy plus zoledronic acid in premenopausal breast cancer. N Engl J Med 2009;360:679–91.

[138] Aft R, Naughton M, Trinkaus K, Watson M, Ylagan L, Chavez-MacGregor M, et al. Effect of zoledronic acid on disseminated tumour cells in women with locally advanced breast cancer: an open label, randomised, phase 2 trial. Lancet Oncol 2010;11:421–8.

[139] Gnant M. The evolving role of zoledronic acid in early breast cancer. Onco Targets Ther 2009;2:95–104.

[140] Tanjore H, Zeisberg EM, Gerami-Naini B, Kalluri R. Beta1 integrin expression on endothelial cells is required for angiogenesis but not for vasculogenesis. Dev Dyn 2008;237:75–82.

[141] Senger DR, Claffey KP, Benes JE, Perruzzi CA, Sergiou AP, Detmar M. Angiogenesis promoted by vascular endothelial growth factor: regulation through alpha1beta1 and alpha2beta1 integrins. Proc Natl Acad Sci U S A 1997;94:13612–7.

[142] Pozzi A, Moberg PE, Miles LA, Wagner S, Soloway P, Gardner HA. Elevated matrix metalloprotease and angiostatin levels in integrin alpha 1 knockout mice cause reduced tumor vascularization. Proc Natl Acad Sci U S A 2000;97:2202–7.

[143] Kim S, Bell K, Mousa SA, Varner JA. Regulation of angiogenesis in vivo by ligation of integrin alpha5beta1 with the central cell-binding domain of fibronectin. Am J Pathol 2000;156:1345–62.

[144] Boudreau NJ, Varner JA. The homeobox transcription factor Hox D3 promotes integrin alpha5beta1 expression and function during angiogenesis. J Biol Chem 2004;279:4862–8.

[145] Garmy-Susini B, Jin H, Zhu Y, Sung RJ, Hwang R, Varner J. Integrin alpha4beta1-VCAM-1-mediated adhesion between endothelial and mural cells is required for blood vessel maturation. J Clin Invest 2005;115:1542–51.

[146] Nikolopoulos SN, Blaikie P, Yoshioka T, Guo W, Giancotti FG. Integrin beta4 signaling promotes tumor angiogenesis. Cancer Cell 2004;6:471–83.

[147] Chung J, Bachelder RE, Lipscomb EA, Shaw LM, Mercurio AM. Integrin (alpha 6 beta 4) regulation of eIF-4E activity and VEGF translation: a survival mechanism for carcinoma cells. J Cell Biol 2002;158:165–74.

[148] Rodriguez-Manzaneque JC, Lane TF, Ortega MA, Hynes RO, Lawler J, Iruela-Arispe ML. Thrombospondin-1 suppresses spontaneous tumor growth and inhibits activation of matrix metalloproteinase-9 and mobilization of vascular endothelial growth factor. Proc Natl Acad Sci U S A 2001;98:12485–90.

[149] John AS, Rothman VL, Tuszynski GP. Thrombospondin-1 (TSP-1) stimulates expression of integrin alpha6 in human breast carcinoma cells: a downstream modulator of TSP-1-induced cellular adhesion. J Oncol 2010;2010:645376.

[150] Eliceiri BP, Cheresh DA. Adhesion events in angiogenesis. Curr Opin Cell Biol 2001;13:563–8.

[151] Calvi LM, Adams GB, Weibrecht KW, Weber JM, Olson DP, Knight MC, et al. Osteoblastic cells regulate the haematopoietic stem cell niche. Nature 2003;425: 841–6.

[152] Brenner S, Whiting-Theobald N, Kawai T, Linton GF, Rudikoff AG, Choi U, et al. CXCR4-transgene expression significantly improves marrow engraftment of cultured hematopoietic stem cells. Stem Cells 2004;22:1128–33.

[153] Kahn J, Byk T, Jansson-Sjostrand L, Petit I, Shivtiel S, Nagler A, et al. Over-expression of CXCR4 on human CD34+ progenitors increases their proliferation, migration, and NOD/SCID repopulation. Blood 2004;103:2942–9.

[154] Zhang J, Niu C, Ye L, Huang H, He X, Tong WG, et al. Identification of the haematopoietic stem cell niche and control of the niche size. Nature 2003;425: 836–41.

[155] Papayannopoulou T. Mechanisms of stem-/progenitor-cell mobilization: the anti-VLA-4 paradigm. Semin Hematol 2000;37:11–8.

[156] Hidalgo A, Peired AJ, Weiss LA, Katayama Y, Frenette PS. The integrin alphaMbeta2 anchors hematopoietic progenitors in the bone marrow during enforced mobilization. Blood 2004;104:993–1001.

[157] Stier S, Ko Y, Forkert R, Lutz C, Neuhaus T, Grunewald E, et al. Osteopontin is a hematopoietic stem cell niche component that negatively regulates stem cell pool size. J Exp Med 2005;201:1781–91.

[158] Christopher MJ, Liu F, Hilton MJ, Long F, Link DC. Suppression of CXCL12 production by bone marrow osteoblasts is a common and critical pathway for cytokine-induced mobilization. Blood 2009;114:1331–9.

[159] Adams GB, Martin RP, Alley IR, Chabner KT, Cohen KS, Calvi LM, et al. Therapeutic targeting of a stem cell niche. Nat Biotechnol 2007;25:238–43.

[160] Mendez-Ferrer S, Frenette PS. Hematopoietic stem cell trafficking: regulated adhesion and attraction to bone marrow microenvironment. Ann N Y Acad Sci 2007;1116:392–413.

[161] Eash KJ, Means JM, White DW, Link DC. CXCR4 is a key regulator of neutrophil release from the bone marrow under basal and stress granulopoiesis conditions. Blood 2009;113:4711–9.

[162] Kollet O, Dar A, Shivtiel S, Kalinkovich A, Lapid K, Sztainberg Y, et al. Osteoclasts degrade endosteal components and promote mobilization of hematopoietic progenitor cells. Nat Med 2006;12:657–64.

[163] Bungartz G, Stiller S, Bauer M, Muller W, Schippers A, Wagner N, et al. Adult murine hematopoiesis can proceed without beta1 and beta7 integrins. Blood 2006;108:1857–64.

[164] Jiang Y, Prosper F, Verfaillie CM. Opposing effects of engagement of integrins and stimulation of cytokine receptors on cell cycle progression of normal human hematopoietic progenitors. Blood 2000;95:846–54.

[165] Voura EB, Billia F, Iscove NN, Hawley RG. Expression mapping of adhesion receptor genes during differentiation of individual hematopoietic precursors. Exp Hematol 1997;25:1172–9.

[166] Hemler ME, Lobb RR. The leukocyte beta 1 integrins. Curr Opin Hematol 1995;2: 61–7.

[167] Coulombel L, Auffray I, Gaugler MH, Rosemblatt M. Expression and function of integrins on hematopoietic progenitor cells. Acta Haematol 1997;97:13–21.

[168] Verfaillie CM, McCarthy JB, McGlave PB. Differentiation of primitive human multipotent hematopoietic progenitors into single lineage clonogenic progenitors is accompanied by alterations in their interaction with fibronectin. J Exp Med 1991;174:693–703.

[169] Oostendorp RA, Reisbach G, Spitzer E, Thalmeier K, Dienemann H, Mergenthaler HG, et al. VLA-4 and VCAM-1 are the principal adhesion molecules involved in the interaction between blast colony-forming cells and bone marrow stromal cells. Br J Haematol 1995;91:275–84.

[170] Liesveld JL, Winslow JM, Frediani KE, Ryan DH, Abboud CN. Expression of integrins and examination of their adhesive function in normal and leukemic hematopoietic cells. Blood 1993;81:112–21.

[171] Qian H, Tryggvason K, Jacobsen SE, Ekblom M. Contribution of alpha6 integrins to hematopoietic stem and progenitor cell homing to bone marrow and collaboration with alpha4 integrins. Blood 2006;107:3503–10.

[172] Schreiber TD, Steinl C, Essl M, Abele H, Geiger K, Muller CA, et al. The integrin alpha9beta1 on hematopoietic stem and progenitor cells: involvement in cell adhesion, proliferation and differentiation. Haematologica 2009;94:1493–501.

[173] Yin T, Li L. The stem cell niches in bone. J Clin Invest 2006;116:1195–201.

[174] Kaplan RN, Riba RD, Zacharoulis S, Bramley AH, Vincent L, Costa C, et al. VEGFR1-positive haematopoietic bone marrow progenitors initiate the pre-metastatic niche. Nature 2005;438:820–7.

[175] Chavakis E, Aicher A, Heeschen C, Sasaki K, Kaiser R, El Makhfi N, et al. Role of beta2-integrins for homing and neovascularization capacity of endothelial progenitor cells. J Exp Med 2005;201:63–72.

[176] McAllister SS, Gifford AM, Greiner AL, Kelleher SP, Saelzler MP, Ince TA, et al. Systemic endocrine instigation of indolent tumor growth requires osteopontin. Cell 2008;133:994–1005.

[177] Lyden D, Hattori K, Dias S, Costa C, Blaikie P, Butros L, et al. Impaired recruitment of bone-marrow-derived endothelial and hematopoietic precursor cells blocks tumor angiogenesis and growth. Nat Med 2001;7:1194–201.

[178] Pazolli E, Luo X, Brehm S, Carbery K, Chung JJ, Prior JL, et al. Senescent stromal-derived osteopontin promotes preneoplastic cell growth. Cancer Res 2009;69:1230–9.

[179] Wei SC, Tsao PN, Yu SC, Shun CT, Tsai-Wu JJ, Wu CH, et al. Placenta growth factor expression is correlated with survival of patients with colorectal cancer. Gut 2005;54:666–72.

[180] Marcellini M, De Luca N, Riccioni T, Ciucci A, Orecchia A, Lacal PM, et al. Increased melanoma growth and metastasis spreading in mice overexpressing placenta growth factor. Am J Pathol 2006;169:643–54.

[181] Kang Y, Siegel PM, Shu W, Drobnjak M, Kakonen SM, Cordon-Cardo C, et al. A multigenic program mediating breast cancer metastasis to bone. Cancer Cell 2003;3:537–49.

[182] Muller A, Homey B, Soto H, Ge N, Catron D, Buchanan ME, et al. Involvement of chemokine receptors in breast cancer metastasis. Nature 2001;410:50–6.

[183] Sun YX, Fang M, Wang J, Cooper CR, Pienta KJ, Taichman RS. Expression and activation of alpha(v)beta(3) integrins by SDF-1/CXC12 increases the aggressiveness of prostate cancer cells. Prostate 2007;67:61–73.

[184] Sun YX, Wang J, Shelburne CE, Lopatin DE, Chinnaiyan AM, Rubin MA, et al. Expression of CXCR4 and CXCL12 (SDF-1) in human prostate cancers (PCa) in vivo. J Cell Biochem 2003;89:462–73.

[185] Sun YX, Schneider A, Jung Y, Wang J, Dai J, Cook K, et al. Skeletal localization and neutralization of the SDF-1(CXCL12)/CXCR4 axis blocks prostate cancer metastasis and growth in osseous sites in vivo. J Bone Miner Res 2005;20:318–29.

[186] Smith MC, Luker KE, Garbow JR, Prior JL, Jackson E, Piwnica-Worms D, et al. CXCR4 regulates growth of both primary and metastatic breast cancer. Cancer Res 2004;64:8604–12.

[187] Parmo-Cabanas M, Bartolome RA, Wright N, Hidalgo A, Drager AM, Teixido J. Integrin alpha4beta1 involvement in stromal cell-derived factor-1alpha-promoted myeloma cell transendothelial migration and adhesion: role of cAMP and the actin cytoskeleton in adhesion. Exp Cell Res 2004;294:571–80.

[188] Mahabeleshwar GH, Feng W, Phillips DR, Byzova TV. Integrin signaling is critical for pathological angiogenesis. J Exp Med 2006;203:2495–507.

[189] Feng W, McCabe NP, Mahabeleshwar GH, Somanath PR, Phillips DR, Byzova TV. The angiogenic response is dictated by beta3 integrin on bone marrow-derived cells. J Cell Biol 2008;183:1145–57.

[190] Gabrilovich DI, Nagaraj S. Myeloid-derived suppressor cells as regulators of the immune system. Nat Rev Immunol 2009;9:162–74.

[191] Yang L, Edwards CM, Mundy GR. Gr-1+CD11b+ myeloid-derived suppressor cells: formidable partners in tumor metastasis. J Bone Miner Res 2010;25:1701–6.

[192] Bingle L, Brown NJ, Lewis CE. The role of tumour-associated macrophages in tumour progression: implications for new anticancer therapies. J Pathol 2002;196:254–65.

[193] Dirkx AE, Oude Egbrink MG, Wagstaff J, Griffioen AW. Monocyte/macrophage infiltration in tumors: modulators of angiogenesis. J Leukoc Biol 2006;80:1183–96.

[194] Jin H, Su J, Garmy-Susini B, Kleeman J, Varner J. Integrin alpha4beta1 promotes monocyte trafficking and angiogenesis in tumors. Cancer Res 2006;66:2146–52.

[195] Hume DA. The mononuclear phagocyte system. Curr Opin Immunol 2006;18:49–53.

[196] Sweet MJ, Hume DA. CSF-1 as a regulator of macrophage activation and immune responses. Arch Immunol Ther Exp (Warsz) 2003;51:169–77.

[197] Sica A, Allavena P, Mantovani A. Cancer related inflammation: the macrophage connection. Cancer Lett 2008;267:204–15.

[198] Gordon S, Taylor PR. Monocyte and macrophage heterogeneity. Nat Rev Immunol 2005;5:953–64.

[199] Martinez FO, Sica A, Mantovani A, Locati M. Macrophage activation and polarization. Front Biosci 2008;13:453–61.

[200] Mantovani A, Sozzani S, Locati M, Allavena P, Sica A. Macrophage polarization: tumor-associated macrophages as a paradigm for polarized M2 mononuclear phagocytes. Trends Immunol 2002;23:549–55.

[201] Chen ZG, Bottazzi B, Wang JM, Mantovani A. Tumor-associated macrophages in metastasizing tumors. Adv Exp Med Biol 1988;233:61–71.

[202] Chambers SK, Kacinski BM, Ivins CM, Carcangiu ML. Overexpression of epithelial macrophage colony-stimulating factor (CSF-1) and CSF-1 receptor: a poor prognostic factor in epithelial ovarian cancer, contrasted with a protective effect of stromal CSF-1. Clin Cancer Res 1997;3:999–1007.

[203] Canioni D, Salles G, Mounier N, Brousse N, Kuppens M, Morchhauser F, et al. High numbers of tumor-associated macrophages have an adverse prognostic value that can be circumvented by rituximab in patients with follicular lymphoma enrolled onto the GELA-GOELAMS FL-2000 trial. J Clin Oncol 2008;26:440–6.

[204] Reyes-Reyes M, Mora N, Gonzalez G, Rosales C. beta1 and beta2 integrins activate different signalling pathways in monocytes. Biochem J 2002;363:273–80.

[205] Jin H, Aiyer A, Su J, Borgstrom P, Stupack D, Friedlander M, et al. A homing mechanism for bone marrow-derived progenitor cell recruitment to the neovasculature. J Clin Invest 2006;116:652–62.

[206] Sato T, Nakai T, Tamura N, Okamoto S, Matsuoka K, Sakuraba A, et al. Osteopontin/Eta-1 upregulated in Crohn's disease regulates the Th1 immune response. Gut 2005;54:1254–62.

[207] Schneider JG, Zhu Y, Coleman T, Semenkovich CF. Macrophage beta3 integrin suppresses hyperlipidemia-induced inflammation by modulating TNFalpha expression. Arterioscler Thromb Vasc Biol 2007;27:2699–706.

[208] Savill J, Dransfield I, Hogg N, Haslett C. Vitronectin receptor-mediated phagocytosis of cells undergoing apoptosis. Nature 1990;343:170–3.

[209] Savill J, Hogg N, Ren Y, Haslett C. Thrombospondin cooperates with CD36 and the vitronectin receptor in macrophage recognition of neutrophils undergoing apoptosis. J Clin Invest 1992;90:1513–22.

[210] Law DA, DeGuzman FR, Heiser P, Ministri-Madrid K, Killeen N, Phillips DR. Integrin cytoplasmic tyrosine motif is required for outside-in alphaIIbbeta3 signalling and platelet function. Nature 1999;401:808–11.

[211] Taverna D, Moher H, Crowley D, Borsig L, Varki A, Hynes RO. Increased primary tumor growth in mice null for beta3- or beta3/beta5-integrins or selectins. Proc Natl Acad Sci U S A 2004;101:763–8.

[212] Kanamori M, Kawaguchi T, Berger MS, Pieper RO. Intracranial microenvironment reveals independent opposing functions of host alphaVbeta3 expression on glioma growth and angiogenesis. J Biol Chem 2006;281:37256–64.

[213] Galarneau H, Villeneuve J, Gowing G, Julien JP, Vallieres L. Increased glioma growth in mice depleted of macrophages. Cancer Res 2007;67:8874–81.

[214] Gabrilovich DI, Bronte V, Chen SH, Colombo MP, Ochoa A, Ostrand-Rosenberg S, et al. The terminology issue for myeloid-derived suppressor cells. Cancer Res 2007;67:425 [author reply 426].

[215] Sinha P, Clements VK, Bunt SK, Albelda SM, Ostrand-Rosenberg S. Cross-talk between myeloid-derived suppressor cells and macrophages subverts tumor immunity toward a type 2 response. J Immunol 2007;179:977–83.

[216] Honn KV, Tang DG, Crissman JD. Platelets and cancer metastasis: a causal relationship? Cancer Metastasis Rev 1992;11:325–51.

[217] Billroth T. Pathology and therapeutics, in fifty lectures. Clin Orthop 1871;2003:4–11.

[218] Gouin-Thibault I, Achkar A, Samama MM. The thrombophilic state in cancer patients. Acta Haematol 2001;106:33–42.

[219] Boucharaba A, Serre CM, Gres S, Saulnier-Blache JS, Bordet JC, Guglielmi J, et al. Platelet-derived lysophosphatidic acid supports the progression of osteolytic bone metastases in breast cancer. J Clin Invest 2004;114:1714–25.

[220] Phillips DR, Charo IF, Scarborough RM. GPIIb–IIIa: the responsive integrin. Cell 1991;65:359–62.

[221] Smyth SS, Reis ED, Vaananen H, Zhang W, Coller BS. Variable protection of beta 3-integrin-deficient mice from thrombosis initiated by different mechanisms. Blood 2001;98:1055–62.

[222] Hodivala-Dilke KM, McHugh KP, Tsakiris DA, Rayburn H, Crowley D, Ullman-Cullere M, et al. Beta3-integrin-deficient mice are a model for Glanzmann thrombasthenia showing placental defects and reduced survival. J Clin Invest 1999;103:229–38.

[223] Jurasz P, Stewart MW, Radomski A, Khadour F, Duszyk M, Radomski MW. Role of von Willebrand factor in tumour cell-induced platelet aggregation: differential regulation by NO and prostacyclin. Br J Pharmacol 2001;134:1104–12.

[224] Karpatkin S. Role of thrombin in tumor angiogenesis, implantation, and metastasis. Pathophysiol Haemost Thromb 2003;33(Suppl 1):54–5.

[225] Nierodzik ML, Karpatkin S. Thrombin induces tumor growth, metastasis, and angiogenesis: evidence for a thrombin-regulated dormant tumor phenotype. Cancer Cell 2006;10:355–62.

[226] Nierodzik ML, Plotkin A, Kajumo F, Karpatkin S. Thrombin stimulates tumor-platelet adhesion in vitro and metastasis in vivo. J Clin Invest 1991;87:229–36.

[227] Gasic GJ, Gasic TB, Stewart CC. Antimetastatic effects associated with platelet reduction. Proc Natl Acad Sci U S A 1968;61:46–52.

[228] Izumi Y, Taniuchi Y, Tsuji T, Smith CW, Nakamori S, Fidler IJ, et al. Characterization of human colon carcinoma variant cells selected for sialyl Lex carbohydrate antigen: liver colonization and adhesion to vascular endothelial cells. Exp Cell Res 1995;216:215–21.

[229] Kim YJ, Borsig L, Varki NM, Varki A. P-selectin deficiency attenuates tumor growth and metastasis. Proc Natl Acad Sci U S A 1998;95:9325–30.

[230] Karpatkin S, Pearlstein E, Ambrogio C, Coller BS. Role of adhesive proteins in platelet tumor interaction in vitro and metastasis formation in vivo. J Clin Invest 1988;81:1012–9.

[231] Lerner WA, Pearlstein E, Ambrogio C, Karpatkin S. A new mechanism for tumor induced platelet aggregation. Comparison with mechanisms shared by other tumor with possible pharmacologic strategy toward prevention of metastases. Int J Cancer 1983;31:463–9.

[232] Nierodzik ML, Bain RM, Liu LX, Shivji M, Takeshita K, Karpatkin S. Presence of the seven transmembrane thrombin receptor on human tumour cells: effect of activation on tumour adhesion to platelets and tumor tyrosine phosphorylation. Br J Haematol 1996;92:452–7.

[233] Mannori G, Crottet P, Cecconi O, Hanasaki K, Aruffo A, Nelson RM, et al. Differential colon cancer cell adhesion to E-, P-, and L-selectin: role of mucin-type glycoproteins. Cancer Res 1995;55:4425–31.

[234] Bromberg ME, Bailly MA, Konigsberg WH. Role of protease-activated receptor 1 in tumor metastasis promoted by tissue factor. Thromb Haemost 2001;86:1210–4.

[235] Camerer E, Qazi AA, Duong DN, Cornelissen I, Advincula R, Coughlin SR. Platelets, protease-activated receptors, and fibrinogen in hematogenous metastasis. Blood 2004;104:397–401.

[236] Francis JL, Amirkhosravi A. Effect of antihemostatic agents on experimental tumor dissemination. Semin Thromb Hemost 2002;28:29–38.

[237] Hu L, Lee M, Campbell W, Perez-Solar R, Karpatkin S. Role of endogenous thrombin in tumor implantation, seeding and spontaneous metastasis. Blood 2004;104:2746–51.

[238] Palumbo JS, Talmage KE, Massari JV, La Jeunesse CM, Flick MJ, Kombrinck KW, et al. Platelets and fibrin(ogen) increase metastatic potential by impeding natural killer cell-mediated elimination of tumor cells. Blood 2005;105:178–85.

[239] Pearlstein E, Ambrogio C, Karpatkin S. Effect of antiplatelet antibody on the development of pulmonary metastases following injection of CT26 colon adenocarcinoma, Lewis lung carcinoma, and B16 amelanotic melanoma tumor cells into mice. Cancer Res 1984;44:3884–7.

[240] Rickles FR, Patierno S, Fernandez PM. Tissue factor, thrombin, and cancer. Chest 2003;124:58S–68S.

[241] Savage B, Almus-Jacobs F, Ruggeri ZM. Specific synergy of multiple substrate–receptor interactions in platelet thrombus formation under flow. Cell 1998;94:657–66.

[242] Shi X, Gangadharan B, Brass LF, Ruf W, Mueller BM. Protease-activated receptors (PAR1 and PAR2) contribute to tumor cell motility and metastasis. Mol Cancer Res 2004;2:395–402.

[243] Amirkhosravi A, Amaya M, Siddiqui FA. Blockade of GpIIb/IIIa inhibits the release of vascular endothelial growth factor (VEGF) from tumor cell-activated platelets and experimental metastasis. Platelets 1999;10:285–92.

[244] Amirkhosravi A, Meyer T, Chang JY, Amaya M, Siddiqui F, Desai H, et al. Tissue factor pathway inhibitor reduces experimental lung metastasis of B16 melanoma. Thromb Haemost 2002;87:930–6.

[245] Rafii DC, Psaila B, Butler J, Jin DK, Lyden D. Regulation of vasculogenesis by platelet-mediated recruitment of bone marrow-derived cells. Arterioscler Thromb Vasc Biol 2008;28:217–22.

[246] Li X, Koh AJ, Wang Z, Soki FN, Park SI, Pienta KJ, et al. Inhibitory effects of megakaryocytic cells in prostate cancer skeletal metastasis. J Bone Miner Res 2010 [Epub ahead of print]

[247] Beeton CA, Bord S, Ireland D, Compston JE. Osteoclast formation and bone resorption are inhibited by megakaryocytes. Bone 2006;39:985–90.

[248] Grundt A, Grafe IA, Liegibel U, Sommer U, Nawroth P, Kasperk C. Direct effects of osteoprotegerin on human bone cell metabolism. Biochem Biophys Res Commun 2009;389:550–5.

[249] Chollet ME, Brouland JP, Bal dit Sollier C, Bauduer F, Drouet L, Bellucci S. Evidence of a colocalisation of osteoprotegerin (OPG) with von Willebrand factor (VWF) in platelets and megakaryocytes alpha granules. Studies from normal and grey platelets. Br J Haematol 2010;148:805–7.

[250] Leven RM, Tablin F. Extracellular matrix stimulation of guinea pig megakaryocyte proplatelet formation in vitro is mediated through the vitronectin receptor. Exp Hematol 1992;20:1316–22.

[251] Schmitz B, Thiele J, Otto F, Farahmand P, Henze F, Frimpong S, et al. Evidence for integrin receptor involvement in megakaryocyte–fibroblast interaction: a possible pathomechanism for the evolution of myelofibrosis. J Cell Physiol 1998;176:445–55.

[252] Lemieux JM, Horowitz MC, Kacena MA. Involvement of integrins alpha(3)beta(1) and alpha(5)beta(1) and glycoprotein IIb in megakaryocyte-induced osteoblast proliferation. J Cell Biochem 2010;109:927–32.

[253] Escudero ND, Lacave M, Ubios AM, Mandalunis PM. Effect of monosodium olpadronate on osteoclasts and megakaryocytes: an in vivo study. J Musculoskelet Neuronal Interact 2009;9:109–20.

[254] Bernasconi S, Matteucci C, Sironi M, Conni M, Colotta F, Mosca M, et al. Effects of granulocyte–monocyte colony-stimulating factor (GM-CSF) on expression of adhesion molecules and production of cytokines in blood monocytes and ovarian cancer-associated macrophages. Int J Cancer 1995;60:300–7.

[255] Zaslavsky A, Baek KH, R.C. Lynch, Short S, Grillo J, Folkman J, et al. Platelet-derived thrombospondin-1 is a critical negative regulator and potential biomarker of angiogenesis. Blood 2010;115:4605–13.

[256] Mizejewski GJ. Role of integrins in cancer: survey of expression patterns. Proc Soc Exp Biol Med 1999;222:124–38.

[257] Khalili P, Arakelian A, Chen G, Plunkett ML, Beck I, Parry GC, et al. A non-RGD-based integrin binding peptide (ATN-161) blocks breast cancer growth and metastasis in vivo. Mol Cancer Ther 2006;5:2271–80.

[258] Trikha M, De Clerck YA, Markland FS. Contortrostatin, a snake venom disintegrin, inhibits beta 1 integrin-mediated human metastatic melanoma cell adhesion and blocks experimental metastasis. Cancer Res 1994;54:4993–8.

[259] Ramos OH, Kauskot A, Cominetti MR, Bechyne I, Salla Pontes CL, Chareyre F, et al. A novel alpha(v)beta (3)-blocking disintegrin containing the RGD motive, DisBa-01, inhibits bFGF-induced angiogenesis and melanoma metastasis. Clin Exp Metastasis 2008;25:53–64.

[260] Avraamides CJ, Garmy-Susini B, Varner JA. Integrins in angiogenesis and lymphangiogenesis. Nat Rev Cancer 2008;8:604–17.

[261] Fujii H, Komazawa H, Mori H, Kojima M, Itoh I, Murata J, et al. Antimetastatic activities of synthetic Arg-Gly-Asp-Ser (RGDS) and Arg-Leu-Asp-Ser (RLDS) peptide analogues and their inhibitory mechanisms. Biol Pharm Bull 1995;18:1681–8.

[262] Brooks PC, Stromblad S, Klemke R, Visscher D, Sarkar FH, Cheresh DA. Antiintegrin alpha v beta 3 blocks human breast cancer growth and angiogenesis in human skin. J Clin Invest 1995;96:1815–22.

[263] Vaillant F, Asselin-Labat ML, Shackleton M, Forrest NC, Lindeman GJ, Visvader JE. The mammary progenitor marker CD61/beta3 integrin identifies cancer stem cells in mouse models of mammary tumorigenesis. Cancer Res 2008;68:7711–7.

[264] Feng X, Novack DV, Faccio R, Ory DS, Aya K, Boyer MI, et al. A Glanzmann's mutation in beta 3 integrin specifically impairs osteoclast function. J Clin Invest 2001;107:1137–44.

[265] Putz E, Witter K, Offner S, Stosiek P, Zippelius A, Johnson J, et al. Phenotypic characteristics of cell lines derived from disseminated cancer cells in bone marrow of patients with solid epithelial tumors: establishment of working models for human micrometastases. Cancer Res 1999;59:241–8.

[266] Felding-Habermann B, O'Toole TE, Smith JW, Fransvea E, Ruggeri ZM, Ginsberg MH, et al. Integrin activation controls metastasis in human breast cancer. Proc Natl Acad Sci U S A 2001;98:1853–8.

[267] Teti A, Migliaccio S, Baron R. The role of the alphaVbeta3 integrin in the development of osteolytic bone metastases: a pharmacological target for alternative therapy? Calcif Tissue Int 2002;71:293–9.

[268] Engelman VW. A peptidomimetic antagonist of the avb3 integrin inhibits bone resorption in vitro and prevents osteoporosis in vivo. J Clin Invest 1997;99:2284–92.

[269] Harms JF, Welch DR, Samant RS, Shevde LA, Miele ME, Babu GR, et al. A small molecule antagonist of the alpha(v)beta3 integrin suppresses MDA-MB-435 skeletal metastasis. Clin Exp Metastasis 2004;21:119–28.

[270] Nemeth JA, Nakada MT, Trikha M, Lang Z, Gordon MS, Jayson GC, et al. Alpha-v integrins as therapeutic targets in oncology. Cancer Invest 2007;25:632–46.

[271] Murphy MG, Cerchio K, Stoch SA, Gottesdiener K, Wu M, Recker R. Effect of L-000845704, an alphaVbeta3 integrin antagonist, on markers of bone turnover and bone mineral density in postmenopausal osteoporotic women. J Clin Endocrinol Metab 2005;90:2022–8.

[272] Smith JW, Ruggeri ZM, Kunicki TJ, Cheresh DA. Interaction of integrins alpha v beta 3 and glycoprotein IIb–IIIa with fibrinogen. Differential peptide recognition accounts for distinct binding sites. J Biol Chem 1990;265:12267–71.

[273] Gramoun A, Shorey S, Bashutski JD, Dixon SJ, Sims SM, Heersche JN, et al. Effects of Vitaxin, a novel therapeutic in trial for metastatic bone tumors, on osteoclast functions in vitro. J Cell Biochem 2007;102:341–52.

[274] Hariharan S, Gustafson D, Holden S, McConkey D, Davis D, Morrow M, et al. Assessment of the biological and pharmacological effects of the alpha nu beta3 and alpha nu beta5 integrin receptor antagonist, cilengitide (EMD 121974), in patients with advanced solid tumors. Ann Oncol 2007;18:1400–7.

[275] Oliveira-Ferrer L, Hauschild J, Fiedler W, Bokemeyer C, Nippgen J, Celik I, et al. Cilengitide induces cellular detachment and apoptosis in endothelial and glioma cells mediated by inhibition of FAK/src/AKT pathway. J Exp Clin Cancer Res 2008;27:86.

[276] Legler DF, Wiedle G, Ross FP, Imhof BA. Superactivation of integrin alphavbeta3 by low antagonist concentrations. J Cell Sci 2001;114:1545–53.

[277] Alghisi GC, Ponsonnet L, Ruegg C. The integrin antagonist cilengitide activates alphaVbeta3, disrupts VE-cadherin localization at cell junctions and enhances permeability in endothelial cells. PLoS One 2009;4:e4449.

[278] Guo W, Giancotti FG. Integrin signalling during tumour progression. Nat Rev Mol Cell Biol 2004;5:816–26.

[279] Sterling JA, Edwards JR, Martin TJ, Mundy GR. Advances in the biology of bone metastasis: how the skeleton affects tumor behavior. Bone. 2010 [Epub ahead of print]

[280] Bisanz K, Yu J, Edlund M, Spohn B, Hung MC, Chung LW, et al. Targeting ECM–integrin interaction with liposome-encapsulated small interfering RNAs inhibits the growth of human prostate cancer in a bone xenograft imaging model. Mol Ther 2005;12:634–43.

[281] Danen EH, Marcinkiewicz C, Cornelissen IM, van Kraats AA, Pachter JA, Ruiter DJ, et al. The disintegrin eristostatin interferes with integrin alpha 4 beta 1 function and with experimental metastasis of human melanoma cells. Exp Cell Res 1998;238:188–96.

[282] Nervi B, Ramirez P, Rettig MP, Uy GL, Holt MS, Ritchey JK, et al. Chemosensitization of acute myeloid leukemia (AML) following mobilization by the CXCR4 antagonist AMD3100. Blood 2009;113:6206–14.

[283] Lane SW, Scadden DT, Gilliland DG. The leukemic stem cell niche: current concepts and therapeutic opportunities. Blood 2009;114:1150–7.

[284] Azab AK, Runnels JM, Pitsillides C, Moreau AS, Azab F, Leleu X, et al. CXCR4 inhibitor AMD3100 disrupts the interaction of multiple myeloma cells with the bone marrow microenvironment and enhances their sensitivity to therapy. Blood 2009;113:4341–51.

Sarah R. Amend

sramend@wustl.edu • (252) 349-5373

PROFESSIONAL PROFILE

Ph.D. with expertise in cancer biology, genetics, and molecular cell biology with a focus on basic research with practical translational application. Proven leadership abilities with a background in teaching, project management, and active collaboration. Committed to contributing to the understanding host contribution and response in cancer metastasis.

HIGHLIGHTS

- Ph.D. researcher with diverse background in basic laboratory science
- National Institute of Health-National Cancer Institute F31 predoctoral fellow
- Comprehensive training in translational science collaboration
- Director of Summer Focus, a youth science outreach program

EDUCATION

Ph.D.
May 2014

Washington University in St. Louis, Saint Louis, MO
Ph.D. in Molecular Genetics and Genomics

B.S.
2008

North Carolina State University, Raleigh, NC
Bachelor of Science in Biological Sciences, minor in Genetics
Summa cum laude

RESEARCH EXPERIENCE

Ph.D. candidate
2009 – present

Washington University in St. Louis, Dept. of Molecular Oncology

Advisor: Katherine Weilbaecher, M.D.

Thesis: Evaluating the microenvironment in bone-resident cancer: host cell contribution and susceptibility to disease

Project 1: Role of Thrombospondin-1 as a coupling factor in bone (osteoclasts, osteoblasts, and bone matrix) under healthy and pathologic states

- Manuscript conditionally accepted at JBMR
- Developed <u>novel protocols</u> to physiologically model bone microenvironment in vitro using syngeneic murine mouse serum and bone powder. Methods paper in progress.

Project 2: Determining the genetic contributions of susceptibility to monoclonal gammopathy of undetermined significance (MGUS), the requisite precursor to multiple myeloma

170

- <u>Discovered</u> that the gene *Samsn1* contributes to susceptibility MGUS, the requisite precursor to multiple myeloma
- Implemented a <u>novel method</u> to combine low-power mouse and human genetics datasets to identify candidate susceptibility loci
- Manuscript in progress.

Research assistant 2009 I**ntern** summer 2008	*The Jackson Laboratory* Laboratory of Beverly Paigen, Ph.D.; Advisor: Ron Korstanje, Ph.D. • Determined the effects of systemic vitamin D levels on susceptibility to kidney disease in mice • Identified causal SNPs in genes underlying HDL cholesterol
Research assistant 2005 – 2008	*North Carolina State University*, *Dept. of Plant Pathology* • Verified a DNA extraction technique for disease peanut plants • Managed field and greenhouse peanut crop studies
Intern 2007 – 2008	*Laboratory Corporation of America, Genetic Services* • Determined the efficacy of an extended carrier mutation panel high-risk populations at high risk for cystic fibrosis

COMPETITIVE RESEARCH SUPPORT

Pre-doctoral fellowship 1F31CA174096-01A1	Role: PI, 2013 - 2016 Impact score: 15; percentile: 4.0 National Institute of Health/National Cancer Institute "Evaluating the role of Thrombospondin-1 – CD47 mediated nitric oxide signaling in the vicious cycle of bone metastasis"
Training grant 5T32HL007088	Role: trainee, 2010 - 2013 Pre- and postgraduate training in Molecular Hematology National Institute of Health National Heart, Lung, and Blood Institute PI: Evan Sadler
Translational research training	Role: trainee, 2010 - 2012 Lucille P. Markey Special Emphasis Pathway in Human Pathobiology Washington University School of Medicine

CLINICAL TRANSLATIONAL EXPERIENCE

Clinical trial methodology working group 2013 - present	Collaborative think-group of clinicians, patient advocates, and biomedical researchers to accelerate investigator-driven clinical trials.

Myeloma Research Program 2011 – present	Multi-disciplinary group of oncologists, basic scientists, bioinformaticians, and clinical trialists to identify and address large-scale problems in the myeloma research and clinical communities.

Pathway in Human Pathobiology
2010 – 2012

Lucille P. Markey Pathway in Human Pathobiology at Washington University School of Medicine

Competitive didactic translational research training program
- Participated in lectures on six pathologies focused on the intersection of basic research and clinical application
- Learned methods to establish dialogue between researchers and clinicians for practical implementation of scientific discovery

PROFESSIONAL EXPERIENCE

IDEA labs
2013 - 2014

Innovation, Design & Engineering in Action (IDEA) Labs

A bioengineering design incubator to invent and implement novel medical devices to solve unmet clinical problems
- Collaborate with engineers to invent the EnteroGauge, a device to measure distance during small bowel enteroscopy
- Analyze product market to determine feasibility of device
- Initiate patenting and commercialization of the prototype

Consultant
2013 - 2014

Biotechnology and Life Science Advising (BALSA) Group

A non-profit organization that provides short-term consulting services to organizations in biotechnology and life sciences

LEADERSHIP EXPERIENCE

Summer Focus Director
2012 – 2013

Young Scientist Program

Summer Focus provides high school students with funded full-time research internships at the Washington University Medical Center with the mission to attract students from disadvantaged backgrounds to STEM careers by emphasizing hands-on research and individual mentoring.
- Oversaw a corps of >100 volunteers
- Managed the program budget (~$40,000)
- Generated a Summer Focus project charter, a living document outlining key personnel, responsibilities, budget, and policies
- Facilitated an active network of university administration, faculty advisors, lab personnel, and program leadership
- Implemented a leadership team for delegation of specialized tasks (assistant director, course instruction, communications)

Teaching Assistant 2011	*Washington University in St. Louis, Department of Genetics* Graduate-level advanced genetics course

- Led weekly discussion groups and study sections
- Lectured on basic genetics concepts
- Facilitated faculty lectures

Laboratory mentor 2009 2011 - 2013	*The Jackson Laboratory* and *Washington University in St. Louis* Individual lab mentoring for a 2 high school students, 2 undergraduates, and 1 graduate rotation student

- Developed challenging short-term independent projects
- Promoted individual experiential learning

PROFESSIONAL HONORS

2012	American Bone and Mineral Society Young Investigator travel grant
	International Bone & Mineral Society/Cancer Induced Bone Disease travel grant
	European Calcified Tissue Society/ASBMR Young Investigator Award
2008	James P. Murphy Memorial Scholarship at The Jackson Laboratory
	The Horace W. Goldsmith Foundation award at The Jackson Laboratory
	Center for Creative Leadership certification
2007	Certificate of Excellence, School of Life Science at the University of Dundee
2005-08	Caldwell Fellow, North Carolina State University
2004-08	University Honors Program, North Carolina State University
2004	Girl Scout Gold Award

PUBLICATIONS

Manuscript Conditionally Accepted:

Amend, SR, O Uluckan, M Hurchla, D Leib, D Novack, M Silva, W Frazier, K Weilbaecher. Thrombospondin-1 regulates bone homeostasis through effects on bone matrix integrity and nitric oxide signaling in osteoclasts. *Journal of Bone and Mineral Research.*

Manuscripts in preparation:

Amend, SR, L Chu, L Lan, D Serie, C Vachon, L Lu, R Vij, G Colditz, K Weilbaecher, MH Tomasson. Deletion of *Samsn1* underlies genetic susceptibility to monoclonal gammopathy of undetermined significance (MGUS) in mice.

Amend, SR, R Zeng. Novel methods for physiologic cell culture of murine osteoclasts using syngeneic serum and bone.

Peer-reviewed manuscript:

Leduc, MS, M Lyons, K Darvishi, K Walsh, S Sheehan, **S Amend**, A Cox, M Orho-Melander, S Kathiresan, B Paigen, and R Korstanje. The Mouse QTL Map Helps Interpret Human Genome-Wide Association Studies for HDL Cholesterol. 2011. *Journal of Lipid Research.*

Invited review:

Schneider, JG, **SR Amend**, KN Weilbaecher. Integrins and bone metastasis: Integrating tumor cell and stromal cell interactions. 2010. *Bone* 48(1):54-65.

NATIONAL and INTERNATIONAL CONFERENCE PRESENTATIONS

Invited talks:

Amend, S, L Chu, D Serie, C Vachon, L Lu, R Vij, G Colditz, K Weilbaecher, and M Tomasson. December 2013. Deletion of *Samsn1* underlies genetic susceptibility to monoclonal gammopathy of undetermined significance (MGUS) in mice. *American Society of Hematology Annual Meeting*, New Orleans, LA.

Amend, S, O Uluckan, M Hurchla, L Jia, W Frazier, and K Weilbaecher. November 2012. Thrombospondin-1 contributes to the vicious cycle of bone metastasis in both the tumor and host microenvironment compartments. *International conference on Cancer Induced Bone Disease*, Lyon, France.

Plenary abstracts:

Amend, S, L Chu, D Serie, C Vachon, L Lu, R Vij, G Colditz, K Weilbaecher, MH Tomasson. November 2013. Samsn1 underlies genetic susceptibility to MGUS, the requisite precursor to multiple myeloma. *International Conference CIBDS*, Miami, FL.

Amend, S, O Uluckan, M Hurchla, L Jia, W Frazier, and K Weilbaecher. October 2012. Thrombospondin-1 regulates bone density in healthy and skeletal metastatic states by regulating osteoclast-osteoblast coupling. *ASBMR*, Minneapolis, MI.

Amend, S, O Uluckan, M Hurchla, L Jia, W Frazier, and K Weilbaecher. July 2012. Thrombospondin-1 regulates bone density through iNOS-mediated effects on nitric oxide signaling on osteoclasts. *International Workshop on Advances in the Molecular Pharmacology and Therapeutics of Bone Disease*, Oxford, United Kingdom